Amir Safaei

Life-cycle Optimization Model for Distributed Generation in Buildings

Thesis submitted in partial fulfillment of the requirements for the degree of Doctor of Philosophy in Sustainable Energy Systems, supervised by Professor Fausto Miguel Cereja Seixas Freire and Professor Carlos Alberto Henggeler de Carvalho Antunes, presented to the Department of Mechanical Engineering of Faculty of Sciences and Technology of the University of Coimbra

November, 2014

In loving memory of my grandfather, who taught me the passion to learn shall never decade with age;

and my grandmother, who showed me the meaning of sincere love.

They both left me during this Ph.D.

Contents

Abstract ***VII***

Sinopse ***IX***

List of Abbreviations ***XI***

List of Figures ***XIII***

List of Tables ***XVII***

Acknowledgments ***XIX***

Chapter 1

Introduction

1.1 Motivation 1

1.2 Statement of the research 3

1.3 Contributions 6

1.4 Structure of the thesis 7

Chapter 2

Literature Review ***9***

2.1 Studies on application of DG in buildings 10

2.2 Optimization models for DG 13

2.3 LCA studies 17

2.4 Summary and conclusions 22

Chapter 3

Life-cycle Assessment of Natural Gas Consumed in Portugal ***27***

3.1 Natural gas in Portugal 27

3.2 Life-cycle of natural gas 29

3.3 Life-cycle model and inventory 31

3.3.1 Goal and scope 31

3.3.2 Life-cycle inventory 33

3.3.2.1 LCI of Nigerian LNG to Portugal 33

3.3.2.2 LCI of Algerian natural gas to Portugal 38

3.3.3 Distribution 40
3.4 Life-cycle impact assessment 41
3.4.1 CED 41
3.4.2 GHG 43
3.4.3 Acidification 45
3.4.4 Eutrophication 48
3.5 Consumption mix in Portugal 51
3.6 Uncertainty assessment of upstream GHG emissions from NG 51
3.6.1 Parameter uncertainty 54
3.6.2 Scenario uncertainty 59
3.7 Summary and conclusions 60
Chapter 4
Life-cycle Assessment of Energy Systems 63
4.1 Goal and ccope 63
4.1.1 Generation of electricity 64
4.1.2 Generation of heating energy 65
4.1.3 Generation of cooling energy 65
4.2 Life-cycle inventory 66
4.2.1 Internal combustion engine cogeneration technology 66
4.2.2 Micro-turbine technology 66
4.2.3 Solid oxide fuel cell cogeneration technology 68
4.2.4 Photovoltaic 69
4.2.5 Solar thermal 69
4.2.6 Boiler 70
4.2.7 Grid 70
4.2.8 Absorption chiller 72
4.2.9 Compression chiller 72
4.3 Life-cycle impact assessment results 77
4.3.1 CED 77
4.3.2 GHG 80
4.3.3 Acidification 84
4.3.4 Eutrophication 88

4.4 Conclusions 92

Chapter 5

A Multi-Objective Mathematical Optimization Model for Design and Operation of Distributed Generation in Buildings 97

5.1 Model description 97

Policy framework for cogeneration systems in Portugal 98

Policy framework for PV systems in Portugal 104

5.2 Mathematical model 105

5.3 Case-study 122

5.4 Multi-objective framework 125

5.5 Summary 126

Chapter 6

Selected Results and Discussions 127

6.1 Economic assessment of distributed generation technologies 127

6.1.1 ICE 128

6.1.2 MT 131

6.1.3 SOFC 133

6.1.4 Cost and PES implications 136

6.2 Pareto frontiers 139

6.2.1 Pareto frontier for cost and CED 141

6.2.2 Pareto frontier for cost and GHG 144

6.2.3 Pareto frontier for cost and Acidification 148

6.2.4 Pareto frontier for cost and Eutrophication 152

6.3 Conclusions 153

Chapter 7

Solar PV economics in Portugal 157

7.1 Methodology 157

7.2 Willingness to pay for PV in Portugal 161

7.3 Implication of FIT on economics of PV in Portugal 162

7.4 Summary and concluding notes 163

Chapter 8

Probabilistic and Robust Optimization Framework ***165***

8.1 Robust modelling framework 165

8.2 Results 167

8.3 Conclusions 173

Chapter 9

Concluding Remarks ***175***

9.1 Summary and dissemination of results 175

9.2 Limitations and recommendations for future studies 177

Bibliographic References ***179***

Extra Readings ***191***

Appendix A ***195***

Appendix B ***199***

Appendix C ***201***

List of Publications ***201***

Abstract

Energy use in the building sector constitutes a major proportion of energy consumption and emissions in European Union. Distributed Generation (DG) sources, namely cogeneration and solar technologies, are expected to play an important role in future energy supply mix of building sector. However, the optimal design and operation of cogeneration is a complex task, due to the diversity of variables in play, namely different types of building energy demands (electrical, heating, cooling) and their variation, dynamic fuel (natural gas) and electricity prices, and fixed and variable costs of different types of DG. This becomes more complex by coupling solar thermal and photovoltaic technologies. At the same time, the liberalization of electricity market allows exporting onsite produced electrical energy to the grid; moreover, the operational strategy of DG should meet the national policy frameworks, if the aim is to benefit from such schemes.

Additionally, considering the high impacts of the building sector, any rigorous assessment of building energy systems should also incorporate environmental aspects, adopting a Life-Cycle (LC) perspective. A LC Assessment (LCA) of DG should include stages related to their construction and operation, as well as their fuel upstream emissions, i.e. Natural Gas (NG). The upstream emissions of NG varies based on its source, type (conventional vs. unconventional) and state of delivery (in the form of Liquefied Natural Gas (LNG) or gas). Similarly, the impact of solar systems is affected by meteorology and solar radiation, which is determined by geographical location. Therefore, a proper assessment of DG calls for an LC framework properly modeled for the location (Portugal), which also incorporates the appropriate fuel input (NG) upstream emissions based on its sources of supply.

The objective of this doctoral research is to present a modelling framework to optimize the design and operation of DG for the Portuguese commercial building sector, while considering the Life-Cycle Impact Assessment (LCIA) and Life-Cycle Costs (LCC) of meeting the building energy demand. Three types of cogeneration technologies (Micro-Turbines (MT), Internal Combustion Engines (ICE), Solid Oxide Fuel Cells (SOFC)), and two types of solar technologies [solar thermal (ST) and Photovoltaic (PV)]

comprise the DG sources that are coupled with conventional sources. An LC model is built taking into account all the impacts related to construction and operation of energy systems, as well as the upstream processes related to their fuel input. For the latter, the mix of NG consumed in Portugal in 2011 (60% from Nigeria, and 40% from Algeria) is identified and the upstream impacts of each route of NG to Portugal are separately assessed for four types of environmental impacts: Cumulative Energy Demand (CED), Greenhouse Gases (GHG), Acidification and Eutrophication. Due to the effect of GHG emissions on policy design, an uncertainty analysis of upstream GHG emissions of NG supplied to Portugal is also performed.

A mathematical model is developed in General Algebraic Modeling System (GAMS; McCarl *et al.*, 2013) that uses the results of LCA of energy systems and their economic implications to minimize the LCC and LCIA of meeting the building demand over a planning horizon. Pareto Optimal frontiers are derived, representing the trade-offs between a type of environmental impact (CED, GHG, Acidification, Eutrophication) and LCC arising from meeting the building energy demand. To increase the model robustness due to uncertainty in energy prices (NG and electricity), a cost robust modeling framework for DG, one that gets least affected by the perturbation of input fuel costs, is also developed. The application of the proposed model is tested on a real-world case-study, a commercial building located in the city of Coimbra, Portugal.

Sinopse

O setor da construção é responsável por uma grande parte do consumo de energia e emissões na União Europeia. A Geração Distribuída (GD) de energia, nomeadamente através de sistemas de cogeração e tecnologias solares, representa um papel importante no futuro energético deste setor. A otimização do funcionamento dos sistemas de cogeração é uma tarefa complexa, devido às diversas variáveis em jogo, designadamente: os diferentes tipos de necessidades energéticas (eletricidade, aquecimento e arrefecimento), os preços dinâmicos dos combustíveis (gás natural) e da eletricidade, e os custos fixos e variáveis dos diferentes sistemas de GD. Tal torna-se mais complexo considerando as tecnologias solares térmicas e fotovoltaicas. Ao mesmo tempo, a liberalização do mercado da eletricidade permite exportar para a rede, a electricidade gerada localmente. Adicionalmente, a operação e planeamento estratégica de um sistema de GD deve ter em conta o enquadramento economico e politico nacional, aos quadros políticos nacionais, para poder beneficiar das regimes especais.

Considerando os elevados impactes ambientais do setor da construção, qualquer avaliação energética de edifícios rigorosa deve também integrar aspetos ambientais, utilizando uma abordagem de Ciclo de Vida (CV). Uma avaliação de Ciclo de Vida (ACV) de um sistema de GD deve incluir as fases relativas à operação e construção do sistema, bem como os impactes associados à produção dos combustíveis. Foram analisadas as emissões da produção de GN, as quais variam de acordo com a origem, tipo (convencional ou não-convencional), e estado (na forma de GN Liquefeito (GNL) ou gás). Do mesmo modo, o impacte dos sistemas solares é afetado pela meteorologia e radiação solar, de acordo com a sua localização geográfica. Sendo assim, uma avaliação adequada dos sistemas de GD exige um modelo de ACV adequado à localização geográfica (Portugal), integrando também a produção de combustível (GN), tendo em conta as suas diferentes fontes de abastecimento.

O principal objetivo desta tese de doutoramento foi desenvolver um modelo para otimizar o desenho e operação de sistemas de GD para o setor da construção de edifícios comerciais em Portugal, considerando os Impactes de Ciclo de Vida (IAVC) e

Custos de Ciclo de Vida (CCV), de modo a satisfazer as necessidades energéticas do edifício.

Três tipos de tecnologias de cogeração (Micro-Turbinas, Motores de combustão interna, e Células combustíveis de óxido sólido), e dois tipos de tecnologias de energia solar (solar térmica e fotovoltaica) constituem os sistemas que foram avaliados. Foi desenvolvido um modelo de CV, tendo em conta todos os impactes relacionados com a construção e operação dos sistemas de energia, bem como os processos a montante relacionados com a produção do GN. Em particular, o mix de GN consumido em Portugal em 2011 foi considerado (60% da Nigéria, 40% da Argélia) e os impactes relativos a cada uma das vias de abastecimento foram avaliados separadamente para quatro categorias de impacte ambiental: Consumo de Energia Primária (CEP), Gases com Efeito de Estufa (GEE), Acidificação, e Eutrofização. Devido à importância das emissões de GEE na formulação de políticas, foi também realizada uma análise de incerteza às emissões de GEE do GN fornecido a Portugal.

Foi desenvolvido um modelo matemático, em "General Algebraic Modeling System" (GAMS), que utiliza os resultados da ACV dos sistemas de energia e as suas implicações económicas para minimizar o CCV e IACV ao longo de um horizonte de planeamento definido pelo decisor. Foram derivadas fronteiras ótimas de Pareto, representando as relações entre o tipo de IACV (CEP, GEE, acidificação, eutrofização) e CCV decorrentes da satisfação das necessidades energéticas do edifício. Para aumentar a robustez do modelo, dada a incerteza dos preços dos combustíveis (GN e eletricidade), foi desenvolvido um modelo de custos robusto para os sistemas de GD, que é menos afetado por perturbações relativas aos custos de combustível. A aplicação do modelo proposto foi testada num caso de estudo real, um edifício comercial localizado na cidade de Coimbra, em Portugal.

List of Abbreviations

Abbreviation	*Meaning*
AC	Absorption Chiller
bcm	Billion Cubic Meters
CC	Compression Chiller
CED	Cumulative Energy Demand
CHP	Combined Heat and Power
CEP	Consumo de Energia Primária
CV	Coefficient of Variation
DG	Distributed Generation
DM	Decision Maker
EAC	Equivalent Annual Costs
FIT	Feed-in Tariff
GAMS	General Algebraic Modeling System
GEE	Gases com Efeito de Estufa
GN	Gás Natural
GHG	Greenhouse Gases
Hrs	Hours
ICE	Internal Combustion Engine
kWh_C	kWh cooling
kWh_e	kWh electricity
kWh_{th}	kWh heat
LC	Life-Cycle
LCA	Life-Cycle Assessment
LCC	Life-Cycle Costs
LCIA	Life-Cycle Impact Assessment
LCI	Life-Cycle Inventory
LNG	Liquefied Natural Gas
MILP	Mixed Integer Linear Programming
LHV	Lower Heating Value
MOLP	Multi-Objective Linear Programming
MT	Micro-Turbine
MW_e	MW electricity
NG	Natural Gas
PES	Primary Energy Savings
PV	Photovoltaic
SD	Standard Deviation
SOFC	Solid Oxide Fuel Cell
ST	Solar Thermal
W	Watt
W_p	Watt Peak
WtT	Well-to-Tank
Yr	Year

List of Figures

Figure 3.1: Euro Maghreb Pipeline Distance and location (Galp Energia, 2012) 28
Figure 3.2: LC stages of NG and LNG 29
Figure 3.3: NG - Annual losses during distribution as a percentage of consumption in Portugal 40
Figure 3.4: CED—Upstream stages of Nigerian LNG (MJ/MJ) 42
Figure 3.5: CED—Upstream stages of Algerian NG (MJ/MJ) 42
Figure 3.6: GHG emissions—upstream stages of Nigerian LNG (100-year time horizon) 43
Figure 3.7: Nigerian LNG GHG: Production breakdown based on LC stage 44
Figure 3.8: GHG emissions—production of NG in Algeria (100-year time horizon)..... 44
Figure 3.9: Algerian NG GHG emissions: Production breakdown based on LC stage 45
Figure 3.10: Acidification potential—upstream stages of Nigerian LNG..... 46
Figure 3.11: Nigerian LNG Acidification: Production breakdown based on LC stage..... 46
Figure 3.12: Acidification potential—production of NG in Algeria..... 47
Figure 3.13: Algerian NG Acidification potential—Production breakdown based on LC stage..... 48
Figure 3.14: Eutrophication potential—upstream stages of Nigerian LNG..... 49
Figure 3.15: Nigerian LNG Eutrophication: Production breakdown based on LC stage. 49
Figure 3.16: Eutrophication potential—upstream stages of Algerian NG..... 50
Figure 3.17: Algerian NG Eutrophication: Production breakdown based on LC stage... 51
Figure 3.18: GHG emission of Nigerian LNG — 90% confidence interval..... 55
Figure 3.19: GHG emission of Algerian NG — 90% confidence interval..... 56
Figure 3.20: Nigerian LNG upstream GHG — sensitivity to input parameters..... 56
Figure 3.21: Algerian NG upstream GHG — sensitivity to input parameters..... 57
Figure 3.22: GHG emission of Portuguese NG mix —90% confidence interval..... 58
Figure 3.23: GHG Sensitivity to input parameters- Portuguese mix 58
Figure 3.24: Upstream GHG emissions of Nigerian LNG and Algerian NG—implications of the selection of the time horizon 59
Figure 3.25: Portuguese NG mix upstream GHG emissions—implications of the selection of the time horizon..... 60
Figure 4.1: Components of a MT cogeneration system 67
Figure 4.2: Evolution of electricity generation mix in Portugal..... 71
Figure 4.3: Electricity generation mix for the current study 71
Figure 4.4: PV, CHP and grid: CED (MJ/kWh$_e$) 77
Figure 4.5: ST, condensing boiler and conventional boiler: CED (MJ/kWh$_{th}$)..... 78
Figure 4.6: CHP—break-down of CED based on LC stage..... 79
Figure 4.7: CED of cooling systems 79
Figure 4.8: PV, CHP and grid—GHG (g CO_2 eq/kWh$_e$) 80

Figure 4.9: ST, condensing boiler and conventional boiler—GHG (g CO_2 eq/kWh_{th}) 81
Figure 4.10: CHP—break-down of GHG based on LC stage 82
Figure 4.11: GHG of cooling systems 84
Figure 4.12: PV, CHP and grid—Acidification of energy systems (g SO_2 eq/kWh_e) 85
Figure 4.13: ST, condensing boiler and conventional boiler— Acidification (g SO_2 eq/kWh_{th}) 85
Figure 4.14: CHP—break-down of Acidification potential based on LC stage 86
Figure 4.15: Acidification impact of cooling systems 88
Figure 4.16: PV, CHP and grid— Eutrophication (g PO_4^{3-} eq/kWh_e) 89
Figure 4.17: ST, condensing boiler and conventional boiler— Eutrophication (g PO_4^{3-} eq/kWh_{th}) 89
Figure 4.18: CHP—break-down of Eutrophication potential based on LC stage 90
Figure 4.19: Eutrophication impact of cooling systems 92
Figure 5.1: Model components and their interrelationship 98
Figure 6.1: Power output in the case of ICE with other energy systems (with export to grid) 130
Figure 6.2: Heat output in the case of ICE with other energy systems (with export to grid) 130
Figure 6.3: Cooling output in the case of ICE with other energy systems (with export to grid) 131
Figure 6.4: Power output in the case of MT with other energy systems (with export to grid) 132
Figure 6.5: Heating output in the case of MT with other energy systems (with export to grid) 133
Figure 6.6: Cooling output in the case of MT with other energy systems (with export to grid) 133
Figure 6.7: Power output in the case of SOFC with other energy systems (with export to grid) 135
Figure 6.8: Heating output in the case of SOFC with other energy systems (with export to grid) 135
Figure 6.9: Cooling output in the case of SOFC with other energy systems (with export to grid) 136
Figure 6.10: NPV—Cogeneration technologies 138
Figure 6.11: ICE- Expected annual cash flows 138
Figure 6.12: Cost vs. CED—Pareto frontier 142
Figure 6.13: Minimizing CED - Optimal operation planning of energy systems to meet Power demand 143
Figure 6.14: Minimizing CED - Optimal operation planning of energy systems to meet heating demand 144
Figure 6.15: Minimizing CED - Optimal operation planning of energy systems to meet cooling demand 144

Figure 6.16: Cost vs. GHG—Pareto frontier 145
Figure 6.17: Minimizing GHG - Optimal operation planning of energy systems to meet Power demand 147
Figure 6.18: Minimizing GHG - Optimal operation planning of energy systems to meet Heat demand 147
Figure 6.19: GHG - Optimal operation planning of energy systems to meet cooling demand 147
Figure 6.20: Cost vs. Acidification—Pareto frontier 149
Figure 6.21: Acidification - Optimal operation planning of energy systems to meet power demand 151
Figure 6.22: Acidification - Optimal operation planning of energy systems to meet heating demand 151
Figure 6.23: Acidification - Optimal operation planning of energy systems to meet cooling demand 151
Figure 6.24: Cost vs. Eutrophication—Pareto frontier 153
Figure 7.1: Map of Portugal—Studied Cities 158
Figure 7.2: Willingness-to-pay for PV— Faro, Évora, Coimbra, Porto, and Bragança 162
Figure 7.3: Implication of FIT on economics of PV—Faro, Èvora, Coimbra, Porto, and Bragança 163

List of Tables

Table 3.1: GHG characterization factors (IPCC, 2007) 32
Table 3.2: Acidification potential characterization factors (Guinee *et al.* 2002) 32
Table 3.3: Eutrophication potential characterization factors (Guinee *et al.* 2002)..... 32
Table 3.4: GHG characterization factor of gases (IPCC, 2007)..... 32
Table 3.5: Raw Nigerian NG and pipeline quality NG from Nigerian LNG: composition on a mass basis 33
Table 3.6: Emission factor of heavy fuel oil and BOG LNG 36
Table 3.7: LNG shipping distance, trip duration and fuel consumption assumptions ... 36
Table 3.8: WtT GHG LCI of Nigerian LNG consumed in Portugal (g/MJ) 37
Table 3.9: WtT Acidification and Eutrophication emissions of Nigerian LNG consumed in Portugal (g/MJ) 37
Table 3.10: WtT energy requirements of Nigerian LNG (MJ/MJ) 37
Table 3.11: Raw Algerian NG and its pipeline quality: composition on a mass basis 38
Table 3.12: WtT GHG emissions of Algerian NG consumed in Portugal (g/MJ) 39
Table 3.13: Acidification and Eutrophication emissions of Algerian NG consumed in Portugal (g/MJ) 39
Table 3.14: WtT energy requirements of Algerian NG consumed in Portugal (MJ/MJ) 39
Table 3.15: LCI of Distribution of NG in Portugal (g/MJ) 41
Table 3.16: CED - Distribution of NG in Portugal (MJ/MJ)..... 41
Table 3.17: LCIA of NG consumed in Portugal 51
Table 3.18: WtT stages of Nigerian LNG- Probability density functions for GHG emissions..... 53
Table 3.19: WtT stages of Algerian NG- Probability density functions for GHG emissions..... 54
Table 4.1: Efficiency parameters of ICE (Osman *et al*., 2008) 66
Table 4.2: Efficiency parameters of MT (EPA ETV, 2003) 68
Table 4.3: Efficiency parameters of SOFC (Osman *et al.*, 2008)..... 69
Table 4.4: LCI of cogeneration systems 73
Table 4.5: LCI of ST, PV, grid and boilers..... 74
Table 4.6: LCI of cooling systems 74
Table 4.7: CED of cogeneration systems 75
Table 4.8: CED of PV and Grid..... 75
Table 4.9: CED of boiler and ST..... 75
Table 4.10: CED of cooling systems 75
Table 5.1: PES implication of cogeneration systems 104
Table 5.2: Site location data for PV system (PVWATTS, 2011)..... 123
Table 5.3: Efficiency parameters of ST systems..... 124
Table 5.4: Case-study demand characteristic and estimation of solar potential..... 124

Table 6.1: PES—Cogeneration technologies 137
Table 6.2: LCIA of cogeneration systems—input to the mathematical model 140
Table 6.3: LCIA of solar and conventional systems—input to the mathematical model 140
Table 6.4: Pay-off values for cost vs CED 141
Table 6.5: Pay-off values for cost vs GHG 145
Table 6.6: Pay-off values for cost vs Acidification 148
Table 6.7: Pay-off values for cost vs. Eutrophication 152
Table 7.1: Meteorological sites specifications— Faro, Évora, Coimbra, Porto, and Bragança (PV-Watts, 2011) 159
Table 7.2: Solar radiation and energy output of PV systems in Faro, Évora, Coimbra, Porto and Bragança 160
Table 7.3: Summary of Willingness-to-pay PV— Faro, Évora, Coimbra, Porto, and Bragança 162
Table 8.1: Expected value of objective function - different energy systems 168
Table 8.2: Sensitivity of results to robustness parameter λ 172

Acknowledgments

This work has been framed under the Initiative Energy for Sustainability of the University of Coimbra and supported by the project Energy and Mobility for Sustainable Regions - EMSURE (CENTRO-07-0224-FEDER-002004). The work was also supported by Faculty of Science and Technology through research grants “BI 1/2011” by Institute for Systems Engineering and Computers at Coimbra (INESC Coimbra), and research grant PTDC/SEN-TRA/117251/2010 in the context of “ Extended “well-to-wheels” assessment of biodiesel for heavy transport vehicles (BioHeavy)” project by Association for the Development of Industrial Aerodynamic (ADAI). I am thankful to committee member of Energy for Sustainability (Efs) initiative for several stages of financial support to visit MIT and present scientific papers in academic conferences during my doctoral studies.

Completing the Ph.D degree has been perhaps the most demanding—and at the same time enjoyable— challenge of my life so far. Being here was not possible without the encouragement and support of many people to whom I would like to express my gratitude.

My first thanks goes to my supervisors— Steve Connors, Carlos Henggeler Antunes, Fausto Freire— for giving me the independence for research. I would like to thank Carlos, who believed in me. His wisdom in problem-solving; and his motto “*we can never win if we don’t try”* will carry me through life. Fausto was the faculty member who welcomed me in Coimbra, and pushed me during the first days I was lost. I am grateful for this, as well as for creating the Center for Industrial Ecology (CIE), which provided the appropriate environment to perform research. Fausto’s persistent “one-step ahead” vision was essential to the quality of this thesis. Finally, my special thanks goes to Steve Connors, who was *coolest* (the way himself pronounces!) host-professor during my period of visit in Massachusetts Institute of Technology (MIT). Apart from his academic excellence, his was-of-being, and his spirit are exemplary for me. I specially thank him for involving me in the “MIT Future of Solar Study” that was a fantastic experience of my Ph.D.

There are two people I would like to mention for their helps and insights to this thesis. Professor José Baranda greatly helped me to better understand cogeneration systems and several meetings with him were greatly valuable to shape chapter 5 of this thesis. Nilton Oliveira kindly gave a hand over to collect and organize the case-study data. Thanks both!

Ana Ramos: thanks for being so responsive and fantastic!

Thanks to my colleagues in CIE and DEM. those who left during my Ph.D and those who are still with me when finishing this work. My gratitude goes to João Malça, who several times helped me out with my scientific doubts. Rita Garcia and Pedro Marques: thanks for all the kindness these years, especially for the hand to calculate the impact of Portuguese grid. Erica, Rita 2 (Domingues!), Carla Caldeira (thought!), Carlos, Pedro Gonçalves, Ronaldo, and others; Thank you for the good times.

A particular thanks goes to Elsa, who was the person beside me in all ups and downs, since the first day of my arrival in Coimbra, till the last moment of writing down this text. Thanks for the all the crazy moments, all the patience, and the sincere support. I could not be luckier in finding you.

Finally, my thanks and love goes to my family: my parents, my grandmother, my aunts, Amoo Andrew, Bahareh, Mohammad-Reza, and my two lovely nephew and niece, Mani and Ava. If you were not there backing me up, I would not have been here. My parents were who foremost encouraged me to pursue education abroad, who have been supporting me unconditionally through my master and now Ph.D. You being there—always kept my heart warm during these years. This is for you!

Chapter 1

Introduction

1.1 Motivation

Energy use in building sector accounts for more than 40 percent of the EU energy consumption (IEA, 2013). Due to this fact and growing environmental awareness, the building sector is under focus to contribute to the reduction of energy use and emissions. A study by the World Business Council for Sustainable Development (WBCSD, 2009) suggests that the building sector needs to cut energy consumption 60 percent by 2050 to assist meeting global climate change mitigation targets. In Portugal, energy consumption in the building stock has consistently increased over the last decade, being the commercial sector the one that registered the largest increase (ADENE, 2012).

The employment of Distributed Generation (DG), also called decentralized generation, is considered as a relevant mean to enhance the energy use in building sector. The generation of energy at the point of consumption is pointed out as a key option for promoting energy efficiency and use of renewable sources in alternative to the traditional generation, its implementation rapidly gaining interest in several countries (Shrestha & Marpaung, 2005). Different technologies have been developed for DG, among which cogeneration, also called Combined Heat and Power (CHP), has been widely recognized for its high global energy efficiency compared to separate production of heat and electricity. Similarly, solar technologies to produce onsite electricity, Photovoltaic (PV), and heating energy, Solar Thermal (ST), are nominated as renewable alternatives to conventional grid and boilers. In this regard, Portugal boasts a favorable climatic situation for benefitting from solar technologies and has employed a Feed-in Tariff (FIT) scheme to promote PV in the building sector.

The conventional setting of energy supply technologies for buildings (grid and boiler) does not leave much space for energy planning and optimization of energy use, as the

price of electricity is generally dictated to the consumer and there is no choice between different energy systems. However, by introduction of DG, different renewable and non-renewable sources, and thus alternative operation strategies can be used that provide a considerable scope for energy planning and optimization. In particular, the optimization of design and operation in CHP systems is complex, due to fuel and electricity dynamic prices, and the variation in energy demands. This becomes more complex by considering hourly variable solar sources and integration of conventional systems, such as grid and gas boilers, with CHP. At the same time, the liberalization of electricity market allows the building owner to be not just a consumer but also a producer and seller of electrical power as long as certain policy framework conditions are met. Therefore, the operational strategy of CHP should also meet the national policy frameworks, if the aim is to benefit from schemes related to exporting electrical power to grid. The joint consideration of these factors establishes that at the current stage there is a significant scope for combination and operational optimization of DG sources for the purpose of meeting the building sector energy demand.

Additionally, considering the high impacts of building sector, it is well established that any rigorous assessment of building energy systems should also incorporate environmental aspects (Alanne & Saari, 2004). Life-Cycle Assessment (LCA), a methodology to assess environmental impacts associated with a product from cradle to grave, is often promoted as the suitable tool. A complete LCA should include stages related to construction of energy systems, their operation, as well as the upstream emissions related to their fuel input, such as Natural Gas (NG) in Portugal. On top of the impacts due to its combustion, NG has impacts associated with its production and transportation, their magnitude depending on the source of NG, its type (conventional vs. unconventional) and state of delivery: in liquid form (LNG) or gas. Similarly, the output and impact of solar systems depend on (many factors including) meteorology and solar radiation received by the system, depending on the geographical location. Therefore, a proper assessment of DG (in Portugal) calls for an LCA framework specifically modeled for the location, one that regards geographical differences and incorporates the correct fuel input (NG) upstream emissions based on its source of supply.

The main impact from cogeneration systems is related to fuel input to the system (Safaei *et al.*, 2012), i.e. NG. NG GHG combustion emissions (downstream) can be estimated based on the composition of NG (API, 2009). On the other hand, a few studies that assessed the uncertainty in NG upstream emissions (Skone *et al.*, 2011; Venkatesh *et al.*, 2011) found a high level of uncertainty from the estimated mean GHG emissions. Thus, and to increase the transparency of LCA results, it is recommended to perform LC studies that are based on probabilistic modeling methods (in addition to conventional deterministic approaches). The ISO standards on LCA (ISO 14044, 2006) also state "whenever feasible, uncertainty analysis should be performed to better explain and support the conclusions".

To summarize, high energy consumptions of building sector and the diffusion of DG calls for a methodological framework for overall energy management. In terms of structure, such a framework should include a set of distributed (including renewable) and centralized energy equipment, and the consideration of its links with the building characteristics. The framework should qualify to incorporate several factors, namely dynamic seasonal and hourly pricing of electricity and NG, different types of building energy demands (electrical, heating, cooling) and their variation, fixed and variable cost implications and environmental performance of components, and existing national legal frameworks and incentives for the promotion of each type of DG. In addition, environmental impact assessment of DG calls for an LC study designed for the location, and should account for different stages related to operation and construction of energy systems, as well as the NG upstream emissions. Moreover, following ISO 14044 (2006) guidelines, whenever feasible uncertainty analysis should be performed to increase the clarity of the LCA results.

1.2 Statement of the research

This work develops an LC optimization framework for design and operation of DG in the Portuguese building sector. Three types of cogeneration technologies ((Micro-Turbines (MT), Internal Combustion Engines (ICE), Solid Oxide Fuel Cells (SOFC)), and two types of solar technologies (solar thermal (ST) and Photovoltaic (PV)) comprise the DG sources that are considered along with conventional sources (two types of NG

boilers, electrical grid) to address the building energy demand. In order to take advantage of the thermal output of the cogeneration systems when cooling demand exists, Absorption Chillers (AC) are added to the model as an alternative to Compression Chillers (CC) that are considered as the current common cooling system in the Portuguese building stock. A mathematical optimization model is developed to minimize the Life-Cycle Costs (LCC) and LC Impact Assessment (LCIA) of meeting the building demand for four types of impacts: Cumulative Energy Demand (CED), Greenhouse Gas (GHG), Acidification, and Eutrophication. An LCA is conducted that takes into account all the impacts related to construction and operation of energy systems, as well as the upstream processes related to their fuel input, i.e. NG. For the latter, the mix of NG consumed in Portugal, based on actual share of supply from exporting countries (Nigeria and Algeria) is identified. Primary data from Nigerian oil and gas industry (NNPC, 2011) and LC databases are collected to build a model assessing the upstream impacts of NG consumed in Portugal. Similarly, average hourly local meteorology and solar radiation data of continental Portugal are used to calculate the output and impacts of solar systems.

The consumption of NG in Portugal has duplicated between 2001 and 2010 (IEA, 2011a). Due to this, and the importance of GHG emissions and their effect on policy design, an uncertainty analysis of upstream GHG emissions of NG supplied to Portugal (from Nigeria and Algeria) is performed. Two types of uncertainty in LC model are assessed: uncertainty in model input parameters (parameter uncertainty) and uncertainty in the modelling choices over the time horizon (20-, 100-, or 500-year) to calculate the GHG intensity (scenario uncertainty). For parameter uncertainty, a distribution function representing upstream GHG emissions of 1 MJ (Lower Heating Value (LHV)) NG consumed in Portugal is derived. For scenario uncertainty, different time horizons are selected to calculate the mean GHG intensity of NG consumed in Portugal and the variety of mean estimate due to selection of different time horizons are shown.

A Mixed Integer Linear Programming (MILP) model is developed in General Algebraic Modeling System (GAMS; McCarl *et al.*, 2013), which uses the results of LCA and economic assessment of energy systems to minimize LCC and LCIA of meeting the

building demand over the planning horizon defined by a Decision Maker (DM). In order to implement the model, an actual commercial building, a 133 room hotel complex located in Coimbra (Portugal), is used as the case-study. Measured hourly electricity consumption, and estimated heating and cooling demands of the complex were used to build up a load diagram, consisting of 7 block-loads for three defined seasons—Hot (H), Mild (M) and Cold (C)— throughout a year of the planning period. Doing this, the varied output profile of the solar units and dynamic pricing of electricity are embedded into the model. The LC model calculates the total impact arising from meeting the building energy demand, including the emissions due to production and decommissioning of energy systems, their operation and upstream NG stages. The following objective functions are used in the model formulation:

- Minimizing LCC;
- Minimizing Cumulative Energy Demand (CED);
- Minimizing Greenhouse Gas (GHG) emissions;
- Minimizing Acidification impact;
- Minimizing Eutrophication impacts.

Using the model, a detailed economic assessment of each individual cogeneration technology, coupled with other energy systems, according to the national regulations in Portugal, is carried out. For PV, since its output depend on the location of installment and meteorology, a detailed economic study according to average local meteorology in different regions in Portugal is carried out. Next, applying multi-objective optimization techniques, four Pareto optimal frontiers are derived, each representing the trade-off between a type of environmental impact (CED, GHG, Acidification, Eutrophication) and LCC arising from meeting the building energy demand throughout a nominal year.

Finally, to increase the model robustness due to uncertainty in fuel (NG and electricity) prices, a probabilistic and robust modeling framework for DG is developed. A probabilistic model incorporates uncertainty in the future fuel costs (in discrete scenarios) to increase the model flexibility and accuracy. A cost robust operation planning for a nominal year, one that gets least affected by the perturbation of fuel

costs, is also offered. The application of the proposed framework was tested by defining a number of scenarios and analyzing the results.

1.3 Contributions

The main contributions of this thesis can be summarized as following:

1- An LC multi-objective model for design and operational optimization of DG for the building sector is developed. The model combines several cogeneration technologies, ST and PV, and conventional sources, and calculates the total LCC and LCIA arising from meeting the building energy demand over a defined time horizon. In order to calculate the environmental impacts, an LC model is developed that considers all the stages related to the construction of energy systems, their operation and fuel input upstream emissions. The model is suitable for selection and optimization of operation of DG according to the level of cost and each type of environmental impact desired by the DM. National policy conditions are included in the model. Additionally, the LC model can be used separately to assess the LC environmental impacts of meeting the energy demand in the building sector.

2- The thesis develops an LC model to assess the upstream impacts of two main routes of LNG and NG imports to Europe from Nigeria and Algeria, based on primary data gathered from national oil and gas companies. Additionally, an analysis to assess the uncertainty in upstream GHG emissions is performed. Nigeria and Algeria together supply virtually the entire Portuguese NG mix (Galp Energia, 2012) and 18% of the NG imported to Europe in 2010 (IEA, 2011a). The uncertainty framework has direct applications in policy design to calculate the upstream emission of NG consumed in EU. This provides useful insights for decision-making within national or regional policy context, when the aim is to mitigate GHG emissions.

3- A novel approach is developed to study the cost-effectiveness of solar PV systems, according to local meteorology, estimated output (kWh/year) of PV systems, market, and financial incentives. Using this methodology, we investigate the key drivers to and status of cost-effectiveness of PV systems in Portugal, according to current national established Feed-In Tariff (FIT).

4- A robust and probabilistic optimization framework for the design and operation of DG in buildings is presented. A cost robust design is the one that gets less affected due to small perturbation in fuel input (NG and electricity) costs.

1.4 Structure of the thesis

This thesis is organized as following:

After this introduction, Chapter 2 presents a comprehensive literature review to demonstrate the contribution of this thesis.

Chapter 3 presents a detailed LCA of upstream stages of Natural Gas (NG) consumed in Portugal. The LC model to assess the upstream impacts of NG is presented, followed by deterministic LCIA results. Next, we include the uncertainty in GHG input parameters and a distribution function is obtained, representing upstream GHG emissions of 1 MJ (LHV) of NG consumed in Portugal. The implications of the selected time horizon on the results (GHG intensity) are also discussed.

Chapter 4 presents the results of LCA of selected DG, conventional energy sources and cooling systems for building sector in Portugal. Data from chapter 3 are used to calculate the upstream impacts of NG, which is the fuel used by cogeneration systems and boilers.

Chapter 5 presents the multi-objective mathematical programming model for the design and optimization of DG in Portugal. It also provides an overview of the policy framework to promote each type of DG, as well as the case-study for the implementation of the model. All these information are embedded in the model, for which the mathematical relations are described in this chapter.

Chapter 6 presents the selected results of the implementation of the model described in chapter 5 on the case-study building. The data from chapter 4, and the case-study data from chapter 5 are used as inputs to the model. The chapter starts with a detailed economic assessment of each individual cogeneration technology according to the policy framework in Portugal. Next, we present and discuss the Pareto frontiers

obtained to show the trade-offs between LCC vis-à-vis other objective functions, i.e. CED, GHG, Acidification, and Eutrophication.

Chapter 7 is devoted to assess the economics of PV system in continental Portugal. A methodology is presented to study the cost-effectiveness of solar PV systems, considering the received solar radiation and meteorology in different geographical locations across the country and the estimated output (kWh/year) of PV systems in those locations.

Chapter 8 deals with uncertainty in the fuel cost data and presents a probabilistic and robust modeling framework for DG. We discuss the application of the proposed framework by defining a number of scenarios and analyzing the model results.

Chapter 9 concludes the thesis with the main contributions of the research and points out a number of recommendations for future studies.

Chapter 2

Literature Review

The purpose of this doctoral thesis was stated in chapter 1. The primary aim of this chapter is to provide an overview of the relevant studies found in literature. This thesis brings together several tools, including Life-Cycle Assessment (LCA) and mathematical optimization, to build a modeling framework for design and operation of Distributed Generation (DG), namely solar and cogeneration technologies. Due to the multi-dimensionality of the topic, a great number of studies could be considered as relevant. In order to narrow down the scope of this chapter, the focus is on the studies that have assessed the application of DG for commercial—and a few residential—applications mainly from economic and environmental aspects. Section 2 provides an overall review of the typology of studies found on the topic of this thesis in literature and presents the studies of application of DG in commercial buildings. These studies are selected to be focused on economic aspects, but some overlaps with environmental studies are unavoidable. Based on these, we demonstrate the necessity to employ an optimization framework for selection and optimal operation of DG. Next, in section 3, mathematical optimization models developed for DG in building sector are discussed. The focus is on the type of model (linear, integer, non-linear), its objective function(s), and novelty of approach. Multi-objective models are also discussed, which without exception consider economic implications as one of the decision criteria. Uncertainty is another topic pointed out here. Finally, section 4 is devoted to relevant studies on environmental aspects, or more specifically studies that employ LCA methodologies to assess DG and Natural Gas (NG) upstream stages.

2.1 Studies on application of DG in buildings

Based on a survey of scientific journals in the last years (1999–2013), the studies on DG in buildings can be classified into three types. Some studies have analyzed technical aspects, such as thermodynamic properties of cogeneration systems, or the design criteria of cogeneration and PV systems. Some have focused on economic aspects, such as the effect of market condition including incentives on the feasibility of DG, or (optimization of) operation and investment planning. In recent years, an increasing number of studies have assessed the environmental aspects of DG, although the number of published studies on this topic is considerably lower compared to technical or economic studies. There are studies that address a combination of the above issues, so there are some overlaps and it is not possible to precisely classify the studies according to the above categorization. The main focus of this thesis and thus this literature review is economic and environmental aspects of DG. Nevertheless, we regard and underline the basic technical aspects of operation of the energy systems that is reported in literature.

A survey of the relevant publications in scientific journals shows that the largest part of these publications is still related to cogeneration. However, the number of research papers related to multi-generation concepts is lately increasing (Chicco & Mancarella, 2009). Several studies solely perform economic or technical feasibility assessments of DG, or study the effect of some variables (e.g. market conditions) on the design and operation of DG systems, and do not specifically develop optimization models. For instance, Xuan *et al.* (2006) examined the application of a gas-fuelled reciprocating Combined Heat and Power (CHP) in a commercial building in China. The CHP system under investigation uses an Absorption Chiller (AC) as the cooling system during warm months. In comparison to the conventional grid connected sources, CHP is capable of reducing primary energy consumption by 23% and CO_2 emission by 36%, with a payback period of 3.8 years. Wu and Rosen (1999) employed an energy equilibrium model to compare conventional and NG cogeneration-based district energy systems for heating, cooling and electrical services. The authors stated that employing cogeneration-based systems can provide potential commercial and environmental benefits and reduce the primary energy consumption, while the delay in implementing

such systems could be costly. Marantan *et al*. (2002) demonstrated the potential of tri-generation NG CHP application in commercial buildings. The study states that the high electricity consumption for cooling and heating purposes could be significantly reduced by using available heat from CHP systems such as micro-turbines and fuel cells. Gunes (2001), who studied the application of fuel cell-based Total Energy System (TES) for residential buildings, claimed that TES introduces 32 to 51 percent primary energy savings for conventional residential energy systems. The feasibility of using fuel cells in commercial buildings was also investigated by Ellis and Gunes (2002). This study found out that employing fuel cells was economically attractive if the initial costs could be reduced to the range of 1000–1500 €/kW_e (kW electricity). The research by Dentice d'Accadia *et al.* (2003) dealt with the application of a small scale fuel cell cogeneration (electrical power <15 kW) to light commercial application users. An energy-based analysis of a CHP system to evaluate its conjunction with domestic household appliances was performed. A test facility was designed and the optimal operation to match the user's thermal and electrical loads was identified. Fuel cell seemed to be promising on the technological aspect. It was also noted that the electricity and gas utilities played an important role for the diffusion of CHPs; with a high rate of gas connection it is more feasible to promote a market for decentralized cogeneration. Another study on fuel cells from Dorer *et al.* (2005) offered a methodology for assessing the performance of SOFC and Polymer Electrolyte Fuel Cells (PEFC), in terms of primary energy demand and CO_2 emissions. Using the building energy simulation software TRNSYS (1976), various configurations were established to analyze the performance of the system with respect to the defined evaluation criteria on a single-family and a multi-family house. The approach analyzes the interaction of the CHP systems with hot water storage, Solar Thermal (ST) collectors and the storage size. It was noted that compared to gas boiler systems, the fuel cell systems could achieve a reduction of 6–48% in non-renewable primary energy demand for all the considered building types and electricity mixes, while the results were strongly dependent on the grid electricity generation mix. Moreover, it was concluded that the primary energy savings decline for the cases with lower heat demand and also in the case of employment of ST collectors.

Some studies emphasize the role of market regulations and prices on the economic attractiveness of cogeneration systems. For instance Mone *et al*. (2001) investigated the underlying factors in economic feasibility of CHP systems using commercially available gas turbines. Waste heat from CHP system was used to satisfy both cooling and heating demand and the authors deduced that the amount of savings by installing a CHP is a function of the cost of NG and the avoided purchased electricity. Bhattacharyya & Quoc Thang (2004) stated that economic feasibility of medium and large scale cogeneration systems is vulnerable to changes in buy-back rate of electricity and investment costs. Andersen & Lund (2007) explored the regulatory tools for the introduction of CHP plants and renewables into the energy market. The authors stated that the introduction of CHP plants into the electricity market can help along the integration of fluctuating electricity generation for renewable energy and therefore strongly advocated further research using different approaches.

In industry, CHP is usually assumed to be heat led, meaning that it turns on when a heat load is present (COGEN Europe, 2004). Electricity is usually considered as a by-product of a Micro-CHP unit heat cogeneration (Harrison & Redford, 2001). Hawkes and Leach (2007) investigated the cost-effective operating strategies for three micro-CHP technologies: Stirling engines, gas engines, and SOFC. The cost of meeting a typical UK residential energy demand was calculated for heat led and electricity led operating strategies, and compared with that of an optimal strategy, i.e. the one that minimizes the cost of meeting the given electricity and heat demand profile subject to the technical constraints of the system. Using estimates of price parameters, and considering some thermal energy storage present in the system, it was shown that the least cost operating strategy for the three technologies was to follow heat *and* electricity load during winter months, rather than using either heat demand or electricity demand as the only dispatch signal. In summer months, the least cost operating strategy varied between technologies. The authors therefore put emphasis on the development of an optimization framework to evaluate the economic and environmental performance of CHPs in an accurate way.

In fact, several studies promote the development of optimization techniques for application of DG in building sector. This is endorsed since several aspects should be taken into account when dealing with the application of DG for buildings (Banos *et al.,*

2011; Chicco & Mancarella, 2009; Connolly *et al*., 2010; Lozano *et al.*, 2010; Rubio-Maya *et al.*, 2011). Firstly, these aspects comprise the characteristics of different types of DG systems, e.g. power to heat ratio of cogeneration systems, efficiency of solar systems according to the location, or the DG application type, e.g. peak shaving or stand-by. Secondly, the market conditions are at stake, such as the spot price of electricity and NG, and national regulations and incentives to employ and promote DG, according to region. Thirdly, the demand characteristics should be addressed, such as the level of different demand types and their volatility. These aspects should be taken into account for optimal operation of DG, regardless of the objective pursued by installation of DG that could be, e.g., reducing costs or certain type of environmental impacts, or increasing the efficiency of energy use. Therefore, there is an extensive use of operational research techniques applied to DG, specifically to cogeneration systems, including linear, integer, and non-linear models that are tackled using mathematical programming algorithms or meta-heuristic approaches such as evolutionary algorithms.

2.2 Optimization models for DG

Cho *et al.* (2009) developed a model to minimize the total cost of energy usage for a building based on energy efficiency constraints for each component: an Internal Combustion Engine (ICE), a gas boiler and the electricity from the grid. The linear programming algorithm provides the on/off signals to each component and results in overall minimum energy cost for the facility. The model was tested on a facility with measured heating and electricity load profile for two days in winter and summer and illustrated that the optimized operation of CHP provides economic gains compared to a baseline operation.

Monteiro *et al.* (2009) developed a model for planning micro-CHP plants in agreement with the Portuguese energy legal framework and also noticed that the price of electricity from the grid is an influential factor in the promotion of CHPs. According to EuroStat (2013) Portugal has the fourth highest electricity prices in the European Union and the authors cited this fact as a “favorable scenario for Micro-CHP generation”. The demand profiles of a number of commercial centers, hypermarkets,

public services and heated swimming pools were extracted and a simple linear model for techno-economic evaluation and optimization of CHP plants was developed. The model is able to design, evaluate and optimize from the techno-economic point of view a micro-CHP plant and it incorporates some databases, such as micro-cogeneration technologies and power consumption profiles.

Lozano *et al.* (2010) also highlighted the importance of considering legal constraints in the design and operation of DG. A Mixed Integer Linear Programming (MILP) optimization model for a tri-generation system with thermal storage was developed, taking into account the legal constraints for cogeneration facilities in Spain. The results showed that adopting different legal scenarios can significantly influence the optimal configuration for the CHP system.

Arcuri *et al*. (2007) put forward a combination of heat pumps, AC and cogeneration systems to delineate the optimal operation strategy of a tri-generation plant maximizing annual short- and long-term economic returns. The model is based on linear constraints, and gives out the optimal design and operational strategies of a tri-generation plant. The model results, for a case-study of a hospital in Athens, stated that a tri-generation plant in which heat pumps were directly fed by a cogenerator could provide economic, energy and environmental benefits. The study also pointed out the diversity of variables in play, such as national regulations, and the importance to regard them when the aim is to determine the optimal capacity and running conditions of CHP.

An equivalent annual cost minimization model was applied to determine the driving factors behind the investment in the technology of SOFC CHP systems for different sized residential and service applications (Hawkes & Leach, 2005a). The model consisted of a hypothetical SOFC system and the connection to grid with the possibility to export electricity. It was shown that under UK market conditions, households with small to average energy demands do not benefit from installation of SOFC, but larger energy demands do benefit under such conditions. A sensitivity analysis showed that the results were sensitive to capital cost, energy import/export prices, plant life-time, and the temporal precision selected for the study (Hawkes & Leach, 2005b).

Mavrotas *et al.* (2008) discussed an optimization framework for energy supply systems in commercial buildings by taking into account the demand uncertainty. The

technologies studied were a CHP, AC and Compression Chiller (CC). The underlying uncertainty in demand was transformed into an objective function, so the model became a multi-objective linear model where the minimization of cost and the maximization of demand satisfaction were the objective functions. A Pareto-optimal front was derived to represent solutions to the problem under uncertainty. A minmax regret approach was finally employed to determine the preferred solutions.

Osman *et al*. (2008) conducted a research combining LCA, energy simulation, and MILP techniques to optimize the cost and the environmental impacts of meeting the energy demand (heating, cooling and electrical) in commercial buildings. Three NG driven CHP technologies [Micro-Turbines (MT), Internal Combustion Engines (ICE), Solid Oxide Fuel Cell (SOFC)] were considered as input to a mathematical model to minimize costs, Green Warming Potential (GWP) and Tropospheric Ozone Precursor (TOP). The study includes detailed operational strategies according to different optimization objectives (costs, GWP, TOP) and the results were depicted on Pareto frontiers. ICE and MT cogeneration systems could result in the reduction of up to 38% in GWP compared to conventional systems and a reduction of up to 94% in TOP was achievable by employing SOFC and MT.

The literature review shows that considerably less studies assess the combination of CHP with renewables (multi DG), although Interesting perspectives are emerging from such integration (Anderson & Lund, 2008). Ren & Gao (2010) developed a single-objective MILP model for the integrated plan and evaluation of DG systems. Given the site's energy loads, local climate data, and utility tariff structure, the model minimizes the overall costs of selection and operation of energy systems for a nominal year. The DG studied included Micro-turbines, gas turbines, fuel cells, PV and wind included. Based on the inputs to the model (building information: load profiles, climate conditions; technical information: power and thermal efficiencies of energy systems; economic information), the model provides the optimal design and operational levels of the energy systems. The operating CO_2 emissions (in the form of carbon tax rate) and efficiency performance of the DG system were also taken into account (as a set of constraints). The results found to be particularly sensitive to the scale of energy demand, gas and electricity price, as well as carbon tax rate. This study also illustrated that employing DG might result in adverse environmental impacts, if not combined

suitably with heat recovery units. The model was developed to a multi-objective model in (Ren *et al.,* 2010), minimizing energy costs and operating CO_2 emissions. A Pareto frontier was obtained and concluded that least CO_2 emitting technologies were also the most costly ones. Moreover, the value of buy-back rate of electricity had more effect on the results when more weight was given to the economic objective function while the carbon tax had marginal equal influence on the results regardless of the weights given to objective functions.

Rubio-Maya *et al.* (2011) proposed a systematic optimization procedure to select and size a cogeneration plant fuelled by NG, evacuated tube solar collectors, and gasified biomass. An MILP model was developed and applied to a Spanish tourist resort. The model has one objective function (minimizing net present value) and considers energy savings and Greenhouse Gas (GHG) emission reduction as constraints. The results show that higher economic profitability was achieved with NG-based technologies, namely ICE systems. Higher energy savings and reduced GHG emissions were also possible through the gradual penetration of renewable energy sources into the energy systems. The study also performed a comparison between heat, electricity, and heat and electricity load following strategies for cogeneration systems and concluded that best economic results were obtained upon following both heat and electricity, then following heat and the worst case was obtained by following only electricity loads.

Some studies take into account the uncertainty in the input parameters for the optimal design and operation of DG. Among the techniques to address uncertainty, robust optimization is a more recent approach (Bertsimas *et al*., 2010), in which the DM seeks a certain level of robustness against uncertainty that is present in input parameters. In robust optimization, uncertainty is considered explicitly ex-ante, contrarily to sensitivity analysis, which is typically applied as a post-optimization tool for computing the change in the objective function for perturbations in the inputs (Mulvey *et al*., 1995). The optimal solution is called “solution robust” if it remains close to the optimal one when uncertain parameters alter. Likewise, it is termed “model robust” if it stays feasible in face of small changes in the input data. Only one study was found that applied robust optimization techniques to a case of DG: Rezvan *et al*. (2012) developed an MILP robust optimization model to determine the optimum capacity of DG for

buildings in the case of demand uncertainty. One type of cogeneration technology (ICE), along with AC, boiler and solar PV systems were modelled as energy systems. The optimization was carried out on three related criteria: economical, primary energy saving, and environmental performance as a multi-objective optimization. Two types of parameters were defined: penalty for shortage of supply, and degrees of robustness, where the trade-off between optimality and feasibility could be determined by adjusting the level of these parameters. The proposed method was applied to a hospital complex and concluded that by demanding model robustness, the capacities of CHP and AC increase to avoid the risk of shortage of supply, while the capacities of renewable sources decrease.

As Chicco & Mancarella (2009) noted, a thorough energy and environmental assessments of DG incorporating renewables calls for a suitable modeling framework. In particular, the chief energy and environmental burdens of fossil-fuelled energy systems relate to their operation (Hayhoe *et al.* , 2002; Pehnt, 2008; Riva *et al*, 2006; Safaei *et al.,* 2012; Venkatesh *et al;* 2011). Conversely, the operation of renewable-based systems is virtually emission-free and the energy requirements and environmental burdens fall within the energy system construction and decommissioning (García-Valverde *et al*., 2009; Kaldellis *et al*, 2009; Safaei *et al.,* 2012; Voorspools *et al*, 2000). These aspects can be suitably addressed by means of cradle-to-grave LCA techniques (Chicco & Mancarella, 2009). However, the review of literature reveals the lack of sufficient research in this area (Osman *et al*., 2008), as we explore in the next section.

2.3 LCA studies

LCA is a cradle-to-grave methodology to assess the environmental impacts associated with a product throughout its life (ISO 14040, 2006). An LCA study basically consists of four steps (ISO 14040, 2006). First, the goal and scope definition describes the product system under analysis, including system boundaries and main data sources, and functional unit: a reference unit to which all the inputs and outputs are related. The second step of an LCA, LC Inventory analysis (LCI), involves data collection, identification and quantification of relevant inputs and outputs to/from the system. A

flow chart model is normally built, based on the system boundaries, which quantifies the relevant flow of energy, material and emissions to/from the system. The data must be related to the functional unit defined in the goal and scope. The third step is the Life-Cycle Impact Assessment (LCIA) that aims at calculating impacts based on the inventory analysis. For this purpose, an LCIA method is selected and the environmental impacts are categorized and aggregated into impact categories. Finally, through the fourth step, interpretation, the recommendations and conclusions of the LCA are framed based on the findings from LCI and LCIA.

There is an increasing recognition that any rigorous and meaningful comparison of energy supply options must be done using LC approaches (Lund & Biswass, 2008). However, the number, and the scope of relevant studies on this topic are limited. Most studies assess solely CO_2 emissions from operation level, neglecting the whole LC and other types of environmental impacts. Moreover, no study was found to develop an LC optimization framework for building energy systems combining both renewable and fossil fuels. In this section, we review the relevant environmental studies.

Canova *et al.* (2008) characterized the CO and NO_x emissions from gas fuelled MT and ICE by using the emission balance approach. The environmental impact of CHP was viewed through local and global emissions balance models and discussed that while cogeneration systems were advocated to be efficient in terms of energy saving and thus of CO_2 emission saving, this may not be the same in the case of local emissions of CO, NO_x and other non-GHG pollutants. The study made a one-to-one comparison of the environmental impacts of ICE and MT CHP systems and showed that neither has absolute dominance over the other with regard to overall environmental impacts. Moreover, the emission factors in the literature that refers to full-load operation of MT should be considered with care if the machines were planned to operate also at part-load. The necessity to adopt further tools, specifically LCA, to analyze the more complex energy scenarios in case of mass adoption of decentralized energy systems, was also underlined.

Pehnt (2008) assessed GHG and Acidification potential of Micro CHP (less than 5 kW) for residential sector in Germany. The CHP technologies analyzed were ICE reciprocating engines, Stirling engines, and SOFC. Using the avoided burden approach to credit for the heat cogenerated with electricity, authors concluded that nearly all

micro cogeneration systems were superior in terms of reduction of GHG emissions, not only to average electricity and heat supply in Germany, but also to separate production of electricity in modern gas power plants and heat in advanced condensing boilers. However, examining the GHG reduction potential at the level of a supply object or case-study (e.g. a multi-family house), the mitigation potential was lower since micro cogeneration systems could not typically supply the whole energy demand, implying that the additional impacts of electricity from the grid and heat from a peak boiler had to be taken into consideration. For this reason, the study recognizes and motivates the role of optimization in DG planning, to not oversize the systems, and to ensure that the full amount of heat is actually used by the building. Pehnt (2008) also found the Acidification emissions of small reciprocating engines to be higher than those in state-of-the-art centralized gas power plants, due to more efficient emission control in the latter.

Another study (Strachan & Farrell, 2006) characterized the emissions (CO_2, SO_2, NO_x, PM_{10}) from distributed versus centralized generation and highlighted the importance of analyzing heat/power demands for potential host sites and more specifically to do so on a seasonal basis to give a better understanding of how to match-up energy demands with technology output. Most importantly, as far as research to date has been concerned with developing emission estimates of CHP plants, the impacts of location and ambient conditions on the results have been mostly ignored and this requires more in depth LCA studies (Strachan & Farrell, 2006).

NG is considered as the main fuel for cogeneration systems (IEA, 2011). On top of the emissions from combustion, the production of NG also has environmental impacts, their magnitude depending on the source of NG, its type (conventional vs. unconventional) and its state of delivery, in the form of Liquefied NG (LNG) or gas. New reports from oil and gas industries (EPA, 2011) have measured more methane release from the upstream production of conventional gas fields and the IEA world energy outlook (IEA, 2011b) warns that an increased share of NG in the world energy mix alone will *not* put us on a carbon emissions reduction path to diminish global warming. In a similar way, Kavalov *et al* (2009) found that LNG chains imported to Europe tend to be more energy and GHG intensive than the supply chain for pipeline

gas, because of the extra life-cycle stages (liquefaction, gasification) involved and higher burden of transportation.

A number of studies (Arteconi *et al.*, 2010; Okamura & Furukawa & Ishitani, 2007; Tamura *et al.,* 2001; Venkatesh *et al.*, 2010) have addressed the LC environmental impacts of NG and LNG supply chains for Europe, Japan and US. Firstly, all these are limited to assess GHG, and no other impact is considered. Secondly, the NG in Portugal comes from Nigeria and Algeria (IEA 2011a, Galp Energia, 2012) and has a different mix from the European average NG mix (which has imports from Russia and Norway among other countries). We did not find any journal article to assess the upstream emissions of Portuguese import gas, or individually assess the upstream emissions of Nigerian and Algerian produced gas. At the same time, applying the upstream emissions of European NG chain provides misleading results regarding the impact of DG systems in Portugal, as some authors have pointed out the limits of applying "generic" LCA data to assessing changes in "unique" environments (Horne *et al*. 2009). To summarize, a proper assessment of DG in Portugal calls for an LC framework that is specifically modeled for Portugal, one that regards geographical differences and incorporate the upstream emission of the imported NG. NG is regarded as a transitional fuel between incumbent fossil fuels (coal and diesel) and renewables and its consumption is expected to grow nationally and globally. Calculating the upstream emissions of NG therefore provides useful insights for decision-making within policy frameworks by estimating the "embedded" upstream emission of NG consumed in EU and Portugal.

GHG emissions due to the combustion of NG can be assessed, as long as the composition of NG under study is known (API, 2009). On the other hand, uncertainty in NG upstream emissions is rather high (Schori & Frischknecht, 2012). The only study (Venkatesh *et al*., 2011) that assessed the GHG uncertainty of LNG consumed in US found a 19% range from the mean value for 1MJ of NG imported in the form of LNG to US. The uncertainty of upstream GHG emissions of NG produced in US was just slightly lower (17% from mean value). The authors therefore recommend performing LC emission studies of NG that are based on probabilistic modeling methods (in addition to conventional deterministic approaches). The ISO standards on LCA (ISO 14044, 2006) also states "whenever feasible, uncertainty analysis should be performed to

better explain and support the (LCA study) conclusions". This thesis develops an LC model to address the uncertainty in GHG emissions of NG imported from Nigeria and Algeria to Portugal.

A number of studies have assessed the LCA of solar system, although the main focus of research has been on GHG emissions. García-Valverde *et al*. (2009) performed a CO_2 assessment of a 4.2 kW_p (kW peak) mono-crystalline PV system. The analysis demonstrated that the biggest energy requirements and emissions are in the construction phase of PV modules and storage system (batteries). The system was compared to other supply options (Spanish grid and diesel generator) and showed lower emissions, possessing an energy payback time of 9.08 years and CO_2 emissions of 131 g/kWh. Kaldellis *et al*. (2009) studied the energy requirement of standalone PV-lead acid battery systems and discussed that in standalone systems battery plays a more important role, constituting 27% of the system LC energy requirements. According to the application results obtained, the size of the optimal energy autonomous PV+battery configurations were significantly affected by the local solar potential. From this aspect, Portugal boasts a favorable climatic situation. According to Suri *et al.* (2007), who studied the potential of solar electricity generation in the European Union, Portugal and the Mediterranean region have the highest potential for solar electricity, mounting over 1200 kWh/kWp per year. This amount is achievable by the solar panels situated at the optimal angle. Moreover, the difference between regions in solar electricity generation can fluctuate up to 16% within Portugal. Chapter 7 of this thesis is devoted to assess the economics of PV system in continental Portugal, considering the received solar radiation and meteorology in different geographical locations across the country.

Using process based LCA approaches, the performance of multi-crystalline and thin film PV technologies was characterized on the basis of three indicators: Net Energy Ratio (NER), Energy Payback Time (EPBT) and CO_2 emissions (Pacca *et al.* 2007). Based on a case study using US energy fuel mix, the NER and EPBT of the multi-crystalline modules were estimated as 2.7 and 7.4 years, respectively, with LC CO_2 emissions of 72.4 g of CO_2/kWh_e (kWh electricity). In fact, reviewing the LCA studies performed for PV technologies reveals a rather noticeable discrepancy among the results. Bhat and

Prakash (2009) and Pearce (2002) believe such inconsistency would be expected of complete LCA studies. This is because different studies use different methods, set up different boundary conditions, depend on different data sources and inventory methods, model different PV technologies at different locations, and even regard different life-times and analytical periods. This once again underlines the importance of an LCA study to accurately assess the environmental impacts of PV systems in Portugal, according to local meteorology and solar radiation.

2.4 Summary and conclusions

1- The review of literature reveals that some studies have assessed the feasibility of DG from the efficiency and economic perspectives; by using techniques other than optimization (Xuan *et al.*, 2006; Wu and Rosen, 1999; Marantan *et al*., 2002; Gunes, 2001; Dentice d'Accadia *et al,* 2003; Dorer *et al.*, 2005; Bhattacharyya & Quoc Thang, 2004; Mone *et al*., 2001; Hawkes & Leach, 2007). We discussed that due to the diversity of variables in play, namely efficiency parameters of different types of DG, demand magnitude and pattern, and market conditions, there is a considerable scope for employing optimization techniques. Among optimization models developed for DG, mostly consider only cogeneration systems (no other DG types), and the focus is mainly on economic aspects (Arcuri *et al*., 2007; Cho *et al.,* 2009; Hawkes & Leach, 2005a & 2005b; Mavrotas *et al.*, 2008; Monteiro *et al.,* 2009; Rezvan *et al*., 2012). Relatively few studies also incorporate environmental aspects (Osman *et al*., 2008; Ren & Gao, 2010a & 2010b; Rubio-Maya *et al.,* 2011; Rezvan *et al*., 2012).

2- Among studies that incorporate environmental aspects into the analysis (Osman *et al*., 2008; Ren & Gao, 2010a & 2010b; Rezvan *et al*, 2012; Rubio-Maya *et al.,* 2011), only one study (Osman *et al.*, 2008) explicitly performs an LCA, and the others are limited to assess the average CO_2 or GHG emissions of DG operation. The same conclusions stand for the study that has assessed multi-DG for the building sector, i.e. Rezvan *et al*. (2012).

3- Most models developed for DG applications in buildings use MILP models. This is partly due to the flexibility offered by using binary variables in formulating problems involving fixed (or setup) costs (Williams, 2013).

4- The findings by (Arcuri *et al*., 2007; Bhattacharyya & Quoc Thang, 2004; Lozano *et al.*, 2010; Mone *et al*., 2001; Monteiro *et al.,* 2009) highlight the importance of considering national regulatory frameworks in the design and operation of DG, including the effects of parameters such as buy-back rate on the results.

5- Some studies (Hawkes and Leach, 2007; Rubio-Maya *et al.*, 2011) have assessed the performance of cogeneration systems when operating in different load following modes, i.e. electricity following, heat following or both. The least cost operating strategy was shown to vary between technologies and the case-study. The development of an optimization framework for cogeneration system is therefore advocated.

6- Robust optimization techniques have not been extensively applied to DG modelling. The only robust model developed (Rezvan *et al.,* 2011) considers uncertainty in demand and no robust modelling has been developed for other uncertain coefficients, such as cost or environmental impacts.

The review of LCA studies performed for DG led to following conclusions:

1- When dealing with DG renewable sources, an analysis framework is required for a thorough energy and environmental assessment (Chicco & Mancarella, 2009). In particular, the energy and environmental burden of conventional generation is mainly laid in its operation, while the environmental burden of renewables is by large due to plant building and decommissioning. These aspects can be adequately addressed by means of cradle-to-grave LCA techniques (Alsema *et al*., 2009; Chicco & Mancarella, 2009; Horne *et al*, 2009).

2- Analyzing upstream processes to produce fuels, and their associated emissions, is important; otherwise, the emissions resulting from electricity generation of the various cogeneration options are underestimated. For NG technology options, upstream GHG emission rates can be up to 25% of the direct emissions from the energy system (Weisser, 2007). The robust design of any policy to mitigate environmental impacts by replacing incumbent fuels with NG therefore requires a proper assessment of upstream emissions of fuels (Howarth *et al.*, 2011 & 2012; Hayhoe *et al*., 2002; Venkatesh *et al*., 2011). No study was found to explicitly consider upstream emissions of NG as the main fuel to DG, while the implications of upstream stages of NG and LNG chains to their total GHG footprint have been recently questioned (Cathles *et al.*, 2012; O'Sullivan & Paltsev, 2012; Skone *et al.*, 2011; Stephenson *et al.*, 2011; Venkatesh *et al* , 2011).

3- A number of studies have assessed the environmental impacts of NG chains for different geographical locations, including for Europe (Arteconi *et al*., 2010; Cathles *et al*., 2011 & 2012; Howarth *et al.*, 2011 & 2012; Okamura *et al.*, 2007; O'Sullivan & Paltsev, 2012; Skone *et al*., 2011; Stephenson *et al.*, 2011; Tamura *et al*., 2001; Venkatesh *et al*., 2010). Portuguese NG supply is different from the European average mix, with possibly higher upstream emissions due to the high share from LNG chain. No LCA study was found to assess the upstream emissions of gas production from Nigeria and Algeria, which together represent the entire Portuguese NG mix and 18% of NG consumed in Europe. On top of the impacts due to liquefaction and transportation of LNG, relatively high production impacts of Nigerian NG have been acknowledged (Anomohanran, 2012).

4- The results of LCA of DG are dependent on the location: the emissions per output from solar systems depend on total energy produced by the system that depends on the location of installation. Cogeneration systems are also connected to NG transmission network, its upstream emissions depending on the supply mix. We established that Portuguese NG network system is detached from the European system and the average upstream emissions from Europe are not representative for

Portugal. Some authors point out the limits of applying "generic" data to assessing changes in "unique" environments (Horne *et al*. 2009). A proper assessment of potential of DG in Portugal therefore asks for an LC study framed specifically for the Portuguese case. This also helps policy designers to reduce the impacts of building sector by knowing the type and magnitude of emissions of DG, both renewable and NG fuelled, in Portugal.

5- Performing LCA on a level of case-study or supply objects (e.g. commercial buildings) provides significant methodological advantages (Pehnt, 2008). By explicitly calculating the different flows of energy between different objects of supply and demand, such framework helps to calculate the "actual" impacts from operation of DG, rather than assuming a constant average load of operation for the system. Moreover, by taking into account the demand side, it is possible to ensure that full amount of heat is actually used, or alternatively, calculate for the level of waste.

This doctoral thesis develops an optimization framework for the operation of DG in Portugal, taking into account both economic and environmental aspects. Four types of environmental impacts are assessed: Cumulative Energy Demand (CED), Greenhouse Gases (GHG), Acidification, and Eutrophication. As advocated by literature and justified in this chapter, cradle-to-grave LCA is the suitable technique employed to assess the environmental impacts of DG. The LCA model calculates the total impact arising from meeting the building energy demand, including the emissions due to production and decommissioning of energy systems. The model presents a detailed LCA of upstream emissions of NG, supplied from Algeria and Nigeria, to calculate the accurate emissions of DG in Portugal. A methodological framework is also developed to capture the uncertainty in upstream GHG emissions of NG, to increase the model robustness and provide insight for policy making.

The results of LCA are used as the input to a multi-objective mathematical optimization model developed for the design and operation of DG in commercial buildings. Two types of solar systems (ST and PV) and three types of cogeneration technologies (MT, ICE, SOFC) comprise the DG that are coupled with conventional energy systems (boiler

and grid) to meet the building energy demand. ACs are coupled with CHP systems while the extra cooling load can be sourced by CC. The possibility of selling on-site produced electricity to the grid in the context of the legal framework of Portugal as well as dynamic pricing of electricity at peak and off-peak hours are also taken into account. The results of the model are tested on a case-study of a hotel complex to illustrate its application. Finally, a cost and demand robust optimization model is developed to deal with demand and cost uncertainty for optimal energy planning of DG.

Chapter 3

Life-cycle Assessment of Natural Gas Consumed in Portugal*

The motivation and relevant studies to this thesis have been presented in chapters 1 and 2. This chapter presents a Life-Cycle Assessment (LCA) of upstream stages to produce and transport the Natural Gas (NG) consumed in Portugal. The chapter is organized as following: section 3.1 provides a background of the NG sector in Portugal and highlights its importance as a fuel in the country energy mix. Section 3.2 discusses the Life-Cycle (LC) stages of NG and the main sources and types of emissions for each stage. Section 3.3 comprises the LC model (including goal and scope) and LC Inventory analysis (LCI). Section 3.4 presents the deterministic LC Impact Assessment (LCIA) results for four impact categories: Cumulative Energy Demand (CED), Greenhouse Gases (GHG), Acidification, and Eutrophication. Section 3.5 calculates the upstream emissions of Portuguese NG mix based on the shares of supply sources. Section 3.6 provides the background and discusses the results of uncertainty analysis of upstream GHG emissions of NG. Finally section 3.7 summarizes the findings and presents the concluding remarks.

3.1 Natural gas in Portugal

NG was introduced in Portugal in 1997. Since then, the demand for NG has solidly increased, except a temporary drop from 2005 to 2006[1]. NG is mainly used for electricity generation (63%), in industry (23%), and commercial and residential sectors (14%) (IEA, 2011a). It is expected that consumption of NG in Portugal continues to

* This chapter is based on two journal articles:
- Safaei, A & Freire, F & Antunes, C (2014a)
- Safaei, A & Freire, F & Antunes, C (2014b)

[1] This was due to reduced demand in the electricity sector as a result of increased production of hydro electricity in 2006.

grow in the mid-term, mainly in industrial, services and residential sectors, and in long-term in electricity generation sector (IEA, 2011a). Since Portugal has no significant proven reserves of NG, it relies on imports to meet its domestic gas demand. In 2012, 55% of the NG was supplied from Nigeria in the form of Liquefied Natural Gas (LNG), and 32% from Algeria (as NG) and the remaining 13% from other sources of NG (mainly Trinidad and Tobago) in the form of LNG (Galp Energia, 2012).

In order to cover the demand for NG in Portugal, Galp Energia has a contract for annual purchase of 2.3 Billion Cubic Meters (bcm) of NG with Sonatrach, an Algerian state-owned company, and three others with Nigeria LNG Ltd, for the purchase of annual 3.5 bcm of LNG (roughly 4.42 bcm NG). NG from Algeria is transported through the Euro-Maghreb Pipeline system to the main NG entry point in Campo Maior, located on the eastern border of Portugal (Figure 3.1), while LNG is transported (via LNG tankers) to the Sines LNG terminal (IEA, 2011a). In Sines terminal, LNG is offloaded and pumped into temporary storage tanks, where it remains until it is gasified prior to delivery into the national gas transmission network along with the Algerian gas. NG distribution network in Portugal has a total length of 1098 km (IEA, 2011a).

Figure 3.1: Euro Maghreb Pipeline Distance and location (Galp Energia, 2012)

3.2 Life-cycle of natural gas

The LC of NG has the following main stages: exploration, extraction, processing (treatment), transportation, storage, distribution and application (utilization). LNG, on top of above, has two more stages: liquefaction of NG and gasification of LNG. Figure 3.2 shows an overview of stages to produce and transport NG, including the LNG route. In this section, we provide a brief description of each stage, focusing on main sources of emissions.

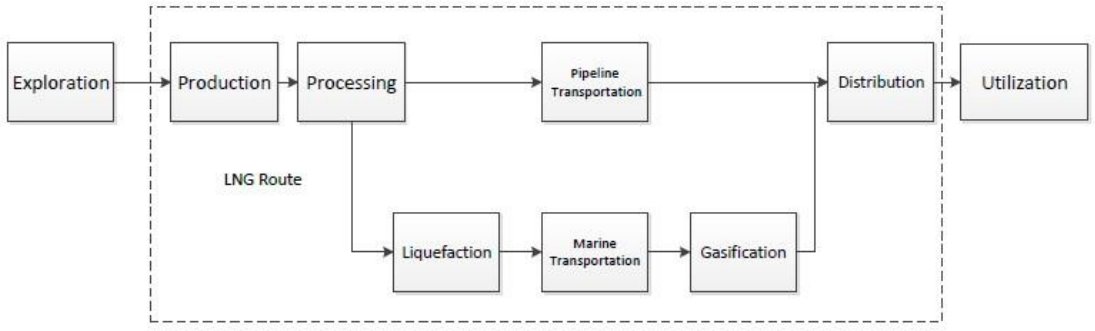

Figure 3.2: LC stages of NG and LNG

The LC of NG starts with the exploration: in the search for NG (and oil) reservoirs, the subsoil is analyzed using geophysical methods. Upon discovery of a gas reservoir, exploration and development wells are drilled (Sevenster & Croezen, 2006). The next stage is the extraction of NG, for which the details of equipments and methods are very site- and technology-specific and depend on several aspects, e.g. if NG is associated with oil or not. The energy needed to extract the (oil and) NG is typically met by burning the onsite produced gas, called lease fuel. On top of the emission from combustion, the extraction of NG is often accompanied by flaring and venting (API, 2009; Schori & Frischknecht, 2012). Flaring refers to deliberate burning of NG that is associated with crude oil and NG production, while venting is the direct (deliberate or not) release of NG to the environment (API, 2009; Buzcu-Guven *et al.*, 2010). Venting and flaring are common practices whenever NG cannot be safely recovered (OGP, 2000). They also occur during well preparations and completions, when the wellhead has not yet been fitted, and when it is not financially preferable to recover the associated NG from an oil well (Buzcu-Guven *et al.*, 2010; EPA, 2011). Extracted NG gives a mixture of raw gas, condensed higher hydrocarbons, free water and carried

along particles (Sevenster & Croezen, 2006; Schori & Frischknecht, 2012). Therefore, it has to be processed (purified) to meet the characteristics of the NG used by consumers. The NG is transported from the extraction sites to processing plants through a system of low-diameter, low-pressure pipeline, called gathering pipelines (API, 2009). There, a number of processes (including vapor absorption, removal of acid gases (CO_2), sulphurous compounds, Nitrogen and heavy hydrocarbons) are performed to give-out a "sweet" NG, ready for pipeline transmissions (Jaramillo *et al.*, 2007). The energy consumed during processing is related to the quality of the gas extracted, i.e. how "sweet" it is (API, 2009).

After being processed, the NG enters the transportation system. Gas should be compressed before entering the pipeline and the pressure loss during the transmission is compensated by intermediate stations. The combustion emission from the station compressors and leakage along transmission comprise the emission sources of pipeline transportation (EPA, 2011). The last stage to deliver the NG to the consumers is distribution. Normally NG is transported from delivery points along the distribution system to local consumers by low-pressure, small-diameter pipeline systems. The sources of emission and energy requirements are similar to pipeline transportation (Schori & Frischknecht, 2012).

In Portugal, in 2012, 60% of the NG supply was in the form of LNG (Galp Energia, 2012). LNG has three further LC stages: liquefaction, marine transportation and gasification. Liquefaction consists of cooling down the NG below its condensation temperature (–162°C) and then pressurizing it convert to liquid form, therefore reducing its volume (Jaramillo *et al.*, 2007). The liquefaction plants are generally located in coastal areas of LNG exporting countries. Emissions are discharged when NG is consumed (as a fuel) to run gas turbines that are sources of power at liquefaction plants as well as venting and flaring. The long-distance transportation of LNG takes place by using LNG carriers. Emissions arise from the combustion of fuel (normally heavy fuel oil) for propulsion system as well as LNG Boil-Off Gas (BOG). BOG refers to the fraction of LNG that is vaporized during transportation due to its cryogenic nature (Faruque Hasan *et al.*, 2009). The current LNG carriers recover the BOG and use it as a fuel along with heavy fuel oil (Arteconi *et al.,* 2010; Faruque Hasan *et al.*, 2009; NETL, 2005). In addition to

BOG, a small amount of LNG (typically ~5%) called heel is retained inside LNG tanks to maintain their low carrying temperature during the voyage back (Faruque Hasan *et al.*, 2009). Before entering the distribution system to reach the final consumers, LNG should pass through gasification, which involves increasing the LNG temperature to return it to gaseous fuel (Schori & Frischknecht, 2012).

3.3 Life-cycle model and inventory

3.3.1 Goal and scope

The importance of natural gas as a low carbon fuel in Portugal was stressed in section 3.1. This LCA aims to assess the upstream impacts of the Portuguese NG mix for four impact categories: Cumulative Energy Demand (CED), Greenhouse Gas emissions (GHG), Acidification, and Eutrophication. GHG emissions are of particular interest due to their influence on climate change and policy planning for implementation of the Portuguese National Program for Climate Change—PNAC (RCM, 2010). A high level of uncertainty was observed for upstream NG GHG emission. ISO 14044 (2006) recommends "whenever feasible, uncertainty analysis should be performed to better explain and support the LCA conclusions". Thus, a probabilistic LC model was additionally developed to assess the underlying uncertainty in upstream GHG emissions of NG mix.

The impact categories were selected from the CML 2001 method (Guinee *et al.* 2002), a problem-oriented LCIA method developed by the Institute of Environmental Sciences of the University of Leiden (CML). Tables 3.1–3.3 display the substances analyzed and their characterization factors for each type of impact category.

Previous studies (Skone *et al.*, 2011; Venkatesh *et al*., 2011) revealed high level of uncertainty in GHG emissions of NG supply chains. Estimating this uncertainty provides useful insights for policy design by calculating the "embedded" upstream emission of Portuguese NG mix. An assessment was performed to address two types of uncertainty in upstream GHG emissions of NG mix of Portugal: parameter uncertainty, concerning uncertainty affecting the LCI parameters; and scenario analysis, related to choice of

time horizon to calculate the GHG intensity. We used the values from IPCC Fourth Assessment Report (2007) to model the GHG characterization factors of methane and Nitrous Oxide for 500-, 100-, and 20-year time horizons (Table 3.4).

Table 3.1: GHG characterization factors (IPCC, 2007)

	Chemical formulation	100-year time horizon (CO_2 eq)
Carbon Dioxide	**CO_2**	1
Methane	**CH_4**	25
Nitrous Oxide	**N_2O**	298

-

Table 3.2: Acidification potential characterization factors (Guinee *et al.* 2002)

	Chemical formulation	Acidification potential
Ammonia	**NH_3**	1.60
Nitrogen oxides	**NO_x**	0.50
Sulfur dioxide	**SO_2**	1.20

-

Table 3.3: Eutrophication potential characterization factors (Guinee *et al.* 2002)

	Chemical formulation	Eutrophication potential
Ammonia	**NH_3**	0.35
Nitrate	**NO_3-**	0.10
Nitrogen oxides	**NO_x**	0.13
Phosphate	**PO_4^{3-}**	1.00
Phosphorus	**P**	3.06

Table 3.4: GHG characterization factor of gases (IPCC, 2007)

	Chemical formulation	500-year time horizon (CO_2 eq)	100-year time horizon (CO_2 eq)	20-year time horizon (CO_2 eq)
Carbon Dioxide	**CO_2**	1	1	1
Methane	**CH_4**	7.6	25	72
Nitrous Oxide	**N_2O**	153	298	289

We chose the year 2010 as the base year of our study. NG consumed in Portugal is imported from Algeria and Nigeria gas (and less amount, 13%, from other countries). This study performs a detailed LCA for each of the two suppliers of NG, i.e. Algeria and Nigeria. For the latter, the model includes the production of NG (in Nigeria), its liquefaction, marine transportation, and gasification. Primary data from Nigerian oil and gas industry (NNPC, 2011) were collected and used to build the LCI. For Algerian

gas, the model includes its production in Algeria in Sonatrach Complex, processing, and pipeline transportation of 1600 km (out of which 45 km is under oceanic pipeline) to Portugal. Primary data from Algerian gas companies were more difficult to obtain; therefore, data were taken from Schori & Frischknecht (2012) to calculate the emissions. The quantity of NG imported from other supply sources (e.g. Trinidad and Tobago) to Portugal is subject to demand conditions and in some years this quantity has been nearly zero (IEA, 2011a). The Portuguese NG mix is therefore determined based on the average share of supply between Algeria and Nigeria in 2010 (Galp Energia, 2012): 3.42 bcm (60%) from Nigeria, and 2.30 bcm (40%) from Algeria. The functional unit of the study is 1 MJ Lower Heating Value (LHV) of Portuguese NG mix. The impact of NG distribution in Portugal is added up to obtain the total upstream impacts of the NG consumed in Portugal.

3.3.2 Life-cycle inventory

3.3.2.1 LCI of Nigerian LNG to Portugal

NG production in Nigeria is associated with oil production. According to NNPC (2013), in 2012, 852 Million barrels of oil and 2580 Billion Standard Cubic Feet (69 billion m^3) of NG were produced. Table 3.5 shows the representative composition on a mass basis of Nigerian raw NG and the pipeline quality NG in Portugal derived from Nigerian LNG. Calculation of GHG emissions presented in this section are based on the gas composition values in Table 3.5, using a mass balance approach, as explained in the Appendix A of this thesis.

Table 3.5: **Raw Nigerian NG and pipeline quality NG from Nigerian LNG: composition on a mass basis**

Component	Raw Natural Gas % mass	Source	Pipeline NG % mass **	Source
CH_4	88	ARI & ICF (2008)*	92.1	REN(2008)
CO_2	1.8		0	
N_2	1.7	API (2009)	<1	
C_2H_6	6.3		4.8	
C_3H_8	2.1		2.1	
C_{3+}	0	n.a.	<1	
***** Data specific for natural gas from Nigeria ****** at LNG terminal in Portugal; LHV = 39.05 MJ/Nm^3				

The first stage of NG LC is its production. The number of wells drilled (to meet the NG demand by Portugal) was estimated by dividing the volume of NG from Nigeria, i.e. 4.42 bcm (Galp Energia, 2012), by the expected average production per well. Estimates of representative Nigerian gas wells production, depth (3050 m) and drilling time (50 days/well) were provided by ARI & ICF (2008). The emission from drilling was calculated considering that a 1500 hp (1100 kW) diesel engine is operating on full-load for 50 days to drill the wells. The energy input requirement (J) and emission factor (per unit fuel input) of the diesel engine was taken from API (2009).

NNPC (2013) reported that, in 2012, 23% (16.46 billion m^3) of NG produced in Nigeria was flared. One way to calculate the impact of flaring on NG GHG intensity is to allocate flaring emissions between the total annual produced crude oil and utilized gas based on their total energy content (calculated based on the lower heating value). In this way, the impact of flaring allocated to NG, considering a 98% flaring efficiency, is calculated as 6.9, 4.4, and 4.5 g CO_2 eq/MJ (100-year time horizon) for years 2010, 2011, and 2012, respectively. However, such approach fails to distinguish between different types of oil and gas fields. This is particularly important since fields with access to gas export likely flare less quantity of NG (Buzcu-Guven *et al.*, 2010). In this way, LNG producers might be burdened with comparably higher flaring emissions by other producers. A way to tackle this is to look only at the fields that their gas was exported for LNG (LNG fields). Therefore, the system boundary addresses the gas fields used for LNG production. The data regarding the flaring emissions of the LNG fields in Nigeria (NNPC, 2013) were gathered. Emissions due to flaring of NG in LNG fields were calculated and allocated between oil and gas production fields (based on their total heating value).

There is a limited set of conflicting data regarding the venting emissions from Nigerian oil and gas production. Schori & Frischknecht (2012), based on a previous LCI report (Jungbluth, 2007), estimated that 0.018 m^3 of NG is vented per unit volume (m^3) NG produced in Nigeria. This alone contributes to 8.5 g CO_2 eq/MJ (100-year time horizon). Kavalov et al (2009) used this value to calculate the GHG intensity of Nigerian NG production as 15 g CO_2 eq/MJ. On the other extreme, a recent publication by the World Bank (Cervigni *et al.* ,2013) assumed no venting practice as a result of NG and oil

activities in Nigeria. Taking into account that the proportion of flaring was considerably less in LNG fields and its quantity has reduced over the years, we assumed that the same applies for venting emissions. In the absence of other reliable LCI, we abided by the zero venting scenario by Cervigni *et al.* (2013) to calculate mean GHG emissions of LNG production in Nigeria. The implications of adopting a higher venting rate are further discussed in section 3.6.

The amount of fuel to extract the NG (lease fuel) was also taken from Schori & Frischknecht (2012). Finally, the energy requirement and emission resulting from transportation of produced gas to the processing facility was accounted for through an average 80 km of unprotected steel gathering pipeline system, based on the emission factors from API (2009).

The energy required for, and the emissions resulting from, processing the NG are highly dependent on the quality of the extracted (raw) gas, and are therefore site-specific. For this reason, we used the values from ARI & ICF (2008) that have estimated the processing emissions for the Nigerian NG.

The liquefaction process consists in cooling down the NG below its condensation temperature and then pressurizing it to convert to liquid form. The emission from NG liquefaction can vary considerably based on the technology used to liquefy NG (Lim *et al*., 2013; Pillarella *et al.*, 2007). Sevenster et al. (2007) estimate that the average existing liquefaction plants have a GHG intensity of 11.4 g CO_2 eq/MJ (100-year time horizon), similar to the values reported by Schori & Frischknecht (2012) for Nigeria and the estimation of Kavalov *et al.* (2009). However, they have used the LCI for vintage liquefaction plants, while modern liquefaction plans are considerably more efficient (Lim *et al*., 2013; Pillarella *et al.*, 2007; Sevenster *et al.*, 2007). NG Liquefaction plants in Nigeria were commissioned in the year 2000, using the Air Products and Chemicals International (APCI) propane pre-cooled, mixed refrigerant (APCI-C3/MR) liquefaction process (Eni-Saipem, 2010). A benchmark of the GHG intensity of LNG plants (Woodside, 2011) recognized Nigeria as one of the most efficient liquefaction projects globally. The estimate by Woodside *et al.* (2011), 11% self-energy consumption, was considered to represent the intensity of Nigerian NG liquefaction, and it also matches

the estimation of Edwards et al. (2014) for liquefaction intensity of average LNG consumed in Europe.

Regarding LNG transportation, a mid-range BOG of 0.125% per day, and a heel of 5% (Faruque Hasan *et al.*, 2009) was assumed to calculate the trips necessary and the corresponding emission from LNG transportation. A total loading and unloading time of 2.5 days per roundtrip and a diesel consumption of 35 tonnes diesel/day in port (Barnett, 2010) was modeled. The main LNG receiver port in Portugal is located in Sines (ERSE, 2011). Table 3.7 summarizes the distance, LNG carrier capacity, travel time, and the fuel and BOG consumption rate. Finally, the energy requirement and emissions resulting from gasification of LNG were taken from Schori & Frischknecht (2012). Tables 3.8, 3.9 and 3.10 summarize the Well-to-Tank (WtT) LCI data of Nigerian LNG supplied to Portugal.

Table 3.6: Emission factor of heavy fuel oil and BOG LNG

Emission Factor **Unit**	**Diesel (Heavy Fuel Oil)**[a] ***(kg/tonne)***	**LNG BOG**[b] ***(kg/tonne)***
CO_2	3151	2176
CH_4	0.02	15.23
N_2O	0.16	0.12

[a] From Danish Maritime Authority (2012)

[b] From Tamura *et al.* (2001)

Table 3.7: LNG shipping distance, trip duration and fuel consumption assumptions

Shipping distance (from Nigeria-Port Harcourt to Portugal-Sines) (km)	6165[a]
LNG tanker capacity (m^3 LNG)	135,000
Speed (Nautical Miles)[b]	19.5
Days per round trip (excluding the days at port)	14.5
Fuel Oil Consumption (t/day)	165
Port turnaround time (days)	2.5
Fuel Consumption in Port* (t/day)	35
LNG BOG consumption (%/day)	0.125
Heel (%)	5
One-way trips necessary to transport the contracted LNG from Nigeria	45
[a] Calculated from http://www.searates.com/reference/portdistance/ [b] Man Diesel (2012).	

Table 3.8: WtT GHG LCI of Nigerian LNG consumed in Portugal (g/MJ)

	g/MJ	Drilling	Venting	Flaring	Lease Fuel	Gathering pipelines	Total Production	Processing	Liquefaction	LNG Transportation	Gasification
Carbon Dioxide	CO_2	3×10^{-2}	0	1.49	1.85	1.07×10^{-4}	3.40	1.67	5.85	2.73	1.60
Methane	CH_4	1.60×10^{-6}	0	6.80×10^{-3}	6.98×10^{-6}	1.17×10^{-5}	2×10^{-5}	3.69×10^{-2}	1×10^{-2}	1.46×10^{-4}	0
Nitrous Oxide	N_2O	2.67×10^{-7}	0	2.7×10^{-10}	6.78×10^{-4}	0	0.0006	2.80×10^{-5}	0	1.35×10^{-5}	0

Table 3.9: WtT Acidification and Eutrophication emissions of Nigerian LNG consumed in Portugal (g/MJ)

g/MJ		Production	Processing	Liquefaction	LNG Transportation	Gasification
Ammonia	NH_3	0	4.74×10^{-6}	9.97×10^{-6}	0	8.19×10^{-6}
Nitrate	NO_3-	1.08×10^{-4}	5.13×10^{-5}	1.10×10^{-4}	1.28×10^{-4}	9.38×10^{-5}
Nitrogen oxides	No_x	2.10×10^{-2}	7.27×10^{-4}	4.55×10^{-3}	9.77×10^{-3}	3.92×10^{-3}
Phosphate	PO_4^{3-}	3.99×10^{-4}	2.04×10^{-4}	4.35×10^{-4}	4.22×10^{-4}	3.73×10^{-4}
Phosphorus	P	0	1.20×10^{-7}	1.67×10^{-6}	0	0
Sulfur dioxide	SO_2	6.10×10^{-4}	2.53×10^{-4}	6.42×10^{-4}	5.42×10^{-4}	4.41×10^{-4}

Table 3.10: WtT energy requirements of Nigerian LNG (MJ/MJ)

MJ/MJ	Production	Processing	Liquefaction	LNG transportation	Gasification
CED	0.06	0.09	0.11	0.051	0.019

3.3.2.2 LCI of Algerian natural gas to Portugal

NG import from Algeria to Portugal has the following Well-to-Tank (WtT) stages: production in Algeria in Sonatrach Complex, processing, and pipeline transportation. NG in Algeria is produced from gas fields, i.e. it is not associated with oil production. The estimated lease fuel to extract the NG is 5.37×10^{-3} m^3 NG per m^3 NG produced, and the flaring and venting rates were assumed to be 0.27% and 1.8% of the total production, accordingly (Schori & Frischknecht, 2012). Venting and flaring emissions factors were calculated based on the NG composition in Table 3.11. Algerian gas is "sweet"; therefore it does not require a high amount of energy for processing. NG goes through dehydration to remove its water content. The pipeline distance between the producing gas company in Algeria (Sonatrach) and the receiving point in Portugal (Campo Maior) is 1613 km, out of which 45 km is offshore (Galp Energia, 2012). A mid-value of 1.9% gas use in compression stations according to (Schori & Frischknecht, 2012) was considered. For fugitive emissions, a loss of 0.02% of NG in pipeline, and 0.006% losses per 1000 km transported NG from compression station were assessed. Tables 3.12 to 3.14 show the LCI of WtT stages of Algerian NG to Portugal.

Table 3.11: Raw Algerian NG and its pipeline quality: composition on a mass basis

Component	**Algerian Raw Natural Gas**	**Source**	**Pipeline Natural gas***	**Source**
	% mass		**% mass**	
CH_4	72.6	Schori & Frischknecht (2012)	87.88	REN(2008)
CO_2	2.4		1.26	
N2	15		1.09	
C_2H_6	5		8.05	
C_3H_8	0		1.37	
C_{3+}	5		<0.05	
***LHV = 38.3 MJ/Nm^3**				

Table 3.12: WtT GHG emissions of Algerian NG consumed in Portugal (g/MJ)

		Drilling and Lease Fuel	Venting	Flaring	Transportation – others	Total Production	Processing	Pipeline Transportation
Carbon Dioxide	**CO_2**	3.84×10^{-1}	4.90×10^{-3}	1.35×1^{-1}	1.06×10^{-4}	5.24×10^{-1}	5.57×10^{-1}	1.51
Methane	**CH_4**	1.28×1^{-5}	1.50×10^{-1}	1.39×10^{-5}	5.34×10^{-6}	1.50×10^{-1}	7.57×10^{-4}	6.90×10^{-3}
Nitrous Oxide	**N_2O**	5.58×10^{-5}	0	6.70×10^{-4}	1.17×10^{-5}	7.38×10^{-4}	5.24×10^{-6}	2.67×10^{-5}

Table 3.13: Acidification and Eutrophication emissions of Algerian NG consumed in Portugal (g/MJ)

		Production	processing	Pipeline Transportation
Ammonia	**NH_3**	4.52×10^{-6}	4.74×10^{-6}	1.22×10^{-6}
Nitrate	**NO_3-**	2.79×10^{-5}	5.13×10^{-5}	3.09×10^{-6}
Nitrogen oxides	**No_x**	4.54×10^{-3}	7.26×10^{-4}	6.95×10^{-4}
Phosphate	**PO_4^{3-}**	1.01×10^{-4}	2.03×10^{-4}	1.25×10^{-4}
Phosphorus	**P**	3.17×10^{-6}	1.19×10^{-7}	8.73×10^{-7}
Sulfur dioxide	**SO_2**	4.07×10^{-4}	2.53×10^{-4}	2.47×10^{-4}

Table 3.14: WtT energy requirements of Algerian NG consumed in Portugal (MJ/MJ)

MJ/MJ	Production	Processing	Pipeline Transportation
CED	2.24×10^{-2}	9.81×10^{-3}	2.86×10^{-2}

3.3.3 Distribution

Distribution is the last upstream phase of NG before consumption. Gasified LNG from Nigeria together with Algerian NG are fed into national grid at corresponding receiving points and transferred through pipelines to reach the consumers. It was assumed that 0.17 % of the distributed NG and 2.6 Wh/m^3 of electricity were used to preheat the gas (Schori & Frischknecht, 2012). This energy includes the energy consumption in high, low and very low pressure pipelines. NG losses due to transport and distribution, including pipeline losses, are reported annually by UNdata (2013). Figure 3.3 displays the total annual import, consumption and losses in Portugal from 2000 to 2010. Venting and fugitive losses were calculated as a percentage of total annual consumption, with a high of 2% for the year 2000 and a low of almost zero for 2009. The losses have decreased in the most recent years, 2009 and 2010. We assumed a value of 0.1% (similar to year 2010) for the venting of NG from the transportation and distribution of NG in Portugal, to account for the recent reductions. This mounts to 5 140 000 m^3 (200 717 000 MJ) of vented NG. The emission factor for venting was calculated based on the NG composition in Table 3.5. Total emissions from the distribution, including energy use and venting emissions in Portugal were calculated per MJ and shown in Tables 3.15 and 3.16.

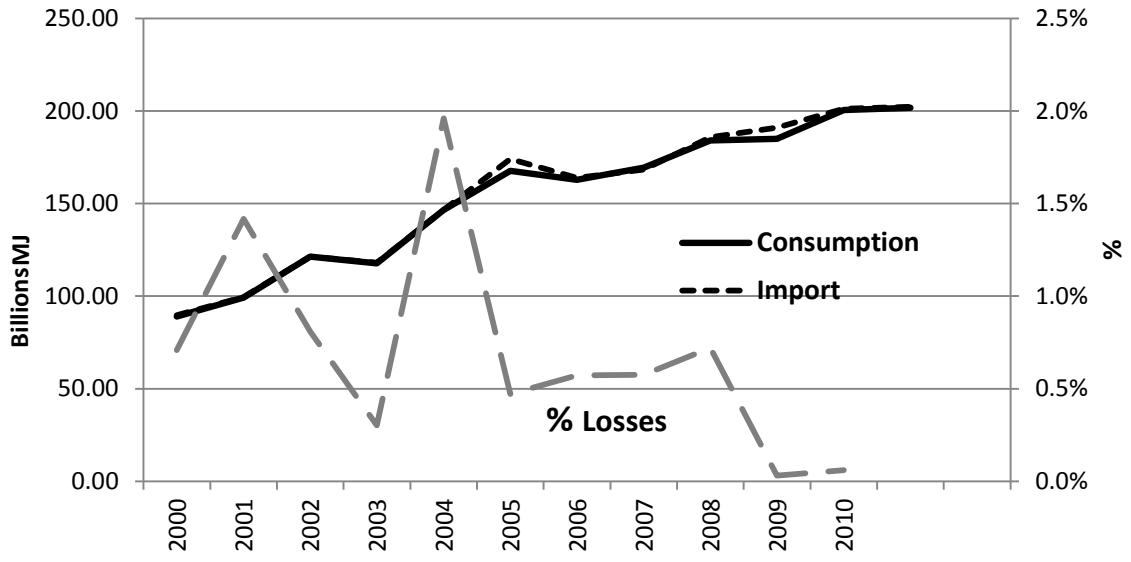

Figure 3.3: NG - Annual losses during distribution as a percentage of consumption in Portugal

Table 3.15: LCI of Distribution of NG in Portugal (g/MJ)

		g/MJ
Ammonia	**NH_3**	2.29×10^{-8}
Carbon dioxide	**CO_2**	1.34×10^{-2}
Nitrous Oxide	**N_2O**	1.44×10^{-7}
Methane	**CH_4**	1.70×10^{-3}
Nitrate	**NO_3-**	7.14×10^{-7}
Nitrogen oxides	**No_x**	1.02×10^{-5}
Phosphate	**PO_4^{3-}**	2.50×10^{-6}
Phosphorus	**P**	1.61×10^{-9}
Sulfur dioxide	**SO_2**	8.05×10^{-6}

Table 3.16: CED - Distribution of NG in Portugal (MJ/MJ)

	MJ/MJ
CED	2.55×10^{-4}

3.4 Life-cycle impact assessment

3.4.1 CED

Nigeria

The total upstream CED to deliver one MJ (LHV) of Nigerian LNG is calculated as roughly 0.253 MJ/MJ, as shown in Figure 3.4. The stage with highest amount of energy requirements is NG liquefaction that contributes to 40% (0.11 MJ/MJ) of the Nigerian NG upstream energy requirements. Next stands the production of NG, with a total CED of 0.0.06 MJ/MJ. The production sub-stages with more energy requirements (destruction) are lease fuel (50%) and flaring of NG (40%). Processing and gasification are the stages with lowest CED. CED of upstream stages of NG is mainly in the form of NG (85%) and Diesel (15%).

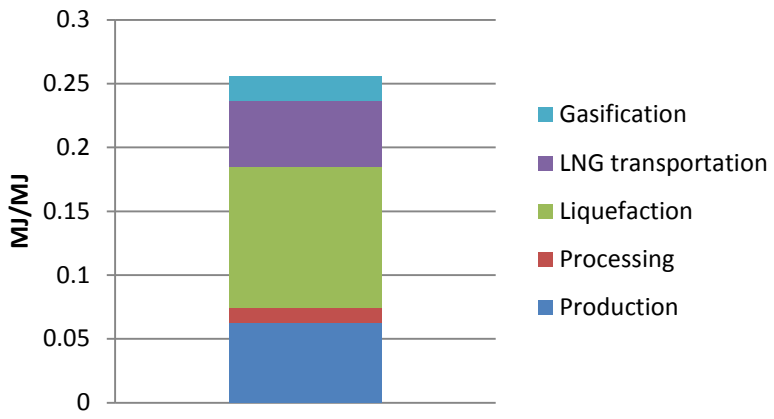

Figure 3.4: CED—Upstream stages of Nigerian LNG (MJ/MJ)

Algeria

The CED of upstream stages of Algerian gas is shown in Figure 3.5. The production and transportation of NG constitute 82% of the total upstream CED of Algerian gas (i.e. 0.065 MJ/MJ) and the remaining 18% (0.02 MJ/MJ) is from processing. Pipeline transportation of NG has slightly more CED than its production. For all these processes, the energy requirement is mainly (80%) in the form of NG and rest from diesel. The CED of production of NG (0.025 MJ/MJ) is due to lease fuel and well-drilling (49%), transportation necessary for production of NG (27%), flaring (17%), and infrastructure (7%).

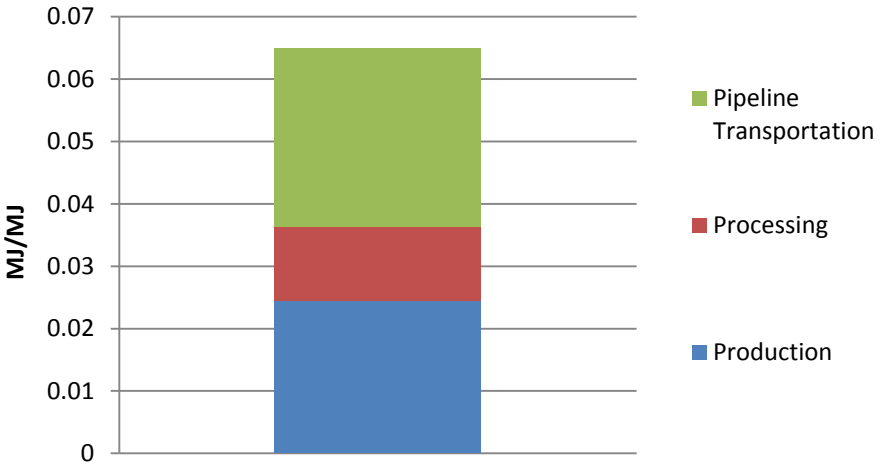

Figure 3.5: CED—Upstream stages of Algerian NG (MJ/MJ)

3.4.2 GHG

Nigeria

Our analysis shows the mean upstream intensity of LNG is 16.65 g CO_2 eq/MJ out of which 37% (6.2 g CO_2 eq/MJ) is from the liquefaction stage of NG (Figure 3.6). Production of NG in Nigeria is the next stage with highest emission (3.8 g CO_2 eq/MJ). These two stages together comprise more than 40% of the total upstream GHG intensity. Processing and transportation of NG show relatively less emissions (around 2.8 CO_2 eq/MJ, respectively) and gasification emission is almost negligible (1.2 g CO_2 eq/MJ). Figure 3.6 displays a breakdown of estimated WtT GHG emissions of the Nigerian LNG.

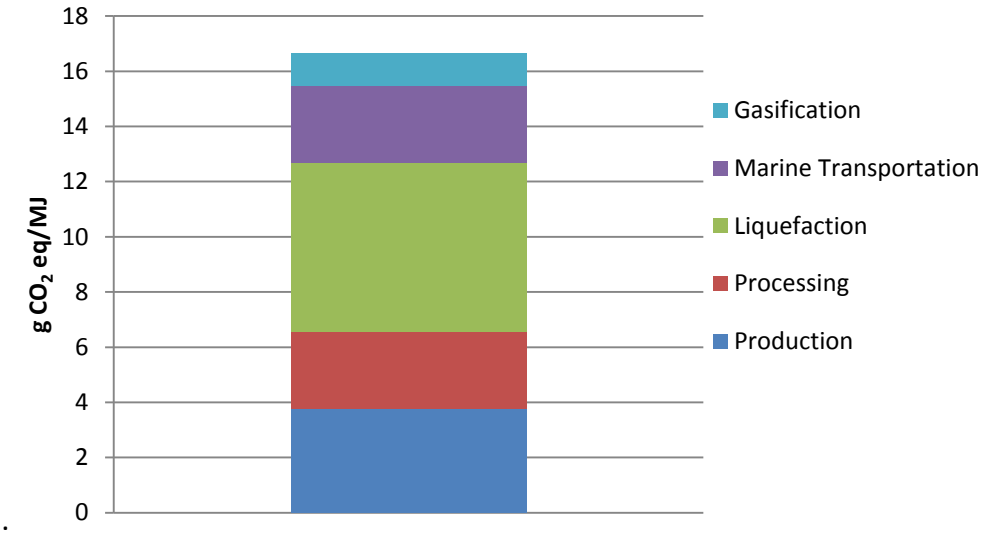

Figure 3.6: GHG emissions—upstream stages of Nigerian LNG (100-year time horizon)

An analysis of the emissions from the production stage of LNG is shown in Figure 3.7. Lease fuel combustion to extract the NG and flaring make up most of the production emissions. Figure 3.7 shows that the emissions from well drilling and transportation of raw NG to processing facility were negligible. The production emission was calculated considering no venting practice as a result of oil and NG extraction in LNG fields.

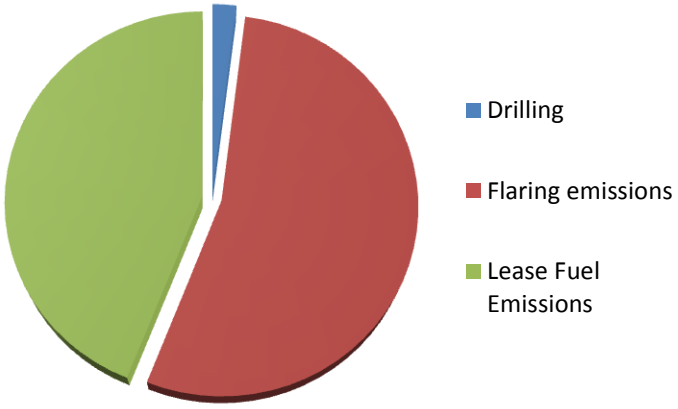

Figure 3.7: Nigerian LNG GHG: Production breakdown based on LC stage

For both processing and liquefaction, emissions are mainly discharged by combusting the NG to meet the energy requirement of these processes. The energy needed for liquefaction is significantly higher than processing and therefore the emissions.. Gasification of LNG represents the stage with the least GHG emissions (0.99 g CO_2 eq/MJ).

Algeria

Figure 3.8 shows the estimated GHG intensity of Algerian NG (6.79 g CO_2 eq/MJ), out of which more than half (4.86 g CO_2 eq/MJ) comes from the production stage of NG. Intensity of pipeline transportation is calculated as 1.70 g CO_2 eq/MJ; mainly (90%) from the energy required to maintain the gas pressure through the pipelines, and the rest (10%) from venting and fugitive emissions.

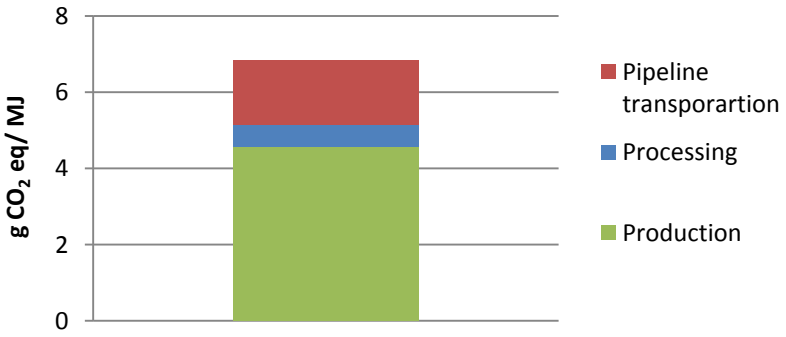

Figure 3.8: GHG emissions—production of NG in Algeria (100-year time horizon)

An analysis of the emission from Algerian gas production shows that GHG emissions are mainly (84%) due to NG venting, which releases methane (Figure 3.9). Emissions from well drilling and lease fuel combustion, and flaring constitute 9% and 7% of the total GHG emission from production, respectively.

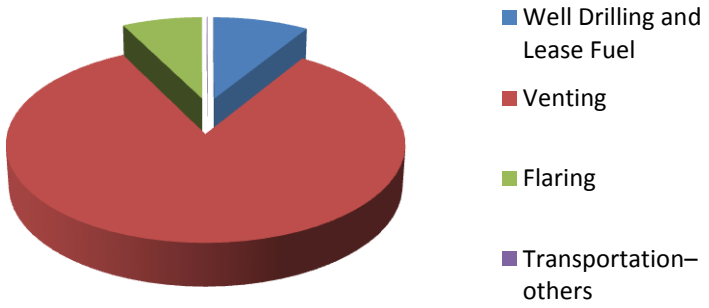

Figure 3.9: Algerian NG GHG emissions: Production breakdown based on LC stage

3.4.3 Acidification

Nigeria

Acidification impact to produce and transport Nigerian LNG is estimated as 2×10^{-2} g SO_2 eq/MJ, from which almost half is from the production stage of NG, followed by transportation, liquefaction and gasification. The impact of processing is negligible compared to other stages.

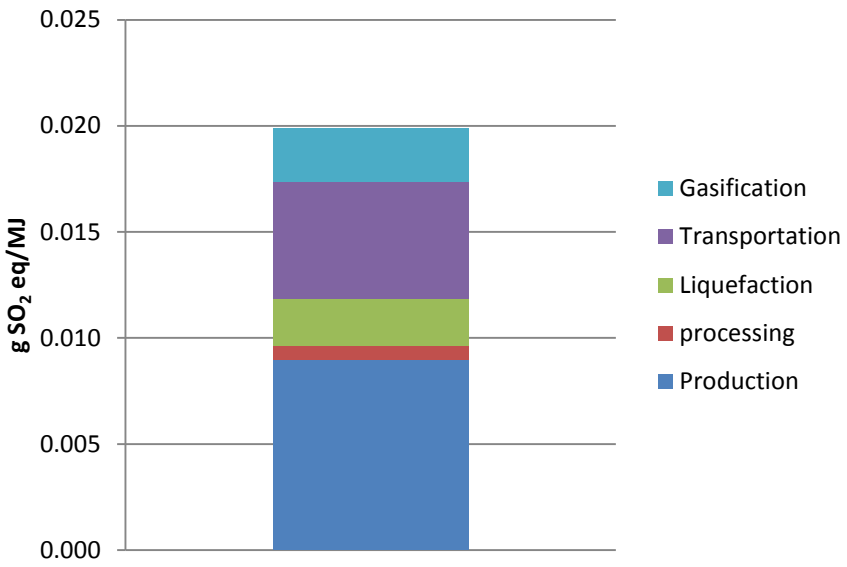

Figure 3.10: Acidification potential—upstream stages of Nigerian LNG

Among the processes to produce Nigerian NG, flaring is the main source of Acidification emissions, due to release of nitrogen oxides. Emissions from lease fuel (NG) and well drilling (diesel) also contribute to the production emissions as shown in Figure 3.11. NO_x dominates (97% of total) the Acidification emissions from production of Nigerian NG.

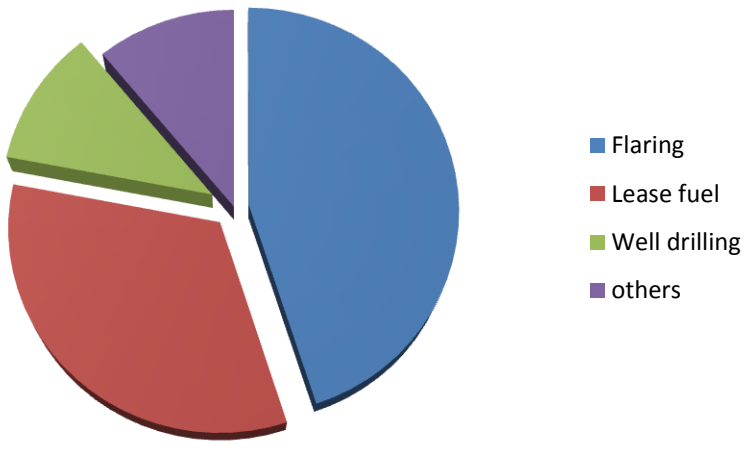

Figure 3.11: Nigerian LNG Acidification: Production breakdown based on LC stage

Acidification emissions are discharged when combusting the NG required for processing and liquefaction stages. Equal shares (74% and 26%) of their impact come from NO_x and SO_2, respectively.

Acidification potential of LNG transportation is caused by the electricity needed in the boarding and unloading ports, and the emissions from burning the heavy fuel oil for propulsion (5.5×10^{-3} g SO_2 eq/MJ) of LNG tanker. For gasification, combustion of NG to meet the energy required for gasification, and infrastructure construction constitute 74% and 26% of total Acidification impact, respectively. The main Acidification emissions of gasification, by order of contribution, are NO_x and SO_2.

Algeria

The Acidification impact of WtT stages of Algerian NG imported to Portugal via pipeline is shown in Figure 3.12. Similarly, NG production is the main contributor to NG LC impact (4.1×10^{-3} g SO_2 eq/MJ), followed by processing and pipeline transportation. The impact of Algerian NG is, however, considerably lower than its Nigerian counterpart, due to lower production and transportation emissions, and less LC stages than the LNG chain.

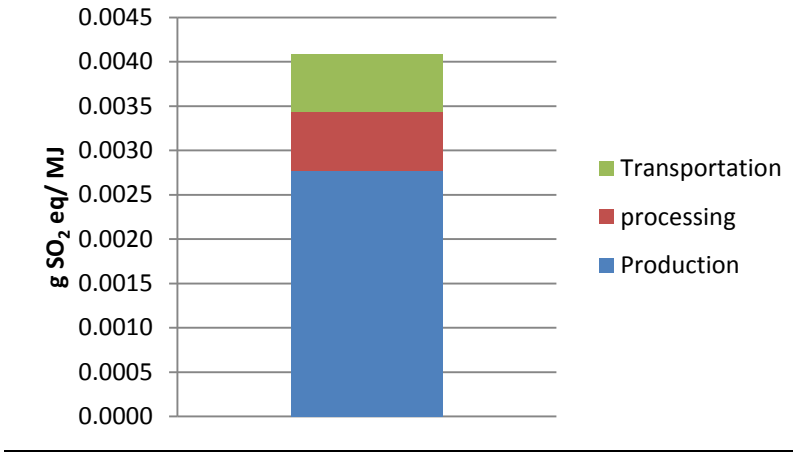

Figure 3.12: Acidification potential—production of NG in Algeria

Since NG flaring (per m^3 produced NG) is considerably lower in Algeria than Nigeria, the resulting Acidification impact is also lower. Twenty percent of impact comes from discharging NO_x from flare stack. Diesel lorry transportation necessary for the upstream activities to produce NG causes 43% of the total production impact—

emitting equal shares of SO_2 and NO_x. Well drilling contributes to the rest (37%) of Algerian NG production Acidification impact.

The Acidification impact from processing is equal to that of Nigerian chain. Pipeline transportation impact is estimated as 6.46×10^{-4} g SO_2 eq/ MJ, most (85%) of which is from combustion of NG in compressor stations to facilitate its transportation. Production of pipeline infrastructure constitutes the remaining impact. The main acidification emissions are NO_x (92%) and SO_2 and the share of ammonia is negligible.

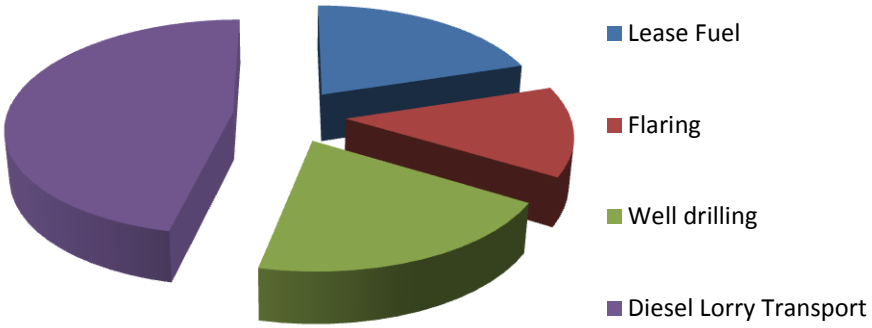

Figure 3.13: Algerian NG Acidification potential—Production breakdown based on LC stage

3.4.4 Eutrophication

Nigeria

The estimated Eutrophication impact of WtT stages to produce and transport Nigerian LNG to Portugal is shown in Figure 3.14. Production of NG contributes significantly to Eutrophication impact, followed by marine transportation, liquefaction, gasification and processing.

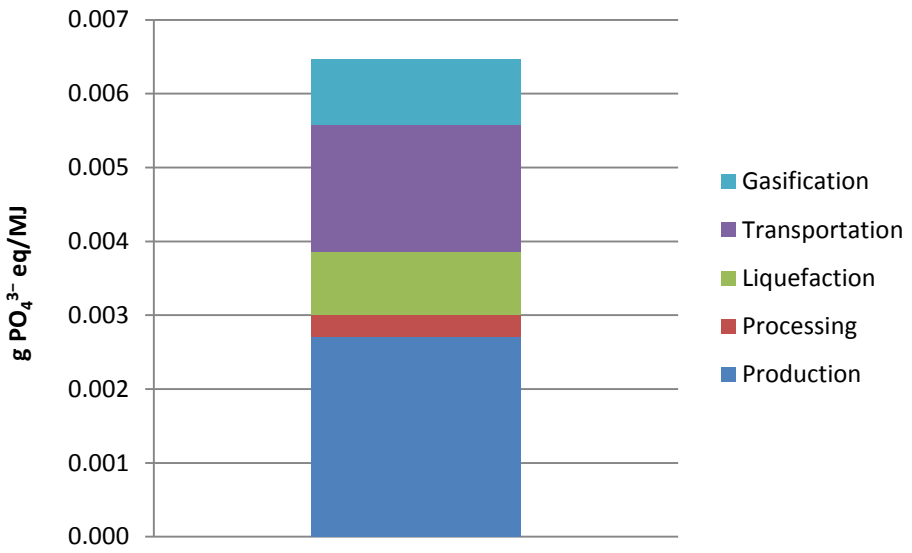

Figure 3.14: Eutrophication potential—upstream stages of Nigerian LNG

Figure 3.15 demonstrates that flaring of NG and lease fuel combustion with well drilling contribute to the major proportion of Nigerian production Eutrophication impact. No_x is the main contributor to the production Eutrophication impact.

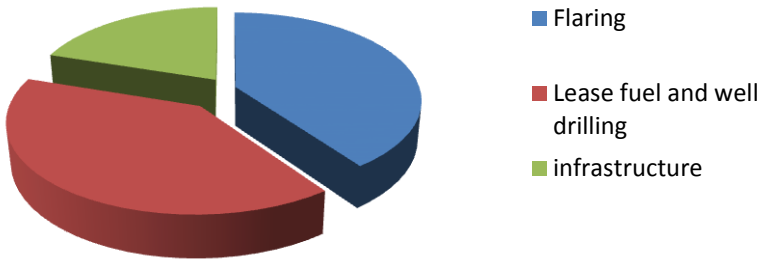

Figure 3.15: Nigerian LNG Eutrophication: Production breakdown based on LC stage

The Eutrophication impact of processing (3.05×10^{-4} g PO_4^{3-} eq/MJ) is due to infrastructure (74%), and NG and electricity needed for processing (26%). For liquefaction, 57% of Eutrophication emissions (1.05×10^{-3} g PO_4^{3-} eq/MJ) are discharged from combustion of NG required to meet the energy for liquefaction. The rest of impacts come from infrastructure construction. 86% of liquefaction emissions are in the form of nitrogen oxides and the rest phosphates. Finally, LNG gasification Eutrophication impact (8.94×10^{-4} g PO_4^{3-} eq/MJ) is due to combustion of NG to meet

the energy, and the infrastructure related to gasify LNG. Emissions of NO_x, phosphate, nitrate and ammonia contribute to Eutrophication impact of gasification.

Algeria

Eutrophication impact of WtT stages of Algerian NG to Portugal is displayed in Figure 3.16. Production is the stage with highest impacts caused by the upstream transportation activities (41%), lease fuel emissions and well drilling (32%), flaring (12%), and construction of infrastructure and disposal (Figure 3.17). From total (1.23×10^{-3} g PO_4^{3-} eq/MJ) Eutrophication impact of Algerian NG production, 65% is from discharging nitrogen oxides, 29% from phosphate and the rest from nitrate and ammonia.

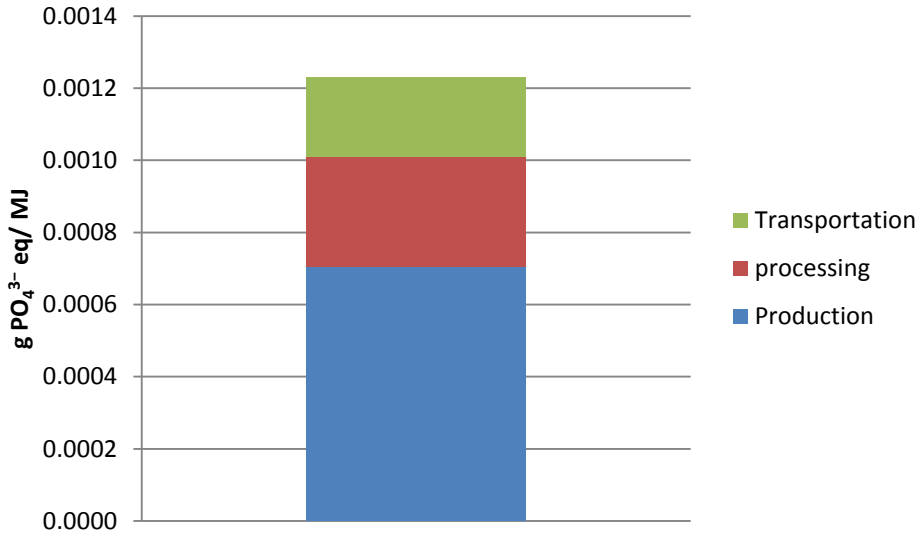

Figure 3.16: Eutrophication potential—upstream stages of Algerian NG

The Eutrophication impact of processing is the same as the Nigerian case, as explained earlier. For pipeline transportation, the combustion of NG to meet the energy required is responsible for 79% of the total emissions and the pipeline infrastructure for the remaining value. Emissions are in the form of NO_x (83%), phosphate (15%), and negligible amounts of phosphorus and ammonia.

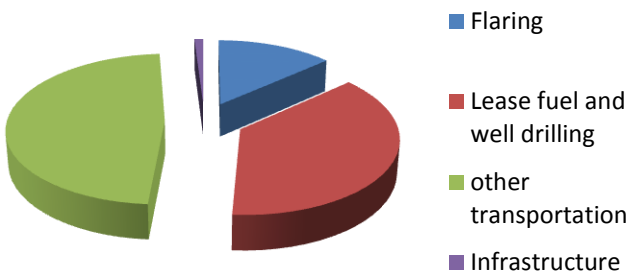

Figure 3.17: Algerian NG Eutrophication: Production breakdown based on LC stage

3.5 Consumption mix in Portugal

Table 3.17 displays a summary of LCIA of upstream stages of two chains of NG (except distribution) discussed in sections 3.1 to 3.4. Portuguese NG mix in Portugal was considered as the average weighted share of supply from Nigeria and Algeria in 2010, i.e. 60% and 40%, correspondingly (Galp Energia, 2012). The last column in Table 3.17 shows the LCIA of Portuguese NG mix. These results were obtained by calculating the weighted sum (60% Nigeria, 40% Algeria) of LCIA results calculated in sections 3.1 to 3.4 (and summarized in corresponding columns in Table 3.17) and adding up the impacts of NG distribution in Portugal (Section 3.3.3).

Table 3.17: LCIA of NG consumed in Portugal

LCIA Category	Unit	Algeria	Nigeria	Distribution	Portuguese mix
CED	**MJ/MJ**	6.08×10^{-2}	2.50×10^{-1}	2.55×10^{-4}	1.74×10^{-1}
GHG	**g CO_2 eq/MJ**	6.76	16.65	5.60×10^{-2}	12.7
Acidification	**g SO_2 eq/MJ**	4.09×10^{-3}	2×10^{-2}	1.48×10^{-5}	1.36×10^{-2}
Eutrophication	**g PO_4^{3-} eq/MJ**	1.23×10^{-3}	6.47×10^{-3}	3.92×10^{-6}	4.37×10^{-3}

3.6 Uncertainty assessment of upstream GHG emissions from NG

Uncertainty is present in all phases of LCA, namely the goal and scope definition, inventory analysis, impact assessment and interpretation. Several sources of uncertainty in LCA can be characterized (Huijbregts, 1998; Lloyd & Ries, 2007; Malça & Freire, 2011): parameter uncertainty, which arises from missing and incomplete

data, and error in measured data; uncertainty in preferences or scenario uncertainty, which reflects the uncertainty in normative choices for constructing LCA models, e.g. choice of functional unit and impact assessment method, or selection of characterization factors; and model uncertainty, which reflects the variability in structure and mathematical relationships in LCA models between model inputs and outputs. In this thesis, we address two types of uncertainty in WtT GHG emission of NG consumed in Portugal: parameter uncertainty, concerning uncertainty affecting the LCI parameters; and scenario analysis related to choice of time horizon to calculate the GHG intensity. In most cases, parameter uncertainty is characterized by means of probability distributions, while uncertainty due to modeling choices is addressed through the development of scenarios (Lloyd and Ries, 2007; Malça and Freire, 2010; 2011).

For parameter uncertainty, we identified the parameters with highest effect on the model outputs, by mean of a sensitivity analysis. A literature review was then conducted to identify the underlying uncertainty and associate probability density functions to the parameters. A Monte-Carlo simulation was employed to obtain the sample distribution for WtT GHG emissions per MJ (LHV) of LNG and NG imported from Nigeria and Algeria to Portugal. Monte-Carlo simulation is a propagation method based on the repetition of many individual model iterations with each iteration using a randomly constructed set of values selected from the represented probability distributions; a probability mixture model then combined the values (emissions) calculated from each iteration to obtain the sample results. Finally, an uncertainty importance analysis was performed to identify the parameters that contribute more to the results variance.

The type of probability distributions of input parameters to the LC model were mainly obtained from literature, in particular Schori & Frischknecht (2012) that assigns a log-normal distribution to the parameters of LC inventory of NG systems. When no distribution was found, a uniform or triangular distribution was assigned to parameters with two or three data points. Finally, for the parameters that we found only one data point, a normal distribution with a Coefficient of Variation (CV) of 10% from the mean value was considered, for which we also assessed the implication of a higher CV (20%).

For venting emissions, since no distribution was found that represented the inherent uncertainty, two scenarios were defined following the two extreme values found in literature (minimum of zero and maximum of 0.018 m^3 per m^3 NG produced). Tables 3.18 and 3.19 include the distribution functions assigned to input parameters of the model.

Several time horizons can be adopted for the estimation of GHG intensity. Although the 100-year horizon is commonly used, the 20- and 500-year time horizons can be also adopted. We include this type of uncertainty into the model by calculating the GHG footprint of each chain of NG and the corresponding Portuguese mix for three different time horizons (20-, 100-, and 500-year time horizons).

Table 3.18: WtT stages of Nigerian LNG- Probability density functions for GHG emissions.

	Mean (g/MJ)	Distribution	SD	CV (%)	Min (g/MJ)	Mid-Value (g/MJ)	Max (g/MJ)
Drilling emissions							
CO_2	3×10^{-2} [a]	Normal		10%			
CH_4	1.60×10^{-6} [a]	Normal		10%			
N_2O	2.67×10^{-7} [a]	Normal		10%			
Venting emissions							
CO_2	0 [b]	n.a			0 [b]		1.58×10^{-2} [c]
CH_4	0 [b]	n.a			0 [b]		2.81×10^{-1} [c]
Flaring emissions							
CO_2	1.49 [d]	Log Normal[c]	1.23 [c]				
CH_4	6.80×10^{-3} [d]	Log Normal[c]	1.23 [c]				
N_2O		Uniform			2.2×10^{-10} [a]		3.1×10^{-10} [a]
Lease Fuel Emissions							
CO_2	1.85 [c]	Log Normal[a]	1.23 [c]				
CH_4	6.98×10^{-6} [c]	Log Normal[a]	1.23 [c]				
N_2O	6.78×10^{-4} [c]	Log Normal[a]	1.23 [c]				
Gathering pipelines							
CO_2 oxidation	1.07×10^{-4} [a, e]	Normal [a]		146% [a]			
CO_2 leak	5.34×10^{-6} [a, e]	Normal [a]		148% [a]			
CH_4	1.17×10^{-5} [a, e]	Normal [a]		148% [a]			
Processing Emission							
CO_2	1.67 [f]	Normal		10%			
CH_4	3.69×10^{-2} [f]	Normal		10%			
N_2O	2.80×10^{-5} [f]	Normal		10%			
Liquefaction							
CO_2	5.85 [g]	Log Normal[a]	1.05 [c]				
CH_4	0.01 [c]	Log Normal[a]	1.50 [c]				

Transportation						
CO_2	2.73	Normal	10%			
CH_4	1.46×10^{-4}	Normal	10%			
N_2O	1.35×10^{-4}	Normal	10%			
Gasification						
CO_2 eq		Triangular		1.85 [h]	1.60 [c]	1.5 [i]

[a] API (2009)
[b] Cervigni et al (2013)
[c] Schori & Frischknecht (2012)
[d] calculated based on NNPC (2013)
[e] WilBros (2011)
[f] ARI & ICF (2008)
[g] Woodside (2011)
[h] Tamura et al. (2001)
[i] Ruether et al. (2005)

Table 3.19: WtT stages of Algerian NG- Probability density functions for GHG emissions.

3.6.1 Parameter uncertainty

The 90% confidence intervals for GHG intensity from Algerian NG and Nigerian LNG LC stages were calculated based on the probability distribution of uncertain input parameters in Tables 3.18 and 3.19. A log-normal distribution was found to best fit the forecast values (Figures 3.18 and 3.19). Nigerian LNG not only has higher GHG emissions than the Algerian counterpart, but also higher associated uncertainty: the interval of the total GHG emission from WtT of LNG spans between 14.77 and 18.82 g CO_2 eq/MJ, with a mean value of 16.59 g CO_2 eq/MJ (Figure 3.18). For Algerian NG, this interval ranges between 4.68 and 11.41 g CO_2 eq/MJ, with a mean of 7.30 g CO_2 eq/MJ (Figure 3.19).

We performed an uncertainty analysis to detect the LC stages that contribute more to GHG intensity of both chains of NG supply (Figures 3.20 and 3.21). The variation range for each parameter, according to the distribution defined in Tables 3.18 and 3.19, was computed using the 5th and 95th percentiles of the intervals. A sensitivity analysis was performed and the 5 parameters that most affect the mean estimated GHG intensity of upstream NG and LNG chains were ranked. Figure 3.20 displays that lease fuel combustion emissions could increase the mean GHG intensity of Nigerian LNG up to 18 g CO_2 eq/MJ. The GHG intensity of Algerian NG is particularly sensitive to venting CH_4 emissions from production stage. Flaring of NG in Nigeria and CO_2 emissions from pipeline transportation of Algerian NG increase their relative upstream GHG by up to

10%. The uncertainty in other parameters in Figures 3.20 and 3.21 only slightly affects the mean GHG intensity. For LNG route, the uncertainty in gasification, liquefaction and transportation would mainly reduce the total GHG results by negligible amounts (2%). Similarly, processing CO_2 emissions would alter the Algerian GHG intensity by 3%. The variability of results due to uncertainty among other input parameters was found to be negligible (less than 0.05%). Moreover, we tested the hypothesis of considering a CV of 20%, instead of CV 10%, for the parameters that we did not find any probability distribution data, i.e. well drilling, processing, and LNG marine transportation. Once again, the changes to the mean value were found to be less than 1% and thus negligible.

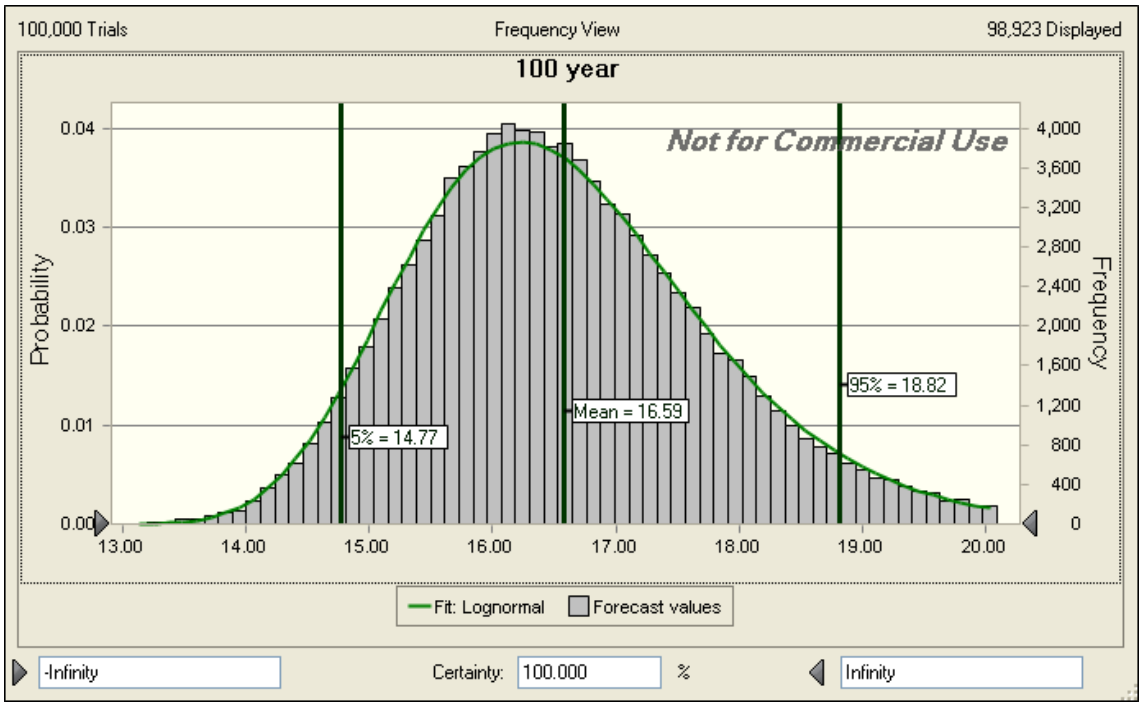

Figure 3.18: GHG emission of Nigerian LNG — 90% confidence interval

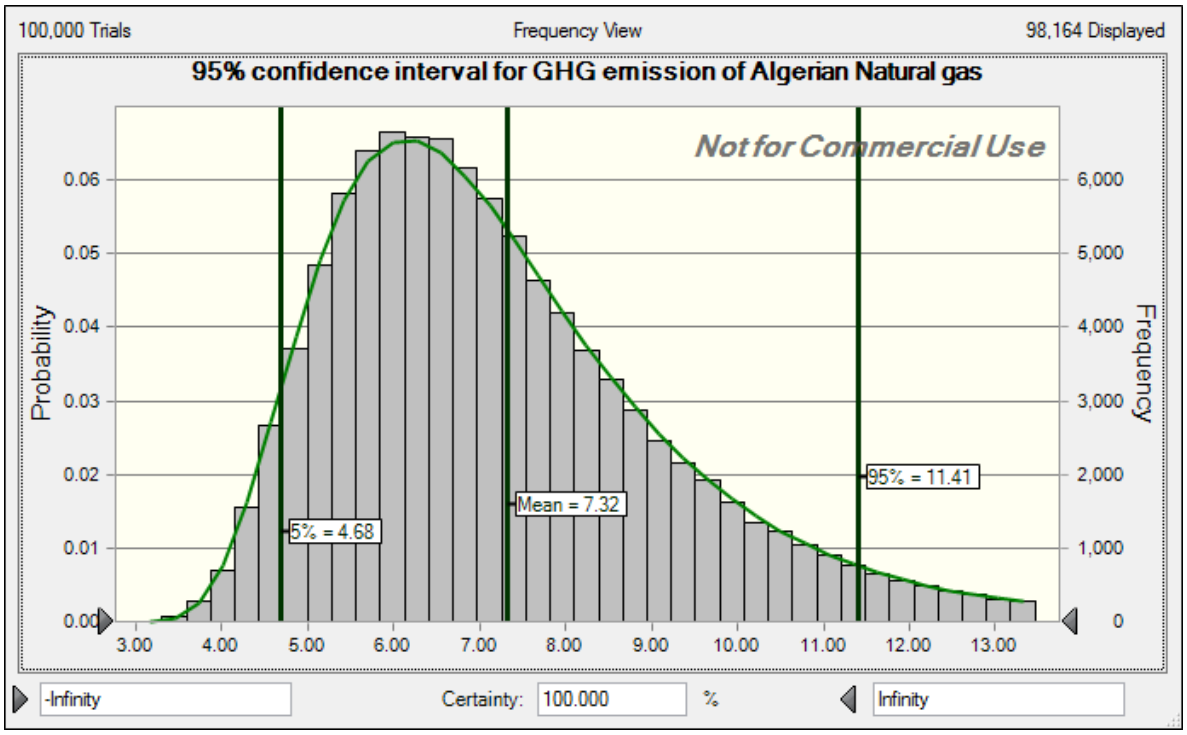

Figure 3.19: GHG emission of Algerian NG — 90% confidence interval

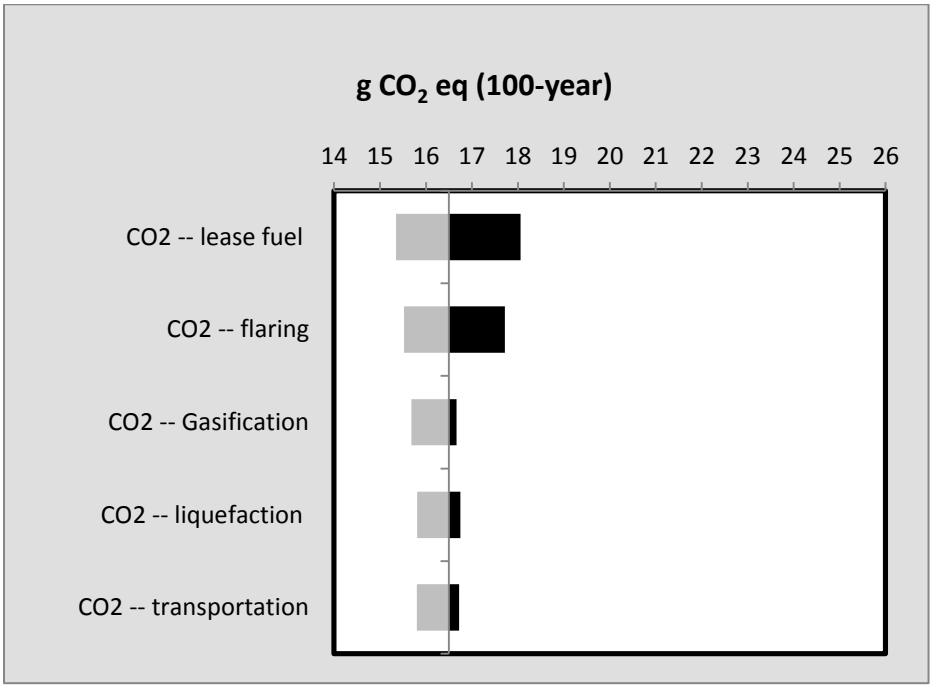

Figure 3.20: Nigerian LNG upstream GHG — sensitivity to input parameters

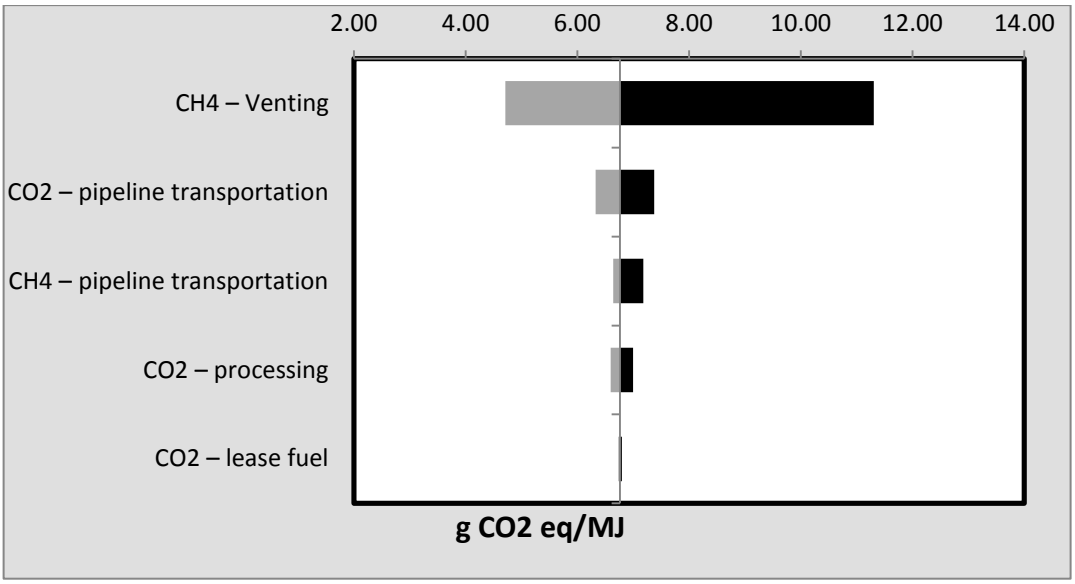

Figure 3.21: Algerian NG upstream GHG — sensitivity to input parameters

Finally, the probability distribution and 90% confidence intervals for the GHG emissions of Portuguese NG mix were obtained. A log-normal distribution (mean = 22.24, standard deviation = 3.29) was found to best fit the forecast values (Figure 3.22). Similarly, an uncertainty analysis was performed to detect the LC stages that most affect the WtT GHG intensity of Portuguese NG mix (Figure 3.23). As expected, GHG intensity of Portuguese gas mix is particularly sensitive to venting CH_4 emissions from production stage of Algerian and Nigerian chains (Figure 3.23). Other parameters with significant effect on the mean GHG intensity are from LNG chain (compare Figures 3.23 and 3.20). These are CO_2 emissions from flaring, lease fuel combustion, gasification and marine transportation. The variability of results due to uncertainty among other input parameters was found to be negligible (less than 0.05%).

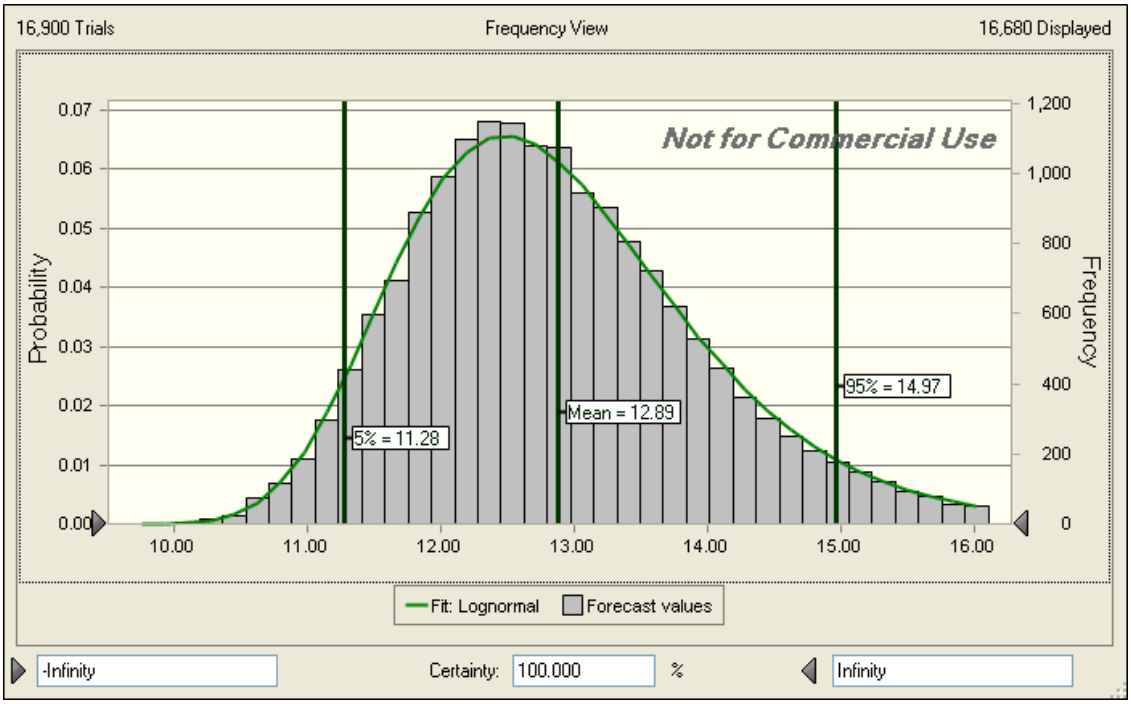

Figure 3.22: GHG emission of Portuguese NG mix —90% confidence interval

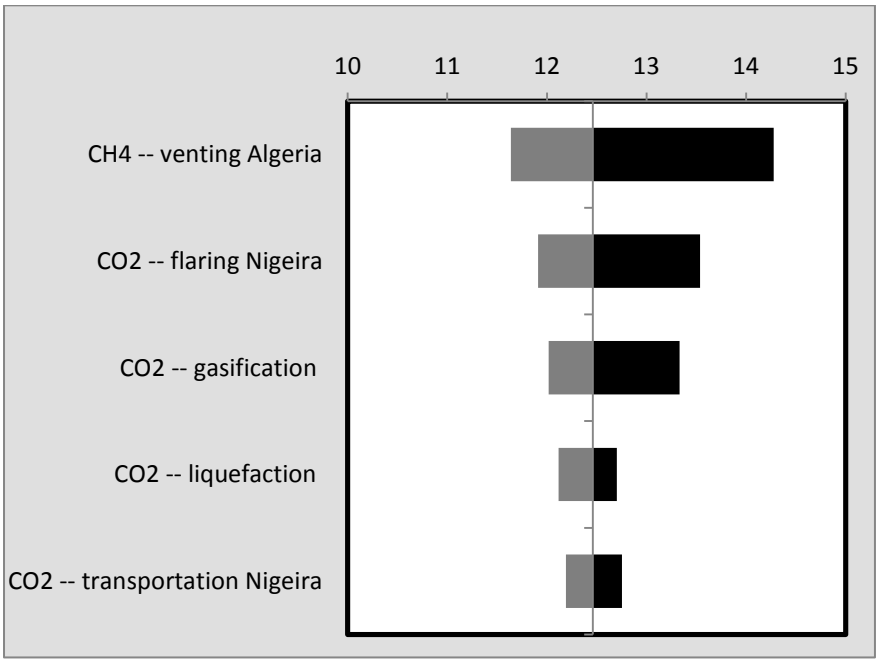

Figure 3.23: GHG Sensitivity to input parameters- Portuguese mix

3.6.2 Scenario uncertainty

The mean estimated GHG intensity (g CO_2 eq/MJ) and the 90% confidence intervals of Nigerian LNG, Algerian NG, and corresponding Portuguese average mix are shown in Figures 3.24 and 3.25 for three defined time horizons. Results were calculated based on the GHG characterization factors in Table 3.4. The shift in the mean GHG intensity as a result of venting emissions is also displayed: NG venting can shift up the mean GHG intensity of Nigerian LNG up to 25 and 40 g CO2 eq/MJ for the 100-and 20-year time horizons, respectively. The 20-year GHG estimations are significantly higher due to higher GHG characterization factor of methane (72 vs. 25 vs. 7.6 kg CO_2 eq for 20-, 100-, and 500-year, respectively). Considering a 20-year time horizon, the mean estimated GHG intensity of Nigerian LNG and Algerian NG were estimated as 18 g CO_2 eq/ MJ and 13.50 g CO_2 eq/ MJ, respectively. Moreover, uncertainty ranges for a 20-year timeframe are significantly higher than 100- and 500-year values, because of high contribution of methane to GHG intensity of NG chains. Conversely, since N_2O hardly contributes to LC GHG emissions of NG, implications of variation of characterization factors between different time horizons are not significant. The break-down of NG and LNG upstream stages also shows that the emissions from production stage, which has a high raw NG (CH_4) venting, and processing vary considerably with the alteration of time horizon chosen, while the variations along other LC stages of NG are insignificant.

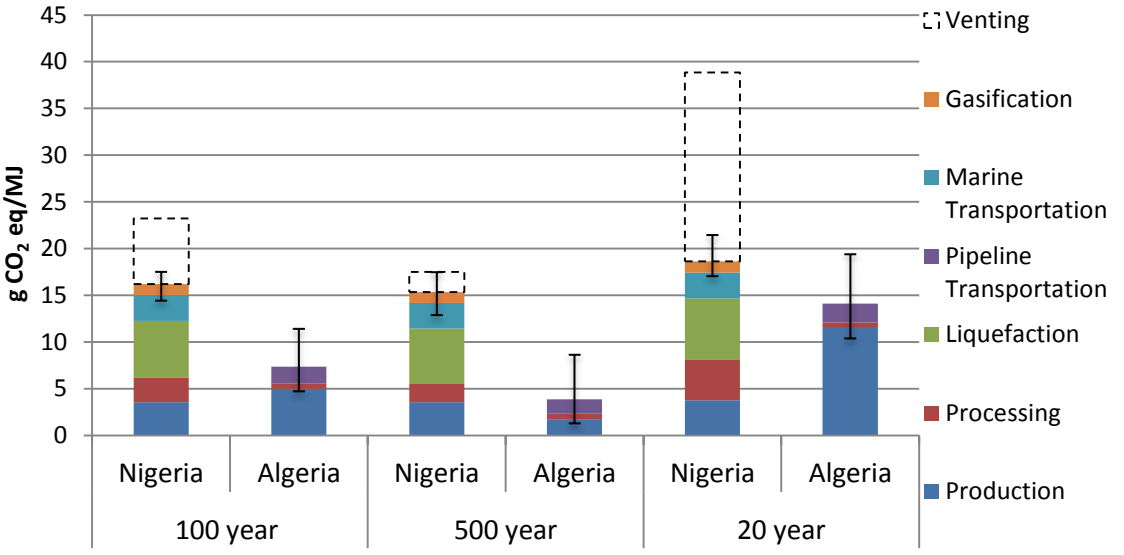

Figure 3.24: Upstream GHG emissions of Nigerian LNG and Algerian NG—implications of the selection of the time horizon

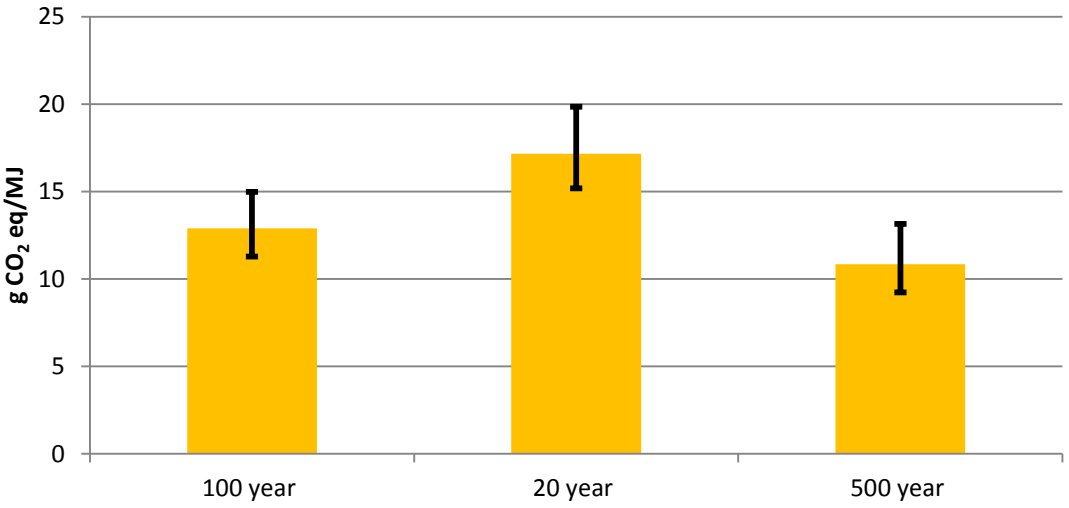

Figure 3.25: Portuguese NG mix upstream GHG emissions—implications of the selection of the time horizon

3.7 Summary and conclusions

This chapter presented the LCA of NG consumed in Portugal. We developed an LC model for two supply sources of NG (Algeria and Nigeria), assessing four impact categories: CED, GHG, Acidification, and Eutrophication. Two types of uncertainty in LC model, scenario and parameter uncertainty, were discussed and analyzed. The findings of chapter are summarized as following:

1- A detailed LCA shows that the LNG chain from Nigeria has considerably higher energy requirements and environmental impacts than the NG chain from Algeria. This conclusion holds regardless of the type of impact and is due to several reasons:

a. Nigerian NG production has higher production emissions, namely higher associated flaring emissions than Algerian counterpart.

b. LNG has two additional LC stages, liquefaction and gasification, among which liquefaction has particularly high energy requirements and emissions.

c. Marine transportation of LNG has slightly more impacts than pipeline transportation of NG.

2- The production of NG is the stage with the highest Acidification and Eutrophication environmental impacts and considerably contributes to GHG emissions of both source of NG (Algeria or Nigeria). Among the processes to produce NG, venting

and flaring are of particular concern as we discussed individually for each type of LCIA categories in sections 3.4.2–3.4.4.

3- Liquefaction of NG has the highest energy requirements (CED) and GHG emissions among upstream stages of NG chains. Liquefaction contributes to more than half of total CED to produce and deliver one unit (MJ) of Nigerian LNG.

4- For GHG, the main emissions from NG chains are in the form of CO_2 and methane; the emission of Nitrous Oxide is negligible. Methane is mainly released from venting of NG during its production; whereas CO_2 emissions contribute significantly to GHG intensity of the other LC stages of the NG chain (except production).

5- The main type of Acidification emissions from NG chains is NO_x, followed by SO_2. NO_x is specifically released from flare stack (incomplete) combustion. The main sources of SO_2 emissions are electricity consumption and burning of diesel to meet the energy requirements of producing and transporting NG. The contribution of ammonia to total Acidification potential of NG chains was found to be negligible.

6- The main type of eutrophication substances from NG chains is NO_x and phosphate. NO_x is the main emission of producing NG, whereas phosphate contributes equally to other stages of NG chains. The contribution of ammonia and nitrate to the Eutrophication impact is negligible.

7- Venting of NG can have influential results on the total GHG footprint of NG chains. The reason is the relatively high GHG characterization factor of methane that is the main component of raw vented NG.

8- Uncertainty analysis of GHG emission of NG chains revealed a high level of uncertainty to the mean value. Specifically, a high level of uncertainty was found regarding the venting emissions of Nigerian NG production.. Flaring can also alter the results by 10% compare to the mean estimation. The contribution of other stages to total GHG intensity was found to be negligible (less than 5%).

9- The estimate for GHG intensity of NG can vary considerably with the alteration of scenario (time horizon) chosen for the study. This is due to higher GHG characterization factor of methane for shorter time horizons. Since N_2O hardly contributes to total GHG emissions of NG chains, its different characterization factor for different time horizons does not affect the mean estimation.

Chapter 4

Life-cycle Assessment of Energy Systems*

The Life-cycle Assessment (LCA) of the upstream stages of Natural Gas (NG) consumed in Portugal was presented in chapter 3. The purpose of this chapter is to present LCA of selected Distributed Generation (DG) sources for the building sector in Portugal. Section 4.1 defines the goal and scope of the LCA. In section 4.2 we present the Life-Cycle Inventory (LCI), including a brief description of energy systems and main assumptions to calculate LCI. The Life-Cycle Impact Assessment (LCIA) is discussed in section 4.3. Finally section 4.4 summarizes the findings and presents the concluding remarks.

4.1 Goal and scope

The environmental impacts of the following types of DG for the commercial building sector in Portugal were assessed: solar Photovoltaic (PV), Solar Thermal (ST), Combined Heat and Power (CHP) technologies, and two types of cooling systems: Absorption Chiller (AC) and Compression Chiller (CC). CHP systems were assumed to be connected to Portuguese NG distribution network, which was assessed in chapter 3. Similarly, solar systems were modeled as they were installed in the city of Coimbra, situated in the central region of Portugal. The average meteorological conditions and solar radiation to calculate the systems output therefore characterizes this region.

PV generates electricity, ST produces heating energy, CHP systems simultaneously generate electricity and heat, and cooling systems produce cooling energy. Due to different types of energy output (electrical, thermal, or both) from energy systems, three distinct LC models were developed to assess their environmental impacts. The

* This chapter is based on the following journal article: Safaei, A & Freire, F & Antunes, C (2014c)

environmental impacts assessed were Cumulative Energy Demand (CED), Greenhouse Gases (GHG), Acidification, and Eutrophication. CML (Guinee *et al.* 2002) was used as the LCIA method.

4.1.1 Generation of electricity

The functional unit of 1 kWh electrical energy (kWh_e) delivered was selected for the LC model developed to assess the environmental impacts of PV and cogeneration systems for the commercial building sector in Portugal. The system boundary includes energy systems production, their use phase and disposal. As a benchmark for (separate) electricity generation, DG was compared with the Portuguese electricity mix in 2011.

Cogeneration systems produce electricity and heat simultaneously. In an LCA perspective, if a process provides more than one function, it is called "multi-functional" (ISO 14044). In this case, energy inputs and emissions linked to the process must be divided between the product of interest and the other co-products in a systematic approach. There are three approaches to do so (ISO 14044):

- system subdivision, i.e. dividing the unit process to be allocated into two or more sub-processes and collecting the input and output data related to these sub-processes;
- system expansion, i.e. expanding the product system to include the additional functions related to the co-products; and
- allocation, i.e. partitioning the inputs and outputs of the system between its different products in such way that reflects the underlying relationships between them.

ISO 14044 (2006) recommends that "wherever possible, allocation should be avoided by using system expansion or sub-division". Following ISO 14044 (2006) guidelines, we adopted the "system-expansion" approach to deal with the multi-functionality of cogeneration process. Since the aim is to compare cogeneration systems against grid, the analysis accounts for the credit of the heat generated as co-product (with electricity) by cogeneration systems. We assumed that thermal energy produced by CHP systems replaces that of a condensing boiler. The selection of the condensing

boiler was to abide by the cogeneration directive (Directive 2004/8/EC, 2004) in Europe, i.e. to compare cogeneration with the state-of-the-art separate production of heat and electricity. In addition to the condensing boiler, and to account for the variability regarding the system replaced to produce thermal energy, a conventional boiler (80% efficiency) was also modeled. The emission per kWh electrical output from cogeneration systems was then calculated considering two alternative systems: a condensing boiler (90% efficiency), and a conventional boiler (80% efficiency).

4.1.2 Generation of heating energy

An LC model was developed to assess the environmental impacts of ST systems for the commercial building sector in Portugal. The functional unit selected is 1 kWh heating energy (kWh_{th}) delivered in the form of hot water (temperature 60 °C) from ST systems. System boundary includes ST production, its use phase and disposal. As benchmarks for heating energy generation, ST was compared with two types of boilers: a modern condensing boiler (90% efficiency), and a conventional boiler (80% efficiency). Fuel input to boilers was considered to be supplied by Portuguese NG distribution network.

4.1.3 Generation of cooling energy

An LC model was developed to assess the environmental impact of AC and CC for the commercial building sector in Portugal. The functional unit selected is 1 kWh delivered cooling energy (kWh_c) e.g. in the form of cool air (temperature 15 °C). System boundary includes cooling systems production, their use phase and disposal. The heating energy input to the AC was considered to be supplied by either a modern condensing boiler (90% efficiency) or a conventional boiler (80% efficiency), both connected to Portuguese NG distribution network (as discussed in 4.1.2). Similarly, the electrical energy required driving the CC, and the negligible amount of electrical energy for the operation of AC and fans was considered to be supplied by the Portuguese electricity mix in 2011.

4.2 Life-cycle inventory

4.2.1 Internal combustion engine cogeneration technology

Reciprocating Internal Combustion Engine (ICE) cogeneration technologies offer relatively low capital costs, fast start-up, excellent load-following characteristics, and significant heat recovery potential. Overall CHP efficiencies for systems range from 65% to 80%. Reciprocating engines are well suited to a variety of DG applications, including standby, peak shaving and grid support. There are two types of reciprocating engines: spark ignition, and compression ignition. Spark ignition engines, the one studied in this thesis, uses a spark plug to ignite a compressed fuel-air mixture within the cylinder (IEA, 2009 & 2011; Onovwiona & Ugursal, 2006; Simader *et al.*, 2006).

The ICE studied here is a NG rich burn engine with a nominal electrical power of 172 kW_e. The life-time of the engine is assumed to be 6 years, with four maintenance sessions required during this period. Table 4.1 displays the efficiency parameters of the ICE. On top of the emissions and energy requirements of construction, the inventory includes the necessary piping requirement for sanitary and venting purposes. A storage tank for hot water can be coupled with CHP systems; however, we exclude it from the scope of our study considering that the building under study does already hold such an equipment to meet its peak hot water demand. Tables 4.4 and 4.7 show the emission inventory and energy requirements of ICE. The values include the emissions due to upstream of NG, as presented in chapter 3.

Table 4.1: Efficiency parameters of ICE (Osman *et al.*, 2008)

	Load	Power	Electric Efficiency (%)	Thermal Efficiency (%)	power-to-heat Ratio
ICE	**100%**	172	33.4	54.8	0.61
	75%	129	30.4	57.8	0.52
	50%	87	26.6	60.8	0.44

4.2.2 Micro-turbine technology

Micro-Turbines (MTs) are combustion turbines whose rated power range between 25 kW and 500 kW (IEA, 2009). MT cogeneration systems consist of a compressor,

combustor, turbine, alternator, recuperator (a device that collects waste heat to improve the efficiency of the compressor stage), generator, and the exhaust gas heat exchanger that transfers the remaining energy from the MT exhaust to a hot water system (IEA, 2009 & 2011; Onovwiona & Ugursal, 2011; Simader *et al.*, 2006). Figure 4.1 illustrates an MT-based cogeneration system. MTs achieve electrical efficiencies in the range of 23% to 32%, and overall efficiencies in the range of 64% to 74% (IEA, 2011). Their applications include peak shaving and base load power (grid parallel) as well as stand-alone power supply. Since MTs reduce power output by reducing mass flow and combustion temperature, efficiency at part load can be below that of full-power efficiency (IEA, 2009).

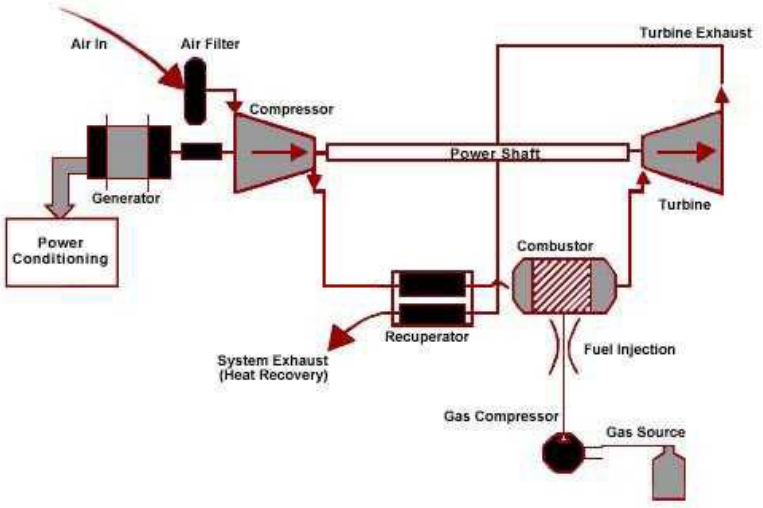

Figure 4.1: Components of a MT cogeneration system

The MT analyzed for this study has a nominal output of 60 kW_e and an electrical efficiency of 26% at full load. As Table 4.2 displays, the efficiency of the system decreases by lowering the operating load. The turbine was assumed to have six years (around 50,000 hours) life-time, with four maintenance sessions for this period. The lubricant consumption is 4.4 liters per year (Primas, 2007). On top of the emission from the construction of the turbine, the inventory also includes the piping for the sanitary equipment, ventilation and the electrical connections. A storage tank for hot water could be employed along with MT; however, we excluded it from the scope of our study considering that the building under study does already hold such equipment.

Table 4.2 displays the efficiency parameters of the MT under study and Tables 4.4 and 4.7 include the LCI of MT per kWh_e output in different operating loads. The NG supplied to turbine was assumed to be from Portuguese NG distribution network.

Table 4.2: Efficiency parameters of MT (EPA ETV, 2003)

	Load	Power	Electric Efficiency (%)	Thermal Efficiency (%)	power-to-heat ratio
MT	**100%**	54.9	26	52	0.50
	75%	39.9	24	56	0.43
	50%	24.8	20	57	0.35
	25%	9.8	13	58	0.22

4.2.3 Solid oxide fuel cell cogeneration technology

SOFCs operate on an electrochemical process to exploit the energy contained in NG or hydrogen fuel to produce electricity. Their size ranges from 100-1200 kW (IEA, 2009). SOFCs offer the potential for low emissions, quiet and efficient power generation, because the fuel is not combusted but instead reacted electrochemically. Since SOFCs have relatively long start-up times they are more applicable to base-load needs. Additionally, they offer the advantage of high power-to-heat ratio and excellent load following characteristic that make them suitable for low-energy buildings (IEA, 2009 & 2011). Each fuel cell system consists of three primary subsystems: 1) the fuel cell stack that generates direct current electricity; 2) the fuel processor that converts the NG into a hydrogen rich feed stream; and 3) the power conditioner that processes the electrical energy into alternating current or regulated direct current.

The SOFC studied here is a 125 kW_e system with tubular cell design. Table 4.3 displays the efficiency parameters of SOFC. The life-time of the unit was considered to be 80,000 hours (full and partial load hours) with eight maintenance sessions including a major overhaul to replace the fuel stack (Primas, 2007). In addition to the infrastructure of SOFC, i.e. piping for sanitary equipment and the electrical connections, a storage tank could be also employed. We excluded the storage tank from the scope of our study considering that the building under study does already hold such equipment. Tables 4.4 and 4.7 show the LCI of 1 kWh_e output of SOFC systems at different operating-loads.

Table 4.3: Efficiency parameters of SOFC (Osman *et al.*, 2008)

	Load	Power	Electric Efficiency (%)	Thermal Efficiency (%)	power-to-heat ratio
SOFC	**104%**	130	44	37	1.20
	100%	125	45	35	1.30
	93%	116	48	32	1.50
	85%	106	49	30	1.63
	78%	98	50	28	1.79
	68%	85	50	24	2.08
	62%	78	51	21	2.43

4.2.4 Photovoltaic

Photovoltaic systems convey solar radiation directly into electricity. Several types of material can be used to produce PV, including mono- and poly-crystalline silicon, amorphous silicon, and cadmium telluride. At the current stage, crystalline based systems dominate the PV market in terms of the total capacity of installation (IEA-PVPS, 2011).

The PV system modeled here is a 4 kW_p (kW peak) mono-crystalline system. The main stages are the production of PV parts (panels and inverters), and the mounting structure and electric installation, which are together called Balance of System (BOS). The production of PV panels include the production of mono-crystalline PV cells, production of aluminum alloys to support the PV system, and solar glass, a glass that protects the PV panels against exposure to rain or dust (Jungbluth *et al*., 2009). The life-time of the PV system was considered to be 20 years, with an annual degradation rate of 0.5% in output (≈10% overall reduction in year 20), according to Denholm *et al*. (2009). Three 2500 W inverters were needed for the operation of the system during its life-time. The annual electrical output of the system was estimated using PV-Watts (2011) application that yields the estimated hour-by-hour power output of the crystalline silicon PV systems. Tables 4.5 and 4.8 display the LCI of PV system.

4.2.5 Solar thermal

Solar Thermal (ST) is a technology to harness thermal energy from solar radiation. ST system in this study is used to produce hot water for sanitary purposes. Such system has normally four components: the absorbing collector including the main framework,

the absorbing plate and the pipes for the thermal fluid flow; the water tank; electric pumps; and the support to secure the system to rooftop. The system requires a small amount of electricity to run the electric pumps.

A 4 kW_{th} ST system was modeled that includes 5.71 m^2 of flat plate collector with black chrome coating on copper, a 2000 liters chrome steel heat storage, 3.55 units of 40 W pumps, and the necessary piping and electric installation for the operation of the system. The life-time of the system was considered to be 20 years. Tables 4.5 and 4.9 display the LCI of ST system.

4.2.6 Boiler

Two 600 kW_{th} NG boilers were modeled for this study: a condensing boiler (90% efficiency) and a conventional boiler (80% efficiency). The life-time of both systems was assumed to be 20 years. The LCI of boilers are shown in Tables 4.5 and 4.9.

4.2.7 Grid

The electricity generation mix of Portugal consists of hydro, coal, NG, wind and PV. The contribution of each type of energy source to the total electricity generation mix changes annually due to weather conditions that affect the output of renewable (hydro, wind and solar) sources. Figure 4.2 shows the annual evolution of national electricity mix of Portugal since 2004 to 2011.

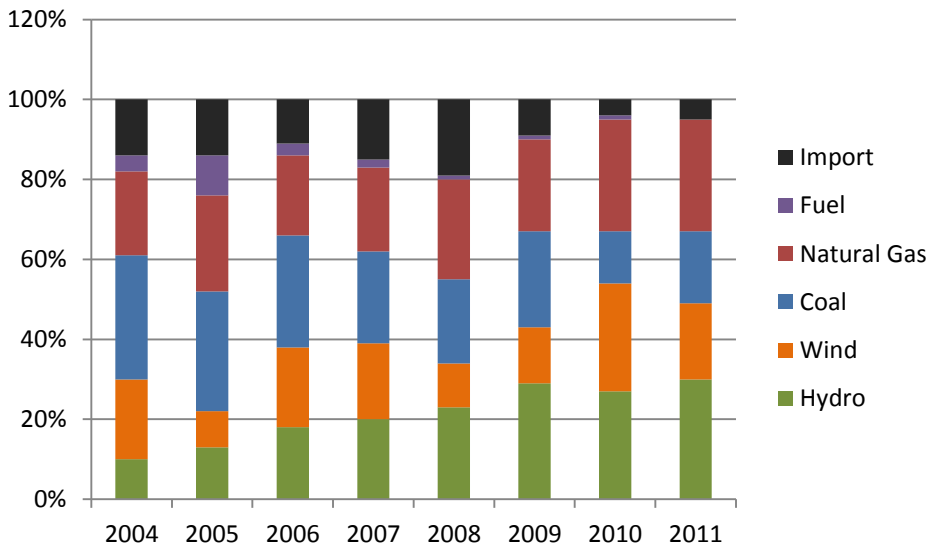

Figure 4.2: Evolution of electricity generation mix in Portugal

The generation mix considered to model the Portuguese grid is parallel to the mix of year 2011, with 20% electricity from coal, 31% NG, 18% wind production, 1% PV, and the rest 6% imported, as shown in Figure 4.3. The estimated LCI of 1 kWh_e supplied by Portuguese grid is shown in Tables 4.5 and 4.8. Portuguese NG mix has been considered as the source of supply of NG to gas plants.

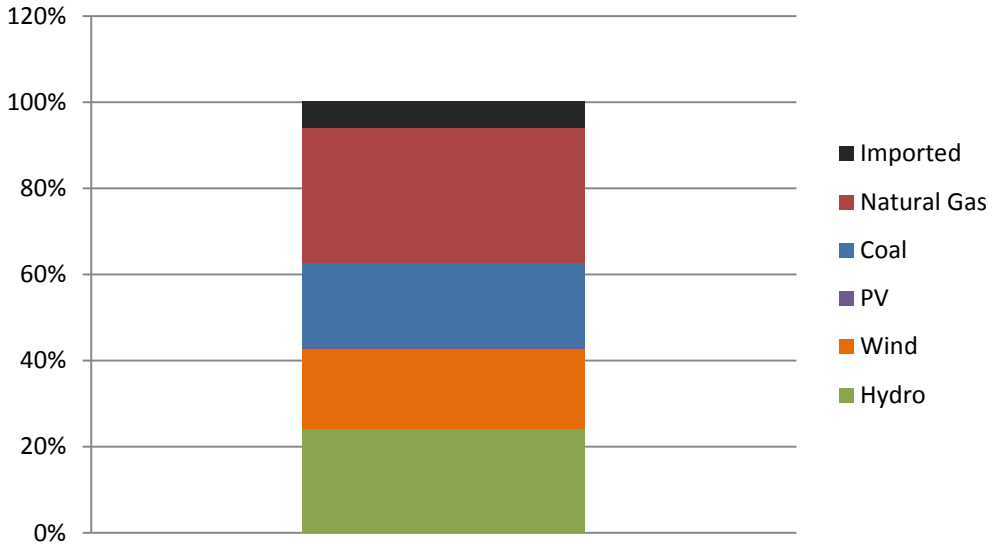

Figure 4.3: Electricity generation mix for the current study

4.2.8 Absorption chiller

An Absorption Chiller (AC) is a cooling system that uses a heat source (e.g., waste heat cogeneration systems) to produce cooling energy. A common AC in large commercial plants uses a solution of lithium bromide salt and water. The cooling cycle works as following: water under low pressure is evaporated from the coils, which are being chilled, and is absorbed by a lithium bromide/water mixture. Using heat, the water is driven off the lithium bromide solution. A Coefficient of Performance (COP) of 0.55 to 0.70 is expected for the system when coupled with cogeneration systems.

A 104 kW AC with a COP of 0.70 was modeled for this study. The life-time of the system was assumed to be 20 years. A small amount of electricity, 0.02 kWh_e per MJ of chilled water output, is required for the energy used during operation. Tables 4.6 and 4.10 show the LCI of AC systems.

4.2.9 Compression chiller

Compression Chillers (CC) are the commercially available technology used for space cooling. They could be air source, ground source, water source or a combination of two or more (hybrid). Air source compression chillers are the most common type used in building sector. An air source CC with a nominal capacity of 15 kW and a COP of 2.2 was modeled for this study. Tables 4.6 and 4.10 show the estimated LCI of CC.

Table 4.4: LCI of cogeneration systems

		ICE 100% load	ICE 75% load	ICE 50% load	MT 100% load	MT 75% load	MT 50% load	MT 25% load	SOFC 104% load	SOFC 100% Load	SOFC 93% load	SOFC 85% load	SOFC 78% load	SOFC 68% load	SOFC 62% load
		g/kWh$_e$													
Ammonia	NH_3	0.0003	0.0003	0.0004	0.0004	0.0005	0.0005	0.0007	0.0033	0.0025	0.0025	0.0025	0.0025	0.0025	0.0025
Carbon dioxide	CO_2	655	711	800	854	895	1022	1552	539	532	530	528	528	528	527
Nitrous Oxide	N_2O	0.0101	0.0112	0.0130	0.0116	0.0126	0.0150	0.0232	0.0611	0.0609	0.0604	0.0602	0.0601	0.0601	0.0599
Methane	CH_4	1.00	1.38	1.99	0.71	1.38	9.13	7.51	0.68	0.63	0.49	0.45	0.51	0.51	0.47
Nitrate	N	0.0011	0.0011	0.0038	0.0041	0.0044	0.0054	0.0084	0.0099	0.0023	0.0022	0.0021	0.0021	0.0021	0.0021
Nitrogen oxides	NO_x	0.25	0.26	0.31	0.42	0.43	0.55	0.85	0.19	0.11	0.0.02	0.02	0.0.02	0.0.02	0.02
Phosphate	PO_4^{3-}	0.0396	0.0772	0.0222	0.0231	0.0246	0.0286	0.0412	0.0439	0.0135	0.0130	0.0128	0.0127	0.0127	0.0125
Phosphorus	P	0.0015	0.0017	0.0098	0.0000	0.0000	0.0000	0.0001	0.0000	0.0151	0.0147	0.0146	0.0145	0.0145	0.0144
Sulfur dioxide	SO_2	0.0400	0.0095	0.0937	0.0285	0.0288	0.0348	0.0541	0.0812	0.0250	0.0241	0.0238	0.0236	0.0236	0.0233

Table 4.5: LCI of ST, PV, grid and boilers

		Conventional Boiler	Condensing Boiler	ST	PV	Grid
		g/kWh_{th}			g/kWh_e	
Ammonia	NH_3	0	0	0.0031	0.0050	0.0161
Carbon dioxide	CO_2	257	224	21	83.99	344
Nitrous Oxide	N_2O	0.0032	0.0029	0.0000	0.00	0.0068
Methane, fossil	CH_4	0.65	0.44	0	0.20	0.48
Nitrate	N	0.0032	0.0028	0.0138	0.0900	0.1290
Nitrogen oxides	NO_x	0.12	0.115	0.059	0.190	0.752
Phosphate	PO_4^{3-}	0.0098	0.0086	0.0932	0.2210	0.405
Phosphorus	P	0.000009	0.000008	0	0.07	0.00137
Sulfur dioxide	SO_2	0.055	0.045	0.101	0.270	0.294

Table 4.6: LCI of cooling systems

		AC Heat supplied by conventional boiler	AC Heat supplied by condensing boiler	CC Electricity supplied by Portuguese grid
			g/kWh_c	
Ammonia	NH_3	0	0	0.007
Carbon dioxide	CO_2	412	368	151
Nitrous Oxide	N_2O	0.01	0.01	0.003
Methane	CH_4	2.97	2.62	0.21
Nitrate	N	0.006	0.005	0.059
Nitrogen oxides	NO_x	0.35	0.31	0.349
Phosphate	PO_4^{3-}	0.02	0.02	0.186
Phosphorus	P	0.00002	0.00001	0.0006
Sulfur dioxide	SO_2	0.1	0.09	0.136

Table 4.7: CED of cogeneration systems

	ICE 100% load	ICE 75% load	ICE 50% load	MT 100% load	MT 75% load	MT 50% load	MT 25% load	SOFC 104% load	SOFC 100% Load	SOFC 93% load	SOFC 85% load	SOFC 78% load	SOFC 68% load	SOFC 62% load
								MJ/kWh$_e$						
CED	12.78	14.03	16.02	16.35	17.70	21.23	32.61	9.85	9.64	9.05	8.87	8.70	8.70	8.54

Table 4.8: CED of PV and Grid

	PV	Grid
		MJ/kWh$_e$
CED	1.80	4.67

Table 4.9: CED of boiler and ST

	ST	Conventional Boiler	Condensing Boiler
		MJ/ kWh$_{th}$	
CED	0.39	5.20	4.71

Table 4.10: CED of cooling systems

	AC Heat supplied by conventional boiler	AC Heat supplied by condensing boiler	CC Electricity supplied by Portuguese grid
	MJ/ kWh$_c$		
CED	8.70	7.79	2.12

This page is intentionally left blank.

4.3 Life-cycle impact assessment results

4.3.1 CED

The CED (MJ) to produce one unit kWh_e by grid, cogeneration systems and PV is shown in Figure 4.4. Similarly, Figure 4.5 shows the CED of the thermal units. The avoided burden heat produced by a 90% efficiency boiler is already subtracted from the total emissions of cogeneration systems (Figure 4.4). The extra savings, obtained as a result of considering a conventional boiler (80% efficiency) instead of a condensing boiler as the avoided burden, are shown as error bars on the total CED of CHP systems. It is visible that the amount of required energy to produce one unit energy output varies according to the type of technology and its operating load. PV systems provide significant energy savings compared to either grid or cogeneration systems to produce a kWh_e (Figure 4.4). ST also has significantly less CED than boilers (Figure 4.5). Employing a condensing boiler (rather than a conventional one) can reduce CED by 12%.

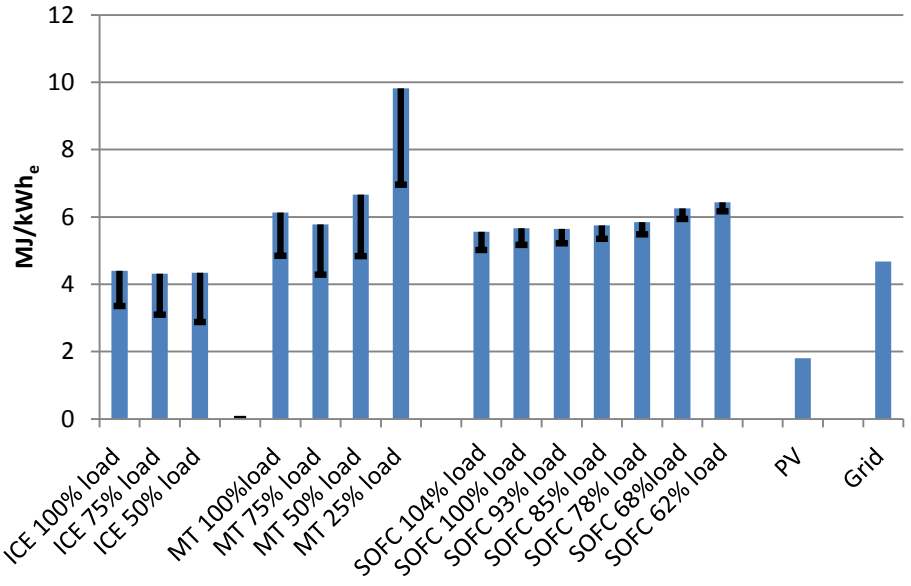

Figure 4.4: PV, CHP and grid: CED (MJ/kWh_e)

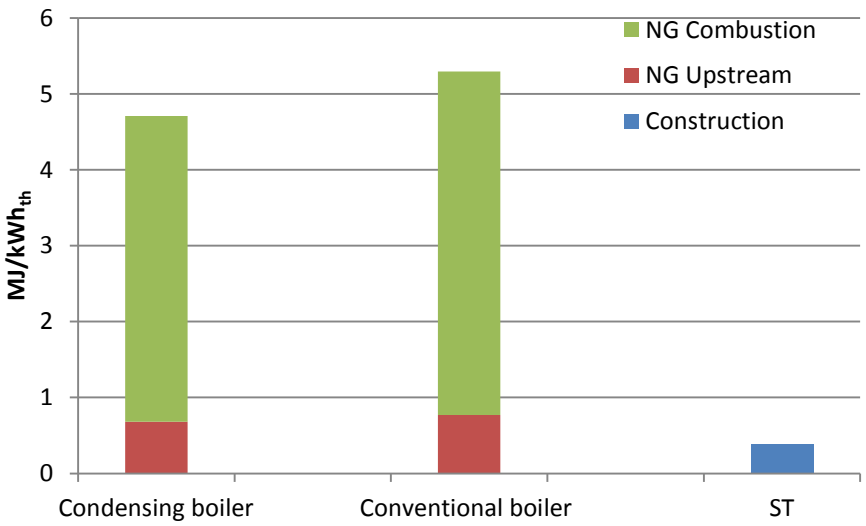

Figure 4.5: ST, condensing boiler and conventional boiler: CED (MJ/kWh$_{th}$)

For CHP systems, Figure 4.6 displays the CED as further broken down based on the three LC stages: construction of CHP, upstream stages to produce and transport NG, and the operation of CHP. The negative bars show the magnitude of emission savings obtained as a result of heat cogenerated with electricity from CHP systems, condensing boiler being selected as the avoided burden. The error bar shows the extra savings if the avoided burden is a conventional boiler. It is visible that the operating phase is the major contributor to CED of cogeneration systems (around 77% of total impact), followed by the upstream stages to produce NG. The CED to construct the energy systems is negligible compared to NG combustion and upstream CED. Moreover, since the amount of NG required producing one unit kWh$_e$ by MT and ICE is higher in part-loads, so is the contribution of NG upstream stages to total CED (Figure 4.6).

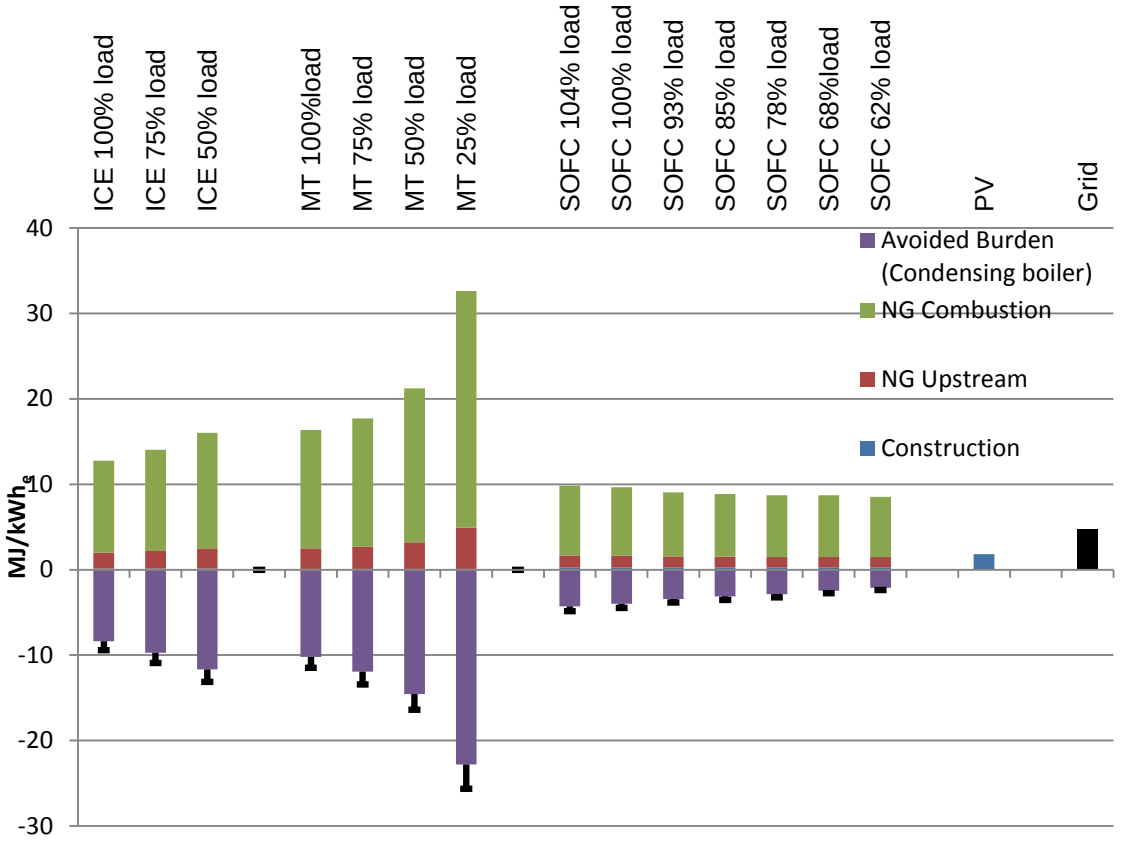

Figure 4.6: CHP—break-down of CED based on LC stage

Finally, Figure 4.7 displays the CED of cooling systems, AC and CC. CC has lower CED, due to combined effect of its higher efficiency and relatively low energy requirement of Portuguese grid, which supplies its electricity. On the other hand, lower COP of AC (0.7) implies higher CED to produce one unit kWh_c. Using a condensing boiler to run the AC can reduce its CED by 12%.

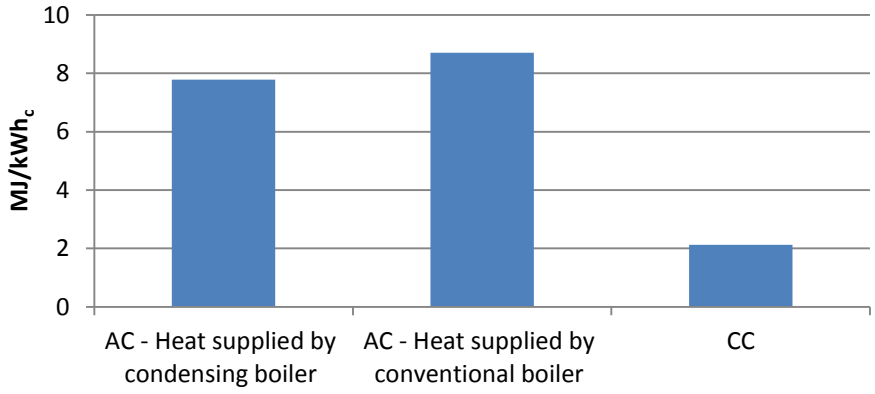

Figure 4.7: CED of cooling systems

4.3.2 GHG

The LC GHG emissions to generate one unit kWh_e by cogeneration, PV and Portuguese grid are shown in Figure 4.8, with the avoided burden heat (produced by a condensing boiler) withdrawn from the total emissions of cogeneration systems. Error bars in Figure 4.8 display the extra savings if the avoided burden was the conventional boiler. In terms of GHG savings, PV by far outweighs the grid and CHP technologies, among which ICE has the lowest emissions. Similarly, Figure 4.9 shows that ST has significantly less GHG emissions compared to boilers. GHG emissions from boilers arise from the combustion of NG (70%) and its upstream stages (30%). Compared to the conventional boiler, condensing boiler has 13% less GHG emissions.

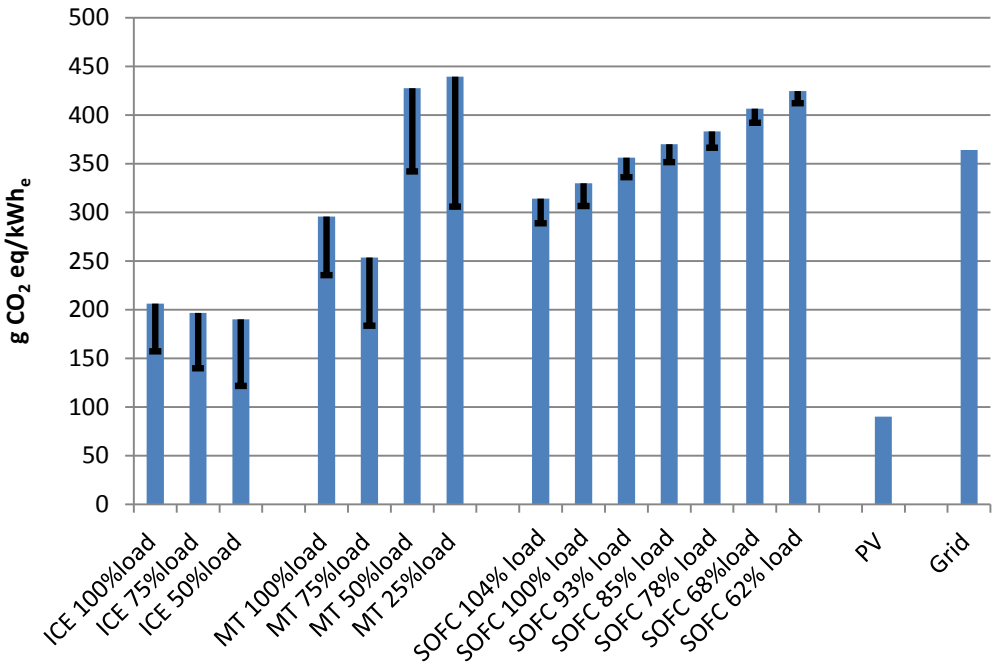

Figure 4.8: PV, CHP and grid—GHG (g CO_2 eq/kWh_e)

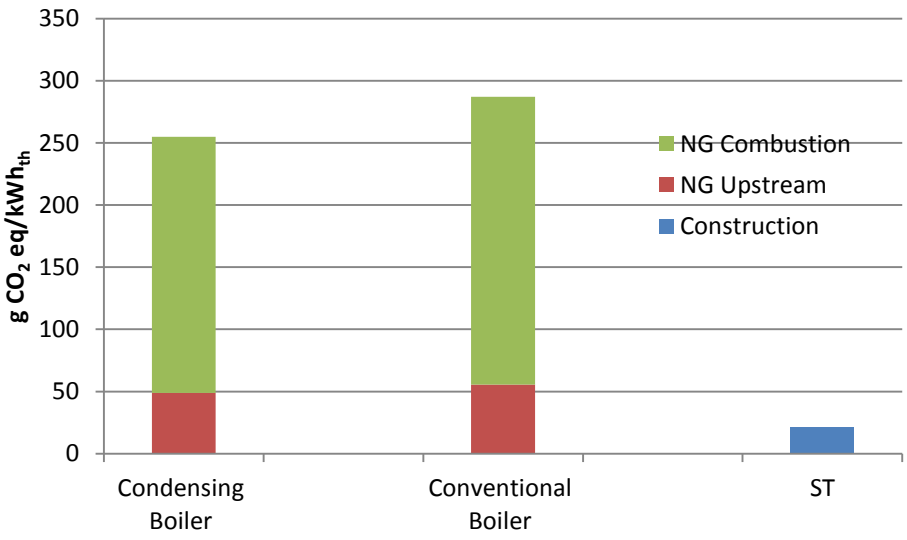

Figure 4.9: ST, condensing boiler and conventional boiler—GHG (g CO_2 eq/kWh_{th})

Figure 4.10 shows GHG emissions of generating one unit kWh_e by energy systems, as further broken down by three stages of LC. Regardless of the type of CHP technology, the stage with more impact is the operation of systems. Between 72% and 76% of the total GHG emissions come from the operation of energy systems, between 26% and 29% from upstream stages of NG, and rest from construction of CHP. For ICE and MT, decreasing the load results in higher operating emissions. The efficiency rates of SOFC in part-loads are similar to full-load, and so its GHG emissions. Regarding boilers (Figure 4.9), about 30% of GHG emissions are from NG upstream stages, the rest being from its combustion.

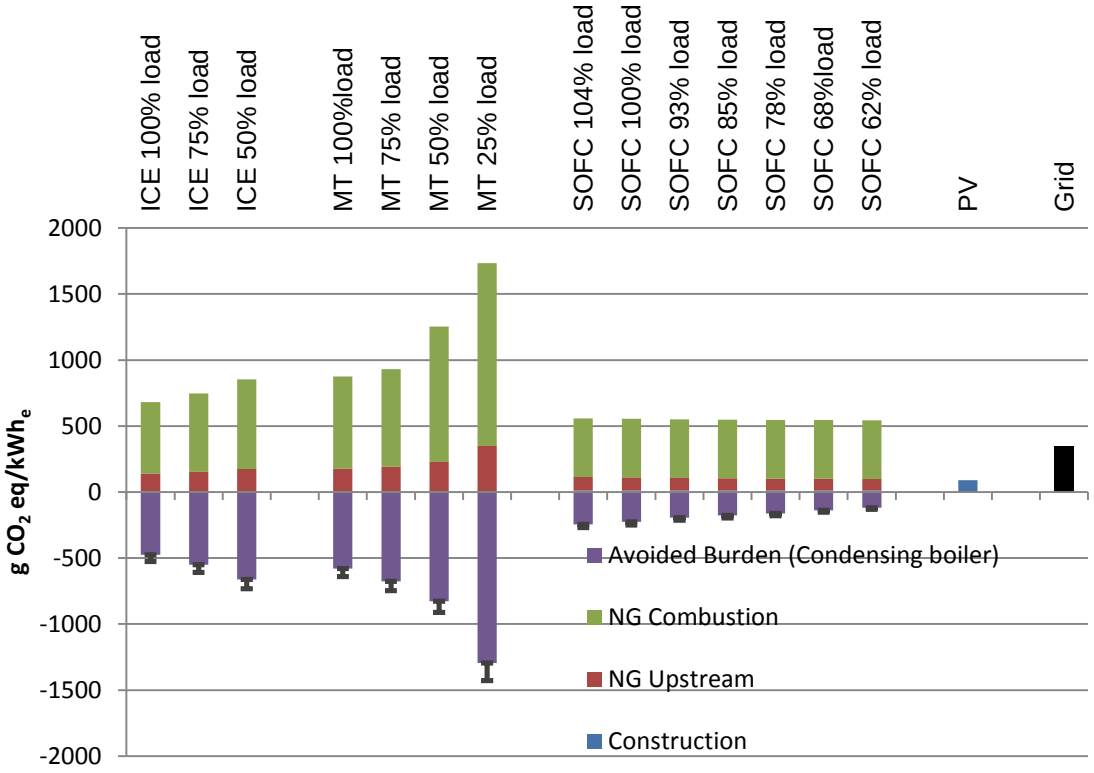

Figure 4.10: CHP—break-down of GHG based on LC stage

For ICE, more than 86% of the total GHG emissions (682 g CO_2 eq/ kWh_e) are caused by the release of CO_2, 12% to 13% (96 g CO_2 eq/ kWh_e) is by methane, and less than 1% (7.5 g CO_2 eq/ kWh_e) is by N_2O. Most of CO_2 emissions come from the combustion of NG, 20% from the upstream emissions of NG, and 1% from engine construction emissions. Conversely, methane and N_2O are mainly (74%) emitted from upstream stage of NG, and less from combustion emissions (construction emissions are negligible).

For MT operating in full load, CO_2 contributes to 90% of total emissions, 9.5% is from methane and less than 0.5% (3 g CO_2 eq/kWh_e) is caused by N_2O. Combustion of NG is the main source of CO_2 emission (around 81%). Methane is almost entirely emitted from upstream stages of NG that signifies very low methane emission from full-load operation of MT. However, methane emissions increase dramatically from 90 g CO_2 eq/kWh_e in full-load to 293 and 253 g CO_2 eq/kWh_e in 50% and 25% loads, respectively. In this way, 20% of GHG emissions of MT in part-loads loads are due to

discharge of methane. Methane emissions from the operation of turbine in 50% and 25% loads even exceed NG upstream methane emissions.

SOFC GHG emissions remain constant with the change of operation load. Once again most of GHG emissions (89% of 557 g CO_2 eq/kWh_e) are by CO_2, 8% (45 g CO_2 eq/kWh_e) by methane and 3% (16.5 g CO_2 eq/kWh_e) by N_2O. The share of methane to total GHG emissions is considerably lower for SOFC compared to other cogeneration systems and nearly all of this methane is from upstream stages to produce NG. Most of CO_2 emissions (80%) are from the operation phase of SOFC. Negligible N_2O emissions are similarly released from the operation of engine (85%), upstream of NG (8%) and the rest from construction of engine.

PV systems have very low LC emissions, mainly due to production of mono-Crystalline PV panels (75%), BOS (16%), inverter (6%), and different types of necessary transportations (3%). CO_2 contributes to 93% (82 g CO_2 eq/kWh_e) of total emissions, followed by methane (6%: 5.4 g CO_2 eq/kWh_e) and Nitrogen Dioxide (1%: .001 g CO_2 eq/kWh_e). Similar to PV, GHG emissions from ST system are essentially caused by the production of hot water tank (42%), ST flat plate collectors (35%), and transportation and installation. The impact of electricity to run the (pump for) ST is negligible. 95% of the total GHG intensity (20 g CO_2 eq/kWh_{th}) is from CO_2 emissions, the rest being from N_2O.

GHG emissions from grid (447 g CO_2 eq/ kWh_e) are mainly caused by the combustion of fossil fuels (coal and NG), which together cause 92% of the GHG intensity, with slightly higher share for coal (52%). The main GHG emissions from NG and coal plants are CO_2 due to combustion (93%) and methane (6%, which is by large from NG chain). The rest of emissions from grid are from the electricity imported (7%: 31.3 g CO_2 eq/kWh_e modeled according to the Spanish mix) and a negligible 2% (9 g CO_2 eq/kWh_e) comes from renewable sources, mainly hydro.

Finally, Figure 4.11 displays the LC GHG emissions of cooling systems. CC shows significantly lower emissions than AC, a joint effect of its higher nominal COP (2.2 CC vs. 0.7 AC) and relatively low GHG emissions of Portuguese grid. For both types of cooling system, the emissions are mainly associated with upstream stages to produce

fuel input (heating or electricity). For AC, the electricity required to drive the system causes only 5% of operating GHG emissions.

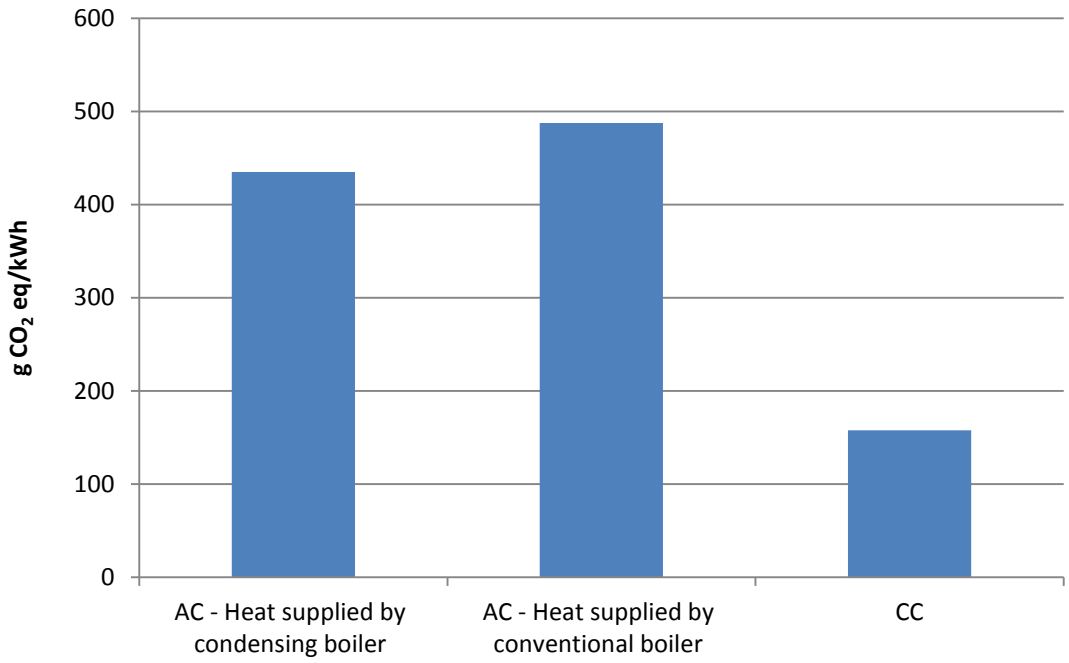

Figure 4.11: GHG of cooling systems

4.3.3 Acidification

Life-cycle Acidification impacts resulting from the production of one kWh_e by CHP technologies, PV and Portuguese generation mix in 2011 are shown in Figure 4.12. Cogeneration systems, regardless of type of technology, bring about significant reductions in Acidification compared to grid and even PV. The highest reduction is possible through the employment of SOFC. Regarding thermal systems, ST has more Acidification impact than the condensing boiler, but lower than the conventional one (Figure 4.13).

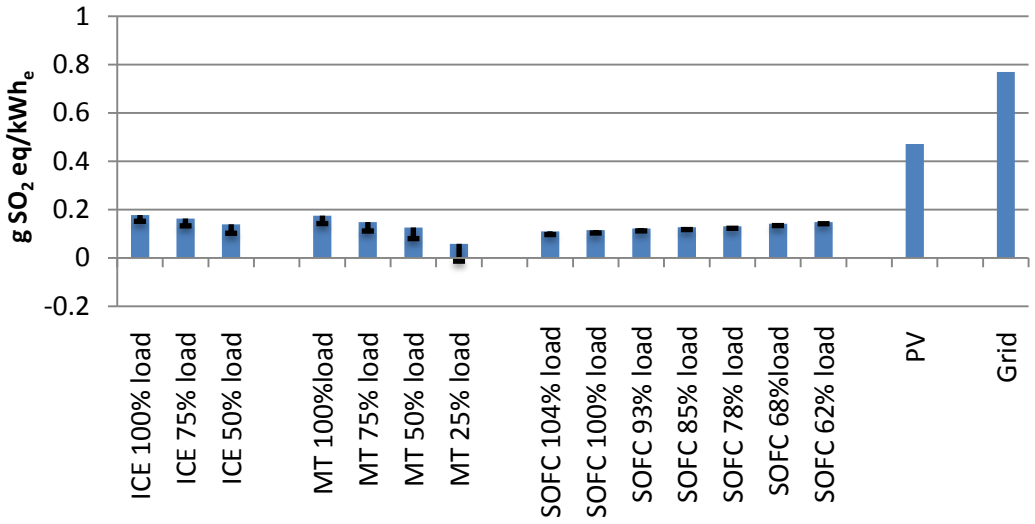

Figure 4.12: PV, CHP and grid—Acidification of energy systems (g SO_2 eq/kWh_e)

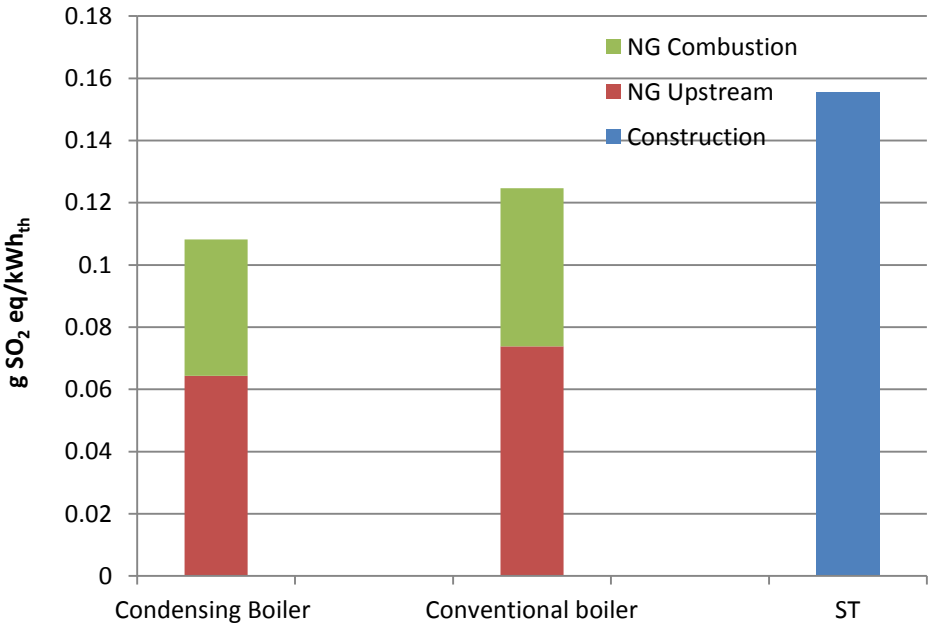

Figure 4.13: ST, condensing boiler and conventional boiler— Acidification (g SO_2 eq/kWh_{th})

Figure 4.14 displays the Acidification of CHP systems as further broken in upstream stages of NG, operation and construction of energy system. Acidification impacts are mainly caused by the upstream stages to produce NG. Moreover, the impact of construction of SOFC and ICE is relatively significant, while the impact of MT construction is negligible.

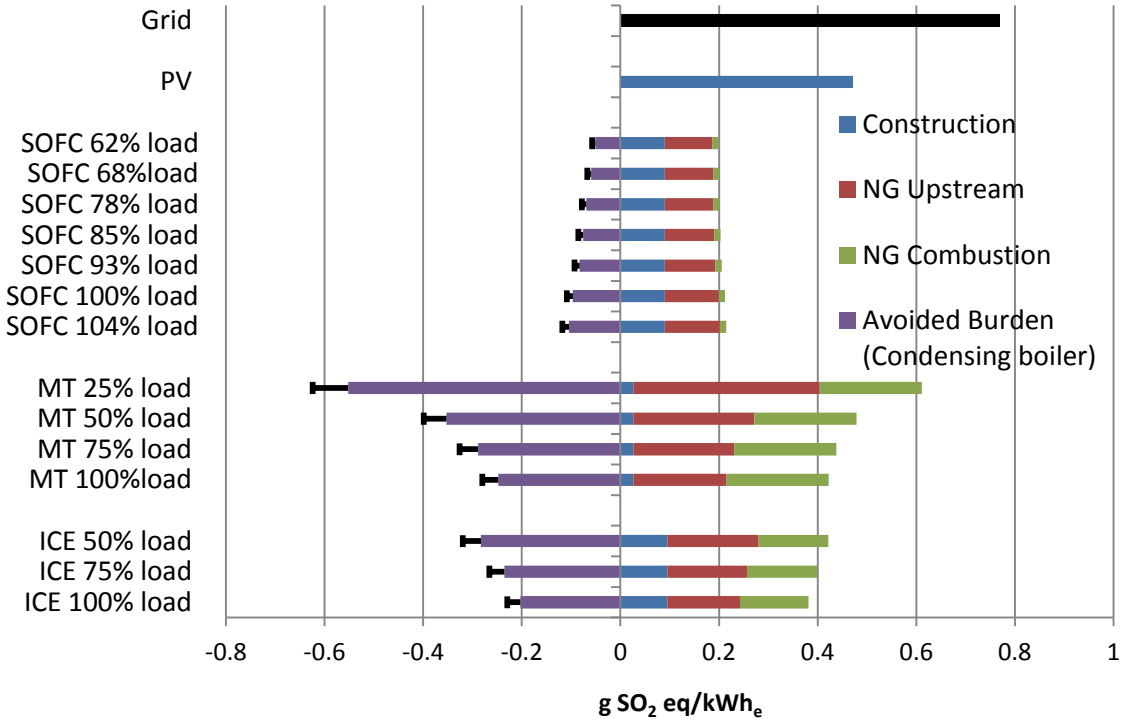

Figure 4.14: CHP—break-down of Acidification potential based on LC stage

ICE has an Acidification potential of 0.4 g SO_2 eq/kWh_e (without crediting the heat). This is mainly caused by SO_2 (80%) and NO_x (20%) emissions from engine. Acidification of ICE is also related to maintenance, involving burning of fuel oil and electricity to meet the energy required, which also releases SO_2 (95% of the total) and NO_x (5%).

Acidification impact of MT is by large caused by upstream emissions of the gas supplied to the turbine. Regarding operation emissions, NO_x that is formed through the operation of turbine is the major (98%) emission and the rest comes from SO_2.

From total Acidification emissions of SOFC (around 0.20 g SO_2 eq/kWh_e), 63% (0.13 g SO_2 eq/kWh_e) is in the form of NO_x , 35% in form of SO_2, and ammonia (2%). SO_2 and NO_x contribute equally to the operating emissions of fuel cell, while upstream activities related to the production of SOFC releases mostly SO_2. As Figure 4.14 shows, most of the emissions resulting from to produce one kWh_e by SOFC are due to upstream of NG, a trend observed for all the systems that run on NG.

The Acidification impact of electricity generation is due to emission of NOx and SO_2. Coal, which constitutes 20% of electricity generation mix (Figure 4.3), causes most of

the impact (i.e. 0.75 g SO_2 eq/kWh_e), followed by NG plants and the imported electricity (that also has coal according to Spanish mix). Overall, SO_2 and NO_x cause 47% and 50% of Acidification potential and 3% is from ammonia.

PV shows a rather high Acidification impact compared to cogeneration systems. The production of PV panels and BOS requires electrical energy that has a generation mix consisting of coal. Moreover, the oceanic and road transportation of PV parts use heavy fuel oil, which also has high Acidification potential. The production of PV panels and BOS generate 78% of Acidification impact, and the rest is from the transportation along upstream stages of production of PV. In terms of substances, 76% of Acidification impact (0.35 g of 0.47 g SO_2 eq/kWh_e) is in form of SO_2, 23% (10.9 g SO_2 eq/kWh_e) NO_x and 1% ammonia.

Regarding ST system, the production stage of flat plate collectors, hot water tank and copper wiring contribute to 90% of the total Acidification impact (0.163 g SO_2 eq/kWh_{th}). The rest of impacts come from ST upstream transportation stages and operation of 40 W pumps. Emissions are in the form of SO_2 (78%), NO_x (19%), and ammonia.

Figure 4.15 displays the Acidification impact of cooling systems. For both systems, construction impact is negligible (less than 1%) and emissions arise from their operation. CC has higher impacts, almost entirely caused by upstream emissions from electricity chain to run CC. Acidification impact of AC is also caused by the heat input from the boiler (75%) and the electricity needed for its operation (25%). Using a condensing boiler to run the AC can improve its impact by 10%.

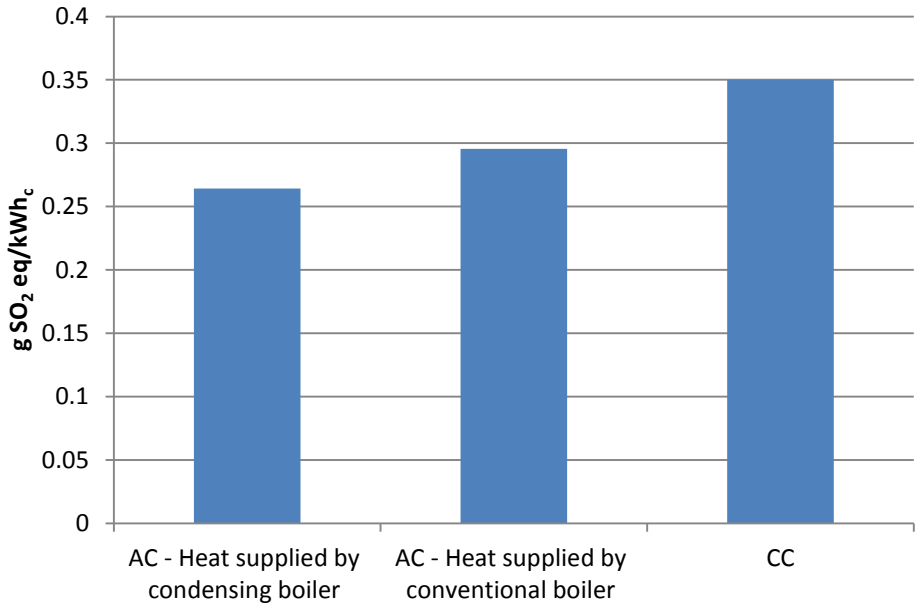

Figure 4.15: Acidification impact of cooling systems

4.3.4 Eutrophication

The Eutrophication impacts of DG (PV and CHP) and grid per kWh_e output of the energy systems are shown in Figure 4.16. Similarly, Figure 4.17 displays the Eutrophication impacts from one kWh_{th} from boilers and ST. CHP systems show significantly lower impacts compared to Portuguese generation mix in 2011. ST, on the contrary, has higher impacts than both conventional and condensing boilers, among which the latter has roughly 12% less impact (Figure 4.17).

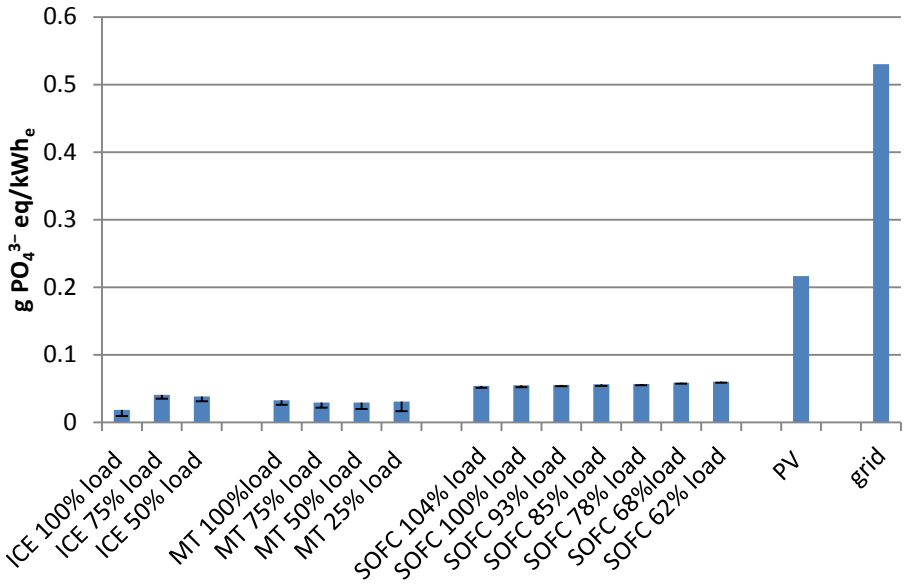

Figure 4.16: PV, CHP and grid— Eutrophication (g PO_4^{3-} eq/kWh_e)

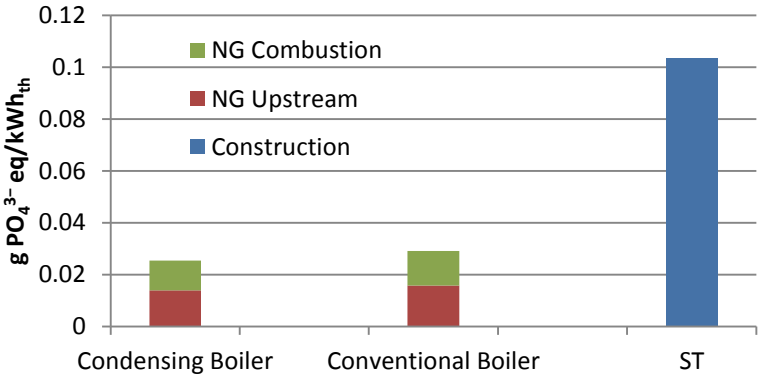

Figure 4.17: ST, condensing boiler and conventional boiler— Eutrophication (g PO_4^{3-} eq/kWh_{th})

Figure 4.18 displays the Eutrophication impact of CHP systems, as further broken down by three stages of LC. For SOFC, Eutrophication arise from the NG upstream stages and construction of the unit; the operating emissions are negligible. For MT and ICE, construction impacts are minor and emissions are discharged by upstream stages to produce NG, and considerably less by the operation of CHP.

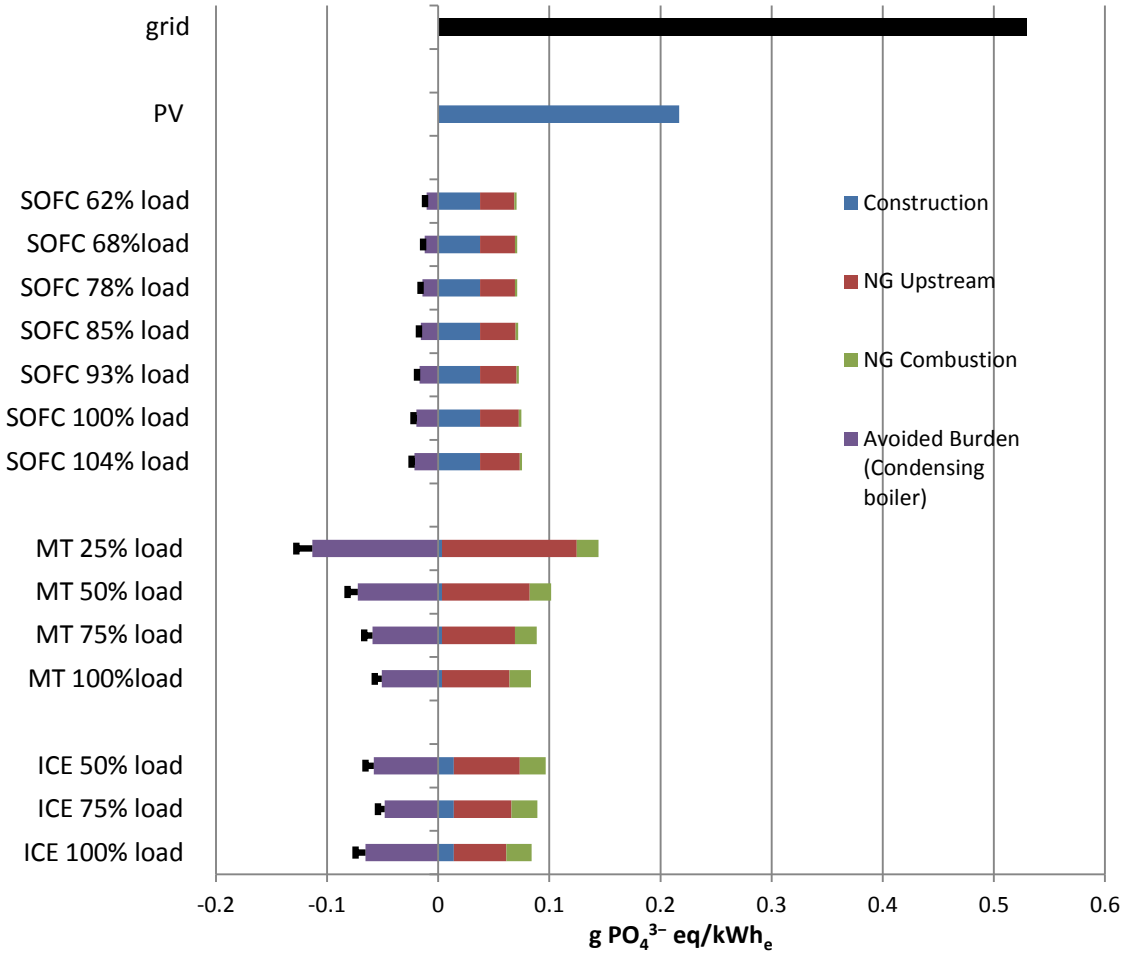

Figure 4.18: CHP—break-down of Eutrophication potential based on LC stage

For ICE, NG upstream stages are the main contributor to Eutrophication impacts, caused by the discharge of NO_x. The low emissions from ICE construction come in form of phosphate (99%) and negligible Nitrogen Oxides. In part-loads, NO_x emissions rate of ICE slightly increases and this is reflected in its Eutrophication impacts (see Figure 4.18).

MT systems have low operating emissions due to catalyst at the exhaust that offsets the NO_x emissions (EPA ETV, 2003). As Figure 4.18 shows, the construction emissions of MTs are also relatively low and NG upstream activities cause the major part of Eutrophication impacts. The NG upstream impacts increases per kWh_e output of the turbine in part-loads, since the electrical efficiency drops. On average, 78.5 % of total

Eutrophication is due to NO_x emissions, 21% phosphate, and other emissions are negligible.

For SOFC, operating impacts are relatively low due to low NO_x emission rate of the cell. Upstream activities to produce SOFC release half of the eutrophication emissions, namely phosphate (83%), Nitrogen Oxides (12%), ammonia and nitrate. The construction of SOFC represents the highest among the cogeneration systems.

High Eutrophication impact of grid is from the release of phosphates (78%) and NO_x (18%). Electricity generation from coal (89%) and imported electricity from Spain (10%) cause the major emissions.

The Eutrophication impact of PV systems (0.22 g PO_4^{3-} eq/ kWh_e) is due to production of PV panels (60%), inverters (22%), BOS (17%) and necessary transport to produce and install PV. The emissions come in the form of nitrate (40%), phosphate (34%), equal shares of Nitrogen and Nitrogen Oxide (12%), and 3% ammonia.

The main contributor to Eutrophication impact of ST (0.11 PO_4^{3-} eq/kWh_{th}) is phosphate, which is emitted by the production of flat plate collectors (60%), hot water tank (17%), and copper wiring (17%). The operation of 40 W pumps has negligible impacts. No_x has minimal contribution (10%) to Eutrophication impact of ST.

Finally, Figure 4.19 shows that utilizing AC brings about significant savings compared to CC to produce one unit kWh_c. For both systems, Eutrophication impacts are caused by the operation of systems and the impacts associated with systems construction are negligible. CC has particularly higher impacts due to higher upstream impact of its fuel input (electricity). For AC, heat only causes 60% of the Eutrophication impact, the rest being caused by the electricity needed to run the system. Using a condensing boiler (instead of a conventional one) can diminish the Eutrophication impacts of AC by 8%.

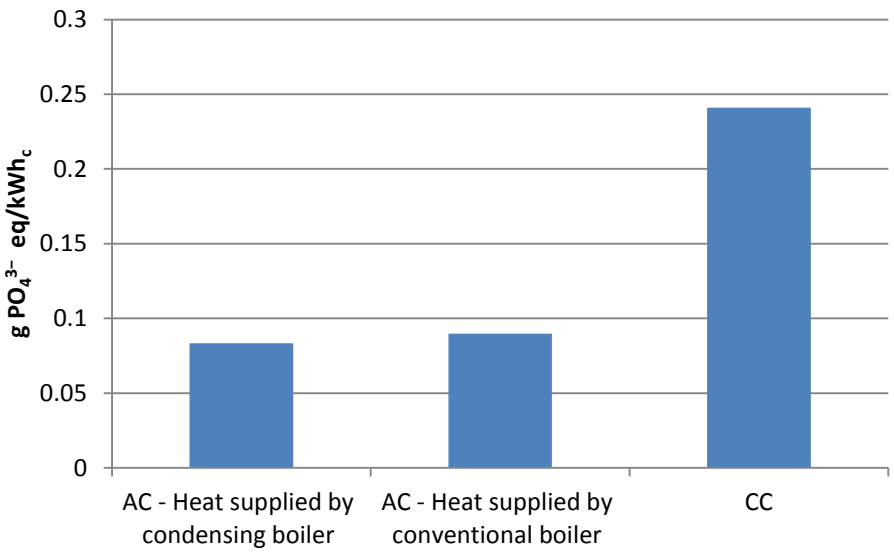

Figure 4.19: Eutrophication impact of cooling systems

4.4 Conclusions

This chapter presented the results of LCA of alternative DG sources for building sector in Portugal. An LC model was specifically designed for Portugal to account for upstream emissions of NG as fuel input to cogeneration systems and boiler, and the amount of solar radiation received by solar systems. Results were presented for four impact categories: CED, GHG, Acidification, and Eutrophication. The findings of the chapter are summarized as following:

1- The relative magnitude of CED of energy systems is similar to their GHG emissions (compare Figures 4.4 and 4.8). Similarly, Eutrophication impacts show virtually the same trend as Acidification impacts (compare Figures 4.12 and 4.16). In other words, the energy systems that have the least CED (PV, grid) also have the minimum GHG emissions. The same association is observed between Acidification and Eutrophication impacts where cogeneration technologies are the type of energy system with least impacts across both.

2- DG could be advantageous to reduce the impact of meeting the building sector energy demand in Portugal. DG is particularly superior to centralized generation for reducing Acidification and Eutrophication impacts where in some cases DG brings

about fourfold emission savings. GHG emissions and CED could also be reduced by employing DG, although the magnitude of emission savings, if any, depends on type of technology and its operating load. This is a result of relatively low GHG emissions and CED of Portuguese grid. PV provides savings compared to grid across both categories, while cogeneration technologies, except ICE for GHG, show relatively more CED and GHG emissions.

Regarding thermal systems, ST has significantly lower CED and GHG than both conventional and condensing boilers, while its Acidification and Eutrophication impacts could be higher. CC, its electricity being source by grid, is also advantageous to AC to reduce GHG emissions and CED, while it shows higher impacts for Acidification and Eutrophication.

3- Neither of the DG technologies has absolute dominance over the other or over centralized generation with regards to overall environmental performance. Solar systems are significantly advantageous to reduce CED and GHG emissions, while the magnitude of savings in Acidification and Eutrophication impacts are relatively less, due to relatively high NO_x emissions from their production stages. CED and GHG emission savings by partially replacing grid with PV could be particularly high. ICE proves the best cogeneration technology to reduce GHG emissions providing savings in Acidification and Eutrophication impacts compared to separate production of heat and electricity. Due to low NO_x and SO_2 exhaust emission, MT can also provide reductions in Acidification and Eutrophication impacts, while its CED and GHG emissions should be considered with care when the turbines operate at part loads. SOFC also has the lowest Acidification and Eutrophication impacts, but higher CED and GHG than other DG or grid.

4- The study highlighted the significance of fuel upstream energy requirements and emissions to the total impacts arising from systems that run on NG (CHPs, boilers). Upstream stages to produce NG contribute to at least 50% of LC Acidification impact from DG in Portugal. Up to 30% of total GHG and CED and Eutrophication impact of DG also come from NG upstream stages. On the other hand, the construction emissions were only significant for Acidification and Eutrophication impacts; the GHG emissions

and CED of construction of energy systems were irrelevant compared to their operating and NG upstream emissions.

5- The importance of proper assessment of part-load performance of cogeneration systems was highlighted. The efficiency of MT and ICE cogeneration systems drops with decreasing the operating load of the systems and this significantly impairs the emission performance of the engines, specifically for MT. SOFC has relatively steady efficiency rates at part-loads; therefore its impact in different operating loads are roughly similar.

6- A comparison between a conventional and a condensing boiler shows that the latter has roughly 12% less impact than a conventional boiler. The choice of a conventional or condensing boiler also affects the performance of AC as most of impacts from AC come from fuel input to the system, as we discuss next.

7- The impact of AC and CC is predominantly related to their upstream fuel input (heat or electricity) emissions to run those systems. The negligible electricity requirement running AC only slightly affects Eutrophication impacts and does not have significant contribution to other impact categories (CED, GHG, Acidification). The impact of AC could be reduced by up to 15%, using a condensing boiler instead of a conventional one.

8- In terms of substances: GHG emissions from distributed and centralized generation are mostly in the form of CO_2 (between 85%-90% of total GHG) and the rest from methane from upstream stages of NG production. This is except MT in part-load, which has very high operating methane emissions.

NO_x and SO_2 are the main Acidification substances from DG, their contribution to total Acidification impact depending on the type of technology. The impact of grid is caused by the emission of SO_2 (76%) and NO_x (23%). The contribution of ammonia to Acidification impacts of energy systems is negligible.

Eutrophication impacts of cogeneration systems are caused almost entirely from the release of NO_x in combustion phase. The main Eutrophication substances from production and BOS of PV are nitrate (40%), phosphate (34%), and less considerably

Nitrogen and NO_x. ST production and installation releases mainly phosphate (60%) and less NO_x (40%). The high Eutrophication impact of electricity generation from grid is due to the emission of phosphate (85%) and NO_x (10%).

Chapter 5

A Multi-Objective Mathematical Optimization Model for Design and Operation of Distributed Generation in Buildings*

The underlying motivations to formulate an optimization model for DG in buildings in Portugal were presented in chapters 1 and 2. This chapter presents the multi-objective mathematical programming model for optimal design and operation of DG in Portuguese commercial buildings. Section 5.1 explains the model, its structure, inputs and outputs. It also provides an overview of the policy framework to promote DG Portugal that is embedded to the model. The description of parameter and variable nomenclature and detailed mathematical relations are presented in section 5.2. Section 5.3 presents the case-study to which the proposed model was applied. Section 5.4 discusses the method used to calculate the Pareto frontiers that are presented in chapter 6. Summary and concluding notes are brought in section 5.5.

5.1 Model description

An optimization model for design and operation of DG was developed and implemented in General Algebraic Modeling System (GAMS; McCarl *et al.*, 2013) to minimize the Life-cycle Costs (LCC) and Life-cycle Impact Assessment (LCIA) of meeting the building energy demand over the defined planning period. Three types of technologies [(Micro-Turbines (MT), Internal Combustion Engines (ICE), Solid Oxide Fuel Cells (SOFC)] comprise the cogeneration systems that are combined with renewable [Solar Thermal (ST) and Photovoltaic (PV)] and conventional sources [Natural Gas (NG) boiler, electrical grid] to meet the building energy demand. In order to take advantage of the thermal output of the cogeneration systems when cooling demand exists, Absorption Chillers (AC) are added to the energy system while the

* This chapter is based on the following journal article:
- Safaei, A & Freire, F & Antunes, C (2013)

extra cooling load can be sourced by Compression Chillers (CC). The possibility of selling on-site produced electricity to the grid, according to the Portuguese legal framework, as well as dynamic pricing of electricity at peak and off-peak hours are also taken into account. A schematic representation of the model and the relationships between energy systems is shown in Figure 5.1. Each type of line in Figure 5.1 represents a form of energy (electrical, heating, cooling) flow. Next, we describe the policy framework for utilization and promotion of PV and cogeneration technologies in Portugal. This information is used as an input to the model.

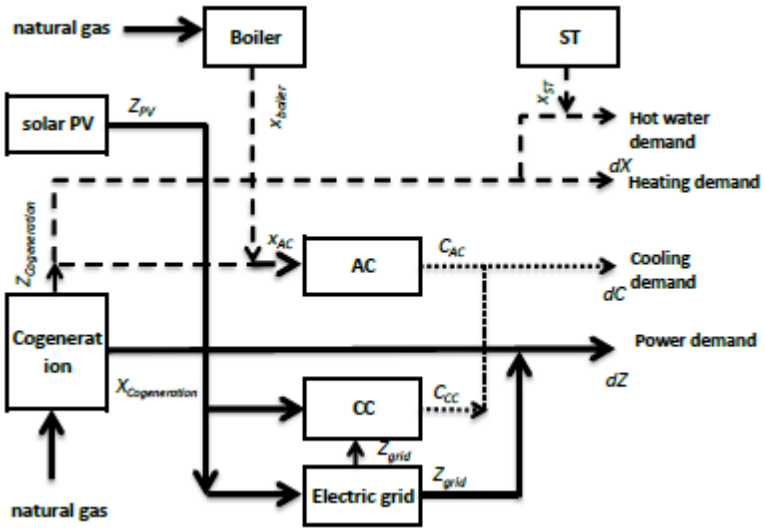

Figure 5.1: Model components and their interrelationship

Policy framework for cogeneration systems in Portugal

The legislative framework for utilization of cogeneration systems in Portuguese buildings and the conditions to export the onsite produced electricity to the grid have been subject to several modifications. The legislation in article 4 of the directive 538/99 (Decree-Law 538/99, 1999) declared that a cogeneration installation was recognized as efficient if the condition in expression (5.1) was met:

$$REE = \frac{E}{C - \frac{T}{0.9 - 0.2\,\frac{CR}{C}}} \geq 0.55 \tag{5.1}$$

in which

REE is the equivalent electrical efficiency of the installation.

E is the annual electrical energy produced by the cogeneration facility, excluding the consumption by internal parts of the systems.

T is the useful thermal energy consumed annually from the thermal energy produced by the cogeneration facility, excluding the consumption by internal parts of the systems.

C is the primary energy consumed annually by the cogeneration facility.

CR is the equivalent renewable energy resources, or industrial, agricultural and urban waste consumed annually by the cogeneration facility.

Provided that the cogeneration installation is recognized as efficient, it is possible to register the cogeneration installation and export the excess power produced onsite to the grid, based on two conditions:

- the electrical energy exported to grid should be less than 60% of the electrical energy produced onsite.
-

$$E_{er} \leq 4.5 \left(\frac{0.5T}{E + 0.5T}\right).E \tag{5.2}$$

where

E_{er} = annual electrical energy supplied to the grid

In 2002, the authorization of decentralized electrical energy production authorized the entity ‘‘producer–consumer” (Decree-Law 68/2002, 2002). Under this regime, decentralized power production in low voltage is allowed provided that

a) at least 50% of the produced electricity is consumed onsite, and

b) the maximum power allowed to be exported to the grid is 150 kW_e.

The compensation of energy injected into the grid is a function of the type of technology, reference values for consumer prices, and the amount of electrical energy supplied to the grid (decree-law 764/2002, 2002). The current legislation was not exclusive to cogeneration technologies, but also allowed the employment of other onsite energy production technologies.

Ultimately, by the introduction of directive 2004/8/EC (2004) of the European Parliament, the previous legislation (Expression 5.1) was overruled and new efficiency measures and market regulations were enacted. This recent directive and its Portuguese adaptation (Decree-law 23/2010, 2010) aims to create

> *"a framework for promotion and development of high efficiency cogeneration of heat and power based on useful heat demand and primary energy savings in the internal energy market" (Directive 2004/8/EC, 2004).*

According to this directive, cogenerations are considered as highly efficient provided that they deliver Primary Energy Savings (PES) of at least 10% compared to the reference for the separate generation of heat and electricity. Micro-cogenerations (maximum capacity below 50 kW_e) and small scale cogenerations (installed capacity below 1 MW_e) providing PES also qualify as highly efficient. The remuneration regime is of two forms: general and special forms. The general form is accessible to all cogeneration plants with no restrictions on engine power. Overall, the compensation of thermal and electric energy produced is to appeal to the market rules, and is calculated monthly as follows:

$$Rem_m = \sum_{i=1}^{2} W_{m,i} \times OMIE_m \times C_i \times f_i \tag{5.3}$$

in which

Rem_m is the remuneration in month m;

i is the period (medium-low) throughout the year;

$W_{m,i}$ is the energy produced in month m in period *i* (kWh);

$OMIE_m$ is the mean closing price of the Portuguese operator of the energy market, the year before, for the same month (€/kWh);

C_i is a coefficient that takes the values of 0.86 and 1.13 for low and medium periods, respectively;

f_i is the adjustment factor to take into account the losses in period *i*. Its value is announced annually by the energy services regulatory authority of Portugal.

The special form is only available to cogeneration plants with an installed capacity equal to or less than 100 MW. In this form, the compensation of thermal energy takes place in market conditions, but the electricity is delivered to the grid for marketing by the Supplier of Last Resort (SLR), in return for a temporary reference rate plus a monthly premium. The remuneration regime has three underlying principles: PES and consequent reduction of CO_2 emissions, utilization of renewable sources, and promoting the participation of cogeneration installations in the electricity market. The reference rate is published periodically by the Ministry of Energy. The monthly premium is based on the efficiency of the installation and the proportion of renewable fuels consumed, and is determined by the SLR. The operation framework of the current legislation takes place pursuant to decree-law 68/2002 (2002), as explained earlier. The value of reference Feed-in Tariff (FIT) for cogeneration systems that run on NG is set to 89.89 €/MWh for 2012 (Administrative rule 140/2012, 2012). The premium of efficiency, which is rewarded monthly, is defined in (5.4):

$$PE_m = PC \times \frac{PES}{1 - PES} \times EEPL_m \times K \times \frac{EP}{EE} \tag{5.4}$$

in which:

PE_m is the value of "premium of efficiency" in month *m* (€);

PC is the reference cost to evaluate PES (28.71€/MWh);

PES is the primary energy saving (%);

$EEPL_m$ is the electrical energy produced by the the cogeneration installation in month m (MWh);

K is a dimensionless factor to distinguish between high and not high efficient cogeneration installations. It assumes a value of 0.5 for high efficient cogeneration systems;

EP/EE is a benchmark ratio between primary energy consumption and electricity produced at the site of cogeneration installation. Since there is no benchmark value for such a ratio, its value is 2.86 and 3.70 for ICE and MT, respectively.

The "premium of renewables", which is applicable to cogeneration systems that utilize renewable sources as their fuel (biomass or biofuel), is calculated as following:

$$PR_m = FIT \times (\frac{CR}{C})_m \times R \times EEPL_m \quad (5.5)$$

PR_m is the value of premium of renewable energy in month *m* (€);

FIT is the reference FIT (€/kWh);

$(\frac{CR}{C})_m$ is the percentage of renewable fuel consumed by the cogeneration installation the year before in month *m*, which is certified by the entity that issues the guarantee of origin.

For the purpose of the current European directive, the PES shall be calculated through (directive 2004/8/EC, 2004; decree-law 23/2010, 2010):

$$PES = \left(1 - \frac{1}{\frac{\eta_{H\ CHP}}{\eta_{H\ Ref}} + \frac{\eta_{E\ CHP}}{\eta_{E\ Ref}}}\right) \times 100 \geq 0.0 \quad (5.6)$$

in which

$\eta_{H\ CHP}$ is the heat efficiency of the cogeneration production;

$\eta_{H\ Ref}$ is the efficiency reference value for separate heat production;

$\eta_{E\ CHP}$ is the electrical efficiency of the cogeneration production;

$\eta_{E\ Ref}$ is the efficiency reference value for separate electricity production.

We analyze the fulfillment of condition in Equation (5.6) for all types of cogeneration systems. The electrical and thermal efficiency values of cogeneration systems have been presented for each technology in chapter 4, section 4.2.4 and also brought in Table 5.1. As regards the efficiency reference values, the directive demands that "each cogeneration unit shall be compared with the best available and economically justifiable technology for separate production of heat and electricity on the market in the year of construction of the cogeneration unit" (directive 2004/8/EC, 2004). Therefore, we calculated the PES employing different cogeneration technologies with reference to the efficiency values of producing electricity in state-of-the-art NG combined cycle (NGCC) power plants and producing thermal power in condensing boilers (90% efficiency). Considering that all the thermal output of the cogeneration systems is utilized onsite, the respective PES obtained by the operation of

cogenerations in different part-loads is shown in Table 5.1. Provided that all the thermal energy of the cogeneration is utilized, i.e. the cogeneration installations reach the thermal efficiency expressed in Table 5.1, the PES for all types of cogeneration installation (except MT working in 25% part-load) would have a positive value. We calculate the threshold for which the PES remains positive as a function of the percentage of thermal energy that should be utilized onsite.

For example, considering MT at 100% load, we conclude:

$$0 \leq PES \leq 0.05 \tag{5.7}$$

Regarding $\eta_{H\ CHP}$ as a variable and solving (6) for PES $>$ 0 results:

$$\eta_{H\ CHP} \geq 0.47 \tag{5.8}$$

So,

$$0.47 \leq \eta_{H\ CHP} \leq 0.52 = \eta_{H\ CHP\ max} \tag{5.9}$$

This can be written as

$$0.91 \times \eta_{H\ CHP\ max} \leq \eta_{H\ CHP} \leq \eta_{H\ CHP\ max} \tag{5.10}$$

In other words, we calculated the threshold for which the PES remains positive as a function of the percentage of thermal output of the cogeneration system that should be utilized onsite. We name this parameter *TT*, whose value is 0.91 for the operation of MT in 100% load. Therefore, satisfying the PES conditions implied by Equation (5.6) indicates that at least *TT* (0.91) of the thermal output of the cogeneration system must be consumed onsite for cooling or heating purposes. Table 5.1 also shows the value of *TT* for other cogeneration technologies/part-loads and the last column of this Table displays the value we used as the input to the model for each cogeneration system.

Table 5.1: PES implication of cogeneration systems

		Cogeneration thermal efficiency	Cogeneration electrical efficiency	Reference thermal efficiency	Reference electrical efficiency	Primary Energy Savings		
		$\eta_{H\,CHP}$	$\eta_{E\,CHP}$	$\eta_{H\,Ref}$	$\eta_{E\,Ref}$	*PES*	*TT*[a]	*TT overall*[b]
MT	100% load	0.52	0.26	0.90	0.55	0.05	91%	100%
	75% load	0.56	0.24	0.90	0.55	0.06	91%	
	50% load	0.57	0.20	0.90	0.55	0.00	100%	
	25% load	0.58	0.13	0.90	0.55	-0.14	-	
SOFC	104% load	0.21	0.51	0.90	0.55	0.14	31%	50%
	100% load	0.24	0.50	0.90	0.55	0.15	34%	
	93% load	0.28	0.50	0.90	0.55	0.18	29%	
	85% load	0.30	0.49	0.90	0.55	0.18	33%	
	78% load	0.32	0.48	0.90	0.55	0.19	36%	
	68% load	0.35	0.45	0.90	0.55	0.17	47%	
	62% load	0.37	0.44	0.90	0.55	0.17	49%	
ICE	100% load	0.55	0.33	0.90	0.55	0.18	64%	77%
	75% load	0.58	0.30	0.90	0.55	0.16	70%	
	50% load	0.6	0.26	0.90	0.55	0.13	77%	

[a] TT for cogeneration at part-load p.

[b] Value of TT (percentage of the thermal output of cogeneration technology that must be consumed onsite) that is used for each cogeneration technology regardless of part-load.

Policy framework for PV systems in Portugal

In Portugal, the generation of electricity from PV sources is mainly promoted through a guaranteed Feed-in Tariff (FIT). A new FIT for the installation of PV systems took off in 2011 with the publication of decree-law 34/2011 (2011). The value of FIT for 2013, in effect for 15 years, is initially set to 0.151 €/kWh with 30% annual reduction (Administrative rule 140/2012, 2012). At least 50% of produced electrical energy by PV systems should be consumed onsite and the amount exported is limited to 2.6

MWh/year. The administrative fee to register the PV installation is set to 2000€ (Administrative rule 140/2012, 2012).

5.2 Mathematical model

The optimization model is a Mixed Integer Linear Programming (MILP) to optimize the selection of and operating strategy for DG in Portuguese commercial buildings. Continuous decision variables are used to describe the energy supplied from a particular source, e.g. the power obtained from the grid, cogeneration or PV systems at a certain time; heating obtained from the boiler cogeneration, or ST units; or cooling obtained from compression or absorption chiller. Three sets of binary variables are used to add capital costs for the energy systems, and maintain the internal consistency of the model. The model is implemented and solved in GAMS (McCarl *et al.*, 2013), using the CPLEX (2010) solver.

It is assumed that the solar and cogeneration systems reach their designed thermal and electrical efficiencies presented in chapter 3. However, in real-world problems factors such as temperature, pressure and working conditions may affect the efficiency of energy systems and introduce some nonlinear effects. The model developed in this thesis is a MILP, so it does not study the effect of these varying factors.

The main input data for the model include:

- Case-study characteristics: Power (*dZ*), heating (*dX*), and cooling demand (*dC*) for each season/block load (in *kW*).
- Economic data: Interest Rate (*% per year*), capital cost and residual value of energy systems (*€*), operating costs of the energy systems ($€/kWh_{output}$), maintenance costs of energy systems [fixed (*€/kW*) and variable ($€/kWh_{output}$)], growth/decline rate of capital and operating costs of energy systems (*% per year*).
- Environmental impact data: LCIA to produce one unit output (kWh_e for PV, grid, CHP; kWh_{th} for boilers and ST, kWh_c for AC and CC) by energy systems (IA/kWh). Four types of LCIA categories are assessed: Cumulative Energy Demand (CED), Greenhouse Gases (GHG), Acidification, and Eutrophication.

- Cogeneration systems: max power (*kW*), min power (*kW*), power-to-heat ratio, fuel (NG) consumption ($m3/kW_e$) for each operating load.
- Boiler, CC, AC: max and min operating region (*kW*), Coefficient of Performance (COP).
- Solar systems: Estimated received solar radiation by the systems (kW/m^2) and their output (kW_e and kW_{th}) for each season/block-load.

Parameters

The demand for electricity (*dZ*), heating (*dX*) and cooling (*dC*) throughout the planning period is estimated using a forecasted growth/decline rate (g_Z, g_X, g_C) with respect to the base year. The capital cost (*capcost*) and operating cost (*opcost*) for each type of generation unit (*m*) is determined using a growth/decline rate with respect to the base year, depending on the type of technology.

Variables

The decision variables assigned to solar systems determine the number of panels installed at each year throughout the planning period (i.e., PVn_t and STn_t determine the number of PV/ST panels installed in year t). For cogeneration, thermal and cooling systems the decision variables are the units installed and their output (power, thermal, or cooling), at part-load p for cogeneration systems, at each season/block-load (e.g., $z_{m,s,b,t,p}$ determines the electrical power output of cogeneration unit *m* in year *t*, season *s*, block-load *b,* part-load *p*).

Three sets of binary variables are introduced in the model to account for:

- annual recurring fixed costs (maintenance costs) associated with energy systems ($\lambda 1_{m,t}$ for unit *m* at year *t*).
- Once occurring fixed costs (capital costs) in the *first year* of employment of energy systems ($\lambda 2_{m,t}$ for unit *m* at year *t*). Index *t* of these variables denotes the installation year of unit *m.*
- Once occurring residual value in the *final year* of employment of energy systems ($\lambda 3_{m,t}$ for unit *m* at year *t*). Index *t* of these variables denotes the retirement year of unit *m.*

Other binary variables (e.g., $\lambda_{m,s,b,t,p}$) are used for model consistency purposes, such as to ensure that if a cogeneration engine is utilized it operates in one part-load only.

Objective Functions

The objective functions (Equations. A.1 and A.2) are defined to minimize the total discounted LCC or LCIA of meeting the building electrical (*dZ*), heating (*dX*), and cooling (*dC*) demand throughout the planning period. LCC comprises the Total Fixed Costs (*TFC*

including capital cost, maintenance and residual value at the end of life) related with the equipment acquisition and installation (Equation A.30), and the Total Variable Costs (*TVC* calculated by Equation A.31), related with the system operation including buying from/selling to the grid as well as variable maintenance costs. Total LCIA (Equation A.32) calculates the impact of meeting the energy demand over the defined horizon by using the energy systems defined in the model, expressed in units MJ for CED, g CO_2 eq for GHG, g SO_2 eq for Acidification, and g PO_4^{3-} eq for Eutrophication.

Constraints

Different categories of constraints are included in the model. They are classified based on their type and cross-referenced to the mathematical model that follows this section.

Demand satisfaction constraints refer to:

- Demand satisfaction for electricity, which can be supplied from the grid, three types of cogeneration systems and PV systems and should also provide running the CCs (Equation A.3).
- Demand satisfaction for heat, which can be supplied by boilers, three types of cogeneration systems and ST units, which should also provide running the AC (Equation A.4).
- Demand satisfaction for cooling, which can be supplied by AC and/or CC (Equation A.5).

Capacity constraints that are employed to:

- Certify that the power output of cogeneration systems (Equation A.6), heat output of the boiler (Equation A.7), and cooling output from the cooling systems (Equation A.8) are within the operating region of that system.
- Warrant that the power and thermal output of PV (Equation A.9) and ST panel (Equation A.10) during each season and at each block-load do not exceed the capacity of the system during the respective season and block-load.
- Limit the number of solar PV and ST installations due to area restrictions (Equation A.11).

National policy constraints that:

- Calculate the electrical energy (kWh) generated onsite that is allowed to be exported to the grid. National regulations establish that at least 50% of the produced electrical energy should be consumed onsite (Equation A.12) and the power exported must be lower than 150 kW (Equation A.13).

- Guarantee the fulfillment of the national policy conditions that TT (refer to Table 5.1) of the thermal output of the cogeneration systems must be consumed onsite (Equation A.14).

Consistency constraints guarantee the internal coherence of the model:

- Warranting that the amount of thermal output from the cogeneration systems (operating at each part-load) is correlated with their electrical output, via the introduction of "power-to-heat" ratio (Equation A.15).
- Relating the amount of cooling obtained from the AC to the energy input (i.e. thermal energy from the cogeneration systems and/or a gas boiler) by using the COP of the AC (Equation A.16).
- Relating the amount of cooling obtained from the CC to the energy input (electrical energy produced onsite or imported from grid) by using the COP of the CC (Equation A.17).
- Maintaining the required relationship between the binary variables for different generation units (Equations. A.18-26).
- Ensuring that for cogeneration systems a single part-load operating level is in use (Equation A.27).
- Establishing the continuous operation of SOFC units (Equation A.28).
- Accounting for fuel cell stack change cost (Equation A.29).

Mathematical programming model

Nomenclature

Capcost	*capital cost of generation units (€)*
Opcost	*Operating cost of generation units (€ /kW)*
OMcost	*Fixed operating and maintenance costs of generation units (annual €)*
VarOMCOST	*Variable operating and maintenance costs of generation units (€ /kWh)*
ResValue	*Residual value of generation units (€)*
opcost-g	*Rate of decrease or increase in operating costs of units (annual %)*
capcost-g	*Rate of decrease or increase in capital costs of*

	units (annual %)
IA	*LCIA of generation units (g CO2 eq/kwh for GHG; g SO_2 eq/kWh for Acidification; g PO_4^{3-} eq/kwh for Eutrophication; MJ/kWh for CED)*
Life-time	*Life-time of generation units (years)*
Mincap	*Minimum capacity of the generation units (kW)*
Maxcap	*Maximum capacity of generation units (kW)*
PHratio	*Power-to-heat ratio of cogeneration units*
COP	*Coefficient of performance (COP)*
dX	*Heat demand of case-study building (kW)*
dZ	*Electricity demand of the case study building (kW)*
dC	*Cooling demand of the case study building (kW)*
Duration	*Duration of demand block (hours)*
Δ	*discount factor*
Ir	*Interest rate (annual %)*
g_Z	*Electricity demand growth rate (annual %)*
g_X	*Heat demand growth rate (annual %)*
g_C	*Cooling demand growth rate (annual %)*
M	*Set of generation units. M = { mPV, mST, mSOFC, mMT, mICE , boiler,mCC, mAC}*
T	*Set of years. T= { 1,2,3,…,n}*
S	*Set of seasons. S = {hot, mild, cold}*
B	*Set of demand block-loads. B = {peak, high, medium, low}*
E	*Set of LCIA categories. E = {CED, GHG, Acidification, Eutrophication}*

Indexes	
t	*Index number for the year, t* ∈ T
s	*Index for the season, s* ∈ S
b	*Index for demand block-load, b* ∈ B
p	*Index for part-load performance of the cogeneration system, p* ∈ *(p1,p2,p3, ..., p7)*
e	*Index for LCIA categories, e* ∈ E
m	*Index for the generation units, m* ∈ M
mPV	*Index for solar PV systems, mPV* ∈ *{mPV-1, mPV-2,… mPV-20}*
mST	*Index for solar thermal systems, mST* ∈ *{mST-1, mST-2,… mST-20}*
mSOFC	*Index for SOFC unit, mSOFC* ∈ *{SOFC-1, SOFC-2,…SOFC-5}*
mICE	*Index for ICE units, mICE* ∈ *{ICE-1, ICE-2,…ICE-5}*
mMT	*Index for MT units, mMT* ∈ *{MT-1, MT-2, … MT-5}*
boiler	*Index for the boiler*
grid	*Index for the national grid*
mAC	*Index for the AC units, mAC* ∈ *{AC-1, AC-2}*
mCC	*Index for the CC units, mCC* ∈ *{CC-1, CC-10}*
Parameters	
$dZ_{s,b,t}$	*Power (electricity) demand by season, block, year (kW)*
$dX_{s,b,t}$	*Heat demand by season, block, year (kW)*
$dC_{s,b,t}$	*Cooling demand by season, block, year (kW)*
$Duration_{s,b}$	*Duration of demand block b in season s (hours)*

$opcost_{m,t}$	*Operating cost of unit m in year t (€/ kWh), m ∈ {boiler, mCC, mAC}, t ∈* T
$opcost_{m,t,p}$	*Operating cost of the cogeneration unit m at year t operating at part-load p (€/kWh$_e$), m ∈ {mMT, mSOFC, mICE}. p ∈ {p1, … , p3}* for ICE, *p ∈ {p1, … , p4}* for MT, *p ∈ {p1, … , p7}* for SOFC
$opcost_{grid,s,b,t}$	*Operating cost of grid in year t, season s, block-load b (€/kWh)*
$sellcost_{s,b,t}$	*Price of selling electricity to the grid in year t, season s, block-load b (€/kWh)*
$capcost_{m,t}$	*capital cost of unit m in year t* (€), *m ∈* M
$ResValue_{m,t}$	*Residual value of unit m in year t* (€)*, m ∈* M
Δ_t	*Discount factor for year t*
$Life\text{-}time_m$	*Life-time of unit m (years), m ∈* M
$zPV_{mPV,s,b,t}$	*Power output of a 4 kW PV system at year t, season s, block-load b (kW per panel)*
$xST_{mST,s,b,t}$	*Heat output of a 4 kW solar thermal system in year t, season s, block-load b (kW per unit)*
$mincap_m$	*Minimum capacity of unit type m (kW), m ∈ {boiler, mCC, mAC}*
$maxcap_m$	*Maximum capacity of unit type m (kW), m ∈ {boiler, mCC, mAC}*
$mincap_{m,p}$	*Minimum capacity of cogeneration system m at part-load p (kW$_e$), m ∈ {mMT,mSOFC, mICE}*
$maxcap_{m,p}$	*Maximum capacity of cogeneration system m at part-load p (kW$_e$), m ∈ {mMT,mSOFC, mICE}*
$maxcap_{m,s,b}$	*Maximum capacity of solar (PV, ST) panels during season s, block-load b (kW/unit), m ∈ {mPV,mST}*
$max\_power\_output_m$	*Maximum power output of cogeneration units (kW), m ∈ {mMT,mSOFC, mICE}*

$max\_annual\_power\_output_m$	*Maximum annual energy output of unit m (kWh), m ∈ {mCC, boiler, mAC}*
Max_Panel	*Maximum number of solar PV and ST panels allowed to be installed due to area constraints.*
$PHratio_{m,p}$	*Power-to-heat ratio of cogeneration m at part-load p, m ∈ {mMT, mSOFC, mICE}*
TT_m	*The percentage of the thermal output (kW) of the cogeneration systems that should be consumed onsite to meet the national regulations, m ∈ {mMT, mSOFC, mICE}*
COP_{AC}	*COP for AC: ratio relating the cooling output to the heat input*
COP_{CC}	*COP for CC : ratio relating the cooling output to the electrical power input*
$Opcost\text{-}rate_m$	*Rate of decrease or increase in operating cost of unit m (annual %)*
$capcost\text{-}rate_m$	*Rate of decrease or increase in capital cost of unit m (annual %)*
$IA_{e,m,p}$	*Impact Assessment (IA) of generation units, e ∈ E, m ∈ M, p ∈ { p1, … , p3}* for ICE, *p ∈ { p1, … , p4}* for MT, *p ∈ { p1, … , p7}* for SOFC
Variables	
LCC	*Total discounted life-cycle costs (€)*
TFC_t	*Total fixed costs in year t (€)*
TVC_t	*Total variable costs in year t (€)*
$LCIA_e$	*Total LCIA category e during the planning period (MJ for CED, g CO_2 eq for GHG; g SO_2 eq for Acidification; g PO_4^{3-} eq for Eutrophication;), e ∈ E*
$TIA_{e,t}$	*Total environmental impacts of type e in year t (MJ for CED; g CO_2 eq for GHG; g SO_2 eq for Acidification; g PO_4^{3-} eq for Eutrophication), e ∈ E*

$x_{m,s,b,t}$	*Heat output of unit m in year t, season s, block-load b (kW), m∈{ mMT, mSOFC, mICE, boiler}*
$z_{grid,s,b,t}$	*Power purchased from grid in year t, season s, block-load b (kW)*
$y_{grid,s,b,t}$	*Power sold to grid in year t, season s, block-load b (kW)*
$z_{m,s,b,t,p}$	*Power output of cogeneration unit m in year t, season s, block-load b (kW), part-load p, m∈{ mMT, mSOFC, mICE}.*
$z_{mCC,s,b,t}$	*Power required to run the CC in year t, season s, block-load b (kW)*
$x_{mAC,s,b,t}$	*Heat required to drive the AC to supply the cooling demand in year t, season s, block-load b (kW)*
$aPVn_t$	*Total number of PV systems installed prior to year t*
PVn_t	*Number of PV panels installed in year t*
$aSTn_t$	*Total number of ST systems installed prior to year t*
STn_t	*Number of ST systems installed in year t*
$\lambda_{m,s,b,t,p}$	*Binary variable for cogeneration units to limit their part-load operation, m ∈ {mMT, mSOFC, mICE}.*
$\lambda 1_{m,t}$	*Binary variable for the units to add the annual recurring (maintenance) fixed costs, m* ∈ M, *t* ∈ T
$\lambda 2_{m,t}$	*Binary variable for the units to add the once occurring fixed (capital) costs, m* ∈ M, *t* ∈ T
$\lambda 3_{m,t}$	*Binary variable for the units to add the once occurring fixed residual value, m* ∈ M, *t* ∈ T
$\lambda 4_{mSOFC,t}$	*Binary variable to add the once occurring fuel cell stack change maintenance cost, t* ∈ T

Mathematical programming Model

Parameters Calculation

Parameters serve as inputs to the mathematical model. The value of parameters (e.g. capital costs or operating costs) for each year of the planning period can be defined with reference to the base-year of the study, as following:

$$dX_{s,b,t+1} = dX_{s,b,t} \times (1 + g_X)^{(t-1)} \quad (5.11)$$
$$dZ_{s,b,t+1} = dZ_{s,b,t} \times (1 + gZ)^{(t-1)} \quad (5.12)$$
$$dC_{s,b,t+1} = dC_{s,b,t} \times (1 + g_C)^{(t-1)} \quad (5.13)$$

($t \in T$; $s \in S$; $b \in B$)

The above relations calculate the demand for electricity (*dZ)*, heat (*dX)* and cooling (*dC)* throughout the planning period. The parameters g_Z, g_X, g_C represent the electricity, heating and cooling demand growth rate, respectively.

$$\Delta_t = (1+ir)^{(t-1)} \quad (5.14)$$
($t \in T$)

Equation (5.14) calculates the discount factor (Δ_t) for the planning period years. The parameter *ir* corresponds to the interest rate.

$$capcost_{m,t+1} = capcost_{m,t} \times (1 + capcost\text{-}rate_m)^{(t)} \quad (5.15)$$

$m \in \{ mPV, mST, mSOFC, mMT, mICE, mCC, boiler, mAC, grid \}$, $t \in \{1,2, \ldots, n-1\}$

The above relations calculate the capital cost of the generating units for each year of the planning period, considering the respective capital cost growth/decline rate for each type of generation unit *m*. Capital cost of the unit *m* in year *t+1* ($capcost_{m,t+1}$) is equal to the capital cost of the unit in year *t* ($capcost_{m,t}$) multiplied by the capital cost growth/decline rate of unit *m* ($capcost\text{-}rate_m$).

$$opcost_{mICE,t+1,p} = opcost_{mICE,t,p} \times (1 + opcost\text{-}rate_{mICE})^{(t)} \quad (5.16)$$

($s \in S$; $b \in B$; $p \in \{ p1, \ldots, p3\}$; $t \in \{1,2, \ldots, n-1\}$)

$$opcost_{mMT,t+1,p} = opcost_{mMT,t,p} \times (1 + opcost\text{-}rate_{mMT})^{(t)} \quad (5.17)$$

($s \in S$; $b \in B$; $p \in \{ p1, \ldots, p4\}$; $t \in \{1,2, \ldots, n-1\}$)

$$opcost_{mSOFC,t+1,p} = opcost_{mSOFC,t,p} \times (1 + opcost\text{-}rate_{mSOFC})^{(t)} \quad (5.18)$$

($s \in S$; $b \in B$; $p \in \{p1, \ldots, p7\}$; $t \in \{1,2, \ldots, n-1\}$)

$$opcost_{grid,s,b,t+1} = opcost_{grid,s,b,t} \times (1 + opcost\text{-}rate_{grid})^{(t)} \quad (5.19)$$

($s \in S$; $b \in B$; $t \in \{1,2, \ldots, n-1\}$)

$$Opcost_{m,t+1} = opcost_{m,t} \times (1 + opcost\text{-}rate_{m})^{(t)} \quad (5.20)$$

(m $\in$ {*mCC*, *boiler*, *mAC* }; $t \in \{1,2, \ldots, n-1\}$)

The above relations calculate the operating cost of the generating units *m* throughout the planning period, with regards to their operating cost growth/decline rate. Operating cost of the unit *m* in year *t+1* ($opcost_{m,t+1}$) is equal to the operating cost of the unit in year *t* ($opcost_{m,t}$) multiplied by the operating cost growth/decline rate of unit *m* ($opcost\text{-}rate_m$). Please note that the price of electricity purchased from grid varies over different seasons/blocks (Equation 5.19).

Objective Functions

$$Min \{LCC = \sum_{t=1}^{n} [\Delta_t \times (TFC_t + TVC_t)]\} \quad (A.1)$$

$$Min \{LCIA_e = \sum_{t=1}^{n} (TIA_{e,t}) \} \quad (A.2)$$

($e \in E$)

The objective functions are defined to minimize the total discounted LCC or LCIA (CED, GHG, Acidification, Eutrophication) of meeting the building energy demand. Total cost of year *t* comprises of Total Fixed Costs (*TFC*) and Total Variable Costs (*TVC*) and *LCC* is the discounted sum of the total annual costs over the time horizon of the study (*n* years). The parameter Δ_t is the discount factor for year *t*. LCIA type *e* of meeting the building energy demand over the planning horizon is the sum of LCIA of individual years *t (TIA)*.

Constraints

$$\sum_{p=p1}^{p3} \sum_{mICE} z_{mICE,s,b,t,p} + \sum_{p=p1}^{p4} \sum_{mMT} z_{mMT,s,b,t,p} + \sum_{p=p1}^{p7} \sum_{mSOFC} z_{mSOFC,s,b,t,p} + z_{grid,s,b,t} + (PVn_t + aPVn_t) \times zPV_{mPV,s,b,t} = dZ_{s,b,t} + z_{mCC,s,b,t,p} + y_{grid,s,b,t} \quad (A.3)$$

($s \in S$; $b \in B$; $t \in T$)

At each *s,b,t*, the power provided by grid ($z_{grid,s,b,t}$), cogeneration systems (MT: $z_{mMT,s,b,t,p}$; ICE: $z_{mICE,s,b,t,p}$; SOFC: $z_{mSOFC,s,b,t,p}$) and PV systems [$(PVn_t + aPVn_t) \times zPV_{mPV,s,b,t}$] must meet the power demand of the building and should be enough to provide the power needed ($z_{mCC,s,b,t,p}$) to run the CC.

$$\sum_{mICE} x_{mICE,s,b,t} + \sum_{mMT} x_{mMT,s,b,t} + \sum_{mSOFC} x_{mSOFC,s,b,t} + (STn_t + aSTn_t) \times xST_{mST,s,b,t} + x_{boilers,b,t} \geq dX_{s,b,t} + x_{mAC,s,b,t} \quad (A.4)$$

($s \in S$; $b \in B$; $t \in T$)

The heat provided by ICE units ($x_{mICE,s,b,t}$),MT units ($x_{mMT,s,b,t}$), SOFC units ($x_{mSOFC,s,b,t}$), the boiler ($xBoiler_{s,b,t}$), and ST systems must meet the heat demand of the building and should be enough to run the AC at each *s,b,t*. $(STn_t + aSTn_t)$ represents the total number of solar thermal units installed and operating in year t.

$$\sum_{mCC} c_{mCC,s,b,t} + \sum_{mAC} c_{mAC,s,b,t} = dC_{s,b,t} \quad (A.5)$$

($t \in T$; $s \in S$; $b \in B$)

The cooling provided by AC ($c_{mAC,s,b,t}$) and CC ($c_{mCC,s,b,t}$) at each *s,b,t* must meet the cooling demand ($dC_{s,b,t}$) of the building.

$$mincap_{m,p} \leq z_{m,s,b,t,p} \leq maxcap_{m,p} \quad (A.6)$$

m $\in$ { *mSOFC*, *mMT*, *mICE* }; $t \in T$; $s \in S$; $b \in B$, $p \in$ { *p1, … , p3*} for ICE, $p \in$ { *p1, … , p4*} for MT, $p \in$ { *p1, … , p7*} for SOFC

$$mincap_{boiler} \leq x_{boilers,b,t} \leq maxcap_{boiler} \quad (A.7)$$

($s \in S$; $b \in B$; $t \in T$)

$$mincap_{m} \leq c_{m,s,b,t} \leq maxcap_{m} \quad (A.8)$$

$$m \in \{mCC, mAC\}, (s \in S; b \in B; t \in T)$$

Above constraints are employed to guarantee that at each *s,b,t*, the power output of cogeneration systems, heat output of the boiler and cooling output from AC and CC are within the operating region of that system.

$$zPV_{mPV,s,b,t} \leq maxcap_{mPV,s,b} \quad (A.9)$$

$$xST_{mST,s,b,t} \leq maxcap_{mST\,s,b} \quad (A.10)$$

$$(s \in S; b \in B; t \in T)$$

Constraints (A.9) and (A.10) warrant that the power output of each PV/ST system during each block-load is not higher than the capacity of the system during the respective block-load.

$$\sum_t PVn_t + STn_t \leq Max\_Panel \quad (A.11)$$

Constraint (A.11) limits the number of PV and ST installations due to area restrictions.

$$\sum_{s,b} y_{grid,s,b,t} \times Duration_{s,b} \leq \sum_{s,b} Duration_{s,b} \times [\sum_{p=p1}^{p3} \sum_{mICE} z_{mICE,s,b,t,p} + \sum_{p=p1}^{p4} \sum_{mMT} z_{mMT,s,b,t,p} + \sum_{p=p1}^{p7} \sum_{mSOFC} z_{mSOFC,s,b,t,p} + (PVn_t + aPVn_t) \times zPV_{mPV,s,b,t}] \times 0.5 \quad (A.12)$$

$$y_{grid,s,b,t} \leq 150 \quad (A.13)$$

$$(t \in T; s \in S; b \in B)$$

Based on Portuguese regulation, the electrical energy (kWh) allowed to be exported to grid should be less than half of onsite production (A.12) and its power should be less than 150 kW (A.13).

$$TT_m \times \sum_{m,t} x_{m,s,b,t} \leq dX_{s,b,t} + \sum_{mAC} x_{mAC,s,b,t} \quad (A.14)$$

$$m \in \{mSOFC, mMT, mICE\}; (t \in T; s \in S; b \in B)$$

At least *TT* of the thermal output of the cogeneration units must be consumed onsite to provide PES compared to separate production of heat and electricity. The above

constraint certifies the fulfillment of this condition, where the thermal output of the cogeneration systems can be used to run the AC or for direct heating purposes.

$$x_{m,s,b,t} = z_{m,s,b,t,p} / PHratio_{m,p} \quad (A.15)$$

m ∈ { *mSOFC*, *mMT*, *mICE* }; $t \in T$; $s \in S$; $b \in B$;$p \in$ { *p1, … , p3*} for ICE, $p \in$ { *p1, … , p4*} for MT, $p \in$ { *p1, … , p7*} for SOFC

The above equation guarantees that the amount of thermal output from the cogeneration systems operating at part-load *p* at each *s,b,t,* is correlated to their electrical output, via the introduction of "Power-to-heat ratio".

$$c_{mAC,s,b,t} = x_{mAC,s,b,t} \times COP_{AC} \quad (A.16)$$

($s \in S$; $b \in B$; $t \in T$)

Equation (A.16) relates the amount of cooling obtained from the AC ($c_{mAC,s,b,t}$) to the energy input (thermal energy from a gas boiler or the cogeneration systems; $x_{mAC,s,b,t}$) by using the COP of AC.

$$c_{CC,s,b,t} = z_{CC,s,b,t} \times COP_{CC} \quad (A.17)$$

($s \in S$; $b \in B$; $t \in T$)

Above equation relates the amount of cooling obtained from CC ($c_{CC,s,b,t}$) to the energy input (power produced by the cogeneration systems, PV system and/or grid; $z_{CC,s,b,t}$) by using the COP of the CC.

$$z_{m,s,b,t,p} \leq maxcap_{m,p} \times \lambda_{m,s,b,t,p} \quad (A.18)$$

m ∈ { *mSOFC*, *mMT*, *mICE* }; $t \in T$; $s \in S$; $b \in B$, $p \in$ { *p1, … , p3*} for ICE, $p \in$ { *p1, … , p4*} for MT, $p \in$ { *p1, … , p7*} for SOFC

The above binary variables for cogeneration systems (MT: $\lambda_{mMT,s,b,t,p}$, ICE: $\lambda_{mICE,s,b,t,p}$, SOFC: $\lambda_{mSOFC,s,b,t,p}$) are employed in consequent equations to ensure that, at each *s,b,t* a single part-load operating level is in use for each MT, ICE and SOFC, respectively. These variables get a value of one when an engine is on; operating at part-load *p* and otherwise zero.

$$\lambda_{m,s,b,t,p} \leq \lambda 1_{m,t} \quad (A.19)$$

m ∈ { *mSOFC*, *mMT*, *mICE* }; $t \in$ T; $s \in$ S; $b \in$ B, $p \in$ { *p1, … , p3*} for ICE, $p \in$ { *p1, … , p4*} for MT, $p \in$ { *p1, … , p7*} for SOFC

At *each* year, if a cogeneration unit *m* is operating (engine is on), the $\lambda 1_{m,s,b,t,p}$ variable gets a value of one. This type of binary is employed to add the *annual* recurring fixed maintenance costs to the total costs.

$$\sum_{s,b} \quad c_{m,s,b,t} \leq maxcap_m \times \lambda 1_{m,t} \quad (A.20)$$

m ∈ {*mCC*, *mAC* }, ($t \in$ T*)*

$$\sum_{s,b} \quad x_{boilers,b,t} \leq maxcap_{boiler} \times \lambda 1_{boiler,t} \quad (A.21)$$

($t \in$ T*)*

The above equations are formulated to introduce the binary variables $\lambda 1_{mCC,t}$, $\lambda 1_{mAC,t}$ and $\lambda 1_{boiler,t}$ for respectively CC*,* AC, and the boiler. For each *t*, these variables get a value of one if the respective engine is on. This type of binary variable is employed to account for *annual* recurring maintenance costs to the total costs.

$$\lambda 1_{m,t+1} = \lambda 1_{m,t} + \lambda 2_{m,t+1} - \lambda 3_{m,t+1} \quad (A.22)$$

($m \in$ M), (t = 1,… , 10)

$$\lambda 1_{m,t} = \lambda 2_{m,t+1} \quad (A.23)$$

($m \in$ M), (t = 1)

Equations (A.22-23) are used to construct a set of variables ($\lambda 2_{m,t}$) to account for capital costs of generating units. If unit *m* is installed in year *t*, $\lambda 2_{m,t}$ = 1. For the first year (t=1), a slightly different formulation is required (A.23*).*

$$\lambda 3_{m,t} = \lambda 2_{m,t+life\text{-}time\ m} \quad (A.24)$$

($m \in$ M), ($t \in$ T)

Equation (A.24) is to construct ($\lambda 3_{m,t}$) binary variables to account for residual value of the generating units at their retirement year. Variable $\lambda 3_{m,t}$ gets a value of one in the retirement year of the unit *m*.

$$\sum_t \quad \lambda 3_{m,t} \leq 1 \qquad (A.25)$$

($m \in$ M), ($t \in$ T)

$$\lambda 3_{m,t} = 0 \qquad (A.26)$$

($m \in$ M), *(t = 1)*

The above constraints are formulated to maintain the internal consistency of the model.

$$\sum_{p \in} \quad \lambda_{m,s,b,t,p} \leq 1 \qquad (A.27)$$

m ∈ { *mSOFC*, *mMT*, *mICE* }; $t \in$ T; $s \in$ S; $b \in$ B, $p \in$ { *p1, … , p3*} for ICE, $p \in$ { *p1, … , p4*} for MT, $p \in$ { *p1, … , p7*} for SOFC

Using the binary variables constructed through Equation (A.18), the above constraints warrant that at each *s,b,t*, if a cogeneration operates, it operates only at one part-load.

$$\lambda 1_{mSOFC,t} = \sum_{p \in \{p1,\dots,p7\}} \quad \lambda_{mSOFC,s,b,t,p} \qquad (A.28)$$

($s \in$ S; $b \in$ B*; t* ∈ T)

Due to their time-consuming start-up (more than 8 hours), SOFC engines are constrained to operate continuously through Equation (A.28).

$$\lambda 4_{mSOFC,t} = \lambda 2_{mSOFC,t+4} \qquad (A.29)$$

($t \in$ T)

Constraint (A.29) is formulated to account for the fuel cell stack change cost that occurs once per the life-time of the SOFC engines.

$$TFC_t = \sum_{mMT} (\lambda 2_{mMT,t} \times capcost_{mMT,t} + \lambda 1_{mMT,t} \times OMcost_{mMT,t} - \lambda 3_{mMT,t} \times ResValue_{mMT,t}) + \sum_{mICE} (\lambda 2_{mICE,t} \times capcost_{mICE,t} + \lambda 1_{mICE,t} \times OMcost_{mICE,t} - \lambda 3_{mICE,t} \times ResValue_{mICE,t}) + \sum_{mSOFC} (\lambda 2_{mSOFC,t} \times capcost_{mSOFC,t} + \lambda 1_{mSOFC,t} \times OMcost_{mSOFC,t} - \lambda 3_{mSOFC,t} \times ResValue_{mSOFC,t}) + \sum_{mCC} (\lambda 2_{mCC,t} \times capcost_{mCC,t} + \lambda 1_{mCC,t} \times OMcost_{mCC,t} - \lambda 3_{mCC,t} \times$$

$ResValue_{mCC,t}) + \sum_{mAC} (\lambda 2_{mAC,t} \times capcost_{mAC,t} + \lambda 1_{mAC,t} \times OMcost_{mAC,t} - \lambda 3_{mAC,t} \times ResValue_{mAC,t}) + (\lambda 2_{boiler,t} \times capcost_{boiler,t} + \lambda 1_{boiler,t} \times OMcost_{boiler,t} - \lambda 3_{boiler,t} \times ResValue_t) + \sum_{mPV} (PVn_t \times capcost_{mPV,t}) + (PVn_t + aPVn_t) \times OMcost_{mPV,t} + \sum_{mST} (STn_t \times capcost_{mST,t}) + (STn_t + aSTn_t) \times OMcost_{mST,t}$ *(A.30)*

($t \in T$)

Equation (A.30) calculates the total discounted fixed annual cost (€) of the energy systems. The three types of binary variables are employed to add the annual recurring maintenance costs ($\lambda 1_{m,t}$), capital costs ($\lambda 2_{m,t}$), and residual value ($\lambda 3_{m,t}$).

$TVC_t = \sum_{mMT,p}^{p4} \sum_{s,b} ((opcost_{mMT,t,p} + VarOMCost_{mMT,t}) \times Duration_{s,b} \times z_{mMT,s,b,t,p}) + \sum_{mICE,p}^{p3} \sum_{s,b} ((opcost_{mICE,t,p} + VarOMCost_{mICE,t}) \times Duration_{s,b} \times z_{mICE,s,b,t,p}) + \sum_{mSOFC,p}^{p7} \sum_{s,b} ((opcost_{mSOFC,t,p} + VarOMCost_{mSOFC,t}) \times Duration_{s,b} \times z_{mSOFC,s,b,t,p}) + \sum_{season,b} (opcost_{grid,s,b,t} \times Duration_{s,b} \times Z_{grid,s,b,t}) + \sum_{season,b} (opcost_{boiler,t} \times x_{boilers,b,t} \times Duration_{s,b}) + \sum_{mCC} \sum_{s,b} (opcost_{mCC,t} \times Duration_{s,b} \times c_{mCC,s,b,t}) + \sum_{s,b} (opcost_{mAC,t} \times Duration_{s,b} \times c_{mAC,s,b,t}) - \sum_{s,b} (y_{grid,s,b,t} \times Duration_{s,b} \times sellcost_{s,b,t})$

(A.31), ($t \in T$)

Equation (A.31) calculates the total discounted operating and variable maintenance costs for the year *t*. This is calculated by multiplying the output of each unit (in kW) into the duration (hours) of the period of operation into the respective operating and variable maintenance costs (both in €/kWh) of that unit in year t.

$TIA_{e,t} = \sum_{mMT} \sum_{p}^{p4} \sum_{s,b} (IA_{e,mMT,p} \times Duration_{s,b} \times z_{mMT,s,b,t,p}) + \sum_{mICE} \sum_{p}^{p3} \sum_{s,b} (IA_{e,mICE,p} \times Duration_{s,b} \times z_{mICE,s,b,t,p}) + \sum_{mSOFC} \sum_{p}^{p7} \sum_{s,b} (IA_{e,mSOFC,p} \times Duration_{s,b} \times z_{mSOFC,s,b,t,p}) + (\sum_{season,b} (IA_{e,grid} \times Duration_{s,b} \times Z_{grid,s,b,t}) + \sum_{season,b} (IA_{e,boiler} \times x_{boilers,b,t} \times Duration_{s,b}) + \sum_{mCC} \sum_{s,b} (IA_{e,CC} \times Duration_{s,b} \times c_{mCC,s,b,t}) + \sum_{mAC} \sum_{s,b} (IA_{e,AC} \times Duration_{s,b} \times c_{mAC,s,b,t}) - \sum_{s,b} (IA_{e,grid} \times y_{grid,s,b,t} \times Duration_{s,b})$ *(A.32)*

($t \in T$, $e \in E$)

Equation (A.32) calculates the annual LCIA (type *e*) of meeting the building energy demand over the planning horizon. Similar to calculation of operating costs, impacts are calculated by multiplying the output of each unit (in kW) into duration (hours) of period of operation into its respective impact (IA/kWh) of unit in year t.

5.3 Case-study

The case study for the implementation of the proposed methodology is a 133 room hotel complex located in Coimbra, Portugal. Electricity consumption of the complex was measured at 15 minutes interval and used to generate the power load demand of the building. Hourly heating and cooling demands were also calculated using building simulation and calibrating the simulation results with the historical energy consumption data of the building. To build up a load diagram, the year was divided into three seasons, Hot (H), Mild (M) and Cold (C), therefore considering the varied output profile of the solar units along the year. The months November, December and January comprised the cold season whereas June, July and August were considered as hot season. The rest of the months were regarded as mild season. Each season possesses a load duration curve (LDC) for each type of cooling, heating and power demand with 7 block-loads: peak1 (P1), peak2 (P2), high1 (H1), high2 (H2), medium1 (M1), medium2 (M2) and low (L). The block-loads were defined with some adjustments in a way to represent the hours for which the price of buying electricity from grid changes and therefore at each of the 4 groups of loads (Peak, High, Medium, Low) the price of purchasing electricity from the grid is constant and different from the rest. Table 5.4 displays the case-study demand data.

Estimation of case-study solar energy potential

In order to estimate the output of Solar PV and thermal systems for case-study, we employed two different tools. As for ST systems, we used the web-application Satel-Light (2012) to estimate the hourly available solar radiation and calculated the output of the system using a simplified approach (ESTIF, 2007). As for the PV systems, the web-application NREL's PVWATTS (PVWATTS, 2011) was used and is discussed next.

PV systems

By selecting the location of the study, the PVWATTS application (2011) yields the hour-by-hour estimated power output of the crystalline silicon PV systems according to the settings defined by the user. The settings comprise the size of the system, tilt angle, azimuth angle and array type (fixed, 1 axis tracking or 2-axis tracking). These values, PV system specifications and the site location details for the current site are shown in

Table 5.2. The expected life-time of the PV system is 20 years, with an annual performance degradation of 0.5% (≈10% overall reduction in year 20) (Denholm *et al.*, 2009), as previously mentioned in chapter 3, section 3.3.

Table 5.2: Site location data for PV system (PVWATTS, 2011)

Site Location		**PV System Specifications**	
City	Coimbra	**DC Rating (kW)**	4.0
Country/Province	Portugal	**DC to AC Derate Factor:**	0.77
Latitude	40.20°N	**Array Type**	Fixed
Longitude	8.42°W	**Array Tilt**	40.20
Elevation	140 m	**Array Azimuth**	180

ST systems

Referring to ST systems, the power output of collectors is calculated as (ESTIF, 2007):

$$P = A \times G \times \eta \tag{5.21}$$

where

$P =$ thermal output of solar collector (W);

$G =$ solar irradiation (W/m^2);

$A =$ collector area (m^2);

$\eta =$ solar thermal collector efficiency.

The collector efficiency, η, is estimated using Equation (5.22).

$$\eta = \eta_0 - a_1 \times (T_m - T_a)/G - a_2 \times (T_m - T_a)^2/G \tag{5.22}$$

where

$T_a =$ ambient air temperature (K);

$T_m =$ collector mean temperature (K);

$\eta_0 =$ Zero-loss efficiency;

$a_1 =$ First order heat loss coefficient (W/Km²)

$a_2 =$ Second order heat loss coefficient (W/K^{2}m²)

We used the typical efficiency values of solar thermal glazed collectors and hourly solar radiation (from Satel-Light, 2012) and hourly ambient temperature data to calculate the efficiency of the collector at each time period. To simplify the calculation, as recommended by ESTIF (2007), the collector mean temperature T_m is assumed constant all the time. This value and the efficiency values used to estimate the output (kW) of ST collectors are shown in Table 5.3. Knowing η and G at each time period, the potential thermal power output of a square meter ST system at each block-load can be calculated. The collector efficiency and the output of a 4kW ST system are shown in Table 5.4.

Table 5.3: Efficiency parameters of ST systems

Solar Thermal systems	
Solar Thermal type	Glazed flat plate collectors
Zero-loss efficiency (η_0)	0.78
first order heat loss coefficient (a_1)	3.2 W/(K×m²)
second heat loss coefficient (a_2)	0.015 W/(K²×m²)
collector mean temperature (T_m)	50^o C (323 K)

Table 5.4: Case-study demand characteristic and estimation of solar potential

Block-load	Index	Duration	Power demand	Heat Demand	Cooling demand	Grid Electricity	ST efficiency	PV output	ST output
		(hrs / yr)	(kW)	(kW)	(kW)	(€/kWh)	%	kW	kW
Hot.peak1	H P1	276	369	0	101	0.2103	0.64	1.69	1.68
Hot.peak2	H P2	276	460	0	106	0.2103	0	0.17	0
Hot.high1	H H1	184	366	0	71	0.1136	0.35	0.8	0.37
Hot.high2	H H2	552	389	0	122	0.1136	0.63	1.02	1.55
Hot.medium1	H M1	184	293	9	25	0. 0757	0	0.14	0
Hot.medium2	H M2	368	363	0	51	0. 0757	0	0	0
Hot.low	H L	368	239	16	23	0. 0704	0	0	0
Mild.peak1	M P1	543	305	86	37	0.2103	0.59	1.72	1.44
Mild.peak2	M P2	543	378	92	52	0.2103	0	0	0
Mild.high1	M H1	362	303	120	28	0.1136	0.29	0.8	0.31
Mild.high2	M H2	1086	306	64	50	0.1136	0.52	1.17	0.9
Mild.medium1	MM1	362	230	133	1	0. 0757	0	0	0
Mild.medium2	MM2	724	287	101	45	0. 0757	0	0.1	0
Mild.low	M L	724	165	132	9	0. 0704	0	0	0
Cold.peak1	C P1	184	284	153	0	0.2103	0.42	1.31	0.69
Cold.peak2	C P2	184	329	107	0	0.2103	0	0	0
Cold.high1	C H1	644	271	97	0	0.1136	0.41	1.35	0.61
Cold.high2	C H2	184	342	123	0	0.1136	0	0	0
Cold.medium1	C M1	276	230	206	0	0. 0757	0	0.06	0
Cold.medium2	C M2	368	249	164	0	0. 0757	0	0	0
Cold.low	C L	368	153	191	0	0. 0704	0	0	0

5.4 Multi-objective framework

In multi-objective problems, since the objective functions are often conflicting, there is no single optimal solution that simultaneously optimizes all the objective functions. Therefore, the notion of optimal solutions is replaced with that of efficient or Pareto optimal solutions. The efficient (Pareto optimal, non-dominated) solutions are solutions that cannot be improved in one objective function without deteriorating their performance in at least one of the rest. Efficient solutions are usually graphed as Pareto optimal frontiers.

In order to enumerate the efficient solutions for our multi-objective problem, which consists of design and operation of t DG for commercial buildings according to cost and environmental criteria, we have used the algorithm presented by Sylva & Crema (2004; 2007). Consider a typical multi-objective mathematical modeling problem as following,

$$\begin{gathered} \text{Min } Z_l \\ l = 1,..,P \\ s.t: Ax \leq b \\ L \leq x \leq U \end{gathered} \tag{5.23}$$

where we have p objective functions. The algorithm consists of repeatedly solving a more constrained version of the original multi-objective problem to generate a new efficient solution at each step. This is done by adding the following constraints to the model:

$$\begin{gathered} Z_l^n \leq \left(Z_l^{n-1} - \delta_l\right) \times Q_l + M_l \times (1 - Q_l) \\ l = 1,..,P \\ \sum_{l=1}^{P} Q_l \geq 1 \\ Q_l \in \{0,1\},\ \delta_l \geq 0, l = 1,..,P \end{gathered} \tag{5.24}$$

In expression (5.24), Z_l^n is the value of the lth objective function in iteration *n*, Z_l^{n-1} is the value of the lth objective function in iteration n-1, δ_l is a parameter (defined by

the user) that determines the minimum (absolute) step of improvement of lth objective function, Q_l are binary variables and M_l is the highest feasible bound for the lth objective function. The set of expression (5.24) implies that, at each iteration, the value of at least one of the objective functions should be improved by no less than its step value δ_l**.** Based on the chosen step value, a series of progressively more constrained version of the model is built and solved until the problem becomes infeasible. For further details on the model applications refer to Sylva & Crema (2004). The algorithm was implemented in GAMS (McCarl *et al.*, 2013) to generate the non-dominated Pareto frontiers for LCC and LCIA, presented in chapter 6.

5.5 Summary

This chapter presented the multi-objective mathematical model developed for the optimization of operation of DG in Portugal. The case-study to implement the proposed model, and the procedure followed to calculate the output of energy systems for the case-study building were also discussed. Finally, the algorithm implemented in GAMS (McCarl *et al.*, 2013) to calculate the Pareto frontiers was presented. The results of implementation of the proposed model are discussed in the next chapter.

Chapter 6

Selected Results and Discussions

The mathematical programming model and the inputs to the model were described in previous chapters. The aim of this chapter is to discuss the results of the optimization model and is organized as following. In section 6.1, we assess the economic implications of each individual cogeneration technology according to the national regulations in Portugal. This is done by considering a single-objective model with Life-Cycle Costs (LCC) as the function to minimize. Next, in section 6.2 we develop a multi-objective model and present the Pareto frontiers of LCC vis-à-vis other objective functions, i.e. Cumulative Energy Demand (CED), Greenhouse Gases (GHG), Acidification and Eutrophication. Finally, summary and concluding notes close the chapter (section 6.3).

6.1 Economic assessment of distributed generation technologies

Cost implications are always present as a deciding factor to plan and employ Distributed Generation (DG) technologies for buildings, regardless of the presence of other criteria of interest. This section discusses the model results when the objective function was to minimize the LC energy costs of meeting the building energy demand (over a planning period of eleven years from 2012 to 2022). In order to facilitate cross-comparison among different technologies, we analyze the combination of each type of cogeneration technology with other kind of energy systems. In other words, we look at each cogeneration technology as a potential DG source and assess its economic implications for the next mid-term planning period. As explained in chapter 5, the model regards the national policy; hence the feasible solutions are limited to the ones that provide PES (defined according to European directive 2004/8/EC through Equation 5.6.) compared to separate production of heat and electricity. We have assumed a

growth rate of 2% for the cost of electricity and Natural Gas (NG) for commercial consumers and all other growth/decline trends along the planning period are ignored. The first year of the study resembles year 2012 regarding cost implications. The results are limited to include the operational level and output of different energy systems for the first year and a randomly selected year throughout the planning period for illustrative purposes. The detailed cost factors of the energy systems are included in Appendix B. In section 6.1 we assess the economic implications of cogeneration technologies for the commercial sector in Portugal. For PV, a more detailed economic assessment according to local meteorology and radiation is followed in the next chapter.

6.1.1 ICE

The analysis shows that under the current policy framework in Portugal, ICE is a cost-effective cogeneration system for commercial sector. For our case-study, on average a 172 kW_e ICE produces 33% of annual power needs of the building while satisfying almost all the thermal demand.

Figure 6.1 shows the electrical output (kW) of different energy systems, according to cost-optimal operation planning, to meet the electrical power demand of the building. Figures 6.2 and 6.3 exhibit the same type of information for heating and cooling power demands, respectively. The output of the energy systems are shown at each block-load of the first year (2012) and a (randomly selected) year of the planning period (refer to Table 5.4 for the complete list of block-loads on the X-axis).

The analysis shows that one unit of ICE is employed, and its electrical output level (kW) at each block-load is shown in Figure 6.1. In this way, ICE satisfies almost all the thermal demand of the building, hence there is no interest to install a backup boiler and ST systems (Figure 6.2). From Figures 6.1 and 6.2[1] we also observe that the electricity purchase price from grid at different block-loads affect the planning pattern with the engine working at low capacity during medium and low block-loads—in which

[1] In Figure 6.2, the heat demand (kW) refers to the total heat demand of the building, while thermal demand is the building heat demand plus the heat needed to run AC to meet the cooling demand during hot or mild seasons.

the purchase price of electricity is at its minimum—and at (almost) full capacity during high and peak block-loads. Moreover, the engine operates mostly at 100% load, however, the upper-bound over its annual thermal output[2] forces its operation at 75% and 50% part-loads in a number of block-loads. Looking at the trend of exporting electrical power to grid, as observed in Figure 6.1, export is not economical during peak loads (HP1, HP2, MP1, MP2, CP1, CP2). In fact, it is economically worthwhile to consume the entire electrical power produced onsite rather than exporting 50% of the production and accordingly purchase the remainder from grid to compensate the amount exported. Finally, Figure 6.3 shows that the cooling demand of the building is addressed by one unit of AC, which runs by the heat from ICE, and the CC that supply the remainder of cooling need in some block-loads.

Since ICE does not address the total electrical demand (Figure 6.1), there is enough demand capacity for installation of PV systems. However, the existing FIT for PV technologies does not trade off their high initial capital cost and PV systems are not deployed. In chapter 7 we explore the economics of PV technologies in more detail.

Regarding cost implications, ICE demonstrates the best cogeneration technology among those analyzed in this study (for a comparative cost analysis, refer to section 6.5). Even when we analyzed the scenario that all cogeneration technologies and solar systems are potential sources to meet the building energy demand, the optimal energy system settings are parallel to the case in which among cogeneration technologies solely ICE is employed with other energy systems, as discussed in this section. The PES achieved by employing ICE, for the building under study, is approximately 12%.

[2] In order to benefit from the remuneration regime, as explained in chapter 5, the overall efficiency of the cogeneration system should satisfy the PES threshold defined in the decree-laws [Decree-Law 23/2010, 2010; Directive 2004/8/EC . 2004]. In chapter 5, section 5.2, we showed that satisfying this threshold dictates that at least 77% of the annual thermal output of the ICE systems should be consumed onsite (Table 5.1).

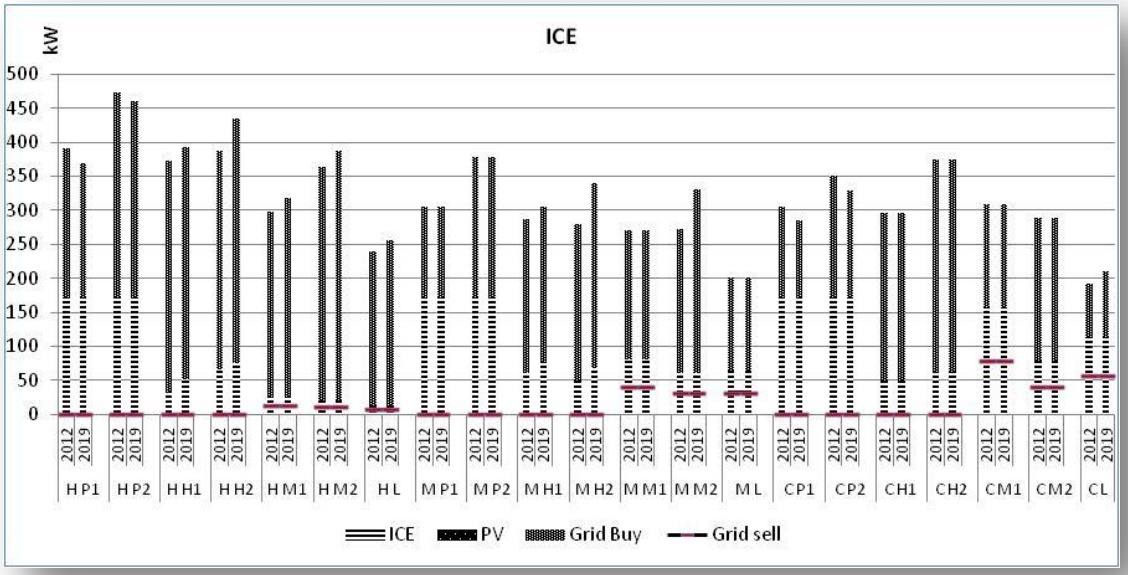

Figure 6.1: Power output in the case of ICE with other energy systems (with export to grid)

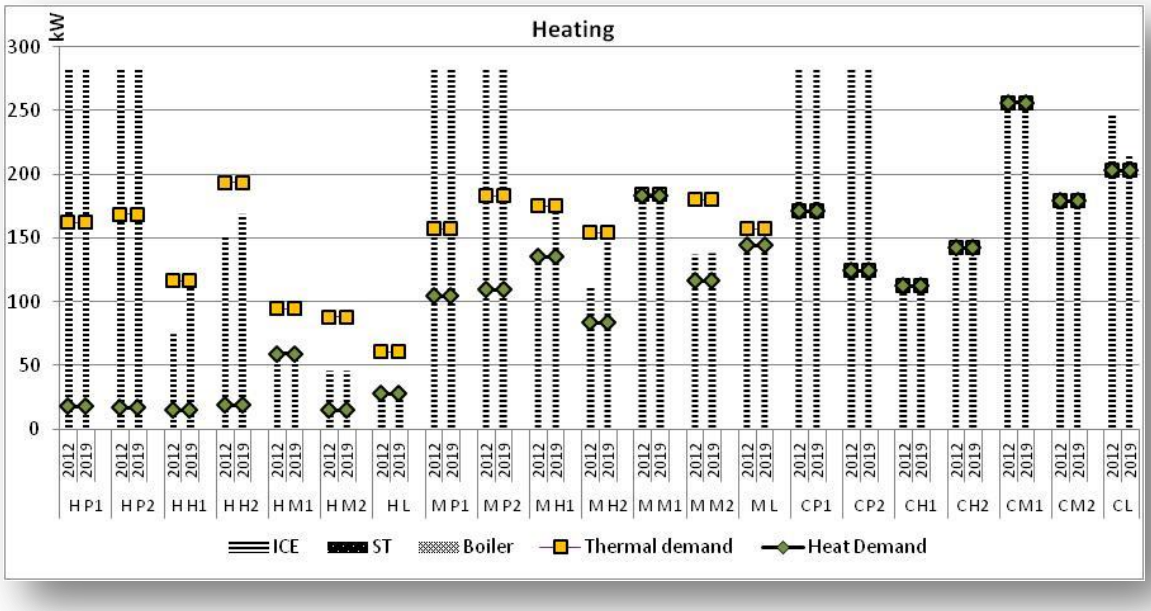

Figure 6.2: Heat output in the case of ICE with other energy systems (with export to grid)

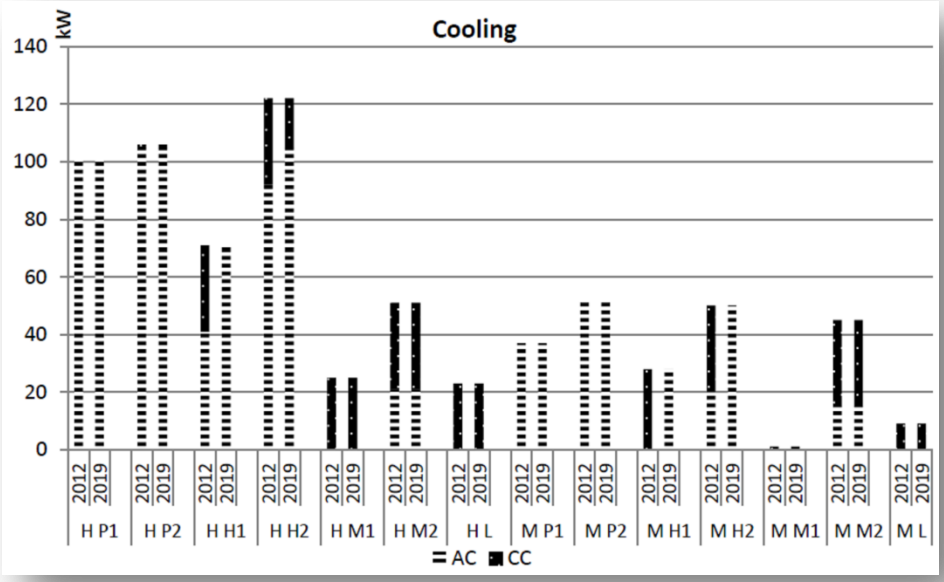

Figure 6.3: Cooling output in the case of ICE with other energy systems (with export to grid)

6.1.2 MT

The optimal operation planning employing MT cogeneration system along with other energy systems (solar and conventional) is shown in Figures 6.4–6.6. The results exhibit that, with existing price conditions for year 2012, MT is not cost-effective against grid and boiler. However, within a 5 year time-scale and with the evolution of cost of electricity and NG, (2% each), MT becomes an economically viable technology for commercial building sector in Portugal. Furthermore, 11 ST (44 kW) systems are installed along with MT that partially meet the need for hot water. This indicates that at the current stage ST systems are cost-competitive technologies with conventional boilers.

Figures 6.4–6.6 exhibit the operation planning of energy systems. In first year, the energy mix consists of conventional sources and ST; MT starts operating in mid-year of planning period (2017). When employed, MT operates at 100% load at majority of the block-loads. In this fashion, the turbine is able to satisfy more than 70% of annual thermal needs jointly with 11 solar thermal systems (44 kW total) and a boiler that meets the rest. Furthermore, same as the trend observed for ICE, Figure 6.4 shows that export of electricity is not economical during peak block-loads. Finally, the

stringent constraint over the thermal output of the MT—100% of the annual production should be consumed onsite—does not justify installation of a second unit, which if employed would be working in part-loads that generally do not expose a cost-effective economic profile.

This combination of energy systems with MT exhibits the most cost-effective operation strategy following the case employing ICEs. For the building under study, MT is capable of providing PES of approximately 5%.

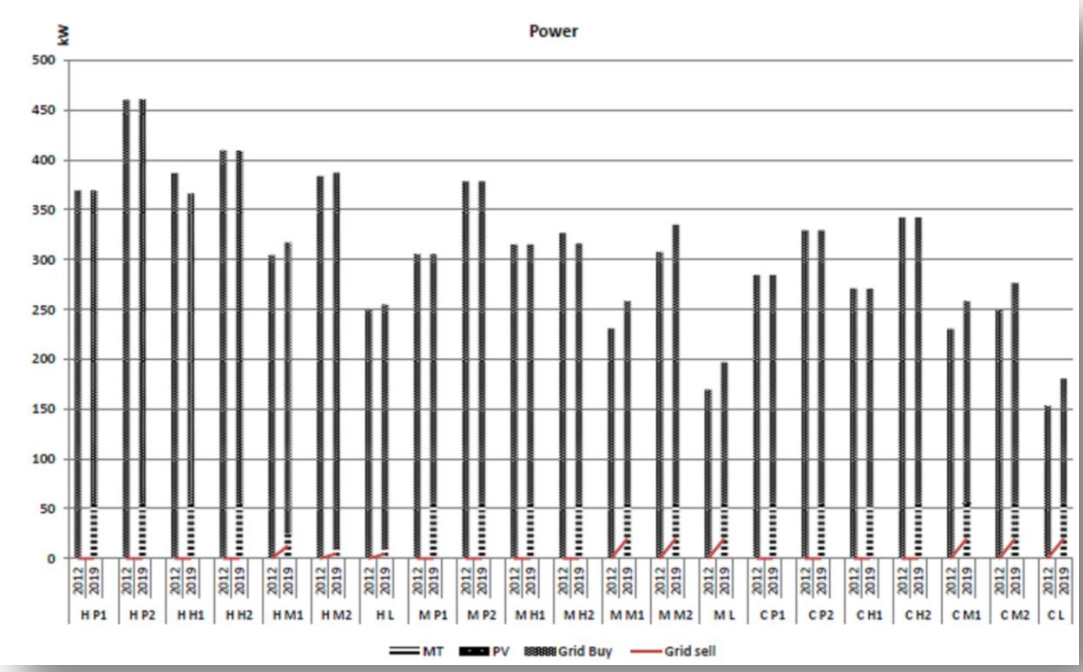

Figure 6.4: Power output in the case of MT with other energy systems (with export to grid)

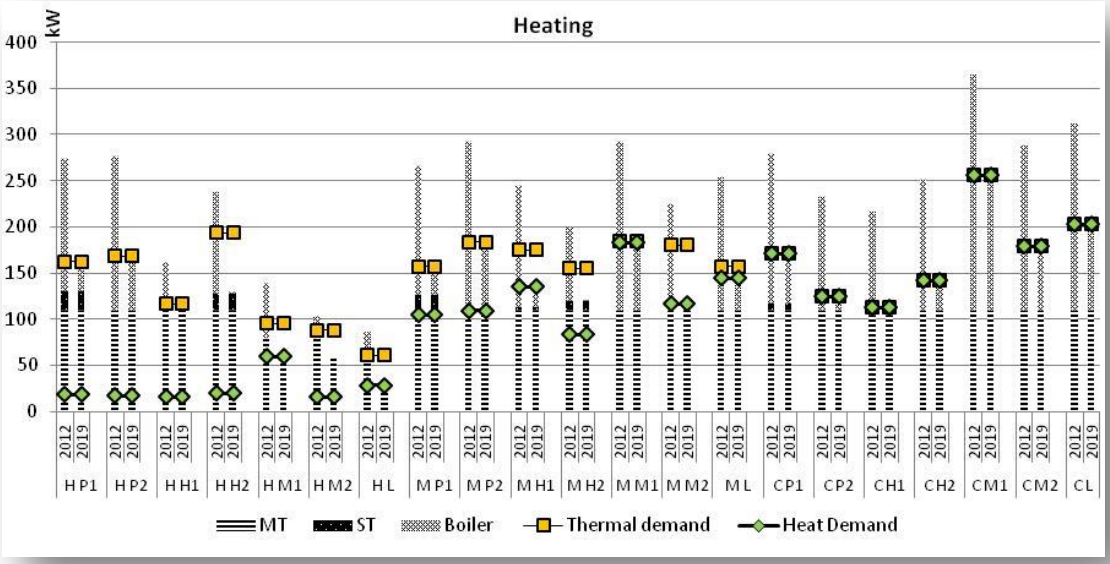

Figure 6.5: Heating output in the case of MT with other energy systems (with export to grid)

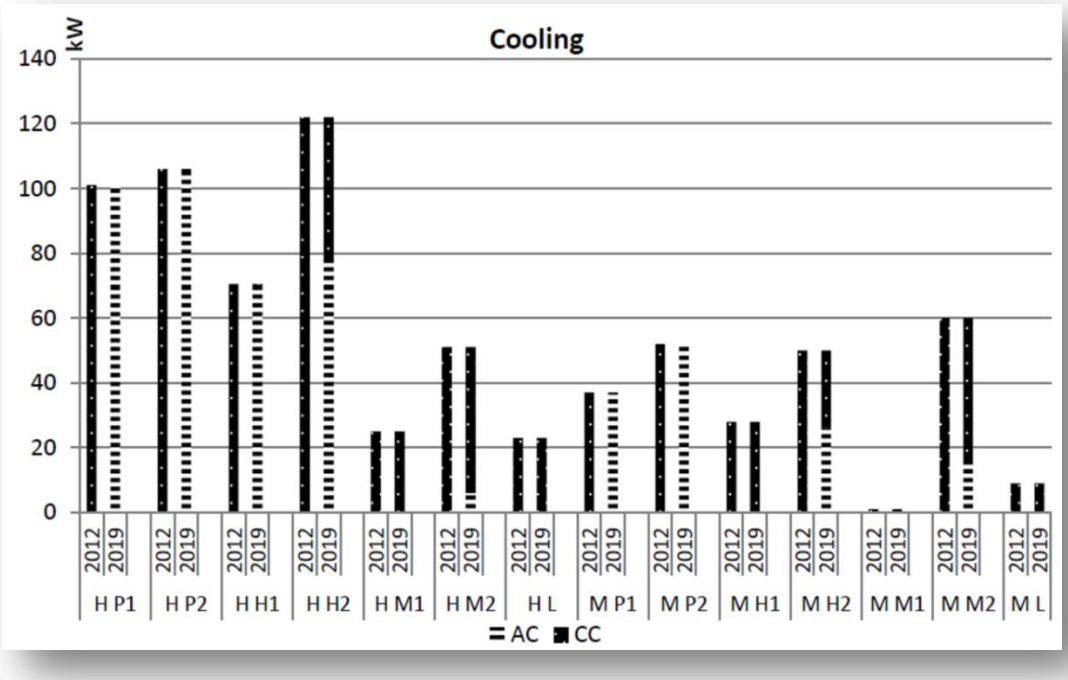

Figure 6.6: Cooling output in the case of MT with other energy systems (with export to grid)

6.1.3 SOFC

The current high price of the SOFC systems delineates that they are not yet cost competitive against conventional energy systems. Therefore, when minimizing LCC of

meeting the energy demand by combining SOFC with other sources, the set of solutions consists of conventional sources and 44 kW ST.

A sensitivity analysis was performed to determine the capital cost reduction that makes the employment of SOFCs a cost effective choice. Considering other cost factors and efficiency parameters constant, approximately 60% reduction in capital cost of fuel cells makes them cost-effective against conventional systems. If so, Figures 6.7–6.9 depict the optimal planning pattern of the energy systems in each block-load through two selected years of the planning period. Two SOFCs are employed and it is noted that the significantly higher electrical efficiency and lower thermal efficiency of the cells as well as their relatively low operating cost causes economic advantage in long-term by exporting more surplus power to grid. Also, Figure 6.7 shows that at medium and low block-loads, SOFC works in 90%-100% load to increase its thermal output to run the AC and meet the cooling demand. Since the thermal output of the SOFC engine is not enough to supply the building demand, a boiler and 11 ST (44 kW total) systems are employed. Here again the cooling demand is met by co-utilizing AC and EC.

While the total cost of co-utilization of SOFC with other energy systems represents a higher level than even conventional sources, the PES achieved by deploying SOFC escalates to approximately 18%, which represents the highest value among cogeneration technologies.

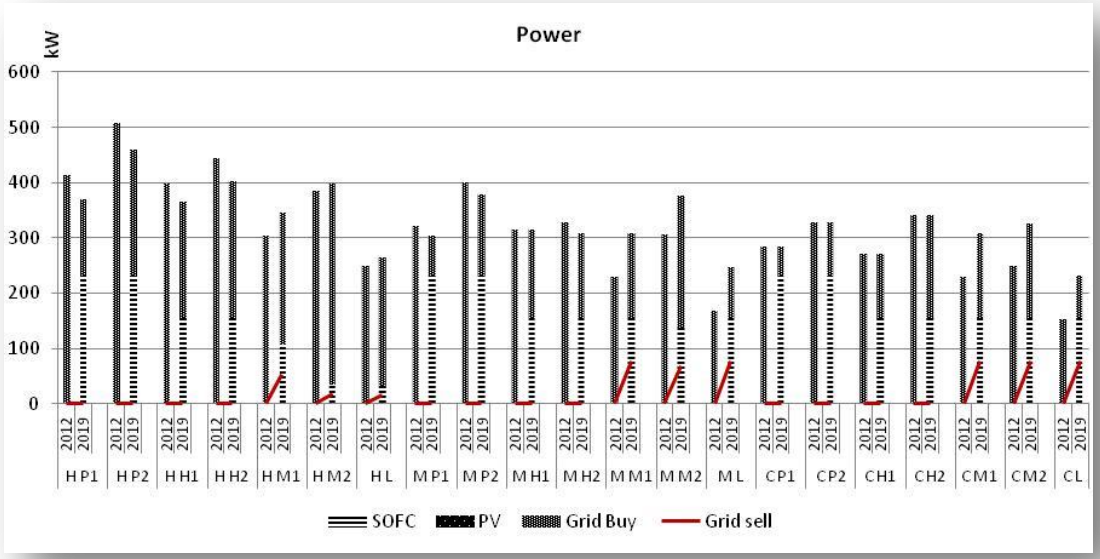

Figure 6.7: Power output in the case of SOFC with other energy systems (with export to grid)

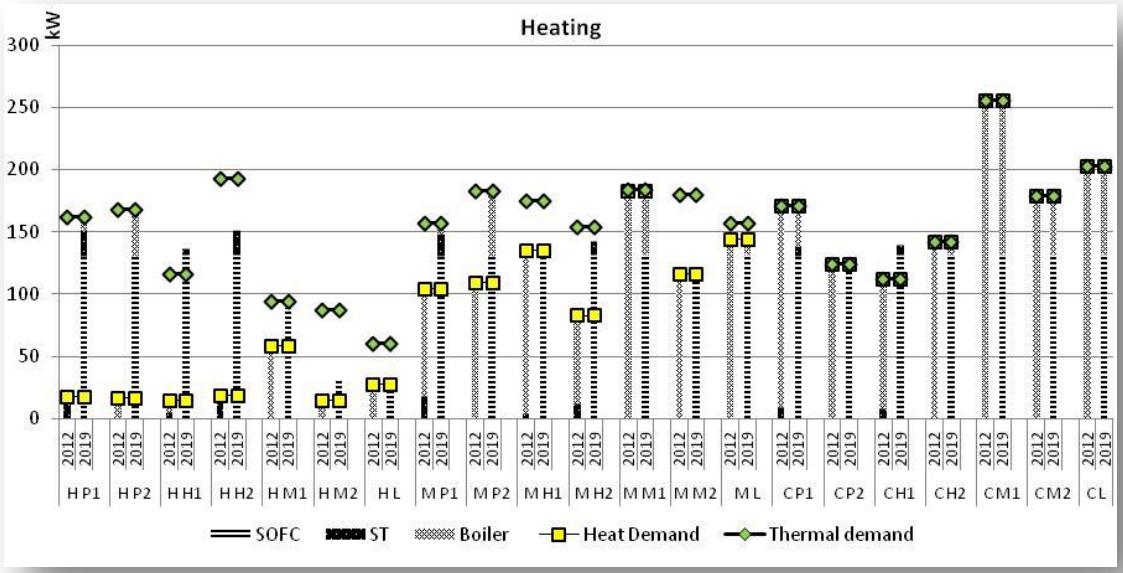

Figure 6.8: Heating output in the case of SOFC with other energy systems (with export to grid)

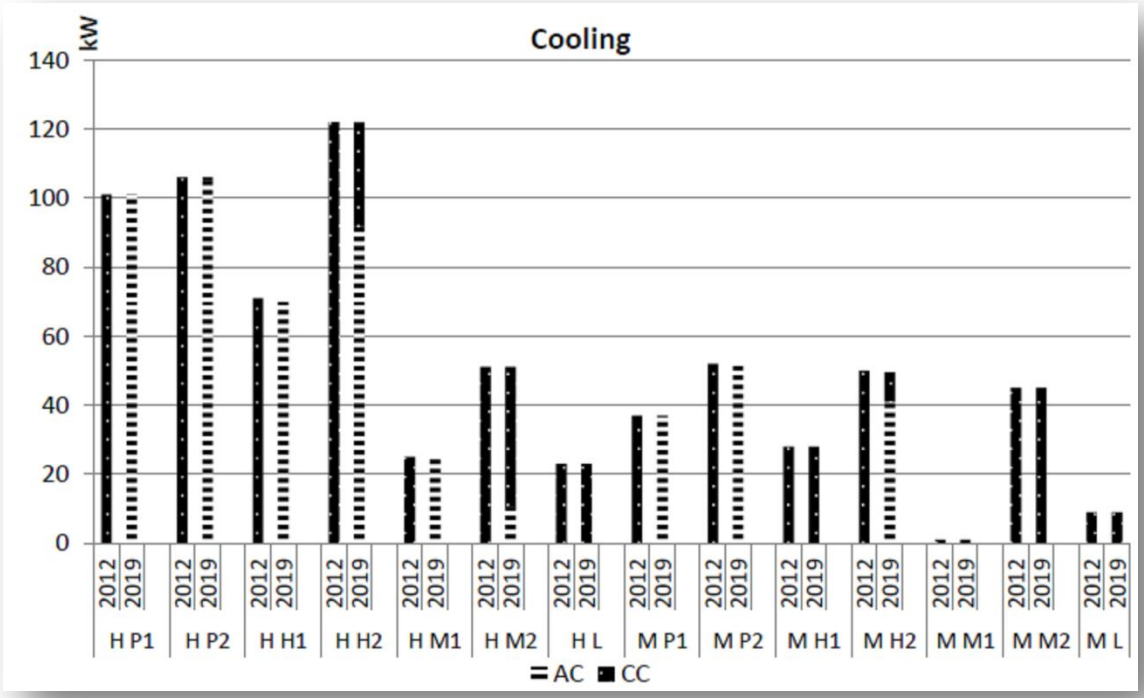

Figure 6.9: Cooling output in the case of SOFC with other energy systems (with export to grid)

6.1.4 Cost and PES implications

This section provides the cost implications of energy systems discussed in section 6.1.1.-6.1.3, and compare cogeneration systems in terms of their PES potential for the case-study. Table 6.1 summarizes the energy systems employed in each of the sections 6.1.1.-6.1.3. It also shows the average annual PES obtained (compared with separate production of heat and electricity) if each cogeneration technology operates according to its cost-optimal plan. PES is calculated according to European directive 2004/8/EC (2004), as discussed in detail in chapter 5, section 5.1. We can see that the PES obtained by deploying SOFC engines is higher than the one by ICEs and MTs. Furthermore, in the case of MT and SOFC, PES is close to the level that the engines are capable to provide (compare with Table 5.1). While ICE engines can provide PES of about 18%, the PES value obtained by ICE is ~12%. This is the result of over supplying the building thermal demand that diminishes the efficiency and consequently the PES obtained by employing the ICE engines.

Similarly, Figure 6.10 shows the LC energy costs of the building for 11 years, if using each of the energy system combinations summarized in Table 6.1. Each column in Figure 6.10 refers to a row of energy systems in Table 6.1. Looking at mid-term (11 years) planning period, the combination of ICE and grid exhibits a cost-effective cogeneration-based technology for commercial sector in Portugal. This is due firstly to their relatively low operating costs and secondly to the higher level of thermal output that fulfills the entire annual heating demand, therefore preventing the operation of (less efficient) boiler. These two factors contribute to reduce the total operating energy costs of the building. Following ICEs, in near future MT exhibits an alternative cost effective cogeneration system with a relatively low initial capital investment. On the contrary, the high initial capital cost of the SOFCs means that they are not yet cost-effective. For our case-study, SOFCs would be employed if their initial capital investment were 30% lower. In terms of solar systems, we discussed that ST systems are cost-effective alternatives against conventional boilers while PV, considering the existing FIT in Portugal, is not yet cost-effective for commercial applications in the central region of Portugal. In our study, 42 kW of ST systems are installed along with MT and SOFC to meet a part of the thermal demand. A detailed cost analysis of PV in Portugal is presented in chapter 7.

Table 6.1: PES—Cogeneration technologies

	Reference Section	Cogeneration/Energy systems deployed	Annual PES (to separate production of heat and electricity)
1	6.1.1	2 ICEs/ GRID	~12%
2	6.1.1	1 MT (from 5th year of planning period)/ 42 kW ST systems, BOILER, GRID	~5%
3	6.1.3	2 SOFCs (from 3rd year) / 42 kW ST systems, BOILER, GRID	~18%
4	-------	BOILER, GRID	-

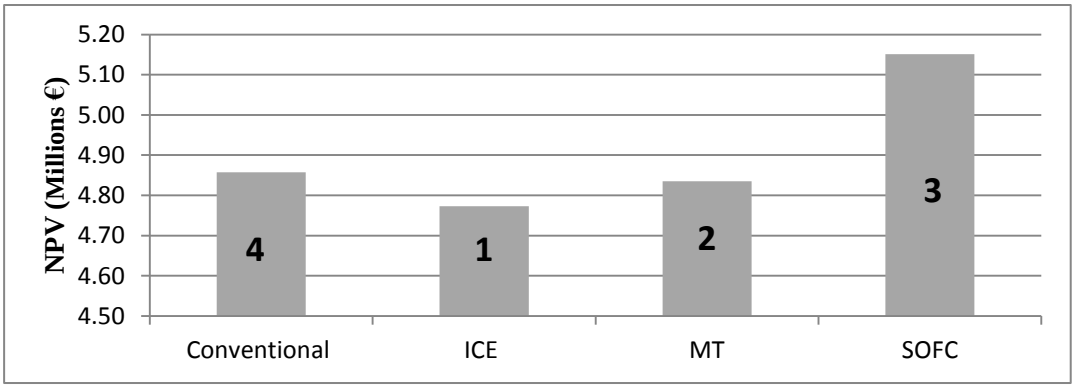

Figure 6.10: NPV—Cogeneration technologies

Finally, Figure 6.11 depicts an example of expected annual cash flows to meet the building energy demand. The positive and negative values signify correspondingly the cash outflows and inflows, if ICEs are employed (energy systems are identical to row 1 of Table 6.1). For instance, the outflow in the first year represents the capital cost incurred to obtain the energy systems. We assumed a salvage value of 10% of capital cost for cogeneration systems. This is credited in year 7 when the first ICE retires after 6 years of life-time. The net income from the export to grid and premium of efficiency have been considered as cash inflows at each respecting year. Figure 6.11 shows that the expected operating energy costs by far outweigh the capital costs. The annually increasing operation charges in Figure 6.11 are the effect of the increase in the price of electricity and NG (2%).

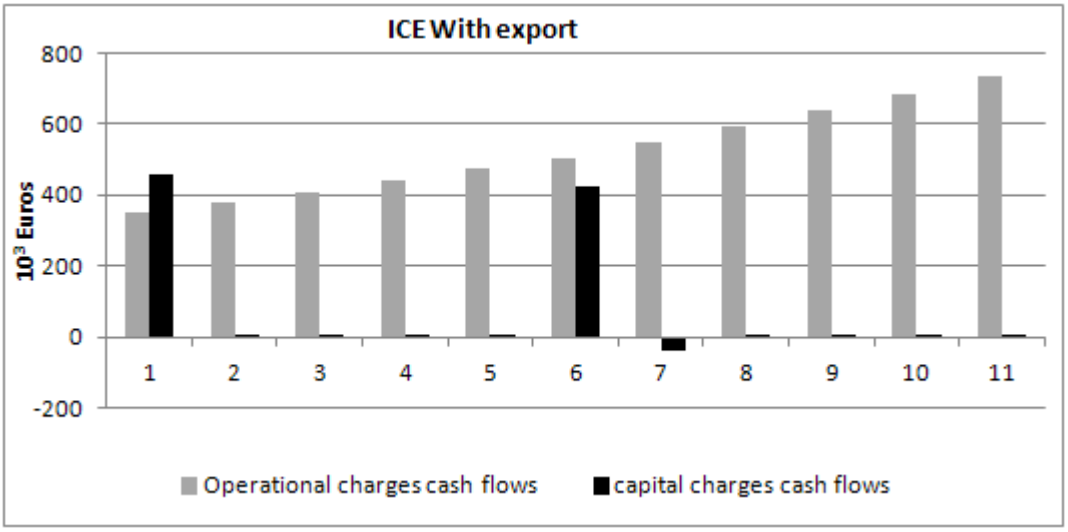

Figure 6.11: ICE- Expected annual cash flows

6.2 Pareto frontiers

This section presents the Pareto frontiers obtained for LCC vis-à-vis environmental impacts for DG investment. Pareto frontiers presented in sections 6.2.1–6.2.4 show the trade-off between cost-efficient solutions, and the solutions with lower CED, GHG, Acidification and Eutrophication impacts values. Each solution consists of a set of energy systems, and their respective operating planning to meet the level of LCC and environmental impact determined by the Decision Maker (DM). For each set of dual-objective problems—LCC vis-à-vis CED, GHG, Acidification and Eutrophication impacts—a minimum step of improvement in the value of objective functions was defined, according to their range of variation at the Pareto optimality level. An algorithm was implemented in GAMS (McCarl *et al.*, 2013), which employs the methodology by Sylva & Crema, 2004 (section 5.4) and outputs the Pareto frontiers.

For this section, the capital and fixed maintenance costs of the energy systems were converted to Equivalent Annual Cost (EAC), i.e. the annual cost owning and operating an asset over its entire lifespan (Fuller & Petersen, 1996; Hawkes & Leach, 2005). EAC is frequently used as a decision making tool when evaluating investment projects of unequal life spans (Fuller & Petersen, 1996). The Life-Cycle Impact Assessment (LCIA: CED, GHG, Acidification , Eutrophication) of energy systems (per kWh) output were calculated and presented in chapter 4 and summarized in Tables 6.2 and 6.3 for reference purposes. The capacity of a conventional boiler for the following analyses is considered as a variable, so the optimal solution (according to the defined objective function) gives out the optimal capacity of the boiler as well as its output throughout the planning period. Moreover, the emissions resulting from the exported power are deducted from the total emissions, since they avoid the generation of electricity (mix production in Portugal). This has been accounted by the model using the “avoided-burden approach” (Clift *et al.,* 2000).

Table 6.2: LCIA of cogeneration systems—input to the mathematical model

		ICE 100% load	ICE 75% load	ICE 50% load	MT 100% load	MT 75% load	MT 50% load	MT 25% load	SOFC 104% load	SOFC 100% load	SOFC 93% load	SOFC 85% load	SOFC 78% load	SOFC 68% load	SOFC 62% load
CED	**MJ/kWh$_e$**	12.78	14.03	16.02	16.35	17.70	21.23	32.61	9.85	9.64	9.05	8.87	8.70	8.70	8.54
GHG	**g CO_2 eq/ kWh$_e$**	682	748	853	876	930	1254	1733	558	555	549	547	546	546	544
Acidification	**g SO_2 eq/ kWh$_e$**	0.38	0.40	0.42	0.42	0.44	0.48	0.61	0.21	0.21	0.21	0.20	0.20	0.20	0.20
Eutrophication	**g PO_4^{3-} eq/ kWh$_e$**	0.08	0.09	0.10	0.08	0.09	0.10	0.14	0.08	0.07	0.07	0.07	0.07	0.07	0.07

Table 6.3: LCIA of solar and conventional systems—input to the mathematical model

		PV	Grid	ST	boiler
		kWh$_e$		kWh$_{th}$	
CED	**MJ**	1.80	4.67	0.39	5.29
GHG	**g CO_2 eq**	90	347	21	287
Acidification	**g SO_2 eq**	0.472	0.770	0.158	0.124
Eutrophication	**g PO_4^{3-} eq**	0.21	0.53	0.10	0.03

6.2.1 Pareto frontier for cost and CED

In this section we discuss the Pareto frontier obtained for CED and LCC objective functions. The Pareto frontier was derived, considering a minimum step of improvement of δ_I = 2,000 for cost and 20,000 for CED. The values correspond to the total LCC and CED of meeting the building energy demand for a nominal year. Table 6.4 shows the pay-off values for LCC versus CED objective functions[4]. The range of variation of CED objective function is considerably higher than that of cost; the magnitude of the best achievable CED (ideal solution) is three times lower than its maximum (nadir value) whereas for cost this difference is less than 12%.

Table 6.4: Pay-off values for cost vs CED

	Min	Max
CED (MJ)	6 048 691	7 682 100
LCC (Euros)	401 654	431 456

The Pareto frontier obtained for CED and LCC objective functions is shown in Figure 6.12. The curve has a steep slope in the beginning and its slope decreases as it progresses towards less CED (or more costs). As discussed in section 6.1, none of the DG systems except ICE and ST are economical based on relative fuel (NG and electricity) cost in Portugal. Thus, the set of energy systems for the most cost-effective results (the solution at the most extreme left part of the Pareto frontier) is composed of an ICE, a boiler with minimal size (5 kW), 1 AC and 30 kW of CC. We explained that with the employment of ICE, there is no interest (financially) to install ST systems, as ICE satisfies almost all of the heat demand of the building. Compared to the case only employing conventional systems, the cost-optimized operation of ICE brings about both financial and energy savings. Thus the case employing conventional systems is dominated by some of the solutions located on the Pareto frontier. For reference purposes, the value of objective functions corresponding to employment of

[4] The pay-off table provides the objective function values, for each non dominated solution, resulting from individually optimizing each objective function of the problem. This allows the DM to have a first global overview about the range of variation of the objective functions in the efficient region. Along with ideal solutions, nadir points are also derived from the pay-off table, by selecting, in each column, the worst value of the corresponding objective function

conventional systems, and conventional systems with 44 kW ST are also displayed in Figure 6.12. The employment of ICE, even at its cost-optimal strategy reduces CED by almost 60% compared to conventional case. Installing 44 kW ST can also reduce CED by 1%, compared to case only employing conventional systems.

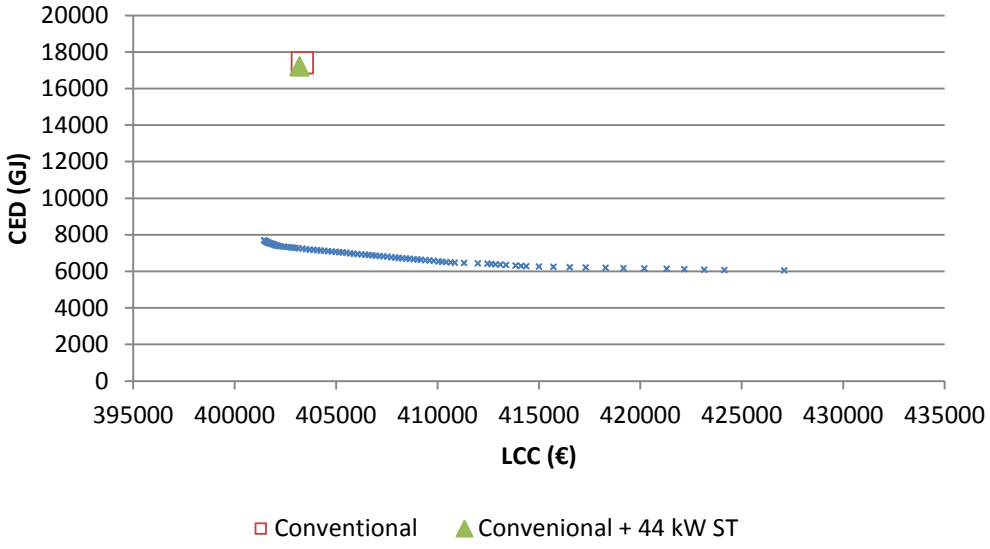

Figure 6.12: Cost vs. CED—Pareto frontier

In order to reduce CED, the output of grid and boiler slightly increases, replacing ICE to partially meet the building energy demand. Therefore, shifting to solutions with less CED (and more cost), the output of ICE gradually decreases whereas import from grid and output from boiler increases. In order to further reduce CED, PV systems are added to energy systems. The number of PV installations gradually increases along the Pareto as the DM desires for less CED; the solution with least CED (11,327,998 MJ; see Table 6.4) employs 80 kW installed PV system, the maximum capacity allowed due to area restrictions of the building.

The operation planning of energy systems to minimize CED are shown in Figures 6.13-6.15. The optimal configuration of energy systems to minimize CED consists of 80 kW PV systems (maximum allowed due to area restriction), an ICE, a boiler sized 25 kW, and 2 ACs (208 kW). This set of energy system corresponds to most extreme right solution (with highest LCC and lowest CED) in Pareto frontier 6.12, referred to in Table 6.4. It is visible that ICE operates as a base-load whereas the extra electricity and heat

needed is met via grid and boiler, respectively. The cooling is completely met by 2 ACs that run on the waste heat from ICE. The output of ICE cannot increase, otherwise it would violate the PES constraint (over its thermal output), so a 25 kW boiler is installed to meet the peak thermal demand. The main difference in the operating plan of ICE—when minimizing CED or LCC—is that for the latter, the output of engine is sensitive to the price of electricity. Therefore, as shown in Figures 6.2 and 6.3, ICE operates in full load during the peak hours (where the price of grid is higher) and in 50–75% load during the medium and low block-loads, in which it is also cost-effective to export electricity to the grid. For the case minimizing CED, however, while 80 kW PV are also added to onsite generation technologies (and so more electricity is available to be exported), export to grid is not recommended to minimize CED. Therefore, onsite produced electricity is only exported in ML and CL block-loads, during which ICE operates to meet the thermal demand and only the extra electricity (above the building electrical power demand level) is exported. In fact, it is energy saving to consume the entire electrical power produced onsite rather than exporting 50% of the production.

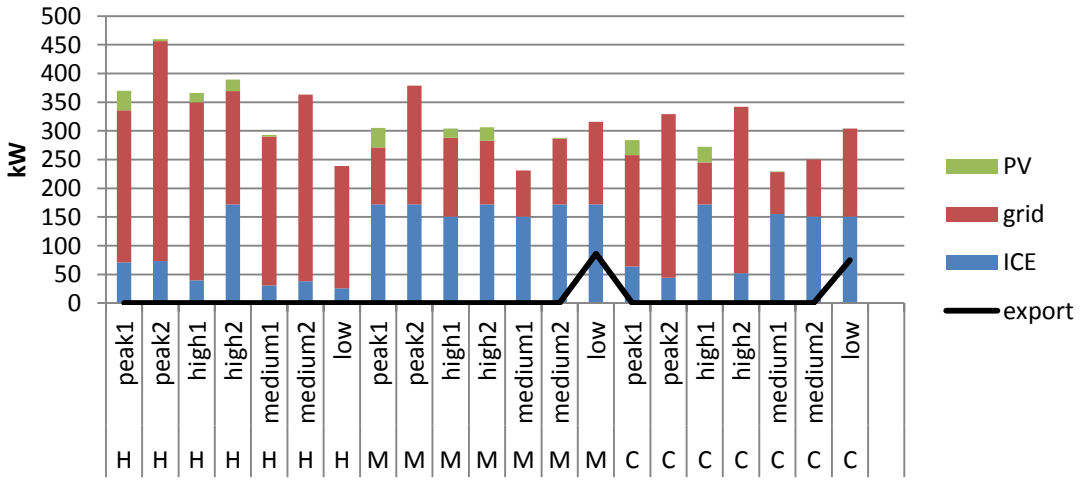

Figure 6.13: Minimizing CED - Optimal operation planning of energy systems to meet Power demand

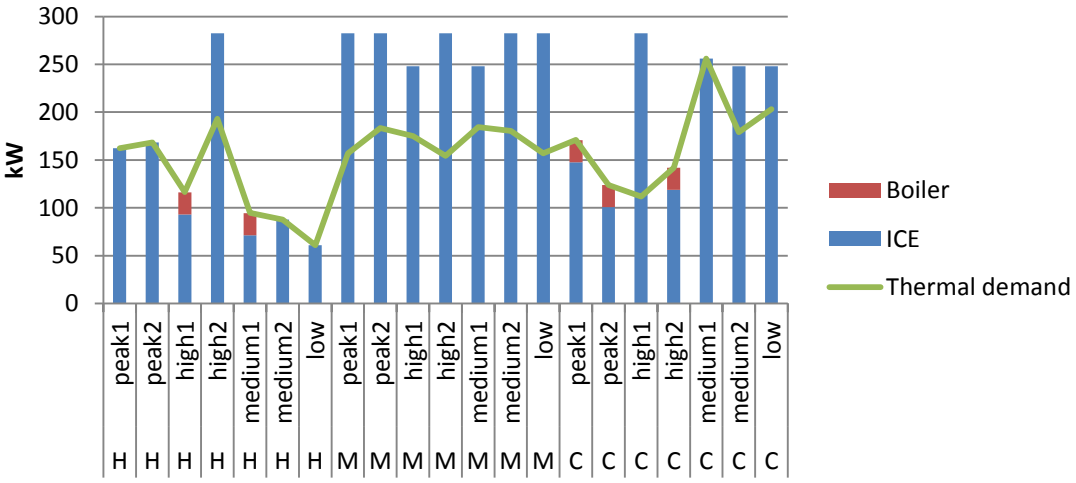

Figure 6.14: Minimizing CED - Optimal operation planning of energy systems to meet heating demand

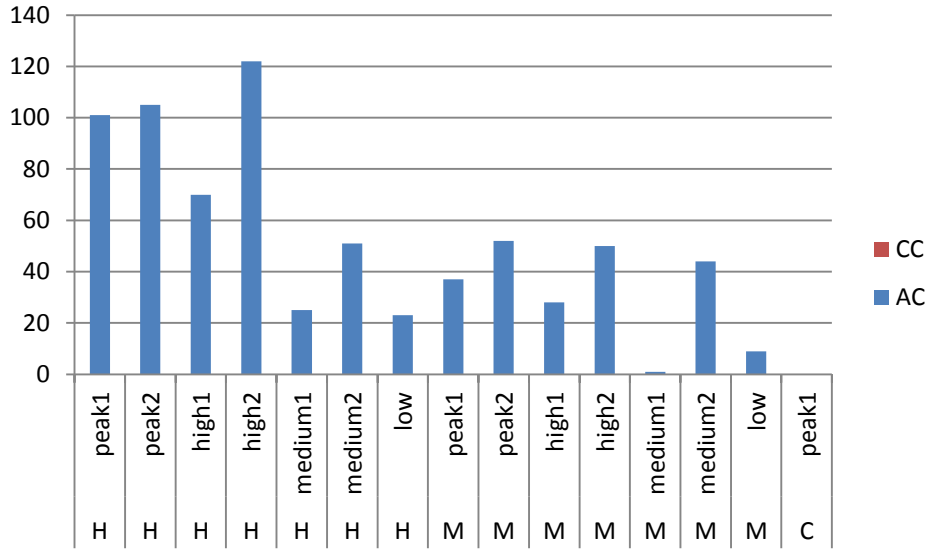

Figure 6.15: Minimizing CED - Optimal operation planning of energy systems to meet cooling demand

6.2.2 Pareto frontier for cost and GHG

In this section we discuss the solutions positioned on the Pareto frontier obtained for GHG and LCC objective functions. The Pareto is derived, considering a minimum step of improvement of $\delta_{I=}$ 2,000 for cost and 200,000 for GHG. The values correspond to the total LCC and GHG emissions of meeting the building energy demand for a nominal year. Pay-off table (Table 6.5) displays the ideal and nadir points of the dual-objective problem. GHG objective function value has a higher range of variability (40%) at the Pareto optimality stage compared to that of LCC objective function (10%).

Table 6.5: Pay-off values for cost vs GHG

	Min	Max
GHG (g CO_2 eq)	522 945 890	697 374 170
LCC (Euros)	401 654	446 188

Figure 6.16 shows the Pareto frontier obtained for GHG and the cost objective functions. The set of energy systems for the solution with minimum cost—pertaining to most extreme left solution of the Pareto frontier—is already known: an ICE, a boiler with minimal size (5 kW), 1 AC and 30 kW of CC. Figure 6.16 also shows the values of GHG and LCC objective functions for the solution only employing conventional energy systems, and for the solutions employing 44 kW ST along with other conventional systems. The conventional settings of energy systems has dramatically higher GHG emissions (almost twice), but only slightly higher LCC (less than 1%) than the case employing ICE. The employment of ICE (and AC) therefore provides both economic and GHG savings for the building.

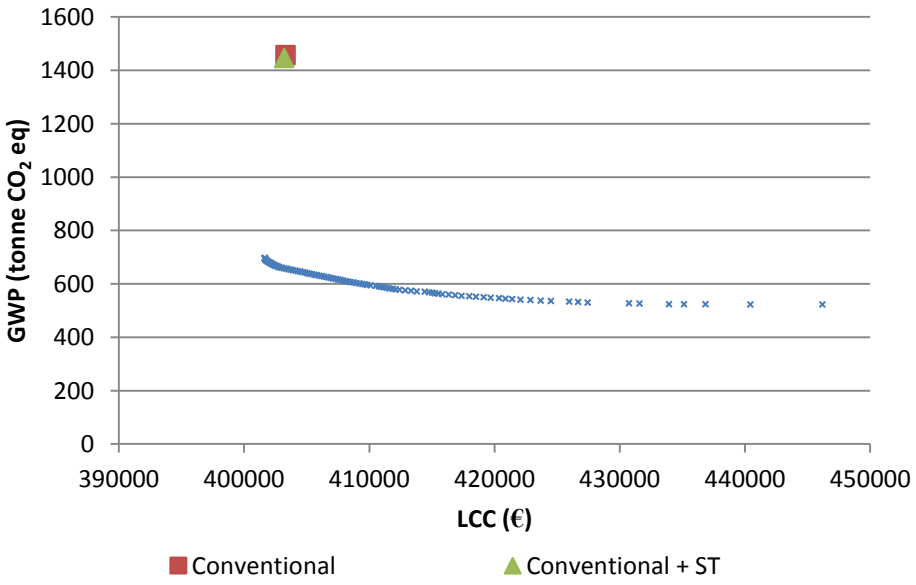

Figure 6.16: Cost vs. GHG—Pareto frontier

In order to reduce GHG, the output of ICE should increase to replace the electricity by the grid. Thus, moving along the Pareto frontier to solutions with less GHG (and more costs), the contribution of ICE to meet the building energy demand gradually increases.

As Figure 6.16 displays, the slope of the Pareto frontier declines towards solutions with higher LCC. This signifies that for such solutions, it bears more costs to reduce GHG by one unit, as ICE is not anymore operating according to its cost optimal design; rather it operates to decrease GHG emissions, even in the block-loads in which its operation is not economical. More electrical output from ICE increases its thermal output to drive the AC, thus the electricity demand for cooling is diminished. Thus, the increased output from ICE directly (via meeting the electricity demand) and indirectly (via reducing the electrical energy needed for cooling) decreases the electricity import from grid. Interestingly, the capacity of installed boiler is higher for solutions with lower GHG. There is a cap over the thermal output of ICE that should be used onsite; it is emission saving if its heat is used for cooling purposes (by driving AC) rather than being used for direct heating purposes. So the ICE operates almost in full-load during hot and medium seasons (to feed AC), and stops in some block-loads during cold seasons, during which the boiler is employed to meet the thermal demand.

Since the ICE meets most of the heating demand, there is no interest to install ST systems. Adversely, the capacity of PV installation increases as the DM opts for solutions with less GHG intensity. The optimal design of the energy systems to minimize GHG is actually composed of an ICE, 80 kW PV systems, 172 kW boiler and 2 ACs.

The optimal operation planning of these energy systems minimizing GHG are shown in Figures 6.17–6.19. This solution has a nominal GHG emission of 522 945 890 g CO_2 eq, as shown in the pay-off Table 6.5. Overall, the ICE operates to meet the base-load whereas the extra electricity and heat needed are met via grid and boiler, respectively. The cooling is completely met by the AC that runs on the waste heat from the ICE and, to a less extent the boiler. The output of the ICE cannot increase: otherwise it violates the PES constraint (over its thermal output), so the ICE stops in cold season through a number of peak block-loads. The heating needed during this season is met by using the boiler. PV is able to satisfy less than 1% needs of the building; in relative terms, this only reduces the building GHG emissions by 3%, but in absolute terms 80 kW installed PV provides an annual savings of 44 tonne CO_2 eq.

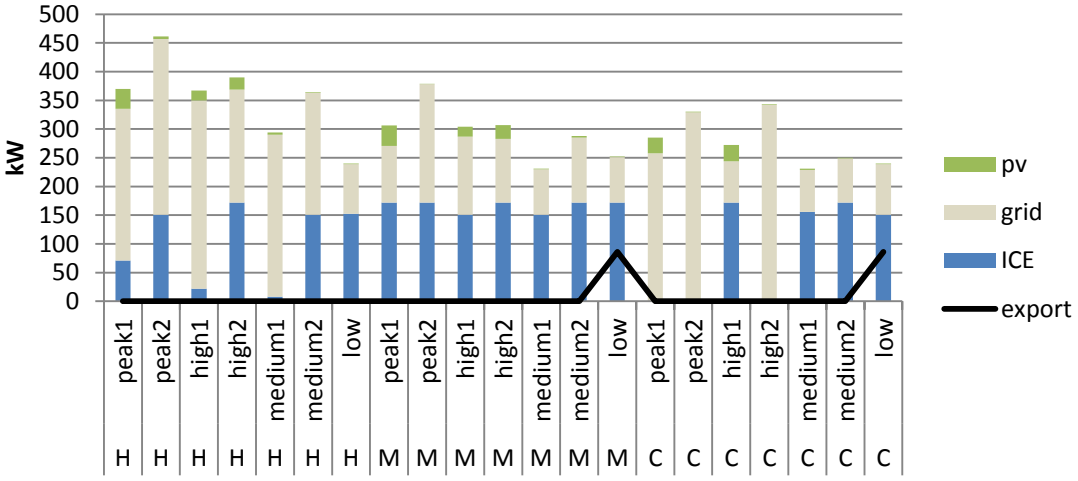

Figure 6.17: Minimizing GHG - Optimal operation planning of energy systems to meet Power demand

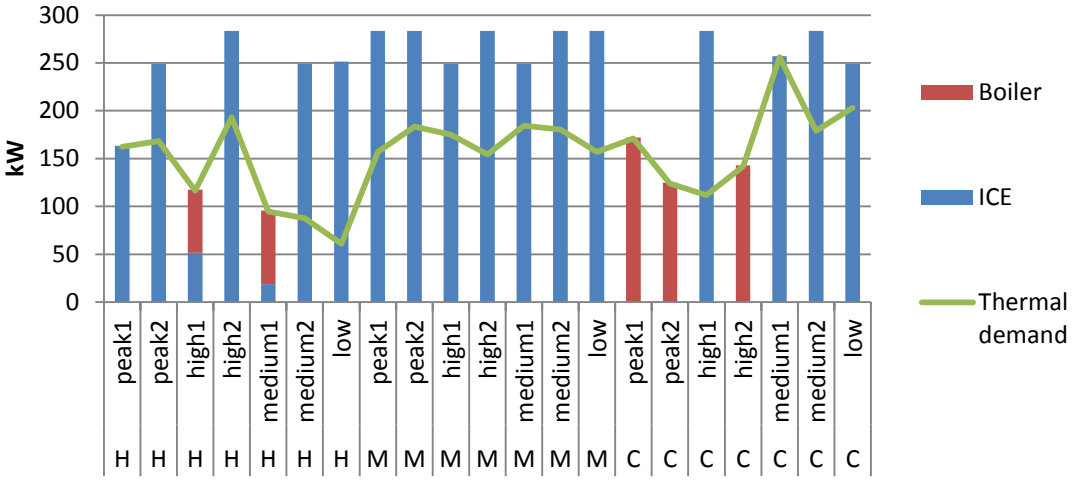

Figure 6.18: Minimizing GHG - Optimal operation planning of energy systems to meet Heat demand

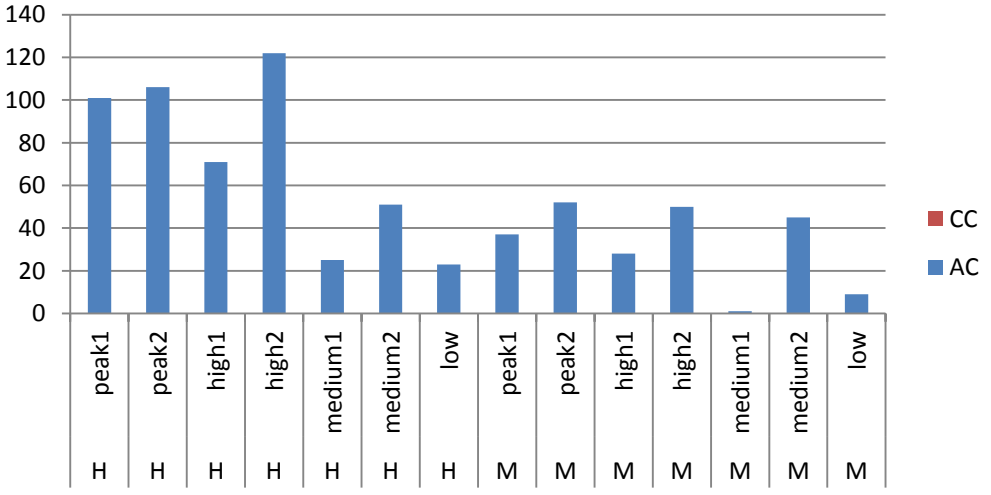

Figure 6.19: GHG - Optimal operation planning of energy systems to meet cooling demand

6.2.3 Pareto frontier for cost and Acidification

In this section we explore the Pareto frontier obtained for LCC vs. Acidification objective functions. As discussed in chapter 4, grid and after then PV have particularly more Acidification impact than CHPs. Thus, in order to reduce the building Acidification impact, imported electricity from grid should be moderated and ultimately avoided. The employment of cogeneration technologies—specifically SOFC—provides significant savings compared to conventional design of energy systems and brings about total negative balance of Acidification emissions for our commercial building. Table 6.6 displays the nadir and ideal values of objective functions. The range of variability of values for Acidification objective function is significantly higher (from -254 $\times 10^3$ to 1217 $\times 10^3$) than LCC objective function (i.e. from 401 $\times 10^3$ to 796 $\times 10^3$).

Table 6.6: Pay-off values for cost vs Acidification

	Min	**Max**
Acidification (g SO_2 eq)	-254 176	1 217 574
LCC (Euros)	401 654	796 050

The Pareto frontier for Acidification and LCC objective functions was derived, considering a minimum step of improvement of $\delta_{I\ =}$ 2,000 for LCC and 15,000 for Acidification (Figure 6.20). The values correspond to the total LCC (€) and Acidification (kg SO_2 eq) of meeting the building energy demand for a nominal year. The Pareto front is composed of five sections. The solutions positioned on section A employ ICE, boiler, AC, and PV systems. The solutions on section B contain the same type energy systems in addition to SOFC systems (see Figure 6.20). The number of SOFC installation increases by one unit for each of the curves on section B towards reduced Acidification impacts. Each jump in the value of LCC objective function therefore represents the employment of an extra SOFC unit.

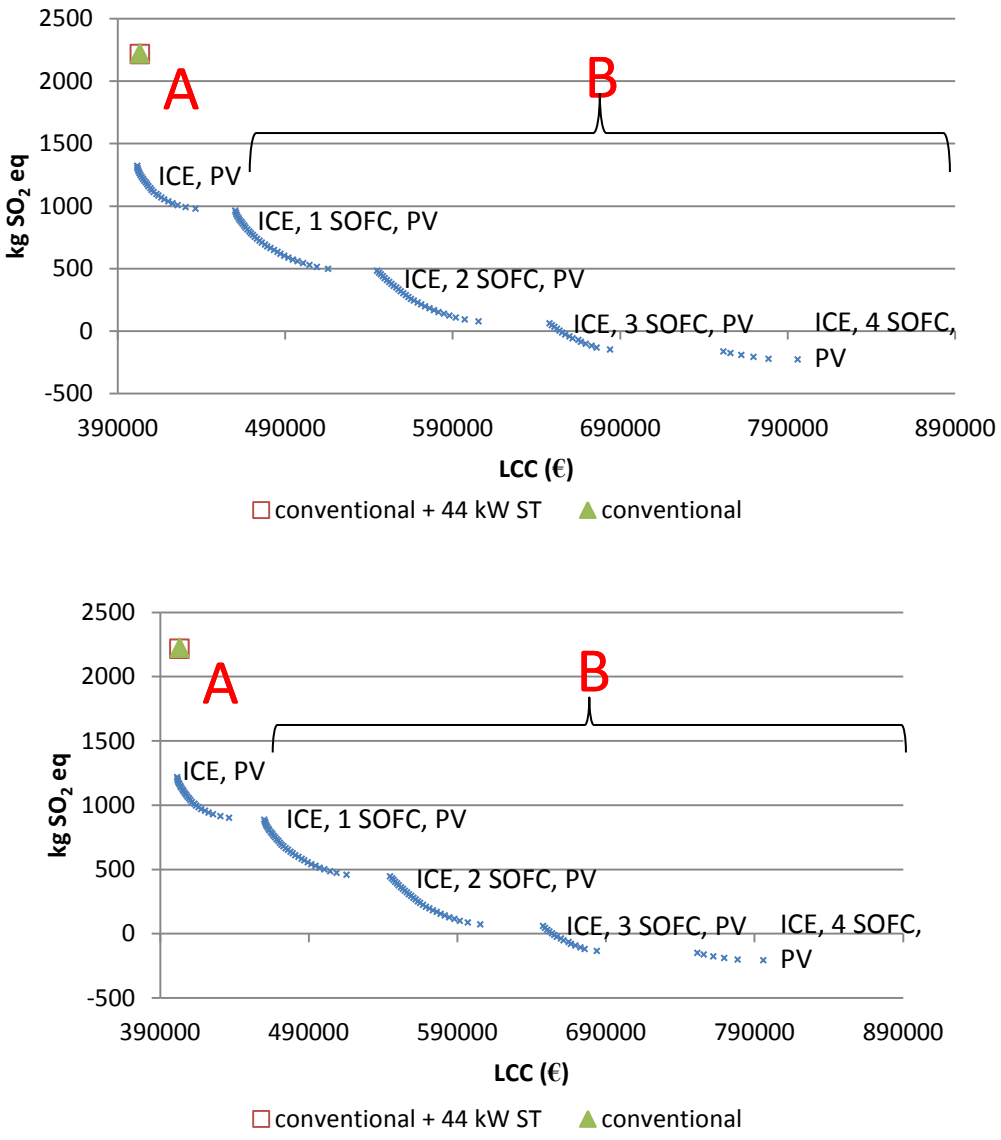

Figure 6.20: Cost vs. Acidification—Pareto frontier

We first explore the solutions located on Part A in Figure 6.20. The profile of the solution with least cost solution is already known (ICE, 5 kW boiler, 1 AC, 30 kW CC). Compared to conventional sources, the employment of the ICE decreases the annual Acidification potential by more than 60%. The values of objective functions corresponding to solution using only conventional sources, and conventional sources with 44 kW ST (which are dominated solutions) are also shown in Figure 6.20. In order to reduce Acidification, the output of the ICE increases to replace that of grid. All the solutions positioned on part A of Pareto frontier in Figure 6.20 employ an ICE; however, the contribution of the ICE to meet the building demand increases towards costlier solutions. The total cost for these solutions increases since the ICE starts

operating in block-loads in which the price of purchased power from grid is low and its operation is not economical. PV also boasts a relatively low cost alternative to decrease the Acidification impacts. The capacity of PV installations also increases, until they occupy the total rooftop space. Acidification can be roughly reduced annually by 500 kg SO_2 eq as an effect of employing 80 kW PV systems. Solutions positioned on the right hand side of Part A of the Pareto front (6.15) all employ 80 kW PV systems.

Moving along the Pareto frontier to the right, the fall in the value of Acidification objective function, from part A to part B, is the result of employment of SOFC in the subsequent solutions. SOFC systems are the most efficient DG technology to reduce Acidification, due to their high power-to-heat ratio, which allows them to supply most of the building electrical power needs while not over-supplying the thermal demand. The environmental impacts of electrical energy exported to grid were considered to be the same as the impact of energy purchased from grid. Therefore, employment of SOFC systems can bring about negative Acidification balance by exporting more onsite power to grid. Acidification is reduced by increasing the output of SOFC as a pay-off by bearing more costs. Consecutive drops in the value of Acidification observed in part B of Figure 6.20 are due to employment of an extra unit of SOFC. Ultimately 4 SOFCs are employed along with an ICE, 80 kW PV, 207 kW boiler, 1 AC and 45 kW CC to meet the building demand. This setting corresponds to optimal configuration of energy systems to minimize the Acidification potential.

Figures 6.21–6.23 depict the optimal planning pattern of the energy systems in each block-load when the objective function is set to minimize Acidification potential. SOFCs are operating to meet the base-loads, while the ICE is employed as the peak shaver. As discussed, Acidification savings can be acquired through exporting extra power to grid; therefore at all the block-loads through the year, 150 kW electrical power, which is the maximum allowed due to policy restrictions, is exported to grid. Clearly, in this way cogeneration system over-supply the building heat demand in a number of block-loads to export more power to grid and this leads to a relatively high annual energy costs.

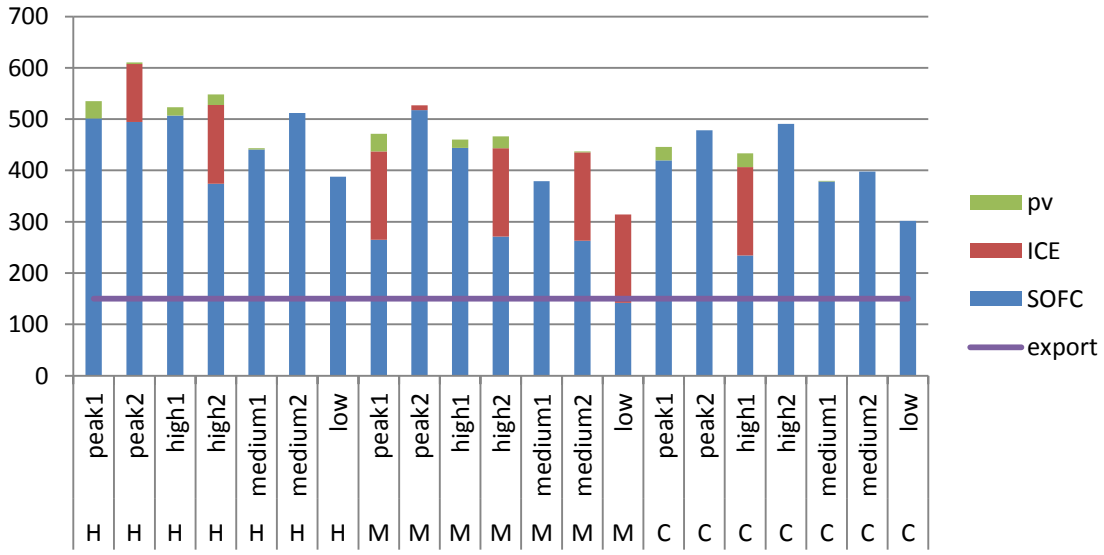

Figure 6.21: Acidification - Optimal operation planning of energy systems to meet power demand

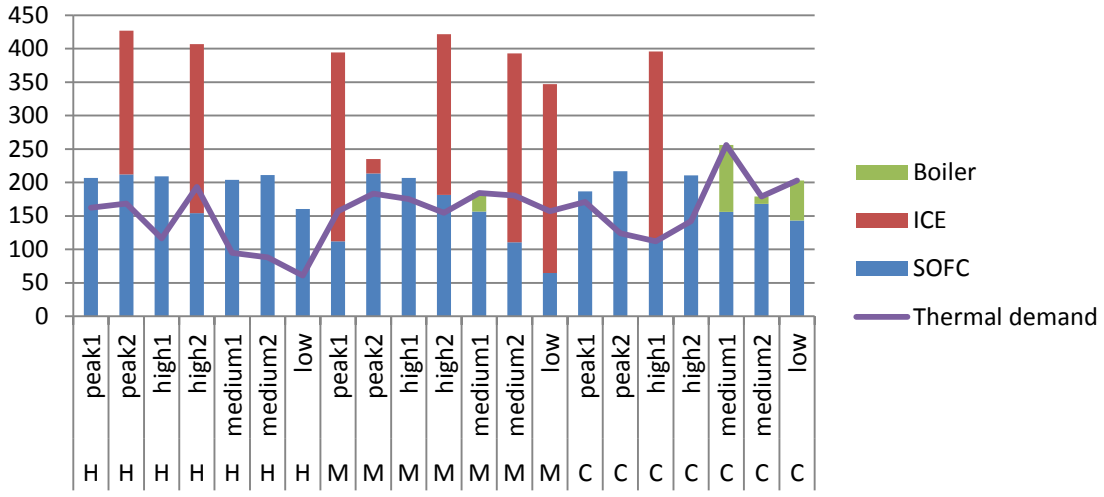

Figure 6.22: Acidification - Optimal operation planning of energy systems to meet heating demand

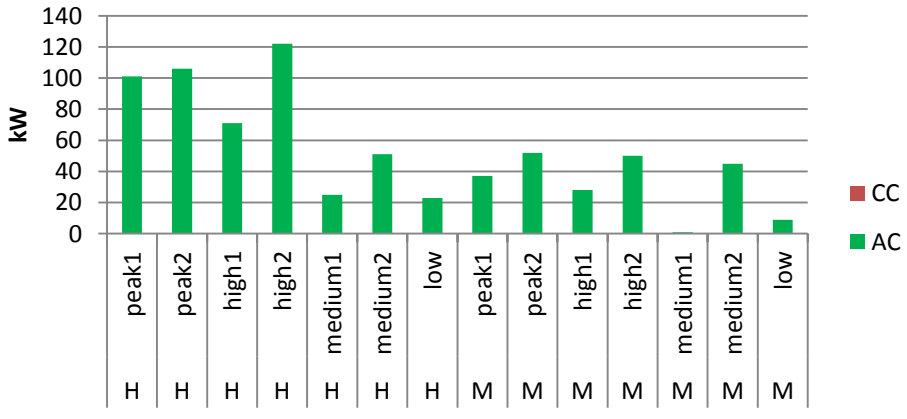

Figure 6.23: Acidification - Optimal operation planning of energy systems to meet cooling demand

6.2.4 Pareto frontier for cost and Eutrophication

This section presents the Pareto frontier obtained for LCC vs. Eutrophication impacts. Pay-off Table 6.7 shows a first global overview of the range of variation of the objective functions in their efficient regions. Significantly higher range of variability is visible for Eutrophication impact objective function values than that for LCC.

Table 6.7: Pay-off values for cost vs. Eutrophication

	Min	**Max**
Eutrophication (g PO_4^{3-} eq)	-350 492	781 453
LCC (Euros)	401 654	797 186

The Pareto frontier for Eutrophication and LCC objective functions was derived, considering a minimum step of improvement of $\delta_{I\,=}$ 2,000 for cost and 50,000 for Eutrophication (Figure 6.24). The values correspond to the total LCC and Eutrophication impact (kg PO_4^{3-} eq) of meeting the building energy demand for a nominal year. The format of the curve, and the energy systems employed in each solution to meet the required level of each objective function (cost and Eutrophication) is very similar to the Pareto obtained for cost vs. Acidification (Figure 6.20). In order to reduce Eutrophication, the imported (exported) electrical energy gradually decreases (increases) to reach its minimum (maximum) value at each block-load (150 kW due to policy restriction). The most viable technology to increase the export to grid (without violating the policy framework) is SOFC (due to high power-to-heat ratio), so its installation capacity increases according to the level of Eutrophication reduction desired by DM. The front is composed of five sections. The number of installed SOFC systems increases by one unit for each section towards less Eutrophication impacts. On top of SOFC and ICE, 80 kW PV systems are also employed that results in an annual saving of up to 410 kg PO_4^{3-} eq for our case-study building.

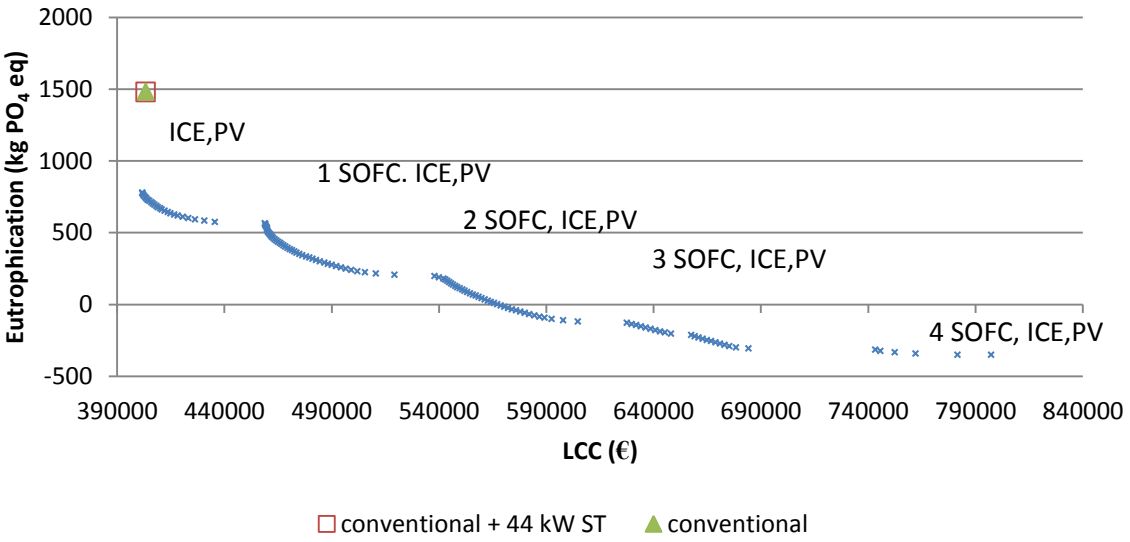

Figure 6.24: Cost vs. Eutrophication—Pareto frontier

The optimal planning patterns of the energy systems in each block-load to minimize Eutrophication impact are parallel to Figures 6.21–6.23. A negative balance of Eutrophication impact can be acquired through exporting the onsite produced electricity to the grid.

6.3 Conclusions

This chapter presented the results of economic and environmental assessment of selected DG for building sector in Portugal. First, a detailed economic assessment of each type of CHP for the building under study was carried out. Next, we presented the Pareto frontiers derived for LCC vis-à-vis four impact categories, namely CED, GHG, Acidification, and Eutrophication. It was shown that each type of DG has its particular cost structure and emissions. Therefore, depending on the objective of DM (that could be reducing the energy costs or one or more types of LCIA categories) a particular DG and operating strategy could be employed. Overall, it is possible to mitigate both energy costs and environmental impacts of the building under study by employing onsite generation technologies, although saving amounts, if any, depend on the type of technology as well as its operating strategy.

A detailed economic analysis of each type of DG, taking into account the current financial incentives to promote them in Portugal, was first undertaken in section 6.1. The combination of each type of cogeneration technology with other energy systems

was presented and showed that at the current stage ICE, and in near future, MTs would be economically viable cogeneration solutions for Portuguese buildings. ST systems also represent cost-effective solutions, whilst SOFC is not yet commercial to deploy. Furthermore, it was shown that the existing FIT in Portugal does not provide enough incentive to promote PV systems. A detailed analysis of economic implications of PV systems according to meteorology and existing national FIT is followed in chapter 7, in which we will compute the level of required FIT to incentivize the deployment of PV technology for commercial applications in different zones of continental Portugal. The significance of including the varied technological profile of cogeneration systems and their interrelationship with the policy frameworks was stressed where it was observed that e.g. utilizing ICE systems leaves no space for the employment of boilers and ST panels, whereas this trend was not replicated for MT and SOFC systems.

The Pareto frontier obtained for CED and GHG shows that ICE is the cogeneration technology that can provide the maximum saving across both categories. Either the DM opts to minimize the energy costs, or reduce the GHG emissions or CED arising from meeting the building energy demands, ICE is the cogeneration technology to employ. The economic advantage of ICE over the conventional energy sources, i.e. grid and a conventional boiler, is not remarkable; however, the magnitude of savings ICE provides compared to conventional settings can be up to 50% for GHG emissions and CED. Moreover, the operating strategy of ICE significantly affects its economic and environmental performance. To illustrate, all the solutions positioned on the Pareto frontiers obtained for CED and GHG vis-à-vis LCC (Figures 6.12 and 6.16), employ ICE cogeneration technology; however, the operating strategy of ICE (and consequently the energy systems coupled with it) differs for each solution according to the level of each objective function (CED, GHG or LCC) aspired by the DM. The optimal configuration of energy systems to minimize CED and GHG emissions are similar, where an ICE and PV are the DG employed. ICE operates mainly in hot seasons (in conjunction with AC), during which its advantage over the combination of grid and CC is more pronounced.

The Pareto frontier obtained for LCC vis-à-vis Eutrophication and Acidification impacts indicate that in order to minimize those impacts, imported power from national grid

should be curbed and ultimately avoided. Employment of any type of DG can mitigate Acidification and Eutrophication impacts; however, the best DG to do so while not over-supplying the building thermal demand is SOFC. This is due to significantly higher power-to-heat ratio of fuel cells compared to other cogeneration systems. SOFC can even bring about negative emission balance for Eutrophication and Acidification impacts.

Regarding solar systems, ST stands as the technology with lower setup costs that make them cost-competitive against the boiler, while PV is not yet commercial against the national grid in Portugal (a detailed assessment of economics of PV technology according to local meteorology and markets is carried out in chapter 7). However, PV combined with cogeneration systems has comparably higher potential to reduce the CED and environmental impacts of the building. This is due to the fact that a cap exists over the thermal output of cogeneration systems, either due to national legal frameworks or basically the demand of the building. For electricity, however, extra produced power could be exported to grid, as long as not violating the policy framework. Therefore, employing CHP might not leave space for the employment of ST systems, since the building thermal demand could be entirely met by CHP. PV, however, has a different position since 50% of its electricity production (as well as that of CHP) could be exported to grid (according to Portuguese legal framework). In other words, although PV has higher installed costs, it also higher potential to reduce the impact of building compared to ST, due to dynamics of national policies and conditions.

Chapter 7

Solar PV economics in Portugal

This chapter proposes a methodology to study the cost-effectiveness of solar PV systems. Using this methodology, we investigate the key drivers to and status of cost-effectiveness of PV systems in Portugal, by taking into account the received solar radiation in different geographical locations across the country and the estimated output (kWh/year) of PV systems. The proposed methodology to assess the economics of PV systems is discussed in section 7.1. Next, we explore the underlying factors behind the willingness-to-pay for PV systems by looking at five different geographical locations in south, center and north of Portugal (section 7.2). The analysis is extended to assess the efficiency of the established Feed-In Tariff (FIT) on the promotion of PV technology in studied locations in Portugal (section 7.3). Summary and concluding notes close the chapter (section 7.4).

7.1 Methodology

The aim of this chapter is to assess the cost-effectiveness of PV systems in continental Portugal, by considering meteorology and solar radiation received by the systems in different geographical locations. The analysis was performed for 5 major cities located at different latitudes across the country: Faro (south), Évora (center-south), Coimbra (center), Porto (center-north) and Bragança (north). Figure 7.1 shows a map of continental Portugal where the studied locations are distinguished with red circles.

Figure 7.1: Map of Portugal—Studied Cities

By selecting the location of the study and the size of the PV system, the PV-WATTS application (PV-WATTS, 2011) yields the hour-by-hour estimated power output of mono-crystalline silicon PV systems according to settings defined by the user. The settings comprise tilt angle, azimuth angle and array type (fixed, 1-axis tracking or 2-axes tracking), etc. For this study, the PV-WATTS default values of the above settings

(that are also the optimal values regarding the azimuth and tilt angles) for each location were used (Table 7.1). PV systems are identical to the description in chapter 4, section 4.2.4. For reference purposes, the current total installed cost and FIT for PV system in Portugal are 4.5€/W_p (Watt-peak) (IEA-PVPS, 2011) and 0.215€/kWh_e (kWh electricity) (Administrative rule 285/2011), respectively.

Table 7.1: Meteorological sites specifications— Faro, Évora, Coimbra, Porto, and Bragança (PV-Watts, 2011)

	Faro (south)	**Évora (center-south)**	**Coimbra (center)**	**Porto (center-north)**	**Bragança (north)**
Latitude	37.02°N	38.57°N	40.20°N	41.23°N	41.80°N
Longitude	7.97°W	7.90°W	8.42°W	8.68° W	6.73° W
Elevation (m)	4	321	140	73	692
DC Rating (kW)	4.00	4.00	4.00	4.00	4.00
AC Rating (kW)	3.08	3.08	3.08	3.08	3.08
Array Type	Fixed	Fixed	Fixed	Fixed	Fixed
Array Tilt	37.02°	38.6°	40.20°	41.23°	41.80°
Array Azimuth	180.00°	180.00°	180.00°	180.00°	180.00°

The solar radiation received and AC energy output of the PV systems in each month, according to the specifications defined in Table 7.1 for each location is shown in Table 7.2. Table 7.2 shows an interesting point: while the total annual solar radiation (kWh/m^2/day) in Coimbra is slightly higher than that in Porto, the AC energy (kWh) output of the PV systems at the two cities is reversed, with Porto being slightly better than Coimbra. This is also shown by the monthly capacity factor of the PV installations (Table 7.2). We see that the capacity factor of systems in Coimbra drops significantly in springtime (May, June) relative to Faro, Évora, Porto and Bragança. The higher ambient temperature in Coimbra explains this trend. The solar resource in Coimbra is actually only slightly better than in Porto; this is why the temperature differences between Coimbra and Porto is enough to cause the unexpected result of higher annual PV generation in Porto, since PV output is reduced by approximately 0.5% for every degree Celsius increase (Denholm *et al*., 2009). With this input data, we calculated the willingness-to-pay for PV systems operating under the same market conditions for the five different meteorological locations.

Table 7.2: Solar radiation and energy output of PV systems in Faro, Évora, Coimbra, Porto and Bragança

	Faro (south)			Évora (center-south)			Coimbra (center)			Porto (center-north)			Bragança (north)		
Month	Solar Radiation (kWh/ m^2/day)	AC Energy (kWh)	Capacity Factor*	Solar Radiation (kWh/ m^2/day)	AC Energy (kWh)	Capacity Factor	Solar Radiation (kWh/ m^2/day)	AC Energy (kWh)	Capacity Factor	Solar Radiation (kWh/ m^2/day)	AC Energy (kWh)	Capacity Factor	Solar Radiation (kWh/ m^2/day)	AC Energy (kWh)	Capacity Factor
1	4.15	384	16.8	3.65	344	15	3.58	324	14.1	2.84	257	11.2	2.76	255	11.1
2	4.76	395	19.1	3.97	333	16.1	3.64	300	14.5	3.87	322	15.6	3.9	328	15.8
3	6.34	574	25.0	6.08	555	24.2	5.04	454	19.8	5.2	476	20.8	5.42	496	21.6
4	6.27	548	24.7	5.49	489	22.1	5.67	490	22.1	6.1	535	24.1	5.18	451	20.3
5	6.78	598	26.1	6.45	567	24.7	5.49	482	21.0	6.12	550	24.0	5.56	497	21.7
6	6.89	580	26.2	6.37	531	23.9	6.03	501	22.6	6.39	529	23.9	6.59	553	24.9
7	7.27	616	26.9	6.90	581	25.4	6.36	538	23.5	6.27	544	23.7	6.88	577	25.2
8	7.01	592	25.8	6.92	589	25.7	6.52	555	24.2	6.37	552	24.1	6.64	566	24.7
9	6.75	566	25.5	5.86	489	22.1	5.57	460	20.7	5.47	457	20.6	6.16	522	23.5
10	5.43	478	20.9	4.71	419	18.3	4.56	396	17.3	4.45	397	17.3	4.26	384	16.8
11	4.32	380	17.1	3.30	293	13.2	3.02	263	11.9	2.61	222	10.0	3.48	304	13.7
12	3.59	328	14.3	2.99	278	12.1	2.8	254	11.1	2.59	227	9.9	2.31	203	8.9
Year	**5.8**	**6040**	**22.4**	**5.23**	**5466**	**20.5**	**4.87**	**5016**	**18.6**	**4.86**	**5069**	**18.8**	**4.93**	**5134**	**19.0**

$$\text{* Monthly Capacity factor} = \frac{\text{PV System AC Output per Month (kWh)}}{3.08\ \text{kW (PV AC rating)} \times \text{hours in the month}}$$

7.2 Willingness to pay for PV in Portugal

We calculated the break-even cost for PV technology for the major cities located in south, center and north of Portugal. Break-even cost for PV technology is defined as "the point where the cost of PV-generated electricity equals the cost of electricity purchased from the grid" (Denholm *et al*., 2009). Break-even points are calculated taking into account the local solar resource and meteorology.

The set of break-even points for one meteorological condition delivers the willingness-to-pay curves for that site. The diagonal lines in Figure 7.2 represent the willingness-to-pay for PV (€/W_{DC}) for Faro, Évora, Coimbra, Porto and Bragança. It is clear that with the current cost of commercial class electricity in Portugal (9 € Cents/ kWh), the willingness-to-pay for solar systems is still substantially lower than the current (unsubsidized) cost of commercial PV systems, or in other words, PV is not cost-effective in any of the regions without subsidization. Figure 7.2 also shows that willingness-to-pay for solar systems is significantly higher in southern cities (Faro and Évora) than in other regions. As a result, the "threshold" (Δ€/W_{DC}) to become cost-effective is lower for south versus other cities. To illustrate, in Faro and Évora, the "cost-effectiveness threshold" (Δ), the gap between the unsubsidized PV cost in Portugal (4.5 €/W_{DC}) and "the willingness-to-pay for PV at 9 € cents", is less than its value for Coimbra, Porto and Bragança. This implies that PV has a shorter path to grid-parity in Faro. Such information is summarized in Table 7.3 in which the values of willingness-to-pay and "cost-effectiveness thresholds" for PV technology in the five locations are shown. The path to grid parity is also lower for Évora than central and northern cities, among which we see that the willingness-to-pay curves for PV systems are almost the same, with Bragança being slightly higher than Porto and next Coimbra.

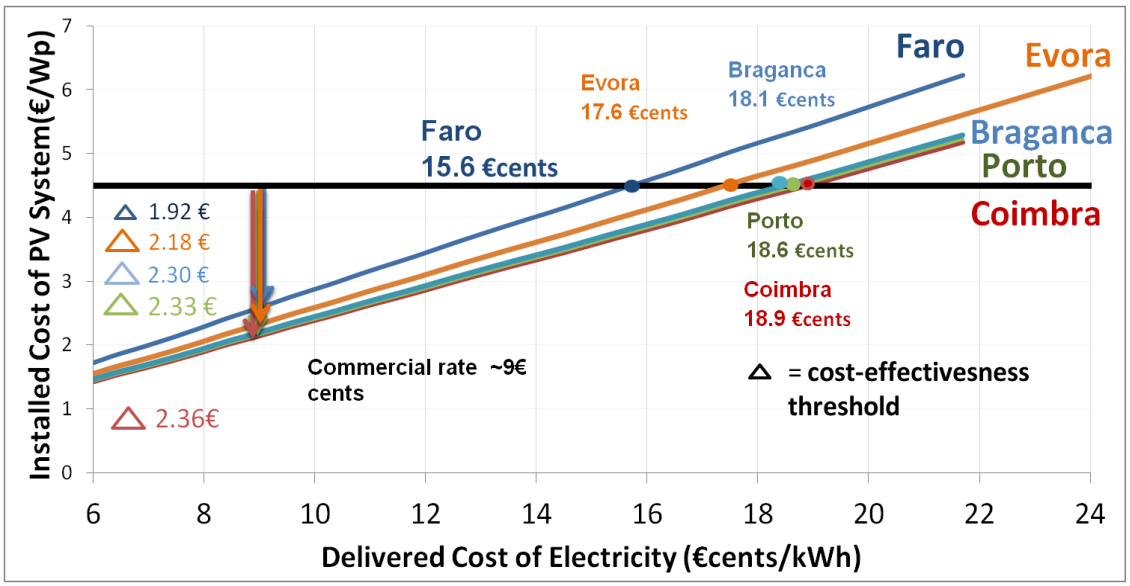

Figure 7.2: Willingness-to-pay for PV— Faro, Évora, Coimbra, Porto, and Bragança

Table 7.3: Summary of Willingness-to-pay PV— Faro, Évora, Coimbra, Porto, and Bragança

	Unit	Locations				
		Faro (south)	**Évora** (center-south)	**Coimbra** (center)	**Porto** (center-North)	**Bragança** (North)
Current average retail price of electricity to commercial customers in 2012	¢/kWh(AC)	9				
Unit Cost of Commercial PV system in Portugal	€/W_{DC}	4.5				
Willingness-to-pay for PV technology (at the current retail price of electricity to commercial customers)	€/W_{DC}	2.58	2.32	2.14	2.17	2.20
"Cost-effectiveness threshold" for PV technology (Δ) [Unit Cost of PV system (€/W_{DC}) – Willingness-to-pay for PV technology]	€/W_{DC}	1.92	2.18	2.36	2.33	2.30

7.3 Implication of FIT on economics of PV in Portugal

We showed that that without financial incentives, PV technology was not cost-effective in any of the studied locations in Portugal. We further explore the implications of the current FIT for the economics of PV across the country. Similar to Figure 7.2, the diagonal lines in Figure 7.3 represent the willingness-to-pay for PV

(€/Wp) technologies, but based on the evolution of FIT. With the current FIT (215 €/MWh), the willingness-to-pay for solar PV systems in center and north (Coimbra, Porto, Bragança) is roughly 3.5 €/W_p, lower than the current cost of PV systems (4.5 €/W_p). This implies that even by considering the current FIT (215 €/MWh), PV is not cost-effective in the mentioned locations. However, PV systems are just about grid-parity in Faro, where the applied FIT seems motivating for the deployment of PV technology. For Évora, the FIT needs to rise to 363 €/MWh for PV to reach grid parity. Regarding center and north, which have similar PV cost structures, either the initial FIT needs to be at the level of 455–485 €/MWh, or alternatively, the installed cost of PV should be reduced to 3.8–4.2 €/W_p.

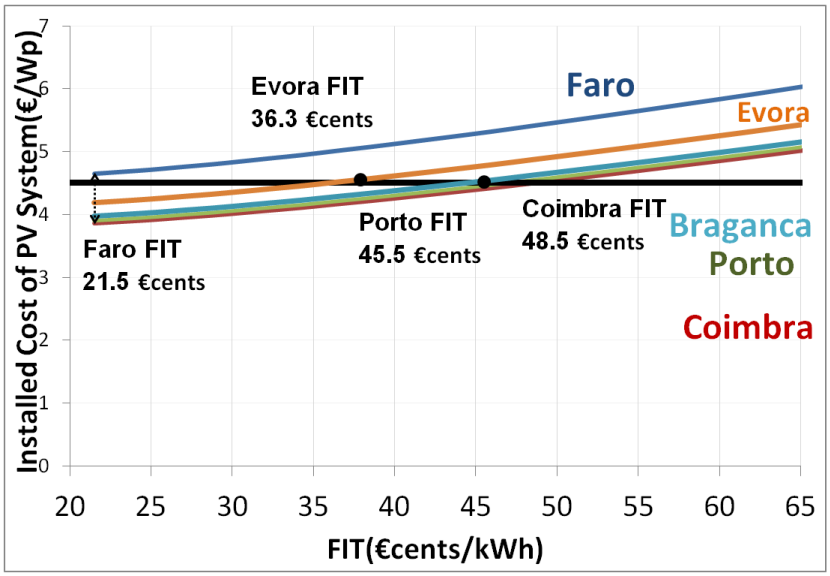

Figure 7.3: Implication of FIT on economics of PV—Faro, Èvora, Coimbra, Porto, and Bragança

7.4 Summary and concluding notes

This chapter explored the cost-effectiveness of PV technology in Portugal. In summary, the relative cost-effectiveness of PV systems depends on a number of key factors. Local solar insolation and meteorological factors impact the output of PV systems. While this impacts the willingness-to-pay for PV systems, the distance to grid parity is also dependent on national electricity rates, the cost of installing PV systems including local permitting and labor costs, and incentives (FIT) to promote PV.

The net result is that the cost-effectiveness of PV systems is impacted by both local meteorology and economics. Policies to get PV to "grid parity" must consider both these factors. The framework developed for economic assessment of PV systems has the advantage that the implication of alteration of deciding parameters (solar PV costs, local electricity costs, FIT) for the promotion of PV can be easily evaluated and updated to reflect the actual distance to grid-parity. For the five locations shown, commercial PV systems were cost effective in south of Portugal (Faro) based upon a good solar resource, while for center and north, distance to grid parity is almost equal—due to uniform solar radiation—and PV is not cost-effective with the existing FIT (215 €/MWh). The required values of FIT required to promote PV in those regions were calculated and discussed. Finally, we highlighted the importance of ambient factors on the net output of PV systems, where we demonstrated the impairment of AC output of PV systems in Coimbra due to high ambient temperatures.

Chapter 8

Probabilistic and Robust Optimization Framework

The purpose of this chapter is to include uncertainty in the energy cost data and present a probabilistic and robust modeling framework for DG. We first provide a general introduction to robust optimization modelling and present the corresponding mathematical formulation. Next, we discuss the application of the proposed framework by defining a number of scenarios and analyzing the model results.

8.1 Robust modelling framework

$$Min\ Z = C\,x + dy \tag{8.1}$$
$$s.t:\ Ax = b$$
$$Bx + cy = e$$
$$x \geq 0, y \geq 0$$

Consider a mathematical programming model (8.1). According to Mulvey *et al.* (1995), we can define two types of decision variables:

x , is the vector of decision variables whose optimal value is not conditioned on the realization of the uncertain parameters and cannot be changed once a specific realization of the data is observed. This type of variable may be associated to the fixed capital costs, which do not get affected by the operation planning or energy costs. Mulvey *et al.* (1995) denote them as “design “variables.

y, denotes the vector of “control” decision variables that get affected by the uncertain parameters as well as the value of design variables. An example is the set of variables associated with operating costs of the energy systems.

The uncertainty is captured through a set of scenarios s ∈ S= {1, 2, ...}, in which each scenario has an associated set of coefficients {d_s, B_s, c_s, e_s,}. The parameter P_s represent the probability that scenario s occurs, where $\sum_{s \in S} P_s = 1$. The optimal solution is

called “solution robust” if remains close to the optimal when uncertain coefficients alter. Likewise, it is termed “model robust” if it stays feasible due to small changes in the input data.

The robust model can be defined as:

$$\begin{aligned} \text{Min } Z = \sigma(x, y_1, y_2, \dots, y_s) + \omega\, \beta(z_1, z_2, \dots, z_s) \\ \text{s.t: } Ax = b \\ B_s x + C_s y = e_s \qquad s \in S \\ x \geq 0, y_s \geq 0, s \in S \end{aligned} \tag{8.2}$$

In (8.2), variables y_s ($s \in S$) are the control variables for each scenario s, and variables z_s ($s \in S$) measure the deviation from feasibility constraints in scenario s. The function σ can be the average of the random variable $\xi_S = c\,x + d_s y_s$ (objective function of the original problem), as in stochastic programming, or the maximum value for all scenarios, as in the minmax formulation. The component $\beta(z_1, z_2, \dots, z_s)$ is a penalty function to penalize violations of constraints for various scenarios. The function σ(.) measures the “solution robustness”, and β(.) measures the “model robustness”, controlled by the parameter ω.

A possible way to formulate $\sigma(.)$ is as following:

$$\sigma(x, y_1, y_2, \dots, y_s) = \sum_{s \in S} P_S \xi_S + \lambda \sum_{s \in S} P_S \left(\xi_S - \sum_{s \in S} P_S \xi_S \right)^2 \tag{8.3}$$

The first term in $\sigma(.)$ represents the average of ξ_S, and the second term represents the variance of ξ_S.

Similarly, $\beta(z_1, z_2, \dots, z_s)$ can be formulated as:

$$\sum_{s \in S} P_S \mid z_S \mid \tag{8.4}$$

With regards to the non-linearity of $\sigma(.)$, we used the approach suggested by Yu & Li (2000). This is done by converting (8.3) to (8.5) by adding an artificial variable (ϕ_s), and adding constraint (8.6) to model:

$$\sigma(x, y_1, y_2, \dots, y_s) = \sum_{s \in S} P_S \xi + \lambda \sum_{s \in S} P_S [(\xi_S - \sum_{s \in S} P_S \xi_S) + 2\phi_S] \tag{8.5}$$

$$\xi_S - \sum_{s\in S} \quad P_S\xi_S \; + \phi_S \geq 0, s \; \in \; S \tag{8.6}$$

The global robust optimization problem can therefore be stated as:

$$\begin{aligned} Min \; Z = = \; \sum_{s\in S} \quad P_S \, \xi_S + \lambda \; \sum_{s\in S} P_S[(\xi_S - \sum_{s\in S} \quad P_S\xi_S) + 2\phi_S \,] \\ + \omega \sum_{s\in S} P_S(Z_S + 2\delta_S \,) \end{aligned} \tag{8.7}$$

s.t:

$$\begin{aligned} \xi_S - \sum_{s\in S} \quad P_S \, \xi_S + \; \phi_S \geq 0 \qquad & s \; \in \; S \\ Z_S + \delta_S \geq 0 \qquad & s \; \in \; S \\ B_s x \; + \; C_s y = \; e_s \qquad & s \; \in \; S \\ x \; \geq 0, y_s \geq 0, s \; \in \; S \end{aligned}$$

where ϕ_S and δ_S are auxiliary variables to linearize the objective function.

The second term in the objective function of (8.7) is the variance, which is considered with aim of providing robust solutions. Parameter λ controls the robustness of the solution. Similarly, the third term in the objective function measures the feasibility violation. Parameter ω is the factor assigned for this matter. Since uncertainty in energy costs only affects the coefficient of variables in objective function (σ), the model never becomes infeasible due to its alteration. In other words, we only seek "solution robustness" against perturbations in energy costs and disregard the robustness in model. In this way, parameter ω can be considered zero.

8.2 Results

Uncertainty in energy (NG and electricity) costs can be stated as uncertainty in the current year costs (around a mean value) or uncertainty in the evolution of costs throughout the planning period. Consider a case where DM has an estimate of the approximate value of this year´s energy costs, but their exact value is unknown and falls within ± α % of their mean value (e.g. due to market conditions). For forthcoming years of planning period, he/she can define a number of plausible scenarios for the evolution of energy costs. The idea is to offer an investment planning that has the minimum expected LCC across different scenarios.

Three scenarios for the future costs of electricity and gas are considered. First scenario, NG and electricity costs (per kWh) increase annually with the rate of 3% and

1%, respectively. Second scenario, energy costs increase annually with the same but reverse order of magnitude: i.e. 1% and 3% for electricity and NG. Finally, for the third scenario energy costs increase by 2%, annually. We first explore the results associated with these scenarios, without considering robustness. Next, we add the robustness factor to provide a robust operation planning. For the first year, we have assumed 100 scenarios in which energy costs fall randomly within $\pm$ 90% of their mean estimated value. We run the model by including all the cogeneration and solar technologies for a period of 11 years, to be consistent with the results presented in chapter 6, sections 6.1.

The results of the running the probabilistic model (no robustness considered i.e., λ = 0), when minimizing the LCC, indicates that one unit of ICE and a boiler are employed to meet the demand throughout the planning period. In fact, the economic advantage of ICE, and cogeneration systems in general, is more pronounced when considering probabilistic modeling rather than a deterministic one (as discussed in section 6.1 of thesis). This is because cogeneration can regulate the operating output at each block-load throughout the (future years of) planning period according to relative fuel price costs. Table 8.1 shows the expected value of the objective function for each of the defined scenarios. Following ICE, while MT was not seen as a cost-effective cogeneration technology against conventional systems in deterministic results (see section 6.1.2), here the employment of MT also proves economical. Once again this is due to the flexibility of the system to shut down (or reduce the operating load) when the NG price is relatively high compared to electricity, and vice versa. For both MT and ICE, the output of EC and AC changes according to the available heat output of cogeneration systems.

Table 8.1: Expected value of objective function - different energy systems

ICE														
Year	2012	2013	2014	2015	2016	2017	2018	2019	2020	2021	2022	Power (KW) ICE	Power (KW) grid	Power (KW) boiler
Scenario 1		406500	414619	422883	431196	439666	448459	457428	466577	475908	485426	11025	21638	297
Scenario 2	398526	407516	416712	425956	435455	445123	454025	463106	472368	481815	491451	11056	21310	281
Scenario 3		405314	412223	419277	426416	433652	442325	451171	460195	469399	478787	10505	22818	23

Conventional													
Year	2012	2013	2014	2015	2016	2017	2018	2019	2020	2021	2022	Power (KW) grid	Power (KW)boiler
Scenario 1		410592	418803	427172	435719	444434	453322	462389	471636	481069	490690	33194	10748
Scenario 2	402539	413816	425429	437388	449694	462357	471604	481036	490657	500470	510479	33194	10748
Scenario 3		407358	412251	417218	422247	427371	435918	444637	453530	462600	471852	33194	10748

						MT								
Year	2012	2013	2014	2015	2016	2017	2018	2019	2020	2021	2022	Power (KW) MT	Power (KW) grid	Power (KW)boiler
Scenario 1		409912	418082	426407	434865	443501	452371	461418	470646	480059	489660	3932	28256	6513
Scenario 2	401820	412276	422932	433855	444999	456454	465583	474895	484393	494081	503962	4219	27905	5846
Scenario 3		407548	413297	419147	425119	431191	439814	448611	457583	466735	476069	3932	28412	6513

Table 8.1 displays the expected value of objective functions, according to defined energy cost evolution scenarios, for three alternative set of energy system combinations: 1- a (172 kW_e) ICE, 104 kW AC and 30 kW CC; 2- one unit (54 kW_e) MT, 44 kW ST, 104 kW AC and 45 kW CC; 3- Conventional systems. As mentioned, when employing cogeneration systems, their output adjusts according to relative energy cost in each scenario to minimize the expected costs. On the other hand, with only conventional systems, the output of energy systems is always fixed and the expected costs only reflect the alteration of energy costs. This example demonstrates the economic benefits of cogeneration systems in face of energy costs uncertainty and reveals that as long as the DM has plausible scenarios for the evolution of energy costs, probabilistic analysis provides more accurate results than a deterministic study.

Next, we include the robustness framework for the selection and optimization of operation of energy systems. As already mentioned, the robustness framework is employed to provide a robust operation planning, one that gets less affected by the relative perturbation of fuel prices (per kWh). One hundred scenarios are considered, in which energy costs fall randomly within $\pm$ 90% of their mean estimated value. Parameter λ in (8.7) controls the solution robustness.

Table 8.2 shows the LCC objective function value and configuration of energy systems as the robustness factor λ increases. As we already know (from 6.1), the most economical set of energy system is ICE and a small sized boiler (5 kW). With this energy systems operating at optimal operation planning to minimize costs (parallel to Figures 6.1 to 6.3), the variance of solutions due to variation of fuel price is 12,862. This is already more robust than conventional energy systems, for which the solution variance due to energy cost perturbations is 16,560. Clearly it is not possible to completely offset the effect of alteration of fuel prices on results and our analysis show that the minimum level of variance—due to 10% random perturbation in energy costs—is 8,154. By gradually increasing the robustness parameter, one can obtain more robust solutions, which get less affected by the alteration of energy costs.

Overall, with increasing the level of λ, the diversity and capacity of cogeneration installation increase. With more desired robustness, MT is also employed along with ICE that operates as peak-shaver (see second row in Table 8.2). It is possible to attain a more robust solution with the same set of energy systems (ICE+ MT + boiler) by changing the operation planning: the contribution and operating hours of cogeneration systems, mainly ICE, slightly increases with more robustness sought. Increasing the robustness factor λ decreases the operating hours of DG in low and medium block-loads (where the grid price is at its lowest), and increases their output in peak-loads (where grid price is at its highest). In this way, the "chance" of conventional systems dominating DG (in terms of costs) decreases to provide a more robust operation planning in face of energy cost changes.

As a trade-off by increasing costs, it is possible to further increase the robustness of solutions. This is done by adding SOFC systems to the set of energy systems. As explored in chapter 6, one specific advantage of SOFC compared to other cogeneration technologies is its high power-to-heat ratio that allows the operation of fuel cell without over-supplying the heat demand. Here, this feature of SOFC, plus the low operating cost of engine, which makes it cost-effective even in some medium-low block-loads, leads to its employment when more robustness is required against energy cost change. Employment of SOFC implicates less electricity import from the grid (which is subject to price volatility), so the effect of fuel price volatility on results is moderated. The higher operating cost of MT and ICE, compared to SOFC, increases the probability that they become inferior to conventional systems when energy costs change, while the lower operating cost of SOFC decreases such probability and therefore provide a more "robust" operation planning due to changes in energy costs. MTs coupled with SOFC mostly operate in peak-loads where they are almost certainly cost-effective in terms of operating costs. The minimum variance attainable, i.e. the most robust solution, has a variance of 8,154 and is achieved by co-employing 2 MTs, 2 SOFCs, and 80 kW PV.

The last rows in Table 8.2 compare the robustness of solutions when PV or ST systems are employed along with conventional systems. Particularly, 80 kW PV can reduce the variance by 681. ST, on the other hand, cannot significantly increase the solution

robustness, only by 14 units as Table 8.2 shows. We reiterate that more robustness (less variance than 8,154) is not attainable with the defined cost volatility scenario, since a part of volatility found in results is due to energy cost price, which cannot be avoided.

Table 8.2: Sensitivity of results to robustness parameter λ

Solution Variance	Energy Systems	LCC (€)	ICE (kW)	MT (kW)	SOFC 8kW)	boiler size (kW)	AC (kW)	CC (kW)	PV (kW)	ST (kW)
16560	Conventional systems	403360	0	0	0	257	0	150	0	0
12862	ICE, boiler	396430	172			6	104	45	0	0
12000	ICE, boiler, CC, AC, PV	397310	172	60	0	207	104	30	80	0
11500	ICE, MT, boiler, CC, AC	403140	172	60	0	96	104	30	0	0
11000	ICE, MT, boiler, CC, AC	404880	172	60	0	96	104	30	0	0
10500	ICE, MT, boiler, CC, AC	407640	172	60	0	96	104	30	0	0
10000	MT, SOFC, boiler, CC, AC	446270	0	60	125	96	104	30	0	0
9500	ICE, MT, 1 SOFC, boiler, CC, AC	457810	172	60	125	96	104	30	0	0
9000	MT, SOFC, boiler, CC, AC	466218	0	60	250	96	104	45	0	0
8500	MT, SOFC, boiler, CC, AC	546360	0	60	250	201	104	60	40	0
8154	MT, SOFC, boiler, CC, AC	655740	0	120	250	207	208	60	80	0
16546	Conventional system + 80 kW ST	397310	0	0	0	257	0	150	0	80
15879	Conventional systems + 80 kW PV	455797		0	0	257	0	150	80	0

8.3 Conclusions

This chapter presented a probabilistic and robust modeling framework for DG. We first discussed that including future energy cost scenario analysis in the model increases its flexibility and accuracy, even without including the robustness factor. By incorporating robustness, the DM is allowed to obtain an operation planning that gets least affected due to perturbations in energy costs.

Chapter 9

Concluding Remarks

9.1 Summary and dissemination of results

Distributed Generation (DG), including renewable sources, is expected to play an important role in the future energy mix of the building sector. This thesis presented a model for optimal design and operation of DG for Portuguese commercial buildings. The model can have extensive application in assessing the economic implications and environmental impacts associated with meeting the building energy demand. In terms of components, it incorporates different combined heat and power technologies, separate production of electricity (grid) and heat (onsite boilers), renewable sources (ST and PV) and auxiliary cooling systems (AC and CC). The national schemes to promote each type of DG, selling electricity produced onsite and dynamic electricity prices are also considered.

The model allows a Decision Maker (DM) to select the design and operational strategies of the energy systems according to preferred level of costs and/or LCIA categories (CED, GHG, Acidification, Eutrophication). LCA techniques were used to calculate the LC impacts rising from of one unit energy output of energy systems. A description of the model, full mathematical relations and the results of economic assessment of DG for Portugal were presented in Safaei *et al*. (2013).

In order to provide the input to the model, a detailed LCA of upstream stages of Portuguese NG mix was performed, based on the weighted share from exporting countries, detecting the main stages and emissions that contribute to each of the LCIA categories studied. By assessing two distinct NG supply chains, we demonstrated that the source of NG and its state of delivery (in liquid form via marine transportation or gas via pipeline) have important implications on its total upstream impacts. In addition, in order to provide insights for policy design, an uncertainty assessment of GHG footprint of NG was also carried out, taking into account the uncertainty in the LC

model input parameters and modeling choices. The underlying uncertainty in upstream GHG intensity of Nigerian LNG to Europe, and the upstream impact of Portuguese NG mix, are dealt with in Safaei *et al*. (2014a) and Safaei *et al*. (2014b).

Using the model developed, we assessed the environmental impacts of distributed and centralized generation sources for building sector in Portugal. We characterized the LC impact of each type of generation technology and discussed the optimal design and operation of energy systems to minimize each individual objective function. It was argued that LCA of CHP can be suitably addressed using a modeling framework that considers the interrelationship between several components in building energy systems, like the optimization model developed in this thesis. In addition, using Pareto frontiers, we showed the trade-off between each type of environmental impact and costs. The Pareto frontiers allow a potential DM to have a firsthand view over the estimated costs and emission of building entity, and select the design and operation of energy systems according to the desired level of each type of objective function. The results of environmental impact analysis of DG for Portuguese buildings and the derived Pareto frontiers are being prepared for publication.

An approach to study the cost-effectiveness of solar PV systems, according to local meteorology, their hourly estimated output (kWh/year), market, and existing financial incentives was presented in chapter 7. We investigated the key drivers to and status of cost-effectiveness of PV systems in Portugal, according to current national established Feed-In Tariff (FIT). Applying the methodology, the cost-effectiveness of PV systems in commercial applications in United States were examined. The latter study is included as a report in “MIT Future of Solar Energy Study” (Peer reviewed by external advisory committee): Safaei & Connors (2014).

Finally, in order to consider the uncertainty in fuel costs into the model, a probabilistic optimization framework for design and operation of DG in buildings, one that is robust against small perturbation in input fuel costs, was presented.

9.2 Limitations and recommendations for future studies

During the course of this doctoral thesis, important questions and limitations have been pointed out that are worth of further research. These are categorized based on their relevance to each chapter.

Chapters 3 and 4:

- High level of uncertainty found in GHG intensity of NG chains suggests that further empirical data and investigation is required to better understand and characterize the source and extent of emissions from NG chains, including other types of NG (conventional or unconventional; LNG) and supply sources. Thus, we strongly recommend further LC studies, including uncertainty analysis for other impact categories, for NG chains. In order to increase the transparency of LCI data, the industry also requires measuring and reducing the methane venting and fugitive emissions from NG production phases (Alvarez *et al.*, 2012).
- Similarly, data availability for construction and operation of DG, including onsite measured emissions, characterizing also their part-load operation, are required.
- Conducting bottom-up studies to estimate the aggregate environmental impacts and energy consumption of the commercial building sector

Chapters 5 to 8:

- In real-world problems factors such as temperature, pressure and working conditions may affect the efficiency of DG and introduce some nonlinear effects. The model developed in this thesis is a Mixed Integer Linear Programming (MILP), and therefore does not assess the implications of these factors. An added value is to assess the effects of those factors by expanding the model considering non-linear aspects.
- This study has considered 4 kW ST and PV systems into analysis. Due to the economies of scale, a solar system with higher size might provide cost advantages, which could be analysed.

- Extending the robustness analysis methodological approach to multiple-objective models and more types of uncertainty

The developed model for design and operation of DG can be improved by

- Adding auxiliary systems, such as heat storage, or diversified technologies, such as other types of PV systems, or tracking PV systems to the model and examine the effects on the results.
- Adapting the mathematical model formulation to include export of thermal energy to district heating systems.
- Including factors that introduce non-linearity into the model.

More suggestions for future studies include:

- Obtaining 3-dimensional Pareto frontiers to display the trade-offs between cost and diverse environmental impacts.
- Performing sensitivity analysis over several input parameters to the model, e.g. efficiency parameters and emission factors of DG.
- Developing a dual-objective robust framework for design and operation of building energy systems, simultaneously considering the underlying uncertainty in costs and environmental impacts.

Bibliographic References

Ackermann, T & Andersson, G & Söder,L (2001) Distributed generation: a definition1. *Electric Power Systems Research*, 57(3): 195-204.

ADENE (2012) Energy Efficiency Policies and Measures in Portugal. *ODYSSEE- MURE 2010; Monitoring of EU and national energy efficiency targets*.

Administrative rule 140/2012 (2012) Administrative rule 140/2 of 14 of May (in Portuguese)

Administrative rule 285/2011 (2011) Administrative rule n.º 285/2011of 28 of October (in Portuguese).

Alanne, K & Saari, A (2004) Sustainable small-scale CHP technologies for buildings: the basis for multi-perspective decision-making. *Renewable and Sustainable Energy Reviews*, 8(5):401-431.

Alsema, E & Fraile, D & Frischknecht, R & Fthenakis, V & Held, M & Kim, H. C & de Wild Scholten, M (2009) Methodology guidelines on life cycle assessment of photovoltaic electricity. *IEA PVPS Task*, *12*.

Andersen, A. N. & Lund, H. (2007) New CHP partnerships offering balancing of fluctuating renewable electricity productions. *Journal of Cleaner Production*, 15(3):288-293.

Anomohanran, O (2012) Determination of greenhouse gas emission resulting from gas flaring activities in Nigeria, *Energy Policy,* (45): 666-670

API (2009) Compendium of Greenhouse Gas Emissions Methodologies for the Oil and Natural Gas Industry. Available at: http://www.api.org/environment-health-and-safety/climate-change/whats-new/compendium-ghg-methodologies-oil-and-gas-industry.aspx

Arcuri, P & Florio, G & Fragiacomo, P (2007) A mixed integer programming model for optimal design of trigeneration in a hospital complex. *Energy*, *32*(8), 1430-1447.

ARI & ICF (2008) Greenhouse Gas Life-Cycle Emissions Study: Fuel Life-Cycle of U.S. Natural Gas Supplies and International LNG.

Arteconi, A & Brandoni, C & Evangelista, D & Polonara, F (2010) Life-cycle greenhouse gas analysis of LNG as a heavy vehicle fuel in Europe. *Applied Energy*. (87) 2005–2013

Baker, J. W & Lepech, M. D (2009) Treatment of uncertainties in life cycle assessment. In *Intl. Congress on Structral Safety and Reliability*. Osaka, Japan

Banos, R & Manzano-Agugliaro, F & Montoya, F. G & Gil, C & Alcayde, A., & Gómez, J. (2011) Optimization methods applied to renewable and sustainable energy: A review. *Renewable and Sustainable Energy Reviews*, *15*(4): 1753-1766.

Barnett, P.J (2010) *Life Cycle Assessment (LCA) of Liquefied Natural Gas (LNG) and its environmental impact as a low carbon energy source*. Published bachelor thesis. University of Southern Queensland. Faculty of Engineering and Surveying.

Bernal-Agustı´n,JL & Dufo-López, R & Rivas-Ascaso, DV (2006) Design of isolated hybrid systems minimizing costs and pollutant emissions. *Renew Energy*; 31: 2227–44.

Bertsimas, D & Brown, D.B & Caramanis, C (2010) Theory and applications of Robust Optimization. *SIAM Rev.* 53(3): 464–501.

Bhat, I.K & Prakash, R (2009) LCA of renewable energy for electricity generation systems—A review. *Renewable and Sustainable Energy Reviews*. 13(5): 1067-1073.

Bhattacharyya, S. C & Quoc Thang, D. N (2004) Economic buy-back rates for electricity from cogeneration: Case of sugar industry in Vietnam. *Energy*, *29*(7): 1039-1051.

Boudghene Stambouli, A & Traversa, E (2002) Fuel cells, an alternative to standard sources of energy. *Renewable and Sustainable Energy Reviews*, 6(3): 295-304.

Boyle, G (2004) *Renewable Energy: Power for a Sustainable Future* – 2nd edition, Oxford Press University, PP 66-82

Buzcu-Guven, B & Harriss, R & Hertzmark, R (2010) Gas Flaring and Venting: Extent, Impacts, and Remedies. James A. Baker III Institute for Public Policy; RICE University

Canova, A & Chicco, G & Genon, G & Mancarella, P (2008) Emission characterization and evaluation of natural gas-fuelled cogeneration microturbines and internal combustion engines. *Energy Conversion and Management*, 49(10): 2900-2909.

Cathles, L.M & Brown, L & Taam, M & Hunter, A (2012) A commentary on “The greenhouse-gas footprint of natural gas in shale formations” by R.W. Howarth, R. Santoro, and Anthony Ingraffea. *Climatic Change*, 113(2): 525-535

Cervigni, R & Dvorak, I & Rogers, J.A (2013). Assessing Low-Carbon Development in Nigeria: An Analysis of Four Sectors. World Bank Publications.

Chevalier, C & Meunier, F (2005) Environmental assessment of biogas co- or tri-generation units by life cycle analysis methodology. *Applied Thermal Engineering*, 25(17-18): 3025-3041.

Chicco, G & Mancarella, P (2009) Distributed multi-generation: A comprehensive view.*Renewable and Sustainable Energy Reviews*, 13(3): 535-551.

Cho, H & Luck, R & Eksioglu, S.D & Chamra, L.M (2009) Cost-optimized real-time operation of CHP systems. *Energy and Buildings*, 41(4): 445-451.

Clark II, W. W. & Lund, H. (2008) Integrated technologies for sustainable stationary and mobile energy infrastructures. *Utilities Policy*, 16(2): 130-140.

Clift, R & Doig, A & Finnveden, G (2000) The Application of Life Cycle Assessment to Integrated Solid Waste Management: Part I – Methodology. *Transactions of the Institute of Chemicals Engineers*, 78 part B:279-289.

COGEN Europe (2004) Micro-CHP needs specific treatment in the European Directive on cogeneration. Brussels: COGEN Europe. [Online]. Available at: http://www.cogeneurope.eu/wp-content/uploads//2009/02/position_paper_microchp.pdf (Accessed 12th Sep 2010)

Connolly, D & Lund, H & Mathiesen, B. V, & Leahy, M (2010) A review of computer tools for analyzing the integration of renewable energy into various energy systems. *Applied Energy*, *87*(4): 1059-1082.

CPLEX IBM ILOG (2010). 12.2 User's Manual

Danish Maritime Authority (2012) North European LNG Infrastructure Project; A feasibility study for an LNG filling station infrastructure and test of recommendations.

De Paepe, M & D'Herdt, P & Mertens, D (2006) Micro-chp systems for residential applications. *Energy Conversion and Management*, 47(18-19): 3435-3446.

Decree-Law 23/2010 (2010) Decree-Law 23/2010 of 25 of March (in Portuguese).

Decree-Law 34/2011 (2011) Decree-Law 34/2011 of 8 of March (in Portuguese).

Decree-Law 538/99 (1999) Decree-Law 538/99 of 27 of July (in Portuguese).

Decree-Law 68/2002 (2002) Decree-Law 68/2002 of 25 of March (in Portuguese).

Decree-Law 764/2002 (2002) Decree-Law 764/2002 of 1st of July (in Portuguese).

Denholm, P & Margolis, R.M & Ong, S & Roberts, B (2009) Break-Even Cost for Residential Photovoltaics in the United States: Key Drivers and Sensitivities. NREL.

Dentice d'Accadia, M & Sasso, M & Sibilio, S & Vanoli, L (2003) Micro-combined heat and power in residential and light commercial applications. *Applied Thermal Engineering*, 23(10): 1247-1259.

Directive 2004/8/EC (2004) Directive 2004/8/EC of the European parliament and the council on the promotion of cogeneration based on a useful heat demand in the

internal energy market. Available at: http://eur-lex.europa.eu/LexUriServ/LexUriServ.do?uri=OJ:L:2004:052:0050:0050:EN:PDF.

Dorer, V & Weber, R & Weber, A (2005) Performance assessment of fuel cell micro-cogeneration systems for residential buildings. *Energy and Buildings*, 37(11): 1132-1146.

Edwards, R & Larivé, J.F & Rickeard, D & Weindorf, W (2014) Well-to-wheels analysis of future automotive fuels and powertrains in the European context. 2006. Version 4a. April 2014

Elhadidy, M. A & Shaahid, S. M (2000) Parametric study of hybrid (wind + solar + diesel) power generating systems. *Renewable Energy*, 21(2): 129-139.

Elhadidy, M. A (2002) Performance evaluation of hybrid (wind/solar/diesel) power systems. *Renewable Energy*, 26(3): 401-413.

Ellis, M.W & Gunes, M (2002) Status of Fuel Cells for combined heat and Power Applications in buildings. *ASHRAE Transactions*, 108, 1032-1044

Eni-Saipem (2010) LNG liquefaction, regasification, and tankage onshore engineering and construction project references. 2010. Available at: http://www.saipem.com/site/download.jsp?idDocument=1919&instance=2

EPA (1996) *Methane Emissions from the U.S. Petroleum Industry (Draft)*. Prepared by Radian. U.S. Environmental Protection Agency. June 1996.

EPA (2011) Greenhouse Gas Emissions Reporting From the Petroleum and Natural Gas Industry; Background Technical Support Document. Available at: http://www.epa.gov/ghgreporting/documents/pdf/2010/Subpart-W_TSD.pdf

EPA ETV (2003) Natural-Gas-Fired Microturbine Combined With Heat Recovery System. *The Environmental Technology Verification Program.*

ERSE (2011) Annual Report to the European Commission. Energy Services Regulatory Authority of Portugal. Available at: http://www.erse.pt.

ESP-r Solar (2005**)** ESP-r Solar; Current capabilities. [Online]. Available at: http://www.esru.strath.ac.uk/Programs/ESP-r_capabilities/solar.html

ESTIF (2007) Simple calculation of energy delivery of (small) ST systems: Objective methodology for simple calculation of the energy delivery of (small) Solar Thermal systems

EuroStat (2013) http://epp.eurostat.ec.europa.eu/portal/page/portal/eurostat/home/

Faruque Hasan, M.M & Zheng, A.M & Karimi, I.A (2009) Minimizing Boil-Off Losses in Liquefied Natural Gas Transportation. *Ind. Eng. Chem. Res*. (48) 9571–9580

Frischknecht, R & Jungbluth, N (2007) Implementation of Life Cycle Impact Assessment Methods. Data v2.0.

Fuller, S.K, & Petersen, S.R (1996) Life-cycle costing manual for the federal energy management program, 1995 Edition. *NIST handbook*, *135*.

Fulton, M & Mellquist, N & Kitsei, S & Bluestein, J (2011) Comparing greenhouse gas emissions from natural gas and coal. Worldwatch Institute/Deutsche Bank. Available at: http://www.worldwatch.org/natural-gas-sustainable-energy

Galp Energia (2012) Natural gas supply. Available at: http://www.galpenergia.com/EN/Investidor/ConhecerGalpEnergia/Os-nossos-negocios/Gas-Power/Gas-Natural/Aprovisionamento/Paginas/Aprovisionamento.aspx (Last Accessed 22 January 2013).

García-Valverde, R & Miguel, C & Martínez-Béjar, R & Urbina, A (2009) Life cycle assessment study of a 4.2 kwp stand-alone photovoltaic system. *Solar Energy*, 83(9): 1434-1445

Guinée, J.B & Gorrée, M. & Heijungs, R & Huppes, G. & Kleijn, R & Koning, A de & Oers, L. van & Wegener Sleeswijk, A & Suh, S & Udo de Haes, H.A. & Bruijn, H de & Duin, R van & Huijbregts, M.A.J (2002) Handbook on life cycle assessment. Operational guide to the ISO standards. I: LCA in perspective. IIa: Guide. IIb: Operational annex. III: Scientific background. Kluwer Academic Publishers, ISBN 1-4020-0228-9, Dordrecht, 2002, 692 pp

Gunes, M.K (2001) "Investigation of a Fuel Cell Based Total Energy System for Residential Applications". *MSc thesis*. Virginia Polytechnic Institute and State University, Virginia.

Harrison, J & Redford, S (2001) Domestic CHP: What are the potential benefits. A report by EA Technology for the Energy Saving Trust, London.

Hawkes, A & Leach, M (2005a) Solid oxide fuel cell systems for residential micro-combined heat and power in the UK: Key economic drivers. *Journal of Power Sources*, 149: 72-83.

Hawkes, A & Leach, M (2005b) Impacts of temporal precision in optimization modelling of micro-combined heat and power. *Energy*, 30(10):1759-1779.

Hawkes, A & Leach, M (2007) Cost-effective operating strategy for residential micro-combined heat and power. *Energy*, 32(5): 711-723.

Hayhoe, K & Kheshgi, H.S & Jain, A.K & Wuebbles, D.J (2002) Substitution of natural gas for coal: climatic effects of utility sector emissions. *Climate Change*. 54: 107–139

Horne, R.E & Grant, T & Verghese, K.L (2009) *Life cycle assessment: principles practice and prospects*. Csiro Publishing.

Howarth, R.W & Santoro, R & Ingraffea, A (2011) Methane and the greenhouse gas footprint of natural gas from shale formations. *Climatic Change*, 106(4): 679-690.

Howarth, R.W & Santoro, R & Ingraffea, A (2012) Venting and leaking of Methane from shale gas development: response to Cathles *et al. Climatic Change*. 113(2): 537-549.

Huijbregts, M (1998) Application of uncertainty and variability in LCA. Part I: A General Framework for the Analysis of Uncertainty and Variability in Life Cycle Assessment. *International Journal of Life Cycle Assessment* 3(5): 273–280.

IEA (2008) Combined Heat and Power; evaluating the benefits of a global greater investment. [Online] Available at: http://www.iea.org/Textbase/Papers/2008/chp_report.pdf (Accessed 27 Feb 2014).

IEA (2009) Cogeneration and District Energy. Sustainable energy technologies for today and tomorrow

IEA (2011) Energy Efficiency in Buildings – Heating and Cooling Technology Roadmap

IEA (2011a) Oil and Gas Security- Emergency response of IEA countries. Country Report: Portugal

IEA (2011b) World Energy Outlook Special Report: Are we entering a Golden Age of Gas?

IEA (2012) World Energy Outlook 2012

IEA (2013) Transition to Sustainable Buildings; Strategies and Opportunities to 2050

IEA-PVPS (2011) Trends in Photovoltaic Applications; Survey Report of Selected IEA countries between 1992 and 2010; Report T1-20

IGU (2011) World LNG report 2011

Intergovernmental Panel on Climate Change (2007) IPCC fourth assessment report (AR4). Working Group 1, The Physical Science Basis. http://www.ipcc.ch/publications_and_data/ar4/wg1/en/contents.html

ISO (2006) ISO 14044 Environmental management—Life cycle assessment—Requirements and guidelines. First edition

Jaramillo, P & Griffin, W. M & Matthews, H. S (2007) Comparative life-cycle air emissions of coal, domestic natural gas, LNG, and SNG for electricity generation. *Environmental Science & Technology*, *41*(17): 6290-6296.

Jungbluth, N & Stucki, M & Frischknecht, R (2009) Eco-Invent report XII: Photovoltaics

Jungbluth, N (2007) Erdöl. In: Sachbilanzen von Energiesystemen: Grundlagen für den ökologischen Vergleich von Energiesystemen und den Einbezug von Energiesystemen in Ökobilanzen für die Schweiz (ed. Dones R.). Swiss Centre for Life Cycle Inventories, Dübendorf, CH.

Kaldellis, J & Zafirakis, D & Kondili, E (2009) Optimum autonomous stand-alone photovoltaic system design on the basis of energy pay-back analysis. *Energy*, 34(9): 1187-1198.

Kavalov, B & Petric´, H & Georgakaki, A (2009) Liquefied Natural Gas for Europe; Some Important Issues for Consideration. JRC-IE report

Kong XQ & Wang, R.Z & Huang, X.H (2007) Energy optimization model for a CCHP system with available gas turbines. *Appl Therm Eng*; 25: 377–91.

Lim, W & Choi, K & Moon, I (2013) Current status and perspectives of liquefied natural gas (LNG) plant design. *Industrial & Engineering Chemistry Research*, *52*(9), 3065-3088.

Lloyd, S & Ries, R (2007) Characterizing, Propagating, and Analyzing Uncertainty in Life Cycle Assessment: A Survey of Quantitative Approaches. *Journal of Industrial Ecology* 11(1): 161–179.

Lozano, M.A & Ramos, J.C & Serra, L.M (2010) Cost optimization of the design of CHCP (combined heat, cooling and power) systems under legal constraints. *Energy*, *35*(2): 794-805.

Lund, C & Biswas, W (2008) A Review of Application of Lifecycle Analysis to Renewable energy systems. *Bulletin of Science, Technology & Society,* 28(3): 200-209.

Lund, H (2005) Large-scale integration of wind power into different energy systems. *Energy*, 30(13): 2402-2412.

Malça, J & Coelho, A & Freire, F (2014) Environmental life-cycle assessment of rapeseed-based biodiesel: Alternative cultivation systems and locations. *Applied Energy*, 114: 837-844.

Malça, J & Freire, F (2010) Uncertainty analysis in biofuel systems; An Application to the Life Cycle of Rapeseed Oil. *Journal of Industrial Ecology*, 14(2): 322-334.

Malça, J & Freire, F (2011) "Uncertainty Analysis of the Life-cycle Greenhouse Gas Emissions and Energy Renewability of Biofuels". In: Environmental Impact of Biofuels, Marco Aurélio dos Santos Bernardes ed., chapter 10, 26 pp., InTech Publishers, Vienna. ISBN: 978-953-307-178-7.

Man Diesel (2012) Propulsion Trends in LNG Carriers; Two-stroke Engines. Online. Available at: http://www.mandieselturbo.com/1008074/Press/Publications/

Marantan, A & Popovic, P & Radermacher, R (2002) The Potential of CHP Technology in Commercial Buildings; Characterizing the CHP Demonstration Building," ASHRAE Symposium on CHP Technologies for the New Century, *ASHRAE Transactions*, vol. 108, part 1

Mavrotas, G & Diakoulaki, D & Florios, K & Georgiou, P (2008) A mathematical programming framework for energy planning in services' sector buildings under uncertainty in load demand: The case of a hospital in Athens. *Energy Policy*, 36(7): 2415-2429.

McCarl, B.A *et al.* (2013) McCarl Expanded GAMS User Guide, GAMS Release 24.2.1. GAMS Development Corporation, Washington, DC, USA. http://www.gams.com/

Mone, C. D & Chau, D.S & Phelan, P.E (2001) Economic feasibility of combined heat and power and absorption refrigeration with commercially available gas turbines. *Energy Conversion and Management*, 42(13):1559-1573.

Monteiro, E & Moreira, N.A & Ferreira, S (2009) Planning of micro-combined heat and power systems in the Portuguese scenario. *Applied Energy*, 86(3):290-298.

Mulvey, J.M & Vanderbei, R. J & Zenios, S. A (1995) Robust optimization of large-scale systems. *Operations research*, *43*(2), 264-281.

NETL (2005) Liquefied Natural Gas; Understanding the basic facts.

NNPC (2011) 2010 Annual Statistical Bulletin. Available at: http://www.nnpcgroup.com/PublicRelations/OilandGasStatistics/AnnualStatisticsBulletin.aspx

O'Sullivan, F & Paltsev, S (2012) Shale gas production: potential versus actual greenhouse gas emissions. *ENVIRONMENTAL RESEARCH LETTERS*. *7*(4): 044030.

OGP (2000) Flaring & venting in the oil & gas exploration & production industry; An overview of purpose, quantities, issues, practices and trends. Report No: 2.79/288

Okamura, T & Furukawa, M & Ishitani, H (2007) Future forecast for life-cycle greenhouse gas emissions of LNG and city gas 13A. *Applied Energy,* (84): 1136-1149.

Onovwiona, H & Ugursal, V (2006) Residential cogeneration systems: review of the current technology. *Renewable and Sustainable Energy Reviews*, 10(5): 389-431.

Osman A & Norman B.A & Ries, R (2008) Life cycle optimization of building energy systems. *Engineering Optimization*, 40(2): 157-178.

Pacca, S & Sivaraman, D & Keoleian, G.A (2007) Parameters affecting the life cycle performance of PV technologies and systems. *Energy Policy*, 35(6): 3316-3326.

Pearce, J.M (2002) Photovoltaics — a path to sustainable futures. *Futures*, 34(7): 663-674.

Pehnt, M (2008) Environmental impacts of distributed energy systems—The case of micro cogeneration. *Environmental science & policy*, *11*(1): 25-37.

Pennington, D.W & Potting, J & Finnveden, E. & Lindeijer,G & Jolliet,O & Rydberg, T & Rebitzer, G (2003) Life cycle assessment Part 2: Current impact assessment practice, *Environment International*, 30(5): 721-739.

Pillarella, M & Liu, YN & Petrowski, J & Bower, R (2007) The C3MR liquefaction Cycle: Versatility for a Fast Growing, Ever Changing LNG Industry. In 15th International Conference on LNG (LNG-15), Barcelona, Spain, April 24–27.

Primas, A (2007) Life Cycle Inventories of new CHP systems. Eco-invent report. Data v2.0

PVWatts (2011) PVWatts Solar PV energy calculator website. [Online]. Available at: http://www.pvwatts.org/ (Accessed 15th Sep 2010)

RCM (2010) RCM 93/2010. PNAC 2020. Programa Nacional para as Alterações Climáticas 2013-2020. Available at: http://dre.pt/pdf1sdip/2010/11/23000/0534905351.pdf

REN (2008) Gas Properties. REN Gasodutos S.A. REDE NACIONAL DE TRANSPORTES DE GÁS NATURAL- PORTUGAL

Ren, H & Gao, W (2010) A MILP model for integrated plan and evaluation of distributed energy systems. *Applied Energy*, *87*(3): 1001-1014.

Ren, H & Zhou, W & Nakagami, K.I & Gao, W & Wu, Q (2010) Multi-objective optimization for the operation of distributed energy systems considering economic and environmental aspects. *Applied Energy*, *87*(12): 3642-3651.

Rezvan, A.T & Gharneh, N.S & Gharehpetian, G.B (2012) Robust optimization of distributed generation investment in buildings. *Energy*, 48(1): 455-463.

Riva, A & D'Angelosante, S & Trebeschi, C (2006) Natural gas and the environmental results of life cycle assessment. *Energy*, 31(1): 138-148.

Rolls-Royce (2007) Rolls-Royce wins order to power new European gas pipeline. Online. Available at: http://www.rolls-royce.com/news/press_releases/2007/rr_wins_order.jsp (Last Accessed 27 Feb 2014).

Rubio-Maya, C & Uche-Marcuello, J & Martínez-Gracia, A & Bayod-Rújula, A.A (2011) Design optimization of a polygeneration plant fuelled by natural gas and renewable energy sources. *Applied energy*, *88*(2): 449-457.

Ruether, J & Ramezan, M & Grol, E (2005) Life Cycle Analysis of Greenhouse Gas Emissions for Hydrogen Fuel Production in the US from LNG and Coal. NETL report

Safaei, A & Connors, S.R (2014) Relative Cost-Effectiveness of Commercial PV Systems – Meteorology and Markets in: *MIT Future of solar energy study* (under preparation).

Safaei, A & Freire, F & Antunes, C (2014a) Life-cycle Greenhouse Gas assessment of Nigerian Liquefied Natural Gas addressing Uncertainty. Submitted

Safaei, A & Freire, F & Antunes, C (2014b) Upstream impacts of Natural Gas mix in Portugal. Submitted

Safaei, A & Freire, F & Antunes, C (2014c) Environmental impacts of Distributed Generation technologies for buildings—the case of Portugal. under preparation

Safaei, A & Freire, F & Antunes, C (2014d) A multi-objective model for integrated economic and environmental assessment of building energy systems. under preparation

Safaei, A & Freire, F & Antunes, C.H (2012) A life-cycle cost optimization model with environmental impact assessment for energy management of service buildings. In *2012 IEEE International Symposium on Sustainable Systems and Technology* (ISSST). pp. 1-6

Safaei, A & Freire, F & Antunes, C.H (2013). A model for optimal energy planning of a commercial building integrating solar and cogeneration systems.*Energy*, *61*, 211-223.

Sakawa, M & Kato, K & Ushiro, S (2002) Operational planning of district heating and cooling plants through genetic algorithms for mixed 0–1 linear programming. *Eur Journal of Operation Research*, 137: 677–87.

Satel-light (2012) The European Database of Daylight and Solar Radiation. Available at: http://www.satel-light.com/

Schori, S & Frischknecht, R (2012) Life Cycle Inventory of Natural Gas Supply. Version 2012. ESU-services Ltd

Sevenster, M.N & Croezen, H.J (2006) The natural gas chain, Toward a global life cycle assessment; Delft

Shrestha, RM & Marpaung, C O.P (2005) Supply- and demand-side effects of power sector planning with demand-side management options and SO_2 emission constraints. *Energy Policy,* 33(6): 815–25

Simader, G.R & Krawinkler, R & Trnka, G (2006) Micro-CHP systems; state of the art. A report prepared for the European Commission Federal Ministry of Economics and Labour.

Skone, T.J & Littlefield, J & Marriott, J (2011) Life Cycle Greenhouse Gas Inventory of Natural Gas Extraction, Delivery and Electricity Production. Final report 24 Oct 2011 (DOE/NETL-2011/1522). U.S. Department of Energy, National Energy Technology Laboratory (NETL), Pittsburgh, PA

Stephenson, T & Valle, J.E & Riera-Palou, X (2011) Modeling the relative GHG emissions of conventional and shale gas production. *Environmental Science & Technology*, 45(24): 10757-10764

Strachan, N & Farrell, A (2006) Emissions from distributed vs. centralized generation: The importance of system performance. *Energy Policy*, 34(17): 2677-2689.

Suri, M & Huld, T.A & Dunlop, E.D & Ossenbrink, H.A (2007) Potential of solar electricity generation in the European union member states and candidate countries. *Solar Energy*, 81(10): 1295-1305.

Sylva, J & Crema, A (2004) A method for finding the set of non-dominated vectors for multiple objective integer linear programs. *European Journal of Operational Research*, 158(1): 46-55.

Sylva, J & Crema, A (2007) A method for finding well-dispersed subsets of non-dominated vectors for multiple objective mixed integer linear programs. *European journal of operational research*, 180(3): 1011-1027.

Tamura, I & Tanaka, T & Kagajo, T & Kuwabara, S & Yoshioka, T & Nagata, T & Ishitani, H (2001) Life cycle CO_2 analysis of LNG and city gas. *Applied Energy* (68): 301-319.

TRNSYS (1976) A transient simulation program. Eng. Experiment Station

U.S. EIA (2012) Nigeria report

UNdata (2013) **http://data.un.org/**.

US EPA (2000) AP 42 Compilation of Air Pollutant Emission Factors. Fifth Edition, Volume I. Chapter 3: Stationary Internal Combustion Sources.

Varun & Bhat, I.K & Prakash, R (2009) LCA of renewable energy for electricity generation systems—a review. *Renewable and Sustainable Energy Reviews*, 13(5): 1067-1073.

Venkatesh, A & Jaramillo, P & Griffin, W.M & Matthews, H.S (2011) Uncertainty in life cycle greenhouse gas emissions from United States natural gas end-uses and its effects on policy. *Environmental science & technology*,*45*(19), 8182-8189. (2011)

Voorspools, K.R & Brouwers, E.A & D'haeseleer, W.D (2000) Energy content and indirect greenhouse gas emissions embedded in 'emission-free power plants: results for the low countries. *Applied Energy*, *67*(3), 307-330.

WBCSD (2009) *Energy Efficiency in Buildings; Transforming the Market*. [Online]. Available at: http://www.wbcsd.org/DocRoot/6aBw3AqwUcwfX4w6qvT4/91719_EEBReport_WEB.pdf (Accessed 27 Feb 2014)

Weisser, D (2007) A guide to life-cycle greenhouse gas (GHG) emissions from electric supply technologies. *Energy*, *32*(9): 1543-1559.

Williams, H. P. (2013) *Model building in mathematical programming*. John Wiley & Sons.

Woodside (2011) Pluto LNG Project Greenhouse Gas Abatement Program. Second Revision. Available at: http://www.woodside.com.au/Our-Business/pluto/sustainability/Pages/Environment.aspx

World Bank (2012) Estimated Flared Volumes from Satellite Data, 2007-2011. Available at: http://go.worldbank.org/G2OAW2DKZ0

Wu, Y.J & Rosen, M.A (1999) Assessing and optimizing the economic and environmental impacts of cogeneration/district energy systems using an energy equilibrium model. *Applied Energy*, 62(3): 141-154.

Xuan, J *et al.* (2006) Evaluation of the Introduction of a Combined Heat and Power System in a Commercial Building in Shanghai. *Journal of Asian Architecture and Building Engineering,* 5(2): 385-390.

Yu, C.S & Li, H.L (2000) A robust optimization model for stochastic logistic problems. *International Journal of Production Economics*, *64*(1): 385-397.

Extra Readings

Ameri, M & Behbahaninia, A & Tanha, A. A (2010) Thermodynamic analysis of a tri-generation system based on micro-gas turbine with a steam ejector refrigeration system. *Energy*, *35*(5), 2203-2209.

Asif, M & Muneer, T (2007) Energy supply, its demand and security issues for developed and emerging economies. *Renew Sustain Energy Rev*; 11(7):1388–413.

Beihong, Z & Weiding, L (2006) An optimal sizing method for cogeneration plants. *J Energy Build*, 38(3): 189-95.

Bernal-Augustı´n,JL & Dufo-López, R & Rivas-Ascaso, DV (2006) Design of isolated hybrid systems minimizing costs and pollutant emissions. *Renew Energy*; 31: 2227–44.

Berta, G.L & Prato, A. P & Garbarino, L (2006) Design criteria for distributed cogeneration plants. *Energy*, *31*(10): 1403-1416.

Boudghene Stambouli, A & Traversa, E (2002) Fuel cells, an alternative to standard sources of energy. *Renewable and Sustainable Energy Reviews*, 6(3): 295-304.

Boyle, G (2004) *Renewable Energy: Power for a Sustainable Future* – 2nd edition, Oxford Press University, PP 66-82

Cooper, J.S. & Fava, J. (2006) Life Cycle Assessment Practitioner Survey: Summary of Results, *Journal of Industrial Ecology*, 10(4): 12-14

Cowie, M & Marantan, A & Garland, P & Radermacher, R (2002) CHP for Buildings: The Challenge of Delivering Value to the Commercial Sector," *ASME Symposium for Emerging and New Technologies for Heat Pump/Refrigeration Cycles, and CHP*. New Orleans.

Dunn, S (2002) Hydrogen futures: toward a sustainable energy system. *International Journal of Hydrogen Energy*, 27(3):235-264.

El-Fadel, M & Chedid, R & Zeinati, M & Hmaidan, W (2003) Mitigating energy-related GHG emissions through renewable energy. *Renewable Energy*, 28, (8), 1257-1276

EPA/GRI (1996) *Methane Emissions from the Natural Gas Industry*. Prepared by Harrison, M., T. Shires, J. Wessels, and R. Cowgill, eds., Radian International LLC for National Risk Management Research Laboratory, Air Pollution Prevention and Control Division, Research Triangle Park, NC. EPA-600/R-96-080a.

Esen H, & Inalli M, & Esen M.A (2007) Techno-economic comparison of ground-coupled and air-coupled heat pump system for space cooling. *Building and Environment*, 42(5): 1955-1965.

Esen, H & Inalli, M & Esen, M (2006) A Technoeconomic appraisal of a ground source heat pump system for a heating season in eastern Turkey. *Energy Conversion and Management*, 47(9–10): 1281-1297.

Fumo, N & Mago, P.J & Chamra, L.M (2009). Energy and economic evaluation of cooling, heating, and power systems based on primary energy. *Applied Thermal Engineering*, 29(13): 2665-2671.

Goodrich, A & James, T & Woodhouse, M (2012) Residential, Commercial, and Utility-Scale Photovoltaic (PV) System Prices in the United States: Current Drivers and Cost-Reduction Opportunities; NREL

Guedes Valente, L.C & Anibal De Almeida, S.V (1998) Economic analysis of a diesel/photovoltaic hybrid system for decentralized power generation in northern Brazil. *Energy,* 23 (4): 317-323

Homer (2010) Energy Modeling Software for Hybrid Renewable Energy Systems. [Online]. Available at: http://www.homerenergy.com/index.html (Accessed 2nd Sep 2010)

Huijbregts, M.A & Gilijamse, W & Ragas, A.M & Reijnders, L (2003) Evaluating Uncertainty in Environmental Life-Cycle Assessment. A Case Study Comparing two Insulation. Options for a Dutch One-Family Dwelling. *Environmental Science & Technology*. 37: 2600-2608.

Hultman, N & Rebois, D & Scholten, M & Ramig, C (2011) The greenhouse impact of unconventional gas for electricity generation. *Environmental Research Letters*, *6*(4): 044008

Lund, H & Münster, E (2006) Integrated energy systems and local energy markets. *Energy Policy*, 34(10): 1152-1160.

Markvart, T (2006) Microgrids power systems for the 21st century? *Refocus*, 7(4): 44-48

Mullins, K.A & Griffin, W. M & Matthews, H. S (2010) Policy impacts of uncertainty in modeling life-cycle greenhouse gas emissions of biofuels. *Environmental Science and Technology*. 45, 132–138.

Muselli, M & Notton, G & Poggi, P & Louche, A (2000) PV-hybrid power systems sizing incorporating battery storage: an analysis via simulation calculations. *Renewable Energy*, 20(1): 1-7.

NETL (2005) Liquefied Natural Gas; Understanding the basic facts.

Nisbet, EG & Manning, MR & Lowry, D & Lassey, KR (2000) Methane and the framework convention on climate change, A61F-10, *Eos Trans*. AGU 81(48), Fall Meet. Suppl

Norris, G.A (2001) Integrating Life Cycle Cost Analysis and LCA, *The International Journal of Life Cycle Assessment*, 6(2): 18–120.

Nosrat, A.H & Swan, L.G & Pearce, J.M (2012) Improved performance of hybrid photovoltaic-trigeneration systems over photovoltaic-cogen systems including effects of battery storage. *Energy*. 49: 366-374.

ONSITE SYCOM Energy (2000) *The Market and Technical Potential for Combined Heat and Power in the Commercial/Institutional Sector*. A Report Prepared for U.S. Department of Energy Information Administration [Online]. Available at: http://www.eere.energy.gov/de/pdfs/chp_comm_market_potential.pdf (Accessed 27 Feb 2014)

Osman, A.E & Ries, R (2006) Optimization for cogeneration systems in buildings based on life cycle assessment, *ITcon Vol. 11*, Special Issue Decision Support Systems for Infrastructure Management: 269-284,

PACE (2009) Life Cycle Assessment of GHG Emissions from LNG and Coal Fired Generation Scenarios: Assumptions and Results.

Papadopoulo, M & Kaddouh, S & Cigni, A & Gullentops, D & Serina, S & Vorgang, J & Veenstra, T & Dupin, F (2005) Life Cycle Assessment of the European Natural Gas Chain – A Eurogas – Marcogaz Study.

PRé Consultants (2009) SimaPro LCA software.

Raugei, M & Frankl, P (2009) Life cycle impacts and costs of photovoltaic systems: Current state of the art and future outlooks. *Energy,* 34(1): 392–399

Rebitzer, G & Ekvall, T & Frischknecht, R & Hunkeler, D & Norris, G & Rydberg, T & Pennington, D.W (2004) Life cycle assessment Part 1: Framework, goal and scope definition, inventory analysis, and applications. *Environment International* 30(5): 701-720.

Tsoutsos, T & Frantzeskaki, N & Gekas, V (2005) Environmental impacts from the solar energy technologies. *Energy Policy* 33: 289–296.

Appendix A

Calculation of GHG emissions from gas flaring and venting

This appendix presents the approach employed for estimating CO_2 and CH_4 emissions due to Natural Gas (NG) venting and flaring processes from its production stage. A material balance approach, based on volume emitted NG and fuel carbon analyses, is the most reliable method for estimating GHG emissions from stationary combustion sources (API, 2009) and is used in calculations of the results presented in chapter 3 of this thesis. This method and the formulations are briefly brought in this appendix.

Calculation of carbon content

In order to measure CO_2 emissions, the carbon content of the NG mixture should be calculated. The carbon content of NG ($Wt\%C_{mixture}$), either in raw or processed form, is a weighted average of its individual component carbon contents *i* ($Wt\%C_{Cj}$).This is shown in Equation (B.1).

$$Wt\%C_{mixture} = \frac{1}{100} \times \sum_{i=1}^{\#components} Wt\%_i \times Wt\%C_i \quad \text{(B.1)}$$

where

$Wt\%C_{mixture}$ = carbon content of mixture, on mass percent basis;

$Wt\%_i$= weight percent of component i; and

$Wt\%C_i$ = carbon content of component i on a weight percent basis.

Carbon content of component *i,* $Wt\%C_i$, is calculated from Equation (B.2).

$$Wt\%C_i = \frac{\frac{12 \text{ lb } C}{\text{lbmole } C} \times \frac{X \text{ lbmole } C}{\text{lbmole } C\ i}}{MWC_i \ (\frac{\text{lb}}{\text{lbmole } i})} \times 100\% \quad \text{(B.2)}$$

where

$Wt\%C_i$ = carbon content of individual hydrocarbon compound on a mass percent basis;

i = any hydrocarbon compound $C_xH_yO_z$

$12 =$ molecular weight of carbon;

$X =$ Stoichiometric coefficient for carbon (for example X=3 for C_3H_8).

and

MWC_i = molecular weight of individual hydrocarbon compound.

Calculation of flaring GHG emissions

CO_2 emissions (kg) due to flaring were calculated by Equation (B.3), considering 98% combustion efficiency at the flare stack (2% of gas is released noncombusted). The composition of Raw NG from Nigeria and Algeria (Tables 3.5 and 3.11) were used to calculate the carbon content of each source of NG (according to Equation B.1) and the corresponding emissions from its flaring.

$$E_{CO2} = V \ / \ MWC \ \times MW_{CO2} \ \times [\ (Wt\%C_{mixture} \times FE) + \frac{B \ mole \ CO2}{mole \ gas}] \quad \text{(B.3)}$$

where

E_{CO2} = CO_2 mass emission (kg) from flare stack;

V = Volume of gas flared (m^3)

MWC = conversion from molar volume to mass (23.685 m^3/kg mole);

MW_{CO2} = CO_2 molecular weight (44);

$Wt\%C_{mixture}$ = carbon content of mixture, on mass percent basis (excluding CO_2);

FE = flare destruction efficiency (98%);

A = the number of CO_2 moles present in the flared gas stream.

Equation B.3 shows that the destruction efficiency and conversion of flare gas carbon to CO_2 does not apply to the CO_2 already contained in the flared stream; the CO_2 present in the flare stream is emitted directly.

CH_4 emissions from flare are calculated by assuming a value (typically 2%) for the amount of residual, unburned CH_4 (Equation B.4).

$$E_{CH4} = V \times MF_{CH4} \times \%\, residual_{CH4} \times \frac{MW_{CH4}}{MWC} \quad \text{(B.4)}$$

where:

E_{CH4} = CH_4 mass emission (kg) from flare stack;

V = Volume of gas flared (m^3);

MF_{CH4}= CH_4 mole fraction;

$\%\, residual_{CH4}$ = noncombusted fraction of flared stream (2%);

MW_{CH4} = CH_4 molecular weight (16);

MWC = conversion from molar volume to mass (23.685 m^3/kg mole).

Calculation of venting GHG emissions

Venting refers to release of emissions without combustion (API, 2009). GHG emissions from venting is calculated using Equation B.5.

$$E_x = V \times F_x \times \frac{MW_x}{MVC} \quad \text{(B.5)}$$

where

E_x = mass emissions of "x" in units of mass (kg);

"x" = the GHG compound of interest (CH_4 or CO_2);

V = Volume of gas vented (m^3)

F_x = the molar fraction of compound "x" in the vent gas stream;

MW_x = molecular weight of compound "x";

MWC = conversion from molar volume to mass (23.685 m^3/kg mole).

Appendix B

Cost Assumptions

Appendix B covers the cost assumptions of the energy systems. The data included in Tables B.1-B.5 serve as the input to the model. The price of natural gas for commercial consumers is assumed to be 0.052 Euros/kWh.

Table B 1: Cost assumptions of Cogeneration systems

	Solid Oxide Fuel Cell (SOFC)	Micro-Turbine (MT)	Internal Combustion Engine (ICE)
Capital cost (€/kW)	5,720	2,718	2,535
Size (kW)	125	60	150
Total Installed Cost	715,000	163,080	380,250
Variable OM cost (€/kWh)	0.01	0.01	0.01
Fixed OM cost (€/kW/year)	6.5	40	10
Fixed OM cost (€/year)	812.5	2,400	1,500
Residual Value (€)	71,500	16,305	38,025
Operating cost P1 (€/kWh)	0.118	0.200	0.158
Operating cost P2 (€/kWh)	0.115	0.217	0.174
Operating cost P3 (€/kWh)	0.108	0.260	0.193
Operating cost P4 (€/kWh)	0.106	0.400	-
Operating cost P5 (€/kWh)	0.104	-	-
Operating cost P6 (€/kWh)	0.104	-	-
Operating cost P7 (€/kWh)	0.102	-	-

Table B 2: cost assumptions of ST systems

Solar Thermal	
Capital cost (€/m^2)	700
Approximate Area(m^2)	4
Total Installed Cost	2,800
Fixed OM cost (€/year)	60
Residual Value (€)	0

Table B 3: cost assumptions of PV systems

Mono-crystalline silicon PV systems	
Capital cost (€/kW)	4,500
Size (kW)	4
Total Installed Cost	18,000
Fixed OM cost (€/year)	60
Residual Value (€)	0
Approximate Area(m^2)	35

Table B 4: Cost assumptions of CC

Compression chillers	
Capital cost (€/kW)	1,000
Size (kW)	15
Total Installed Cost	15,000
Fixed OM cost (€/year)	0
Residual Value (€)	0

Table C 5: cost assumption of AC

Absorption chillers	
Capital cost (€/kW)	1,500
Size (kW)	104
Total Installed Cost	156,000
Fixed OM cost (€/year)	0
Residual Value (€)	0

Appendix C

List of Publications

Journal Articles

1. Safaei, A & Freire, F & Antunes, C (2013). A model for optimal energy planning of a commercial building integrating solar and cogeneration systems. *Energy*, *61*, 211-223.
2. Safaei, A & Freire, F & Antunes, C (2014a) Life-cycle Greenhouse Gas assessment of Nigerian Liquefied Natural Gas addresrstsing Uncertainty. *Submitted*
3. Safaei, A & Freire, F & Antunes, C (2014b) Upstream impacts of Natural Gas mix in Portugal. *Submitted*
4. Safaei, A & Freire, F & Antunes, C (2014c) Environmental impacts of Distributed Generation technologies for buildings—the case of Portugal. *under preparation*
5. Safaei, A & Freire, F & Antunes, C (2014d) An integrated economic and environmental assessment of building distributed generation technologies for buildings. *under preparation*

Conference Papers

1. Safaei, A., Freire, F., Henggeler Antunes, C. (2012). “Economic implications of solar and cogeneration technologies for the building sector in Portugal”. Abstract book of the 1st International Conference on Energy, Environment and Sustainability, pp 50-51. 16-17 September. Porto.
2. Safaei, A., Freire, F., Antunes, C.H. "Life-cycle cost optimization model extended with environmental impact assessment for energy management of service

buildings". 2012 IEEE International Symposium on Sustainable Systems and Technology (ISSST), 5 pages. http://dx.doi.org/10.1109/ISSST.2012.6227981

3. Safaei, A., Freire, F., Antunes, H. (2011). "A Mixed Integer Linear Programming Model to Minimize the Life-Cycle Costs of Meeting Energy Demand in Service Sector Buildings". ICEET 2011 - International Conference on Environmental Engineering and Technology, July 13-15, Amsterdam, Netherlands

Chapters in Books

Safaei, A & Connors, S.R (2014) Relative Cost-Effectiveness of Commercial PV Systems – Meteorology and Markets in: *MIT Future of solar energy study* (under preparation).